The immunological profile of the skin in DRESS and SJS/TEN reactions to first-line tuberculosis drugs in HIV-infected patients.

CHIMBETETE TAFADZWA EDWIN

(CHMTAF003)

Submitted to the University of Cape Town

In fulfilment of the requirements for the degree

MSc (Med) in Clinical Science and Immunology

Department of Medicine

Faculty of Health Sciences

University of Cape Town

14 November 2022

Supervisors:

A/Prof Jonny Peter

Dr Riyaadh Roberts

Dr Sarah Pedretti

DECLARATION

I, TAFADZWA EDWIN CHIMBETETE, hereby declare that the work on which this dissertation/thesis is based is my original work (except where acknowledgements indicate otherwise) and that neither the whole work nor any part of it has been, is being, or is to be submitted for another degree in this or any other university.

I empower the university to reproduce for the purpose of research either the whole or any portion of the contents in any manner whatsoever.

Signature: Signed by candidate

Date: 14th of November 2022

ABSTRACT

Introduction: A greater incidence of severe cutaneous adverse drug reaction (SCAR) such as Drug Reaction with Eosinophilia Systemic Symptoms (DRESS) and Stevens-Johnson syndrome/toxic epidermal necrolysis (SJS/TEN) occur among HIV-infected patients. We sought to characterize the immunohistological phenotype of the skin in these reactions to first-line TB drugs in HIV-infected cases, with a hypothesis that a possible depletion of T-regulatory cells (Tregs) and increased infiltration of effector cells may contribute to SCAR in the context of HIV.

Participants and Methods: HIV cases with validated SCAR phenotypes (probable or definite) and confirmed reactions to either one or multiple first-line anti-TB (FLTB) drugs were chosen (n=20). These cases were matched against controls of HIV-uninfected patients who develop SCAR (n=6). Immunohistochemistry assays were carried out with the following antibodies: CD3, CD4, CD8, CD45RO and FOXP3. Positive cells were normalized to the number of CD3+ cells present.

Results: Infiltrated immunoreactive T cells in SCAR were mainly found in the dermis. Dermal and epidermal CD4+ T-cells (and CD4+/CD8+ ratios) were lower in HIV-infected versus uninfected DRESS; $p < 0.001$ and $p = 0.004$, respectively. In contrast, no difference in dermal CD4+FOXP3+ Tregs were found in HIV-infected versus uninfected DRESS; median (IQR) CD4+FOXP3+ Tregs: [10 (0 - 30) cells/mm^2 versus 4 (3 - 8) cells/mm^2, $p = 0.325$]. HIV-infected SCAR patients clinically reacting to more than one FLTB drug (n=4) showed increased dermal CD4+ T-cells compared to single drug reactors (n=12), [32 (23 - 41) versus 15 (11 - 20) cells/high-powered field, $p = 0.03$]. This was associated with increased dermal CD4+FOXP3+ Tregs in multiple drug reactors, [39 (36-48) versus 10 (1-22), $p = 0.02$]

Conclusion: HIV-infected and uninfected SCAR was associated with an increased infiltration of cytotoxic CD8+ T-cells compared to normal skin, displaying their role as key mediators of tissue damage. CD4+ T-cells were decreased in HIV-infected SCAR, in line with known HIV pathology and higher dermal infiltrates were associated with risk for reactivity to multiple unrelated medications. While inter-individual variation was high, dermal Tregs were in fact increased in HIV-infected DRESS, and this requires further research to understand their role and any possible impact on lower SCAR mortality amongst HIV-infected patients.

CONFERENCES AND MEETING PRESENTATIONS

- **Tafadzwa Chimbetete**, The immunological profile of the skin in DRESS and SJS/TEN reactions to first line tuberculosis drugs in HIV-infected patients. Fogarty HIV-Associated Tuberculosis Training Program Annual Scientific Meeting, November 2020 and February 2022, Cape Town, South Africa.
- **Tafadzwa Chimbetete**, Choshi P., Pedretti S., Roberts R., Lehloenya R., Peter J. The immunological profile of the skin in DRESS and SJS/TEN reactions to first line tuberculosis drugs in HIV-infected patients. 8th South African Immunology Society Virtual Conference, August 2021.
- **Tafadzwa Chimbetete**, The immunological profile of the skin in DRESS and SJS/TEN reactions to first line tuberculosis drugs in HIV-infected patients. University of Cape Town, Department of Medicine Annual Research Symposium, October 2021.
- **Tafadzwa Chimbetete**, Skin immunology and implications for drug hypersensitivity**.** Allergy in Africa Webinar, Department of Paediatrics and Child Health, University of Cape Town, April 2022.
- **Tafadzwa Chimbetete**, Choshi P., Pedretti S., Roberts R., Lehloenya R., Peter J. The immunological profile of the skin in DRESS and SJS/TEN reactions to first line tuberculosis drugs in HIV-infected patients. European Academy of Allergy and Clinical Immunology (EAACI) Prague Hybrid Congress, 1-2 July 2022.
- **Tafadzwa Chimbetete,** Choshi P., Pedretti S., Roberts R., Lehloenya R., Peter J. The immunological profile of the skin in DRESS reactions to first line tuberculosis drugs in HIV-infected patients. DRESS Syndrome Global Conference 2022, 5-6 November 2022.

PUBLICATIONS

- **Chimbetete T.**, Buck C., Choshi P., Selim R., Pedretti S., Divito S.J., Phillips E.J., Lehloenya R., Peter J. 2022. HIV-Associated Immune Dysregulation in the Skin: A Crucible for Exaggerated Inflammation and Hypersensitivity. In Press: Journal of Investigative Dermatology.
- Porter M., Choshi P., Pedretti S., **Chimbetete T.**, Smith R., Meintjes G., Phillips E., Lehloenya R., Peter J. IFN-γ ELISpot in Severe Cutaneous Adverse Reactions to First-Line Antituberculosis Drugs in an HIV Endemic Setting. Journal of Investigative Dermatology, 142 (11), P2920-2928.

ACKNOWLEDGEMENTS

Firstly, all thanks to God Almighty for blessing me with this opportunity and seeing me throughout my journey.

I would like to express my sincere gratitude to my supervisor A/Prof Jonny Peter for giving me the opportunity be a part of his research group. I'm thankful for your guidance, support, and encouragement throughout my MSc, I've definitely learnt a lot from you during this time, and I'm looking forward to many more lessons. To my co-supervisors Dr. Riyaadh Roberts and Dr. Sarah Pedretti for your expertise and continued guidance and support, you are greatly appreciated.

I am thankful to the IMARI Registry team. Thank you for welcoming me into the team and I can say I have learnt so much from each and every one of you. I am grateful for all your contributions towards my research, I definitely would not have done it all by myself. I am excited to continue this great work we are doing, and to achieving more.

To the Allergy and Immunology lab, I am grateful to each one of you for the support and encouragement. Thank you for creating such a great working environment, and for all the memories we shared outside of the lab. Special mention to Talitha Muller for helping with data analysis and making figures, wouldn't have done it without you.

Thank you to Lizette Fick for your assistance with histology and the many hours you spent helping optimize my work. Thank you to Prof Dirk Lang for your expertise and assistance with confocal imaging.

My sincere appreciation to the UCT Department of Medicine Research Committee, National Institute of Health (NIH) Fogarty and EDCTP for all the financial support and for funding my research.

My heartfelt gratitude to my parents, my siblings Tatenda, Tanya and Bo, and my partner Naomi for their continuous support and prayers. Thank you for being there every step of the way, through the highs and low. Grateful for you, always.

TABLE OF CONTENTS

LIST OF FIGURES

LIST OF TABLES

LIST OF ABBREVIATIONS

ADR	Adverse drug reaction
ALP	Alkaline phosphatase
ALT	Alanine aminotransferase
APC	Antigen presenting cell
ART	Antiretroviral therapy
AST	Aspartate aminotransferase
CADR	Cutaneous adverse drug reaction
CMV	Cytomegalovirus
DC	Dendritic cell
DILI	Drug induced liver injury
DRESS	Drug reaction with eosinophilia and systemic symptoms
EBV	Epstein-Barr virus
ELISpot	Enzyme-linked Immunospot assay
EMB	Ethambutol
FDE	Fixed drug eruption
FFPE	Formalin fixed paraffin embedded
FOXP3	Forkhead box protein 3
FLTD	First-line tuberculosis drug
GGT	Gamma glutamyl-transferase
IFN	Interferon
IHC	Immunohistochemistry
IM-ADR	Immune-mediated adverse drug reaction
INH	Isoniazid
cART	Combination active antiretroviral therapy
H&E	Hematoxylin and eosin
HIV	Human immunodeficiency virus
HHV	Human herpes virus
HLA	Human leukocyte antigen
MHC	Major histocompatibility complex
PZA	Pyrazinamide
RegiSCAR	The Registry of Severe Cutaneous Adverse Drug Reactions
RIF	Rifampicin
SCAR	Severe cutaneous adverse drug reaction

SDC	Sequential drug rechallenge
SJS/TEN	Stevens-Johnson syndrome/toxic epidermal necrolysis
TB	Tuberculosis
TCM	Central memory T-cell
TEM	Effector memory T-cell
TNF	Tumor necrosis factor
Treg	Regulatory T-cell
TRM	Tissue resident memory T-cell

1. LITERATURE REVIEW

1.1. Introduction

Adverse drug reactions (ADRs) are unintended harmful reactions to medications and contribute to a high number of admissions to hospital, with approximately 1 in 12 admissions being ADR-related in South African hospitals (Mounton et al., 2016). ADRs have significant morbidity and mortality, with a study of four hospitals in South Africa, including Groote Schuur Hospital, revealing that ADRs contribute to the death of 2.9% of medical admissions in adult medical wards (Mouton et al., 2015). ADRs can result from either on-target or off-target effects. On-target ADRs are predictable reactions caused by the intended pharmacological action of the drug (type A) and are the most common. Off-target ADRs (type B) are heterogenous reactions that have varying clinical manifestations and mechanisms and are often immune-mediated, termed immune mediated adverse drug reactions (IM-ADRs). They are unpredictable, and comprise 15-20% of all ADRs (Peter et al., 2017). Existing IM-ADRs classifications are based on the primary immune effector/trigger involved in the reaction, and include B-cell antibody mediated reactions (Gell-Coombs type I-III) and T-cell mediated delayed hypersensitivity reactions (Gell-Coombs type IV) (Karnes et al., 2019). In addition to IM-ADRs, there is also a growing recognition of non-immune contributions and novel immune receptors to ADRs (Blumenthal et al., 2019).

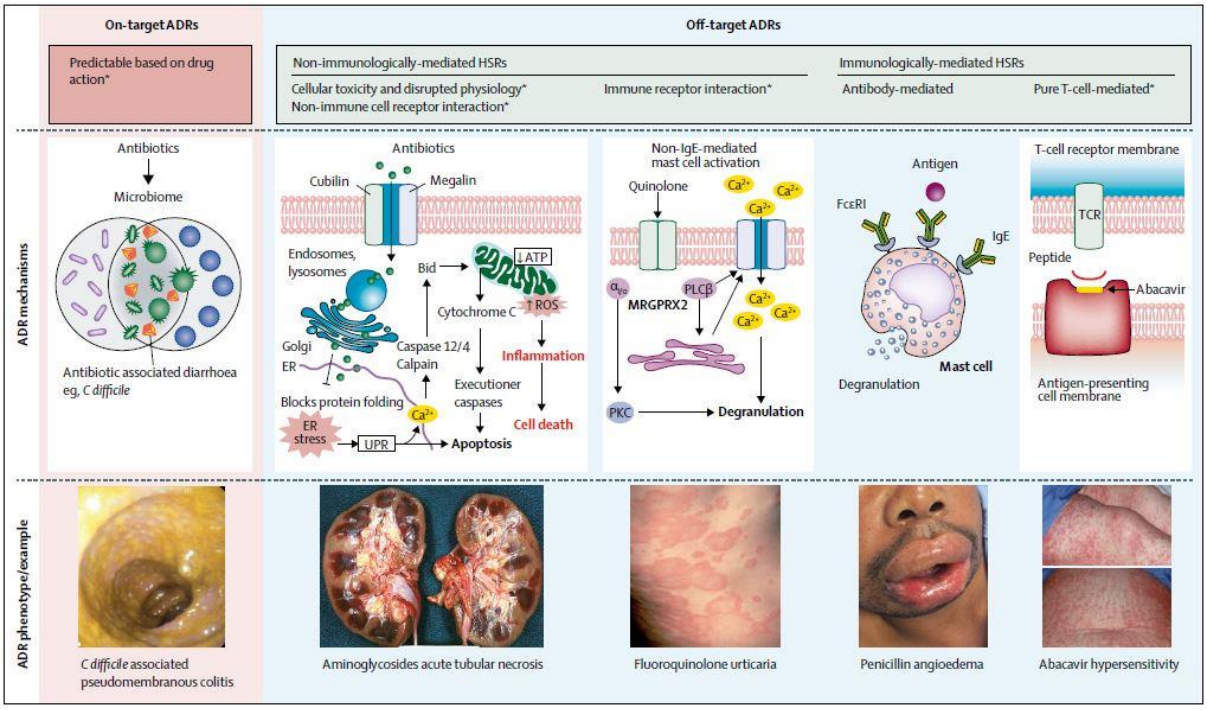

Figure 1-1: Classification of on-target and off-target ADRS (blue panel). Off-target effects that are not immunologically mediated (left) include direct cellular toxicity or disruption of normal physiology, interaction with non-immune receptors, and interaction with non-immune receptors. Adaptive immune

responses that are immunologically mediated (right) can be antibody mediated (e.g., IgE) immediate reactions or T-cell-mediated delayed reactions. Adapted from (Blumenthal et al., 2019).

Cutaneous adverse drug reactions (CADR) are frequent ADRs that involve the skin, with non-life-threatening presentations including maculopapular eruption (MPE), fixed drug eruptions (FDE) and urticaria. Severe cutaneous adverse drug reactions (SCARS) are off-target T-cell-mediated CADRs that, albeit uncommon, are potentially life-threatening and are associated with high morbidity and mortality. The most common SCAR clinical manifestations globally are drug reaction with eosinophilia and systemic symptoms (DRESS) and Stevens-Johnson syndrome/toxic epidermal necrolysis (SJS/TEN) with prevalence data of 4/10 000 and 1-7/1 000 000 respectively (Peter et al., 2017). It is well established that patients with Human Immunodeficiency Virus (HIV) suffer from ADRs at a higher rate than HIV-uninfected people. ADRs are a major obstacle to treatment success in tuberculosis (TB) and HIV and are a source of tremendous economic burden (Knight et al., 2019). IM-ADRs occur 2-100 times more commonly in HIV patients, with 1 in 10 HIV patients required to stop an offending drug/drugs in multi drug resistant tuberculosis regimens due to ADRs (Dheda et al., 2016, Lehloenya and Dheda, 2012).

Although SCARs are less common than low severity CADRs (20% of all HIV-infected patients), these severe reactions result in prolonged and high cost of hospitalization, and substantial long-term morbidity (Lehloenya and Dheda, 2012, Knight et al., 2019). They are particularly problematic in the context of HIV TB co-infection. HIV patients are immunologically vulnerable, with an annual incidence for active TB of 10%, and TB the leading cause of death (Dheda et al., 2016). Unfortunately, first-line anti-TB drugs are the commonest offending agents causing SCAR in the South African setting (3-5 cases/month in a single tertiary hospital) (Peter et al., 2017). Interestingly, some patients report tolerance to anti-TB drugs prior to the development of HIV but develop SCAR on subsequent exposures to first-line anti-TB drugs (FLTB) when co-infected with HIV, TB-HIV co-infected patients can ill afford treatment interruptions, which occur as a consequence of SCAR. Identifying the culprit drug is a major challenge in the context of 4-8 drug polypharmacy. Premature interruption can also worsen transmission of disease and hasten the development of drug resistant TB, with significant public health consequences. Furthermore, approximately 25% of HIV-infected patients will react to more than one of the anti-TB drugs during sequential drug rechallenge (SDC), despite diversity in the chemical structure of offending drugs (Lehloenya and Dheda, 2012, Lehloenya et al., 2012).

1.2. Drugs associated with hypersensitivity in HIV.

Offending SCAR drugs depend on disease burden and prescribing patterns. Several drugs have been implicated with SCAR, but the main culprits include anticonvulsants (i.e., carbamazepine and phenytoin), allopurinol, antiretrovirals, antimicrobials and nonsteroidal anti-inflammatory drugs (Karnes et al., 2019). In contrast, the most common offending drugs causing IM-ADRs in South Africa are FLTD, antiretrovirals and cotrimoxazole. Table 1-1 shows key drugs that are associated with IM-ADRs in an HIV TB endemic setting (Peter et al., 2019).

Antituberculosis drugs are associated with significant ADRs. The combined use of drugs including rifampicin, pyrazinamide, ethambutol, and isoniazid for first-line anti-tuberculosis drugs are responsible for the majority of delayed hypersensitivity reactions. Isoniazid, rifampicin, and pyrazinamide are the most often implicated drugs for both SCAR and drug induced liver injury (DILI) (Nalitye Haitembu et al., 2021). The increased use of second line regimens due to the increase in drug resistant TB, has also seen them being contributors to ADRs (Nagarajan and Whitaker, 2018). Given South Africa's high prevalence of HIV-TB coinfection, the number of people initiating combinational ART (cART) while on anti-tuberculosis treatment has increased. Several drugs in cART are also well-recognized cause of IM-ADRs, with nonnucleoside reverse transcriptase inhibitors (NNRTIs) the most prevalent. Nevirapine is the highest contributor to CADR, SCAR and DILI (Sarfo et al., 2014, Stewart et al., 2016, Wu et al., 2017). Hypersensitivity to NNRTIs such as abacavir is population dependent, as it has been eliminated in areas with routine HLA-B:57:01 testing in cART treatment programs (Peter et al., 2019, Stainsby et al., 2019). Drug hypersensitivity syndrome, CADRs, and case reports of DILI to integrase stand transfer inhibitors such as dolutegravir have also been reported (Thomas et al., 2017, Wang et al., 2018). Cotrimoxazole used for prophylaxis and *Pneumocystis jirovecii* treatment is frequently initiated at a similar time as anti-tuberculosis therapy and also causes SCAR, with DRESS, SJS/TEN and FDE being reported (Hiransuthikul et al., 2016, Mockenhaupt et al., 2008). When patients with HIV-TB coinfection develop SCAR and are on cART as well as drugs used for prophylaxis or treatment of opportunistic infections, all treatment needs to be stopped, bridging therapy given and then a rigorous effort made to identify the offending drug due to overlapping adverse effect profiles of these drugs (Lehloenya and Dheda, 2012).

Table 1-1: Key drugs associated with IM-ADRs in the context of HIV.

Drug	Type of IM-ADR	Prevalence
Antiretrovirals		
Nevirapine	CADR, SCAR: SJS/TEN, DRESS	CADR: 15-32%, DRESS: 5%, SJS/TEN: 0.3-10% (Sarfo et al., 2014, Stewart et al., 2016, Yunihastuti et al., 2014)
Efavirenz	CADR, SCAR	CADR: 6%, SCAR: 0.1% (Colebunders et al., 2004, Sarfo et al., 2014)
Abacavir	Abacavir hypersensitivity resections	2.3-9% (Borras-Blasco et al., 2008, Ma et al., 2010)
Dolutegravir	DHS, DILI	1% (Walmsley et al., 2013)
Anti-TB Drugs		
First-line		
Rifampicin	CADR, SCAR, DILI, AIN	(Lehloenya et al., 2016, Girling, 1997)
Isoniazid	CADR, SCAR, DILI	(Bakkum et al., 2002, Viswanath et al., 2012)
Pyrazinamide	CADR, SCAR	23% of HIV-infected patients receiving anti-CADR: 2.8%, SCAR, DILI (Yunihastuti et al., 2014, Tan et al., 2007)
Ethambutol	SCAR: SJS/TEN, DRESS	(Bakkum et al., 2002, Sanchez-Borges et al., 2013, Surjapranata and Rahaju, 1979, Pegram et al., 1981)
Rifafour (fixed dose combination)	Mainly case reports	Mostly case reports (Lehloenya and Kgokolo, 2014)
Second-line		
Fluoroquinolones Ethionamide Kanamycin/Amikacin	SCAR: DRESS & SJS	~20% in HIV-infected patients (Lehloenya et al., 2012)
Anti-bacterial		
PJP prophylaxis		
Cotrimoxazole (TMP/SMX)	CADR, SCAR: SJS/TEN, DRESS, FDE	CADR: 10.9% (Sisay et al., 2018), SCAR (Mockenhaupt et al., 2008, Hiransuthikul et al., 2016)

Abbreviations: AIN – acute interstitial nephritis, CADR – cutaneous adverse drug reactions, DILI – drug-induced liver injury, DRESS – drug reaction with eosinophils and systemic symptoms, HIV – human immunodeficiency virus; IM-ADR – immune mediated adverse drug reactions; PJP – *Pneumocystis jeroveci* pneumonia, SCAR – severe cutaneous adverse Reactions, SJS/TEN – Stevens-Johnson syndrome/toxic epidermal necrosis, TB – tuberculosis; TLR – treatment limiting reactions; TMP-SMX – trimethoprim sulfamethoxazole. Table adapted from (Peter et al., 2019).

1.3. Most common phenotypes of SCAR

1.3.1. Drug reaction with eosinophilia and systemic symptoms (DRESS)

Figure 1-2: Montage of images to illustrate the important features of drug reaction with eosinophilia and systemic symptoms (DRESS). (**a**) exfoliative dermatitis with severe scaling in a background of erythema. (**b**) indurated erythematous macules and papules. (**c**) confluent and infiltrated plaques, indurated erythema. (**d**) mildly erythematous maculopapular rash with some coalescence into plaques. Images (a) and (b) were adapted from (Peter et al., 2017) and image (d) from (Oladokun et al., 2018)

Drug reaction with eosinophilia and systemic symptoms (DRESS), also known as drug-induced hypersensitivity syndrome (DIHS) or drug hypersensitivity syndrome (DHS), can be associated with mortality of up to 10% (Lehloenya and Dheda, 2012). It is characterized by a delayed onset of clinical symptoms, which typically occurs 2-8 weeks after the start of treatment. Clinical symptoms may also persist even after cessation of treatment (Miyagawa and Asada, 2021). DRESS has diverse skin lesions that often start as a symmetrical MPE, that may progress to coalescent

erythema, infiltrate plaques, purpura, exfoliative dermatitis, and facial oedema. The rash is accompanied by fever, haematologic alterations such as eosinophilia, leucocytosis and/or lymphocytosis, and internal organ involvement such as liver injury (Lehloenya and Dheda, 2012). Although incidence is lower, other visceral organs such as pneumonitis, pancreatitis, nephritis and myocarditis can be involved (Cho et al., 2017). An expansion of CD4+FOXP3+ regulatory (Treg) T cells in circulation and those trafficking to the skin has also been associated with DRESS, and a sequential reactivation of human herpes viruses including cytomegalovirus (CMV), human herpes virus (HHV)-6, HHV7 and Epstein-Barr Virus (EBV) usually detected 2-4 weeks after onset, has been reported (Cho et al., 2017). Autoimmune manifestations also occur as short or long term sequalae i.e., systemic lupus erythematous (SLE), thyroiditis and type 1 diabetes (Karnes et al., 2019). Renal failure and as well advanced age are associated risk factors of disease (Peter et al., 2017).

1.3.2. Stevens-Johnson syndrome/toxic epidermal necrolysis (SJS/TEN)

Stevens-Johnson syndrome (SJS) and toxic epidermal necrolysis (TEN) are phenotypes of the same disease and are characterized by differences in the percentage of body surface area affected by epidermal necrosis and detachment. When less than 10% of epidermal detachment is observed, the disease is termed SJS, and when more than 30% is observed, it is designated TEN (Peter et al., 2017). Where there is 10-30% detached body surface area, it is considered as SJS/TEN overlap. Typical manifestations of SJS/TEN include erythematous macules and atypical target lesions on which blisters occur, leading to skin detachment. This detachment also affects the mucosa and reveals subepithelial erosions which are often haemorrhagic. A key feature of SJS/TEN is the early onset of painful erythema on the palms and soles (Lehloenya and Dheda, 2012). HIV infection, population clustered HLA alleles, renal failure, and radiotherapy are risk factors for SJS/TEN (Lin et al., 2020).

Figure 1-3: Montage of images to illustrate the important features of Stevens Johnson syndrome (SJS) and toxic epidermal necrolysis (TEN). (**a**) focal tender erythematous macules on the palms in SJS. (**b**) focal areas of early epidermal necrosis in a background of erythema in a patient with SJS. (**c** and d) stripping of the epidermis on the back and palms in TEN. Adapted from (Peter et al., 2017).

1.3.2.1. Case validation

Due to the lack of a universal consensus about case definitions of different SCAR, developing cohorts of standardised cases for mechanistic study and comparison across published datasets is a challenge. SCARs can be mimicked by multiple differential diagnoses, and hence careful clinical observation and thorough laboratory examination is required. A series of inclusion criteria have been proposed by the international Registry of Severe Cutaneous Adverse Reactions (RegiSCAR) for cases with suspected DRESS or SJS/TEN. For a suspected DRESS case, the inclusion criteria include hospitalized patients with the following systemic features: acute skin rash, fever above 38℃, enlarged lymph nodes, internal organ involvement; and haematological abnormalities including lymphocytosis or lymphocytopenia, eosinophilia and thrombocytopenia (Kardaun et al.,

2007, Chen et al., 2013, Kardaun et al., 2014). The inclusion criteria sets for SJS/TEN include erythema, skin blister/erosions, epidermal detachment, mucosal involvement, Nikolsky sign, atypical targets, and fever above 38℃ (Bastuji-Garin et al., 1993, Rzany et al., 1999). These two inclusion criteria for suspected DRESS or SJS/TEN are followed by a validation scoring system that categorizes cases as possible, probable, or definite. Other scoring systems also existing for other aspects of SJS/TEN, such as SCORTEN - an illness severity score that has been developed to predict mortality in SJS/TEN cases based on clinical characteristics (i.e., age, associated malignancy, heart rate, serum blood urea nitrogen (BUN), body surface area involvement, serum bicarbonate, and serum glucose) (Fouchard et al., 2000). In this study, all cases were validated according to the RegiSCAR case definitions.

1.3.2.2. Drug causality assessment tools

Upon diagnosis of a SCAR reaction, immediate withdrawal of all possible offending drug(s) is required (Peter et al., 2017). In the case of polypharmacy and cessation of multiple possible offending agents, a standardised approach is necessary to identify the offending drug which can be a challenge. Validated drug causality tools are used to try and rank likely offending drugs and identify the culprit or indicate the level of uncertainty in advising exclusion of particular drugs in the future. The Naranjo scoring system is widely used, and can be applied across all types of ADRs (Naranjo et al., 1981). Naranjo has several limitations, and in the case of SJS/TEN, a more disease-specific algorithm for drug causality for epidermal necrolysis (ALDEN) has been developed (Sassola et al., 2010).

1.4. Immunopathogenesis

The immunopathogenesis of SCAR is incompletely understood; the major mechanism is the crucial role of effector T-cells that are highlighted in Figure 1-4. Both CD8+ and CD4+ T cells are thought to mediate DRESS. Enhanced dermal lymphatic infiltration of lymphocytes and eosinophils, together with an increased secretion of inflammatory cytokines including TNF-α and interferon-gamma (IFN-γ), are the main characteristics of DRESS. In SJS/TEN, the drug most likely interacts with the human leukocyte antigen protein (HLA) on antigen presenting cells (APCs) such as keratinocytes, which further activate drug specific CD8+ cytotoxic T cells (CTL). This results in accumulation of cytotoxic CD8+ T cells releasing perforin and granzyme B within epidermal blisters and meditating keratinocyte cell death (Peter et al., 2017, Nassif et al., 2004). Additionally, CTL, natural killer (NK) cells, and NK T cells are also stimulated to release granulysin, a crucial cytotoxic mediator in SJS/TEN that mediates keratinocyte death without the need for cell contact and is correlated with severity of disease.

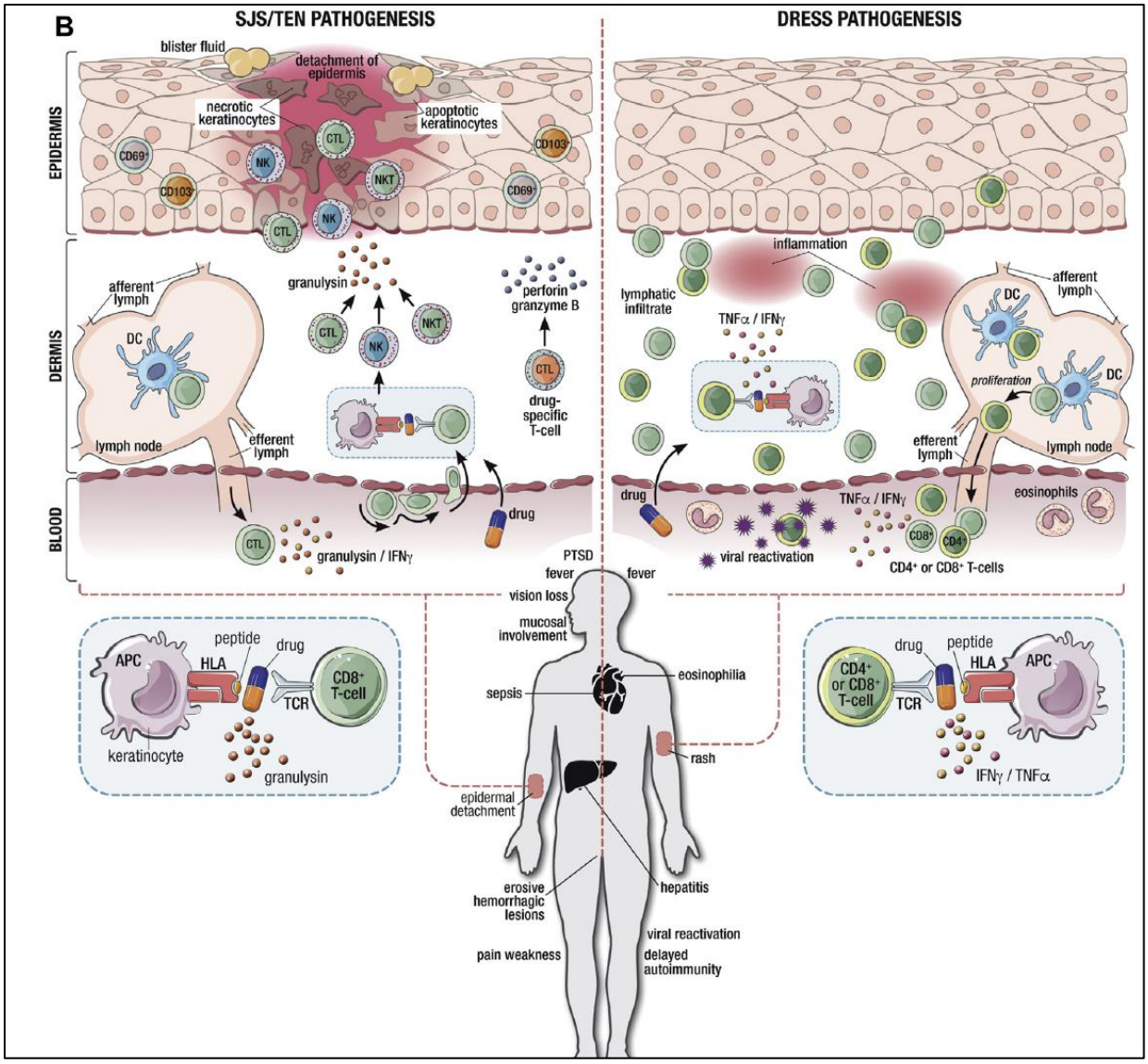

Figure 1-4: Proposed major pathogenic mechanisms in drug induced SJS/TEN and DRESS. Adapted from: (Peter et al., 2017).

Models describing how drugs might mediate activation of T cells have been proposed (Figure 1-5). In the hapten/prohapten model, chemically reactive groups in drugs or reactive drug intermediates form covalent bonds with endogenous peptides. These modified peptides are processed by APCs and presented by the major histocompatibility complex (MHC) molecule, eliciting a T cell response. In the pharmacological-interaction model (p-i), the drug forms a direct non-covalent bond with the MHC or TCR, stimulating an immune response without the need for peptide. As this model does not require antigen processing it explains how some T cell-mediated reactions occur immediately after drug ingestion and after single exposure. The altered peptide repertoire binding model stipulates that the drug can non-covalently bind to the MHC, altering stereochemistry of the binding cleft resulting in an altered repertoire of self-peptides that are

recognized and presented to the TCR (Karnes et al., 2019). This is exemplified by the crystal structure of HLA-B*57:01 with abacavir and peptide which reveals that abacavir binds to the F pocket of the peptide binding groove, changing its stereochemistry and the sequence of the peptide presented to the TCR (Ostrov et al., 2012, Illing et al., 2012).

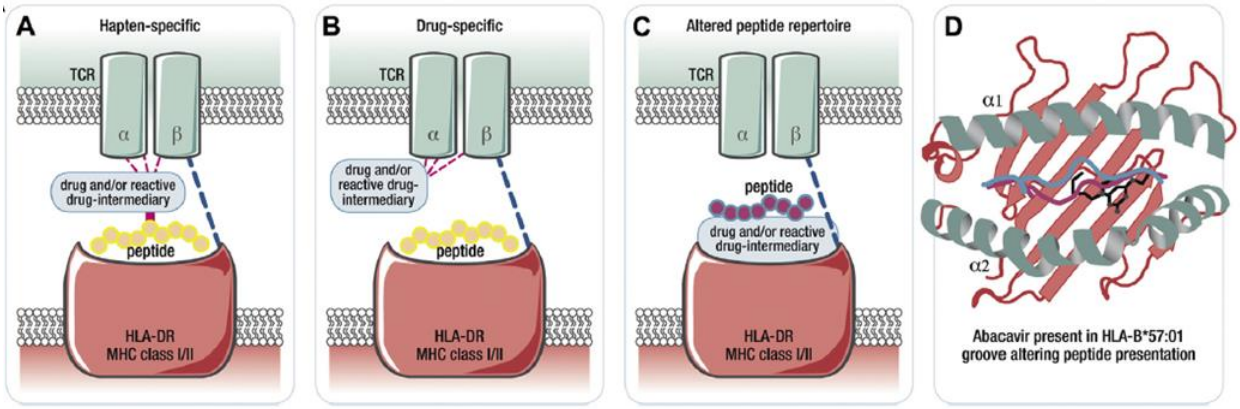

Figure 1-5: Proposed models of drug hypersensitivity in SCAR immunopathogenesis (a) The hapten/prohapten model, (b) drug-specific pharmacological-interaction (p-i) model, (c) altered peptide repertoire model and (d) altered peptide repertoire model exemplified by the interaction between abacavir and HLA-B*57:01 that occurs in abacavir hypersensitivity syndrome. Adapted from: (Peter et al., 2017).

1.5. HLA risk and TCR diversity: current paradigms in SCAR pathogenesis

The HLA molecule, like the CDR3 of TCRs, displays high sequence diversity at its peptide binding grooves and allelic variety in the genes that encode it has been associated with risk of T cell-mediated SCAR development in specific ethnic populations (White et al., 2015). Strong class I HLA associations have been elucidated for abacavir drug hypersensitivity across populations, with HLA-B57:01 allele having a negative predictive value of 100% and positive predictive value of 47.9% (Mallal et al., 2008). Other HLA-associations include HLA-B*15:02 in carbamazepine induced SJS/TEN in Asian populations and the HLA-B*35:05 allele for HIV-infected Thai patients (Chantarangsu et al., 2009, Chung et al., 2004). These discoveries have been translated into pretreatment pharmacogenetic screening strategies where population allele frequencies are high enough to make the number needed to test to prevent a hypersensitivity reaction sufficiently cost-effective (Phillips and Mallal, 2009).

Class I HLA restriction is necessary but not sufficient for SCAR, with many risk alleles carrying 100% negative predictive values, but low positive predictive value and why some tolerant patients carrying the risk allele will not develop SCAR, indicates that additional determining factors must be present to develop these reactions. The same HLA risk allele for a particular drug can also result

in different clinical phenotypes, for instance B*58:01 is associated with both allopurinol-induced DRESS and SJS/TEN and HLA-A*31:01 with carbamazepine-induced DRESS and SJS/TEN (McCormack et al., 2011, Ozeki et al., 2010). The factors that determine the phenotype of SCAR in such cases are unknown. Cross reactive expanded effector memory T-cell clones are suggested as an important additional factor in SCAR development. For instance, a dominant TCR clonotype has been identified from 84% of carbamazepine-associated SJS/TEN patients, absent in carbamazepine-tolerant controls (Ko et al., 2011). Next generation sequencing of T cells isolated from blister fluid of Taiwanese patients with HLA-B*15:02 restricted carbamazepine-SJS/TEN has also been carried out, identifying a T cell clonotype with a specific public TCR (White et al., 2015).

Several of the offending drugs implicated in SCAR amongst patients living with HIV have not had a clear HLA risk allele or dominant clonal TCR identified. To date, our research group and international collaborators have identified HLA-C*04:01 as a requirement for nevirapine-induced SJS/TEN and DRESS in South African populations, with a 100% negative predictive value. In a single case of nevirapine-induced TEN we have also identified oligoclonality of activated T-cells in blister fluid. We have also identified a putative HLA-B risk allele associated with rifampicin-induced DRESS in a South African population. However, in both nevirapine-induced TEN and rifampicin-induced DRESS, the positive predictive value of the HLA risk allele remains very low.

1.6. Immunological and physiological changes in HIV infection

The increased likelihood to develop SCAR in HIV is not fully elucidated, but potential mechanisms include immunological and physiological changes through the life cycle of HIV/AIDS, as highlighted in Figure 1-6. Prior to HIV infection, individuals or populations may be genetically predisposed, carrying HLA or pharmacogenomic risk alleles. Upon infection and disease progression, this genetic risk is coupled with immunologic changes associated with immune hyperactivation and altered immunoregulatory pathways. With advanced HIV infection, additional risks include drug-specific factors; for example, polypharmacy or interrupted drug therapies; the rise of opportunistic co-infections such as TB or HHV; and metabolic disturbances. During chronic infection, there is a state of progressive immune dysregulation, and this likely contributes to the clinical manifestation of SCAR. Normal skin immunology is detailed in Figure 1-7, and the current understanding of cutaneous changes associated with progressive HIV-related infection and immunosuppression which are likely to contribute to SCAR are highlighted in Figure 1-8.

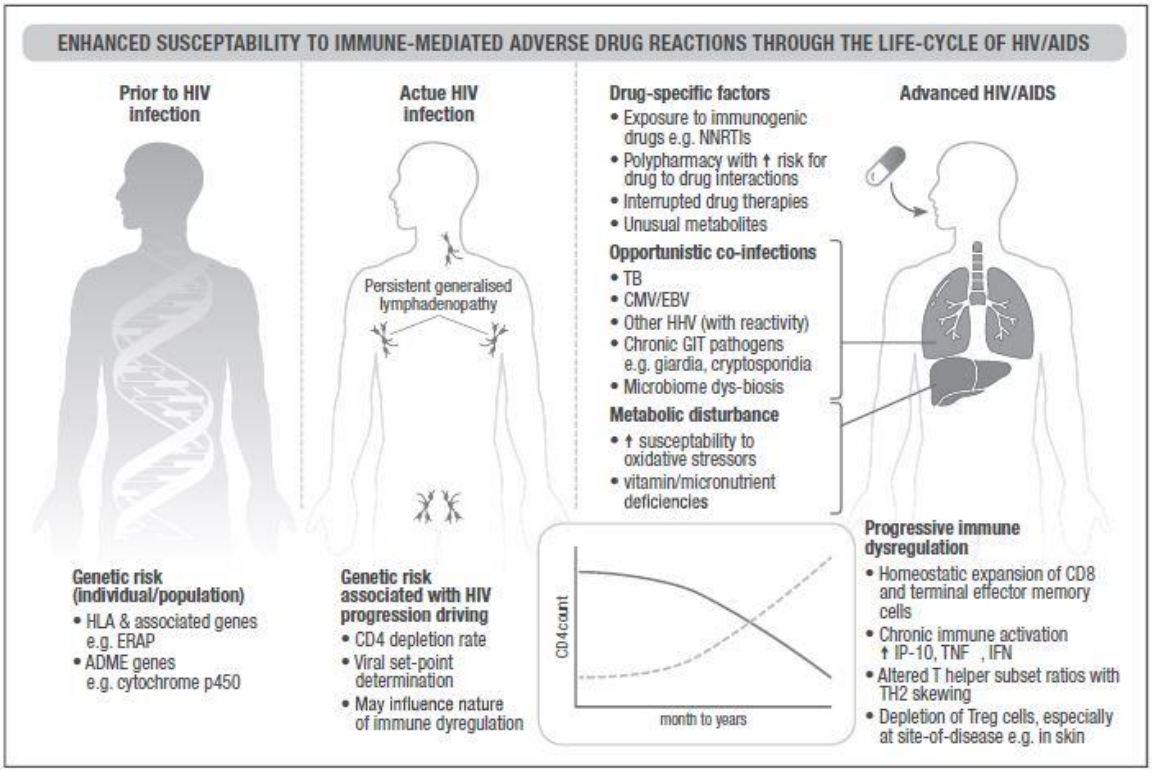

Figure 1-6: Increased susceptibility to immune-mediated adverse drug reactions through the course of HIV/AIDS disease. Adapted from (Peter et al., 2019)

1.6.1. Normal skin immunology

Innate and adaptive immune cell populations residing in normal skin, and their protective interactions, are highlighted in Figure 1-7. The primary function of the skin is to serve as a first line immunological barrier that prevents entry of any harmful substances or microorganisms (Pasparakis et al., 2014). The skin is made up of three major layers which include the epidermis, dermis and subcutis. Keratinocytes are the main cell type residing in the epidermis, with the stratum corneum forming the outermost layer responsible for barrier function, while tight junctions between keratinocytes form in the deep granular layer, creating an impermeable layer to microbes (Coates et al., 2019). Keratinocytes express pattern recognition receptors (PRRs) that recognize pathogen- and damage associated molecular patterns (PAMPS and DAMPS respectively) and are also a source for antimicrobial peptides (AMPs) including β-defensins and cathelicidins (Nestle et al., 2009, Pivarcsi et al., 2004). Langerhans cells are the main APCs in the epidermis, and they express the receptor langerin that recognizes PAMPS, as well as CD1a and MHC-II molecules which activate T helper responses and cross-present antigens to cytotoxic CD8 T cells (Haniffa et al., 2015). Interepithelial lymphocytes, mainly memory CD8+ T cells, also reside in the epidermis, providing immunosurveillance against specific pathogens (Kupper and Fuhlbrigge, 2004).

The dermis consists of dermal dendritic cells (dDCs), macrophages, NK cells, granulocytes (i.e., mast cells), innate lymphoid cells (ILCs) and tissue resident memory (T_{RM}) T cells (CD8+/CD4+) (Nguyen and Soulika, 2019). In the steady state, they promote physiological functions in the skin. DCs are the first to encounter pathogen, and they present antigens to skin resident immune cells, activating inflammatory responses, or migrate to skin draining lymph nodes where they present antigens to naïve T cells (Kabashima et al., 2019, Kupper and Fuhlbrigge, 2004). Activation of naïve T cells result in production of antigen-specific T-cells with effector functions, which further differentiate into effector memory T cells (Sallusto et al., 1999). Mast cells contribute to allergic responses, as well as helping clear bacterial infection and promote healing through receptor-MRGPRX2 AMP-ligand activation (Chompunud Na Ayudhya et al., 2020). Other granulocytes i.e., eosinophils contribute quickly to pathogen exposure through rapid recruitment to skin in response to chemokines. Innate lymphoid cells (ILCs), which consist of IL1, IL2 and IL3 populations, have parallel functions to CD4+ T cell respond to innate signals in the absence of antigen-specific receptor expression (Panda and Colonna, 2019, Polese et al., 2020).

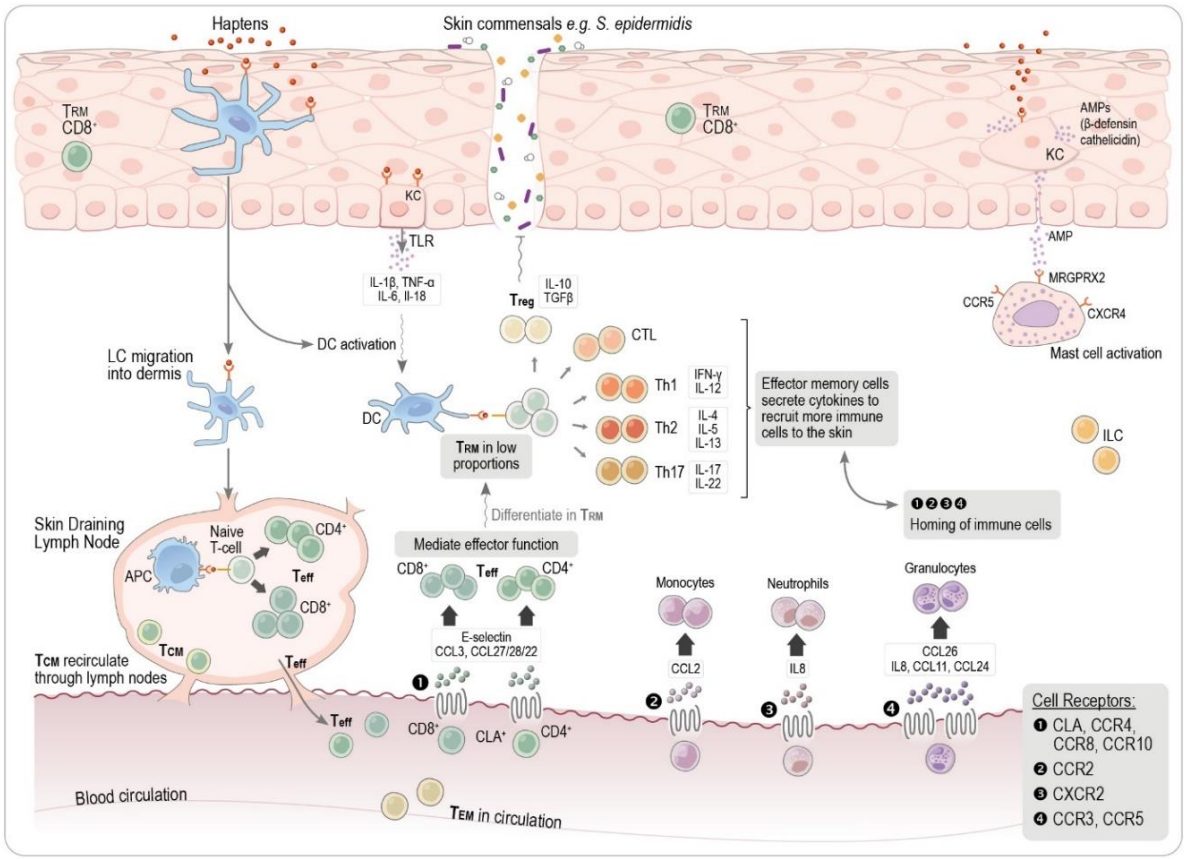

Figure 1-7: A figure showing normal cutaneous immunology. Langerhans cells and keratinocytes, and a small number of CD8+ TRM are immune cells residing in the epidermis; while dDC, mast cells, TRM (CD8+/CD4+), macrophages and ILC populate the dermis. In response to pathogen, APCs migrate into

skin draining lymph nodes, presenting antigens to naive T cells, and stimulating their clonal expansion and differentiation into Teff cells. Chemokines and cytokines secreted by resident immune cells i.e., keratinocytes, upregulate expression of endothelial adhesion molecules and skin homing receptors on circulating immune cells. 1. Lymphocyte recruitment to skin is mediated by the CLA which binds E-selectin on endothelial walls. CLA+ T cells co-express skin-homing receptors CCR4, CCR8 and CCR10 for chemokine ligands CCL3, CCL17, CCL22 and CCL27 2. Monocytes express CCR2 and migrate to skin in response to CCL2 ligand secreted by keratinocytes 3. IL8 mediates neutrophil recruitment through chemokine receptor CXCR2 4. Other granulocytes i.e., eosinophils and basophils express CCR3 and CCR8 and respond to chemokines CCL11, CCL24 and CCL26. **Abbreviations**: APC – antigen presenting cell, CLA – cutaneous lymphocyte antigen, CCL3 – chemokine ligand, CCR4 – chemokine receptor, CXCR2: C-X-C motif chemokine receptor 2, ILC – innate lymphoid cell, TRM – tissue resident memory. Adapted from Chimbetete et al. (In press: *Journal of Investigative Dermatology*, 2022).

1.6.2. HIV immune dysregulation in the skin

An increased number of cutaneous disorders occur during the course of HIV infection (Coldiron and Bergstresser, 1989, Uthayakumar et al., 1997). HIV-induced immune dysregulation in the skin is consistently thought to be the main driver of inflammatory and hypersensitivity skin disorders onset (Galhardo et al., 2004). The main cutaneous immunological changes following HIV infection are highlighted in Figure 1-8. Progressive loss of CD4+ T cells marks the hallmark of HIV infection (Okoye and Picker, 2013). The depletion of CD4+ T-cells may result in alterations of other CD4+ T cell subsets; for example, the immunosuppressive function and frequency of protective CD4+ Treg cells, as well as possible depletion of Th17 cells which contribute to epithelial barrier integrity (Okoye and Picker, 2013, Brenchley et al., 2008). Ongoing HIV viremia is associated with an expansion of HIV-specific effector CD8+ T-cells and marked immune hyperactivation characterized by excessive inflammatory cytokine levels (Peter et al., 2019, Galhardo et al., 2004). HIV-specific CD8+ T_{RM} which are retained in the skin to mediate antiviral function, have been described to play a role in mediating skin disorders such as psoriasis and allergic contact dermatitis (Clark, 2015, Gaide et al., 2015, Suarez-Farinas et al., 2011), and are thought to contribute to the onset of SCAR.

Langerhans cells and dDC are the first cells to encounter HIV at mucosal sites and are therefore the preferred targets for HIV infection (Gray et al., 2020b, Miller and Bhardwaj, 2013). DCs play a central role in viral transmission, target cell infection, and presentation of HIV antigens (Manches et al., 2014). Other innate immune cells such as macrophages, and mast cells expressing HIV receptors CCR5 and CXCR4, contribute to increased HIV viral load and

become reservoirs for latent HIV (Campbell et al., 2019, Sundstrom et al., 2007). Keratinocytes, although not directly infected with HIV, secrete inflammatory cytokines which may enhance viral replication and dissemination (Galhardo et al., 2004, Blauvelt and Katz, 1995). Put together, this HIV-driven immune dysregulation in the skin creates a crucible for exaggerated inflammation and hypersensitivity, resulting in the onset of various skin disorders. These HIV-induced cutaneous immunological changes have been well characterized systemically, however, at the level of the skin there is limited data reported in literature.

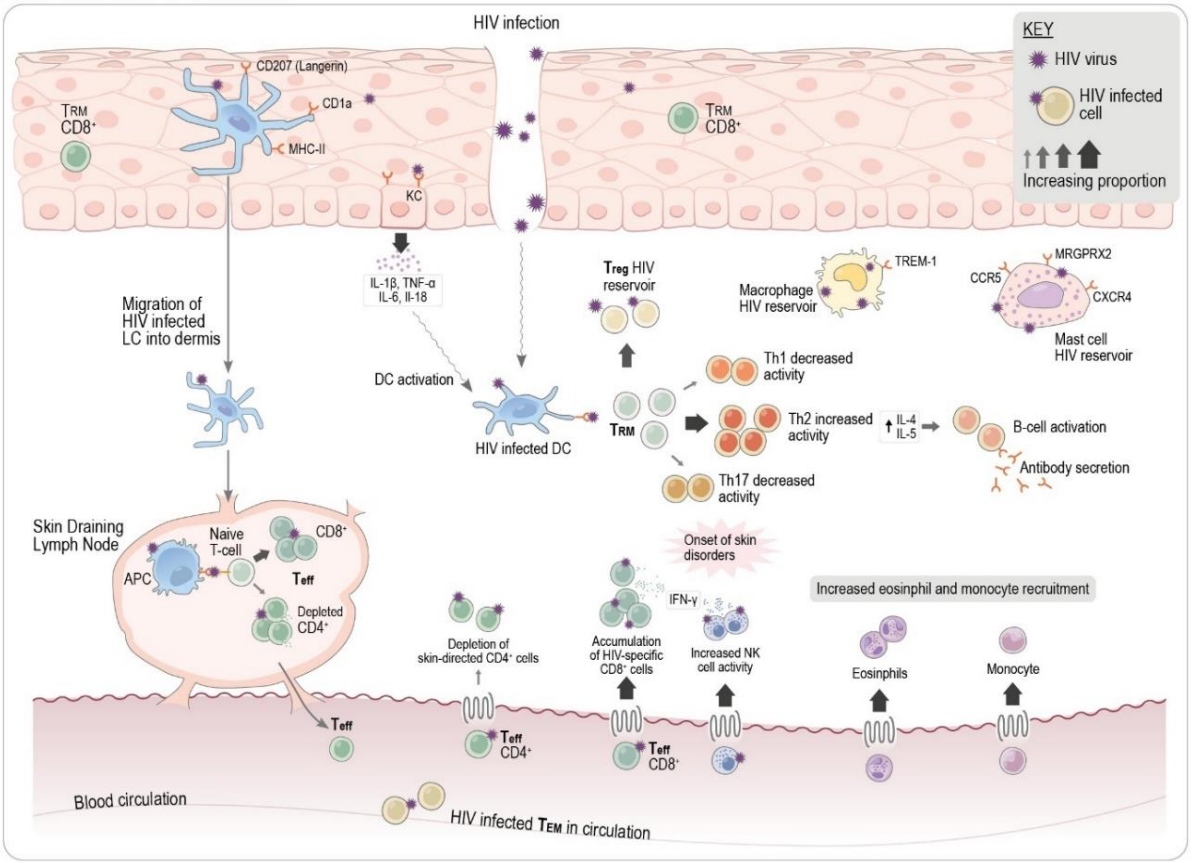

Figure 1-8: Cutaneous immune dysregulation as a result of HIV infection. HIV infection results in alteration of both innate and adaptive immune response pathways. LCs and DCs, being the first immune cells to encounter HIV, transmit it to naïve T cells in skin draining lymph nodes. CD4+ T cells in circulation and those homing to the skin are depleted and an expansion of antiviral CD8+ and NK cells follows. A shift towards a Th2 cytokine profile is observed in advanced HIV infection resulting in increased monocyte and eosinophils infiltration, as well as B cell activation. This results in a state of high immune activation and dysfunction of immunoregulatory mechanisms, leading to the onset of inflammatory and hypersensitivity skin disorders. Adapted from Chimbetete et al. (In press: *Journal of Investigative Dermatology*, 2022).

1.7. Histopathology

1.7.1. DRESS

DRESS can exhibit different morphological patterns of inflammatory skin diseases. Although no single pathological finding is specific enough to confirm diagnosis, the presence of two or more distinct patterns in a single biopsy often served as a diagnostic clue for drug reaction (Cho et al., 2017). Frequently reported histopathological findings include epidermal spongiosis, apoptotic (Civatte bodies) and necrotic keratinocytes, basal vacuolization, interface dermatitis and superficial perivascular infiltration of predominantly lymphocytes with or without eosinophils (Bellon, 2019, Orime, 2017); as highlighted in Figure 1-9. Interface dermatitis is the most common histopathological pattern in DRESS, consisting of interface inflammation (with inflammatory cells extending from the dermis traverse to the epidermal basement membrane) and/or lichenoid dermal inflammation. Interface dermatitis often leads to basal cell vacuolar degeneration accompanied by variably dense perivascular and interstitial infiltrates of lymphocytes, often resulting in exocytosis. Lichenoid dermatitis is associated with a dense band-like infiltrate in the papillary dermis comprising of lymphocytes. Apoptotic keratinocytes as a result of interface dermatitis have been shown to be closely related to liver and/or renal complications (Ortonne et al., 2015, Walsh et al., 2013, Chi et al., 2014). The assumption being that the higher the degree of apoptotic keratinocytes usually mediated by CD8 effector T-cells, is indicative of a higher degree of cytotoxicity and hence the more severe levels of tissue damage (Cho et al., 2017). A perivascular infiltration comprising of lymphocytes, eosinophils, neutrophils, and atypical lymphocytes in the dermis is also characteristic of DRESS, with the intensity of lymphocytic infiltration reported to be linked to severity of liver injury and blood eosinophilia (Goncalo et al., 2016). Epidermal spongiosis, another common feature of DRESS, which often leads to intraepidermal vesicles, has been associated with non-severe forms of DRESS as well as absence of renal complications (Skowron et al., 2015).

There are secondary morphological changes characteristic of DRESS that develop in epidermal or dermal compartments. Common epidermal morphological changes include orthokeratosis, hyperkeratosis, or parakeratosis of the stratum corneum. Additionally, there may be acanthosis of the spinous layer and dyskeratosis of the stratum granulosum (Ortonne et al., 2015). Pigmentary incontinence is often reported, which is seen as accumulation of melanin pigment in the upper dermis. This melanin is often noted as coarse granular, non-refractile brown pigment accumulations within the cytoplasm of dermal macrophages.

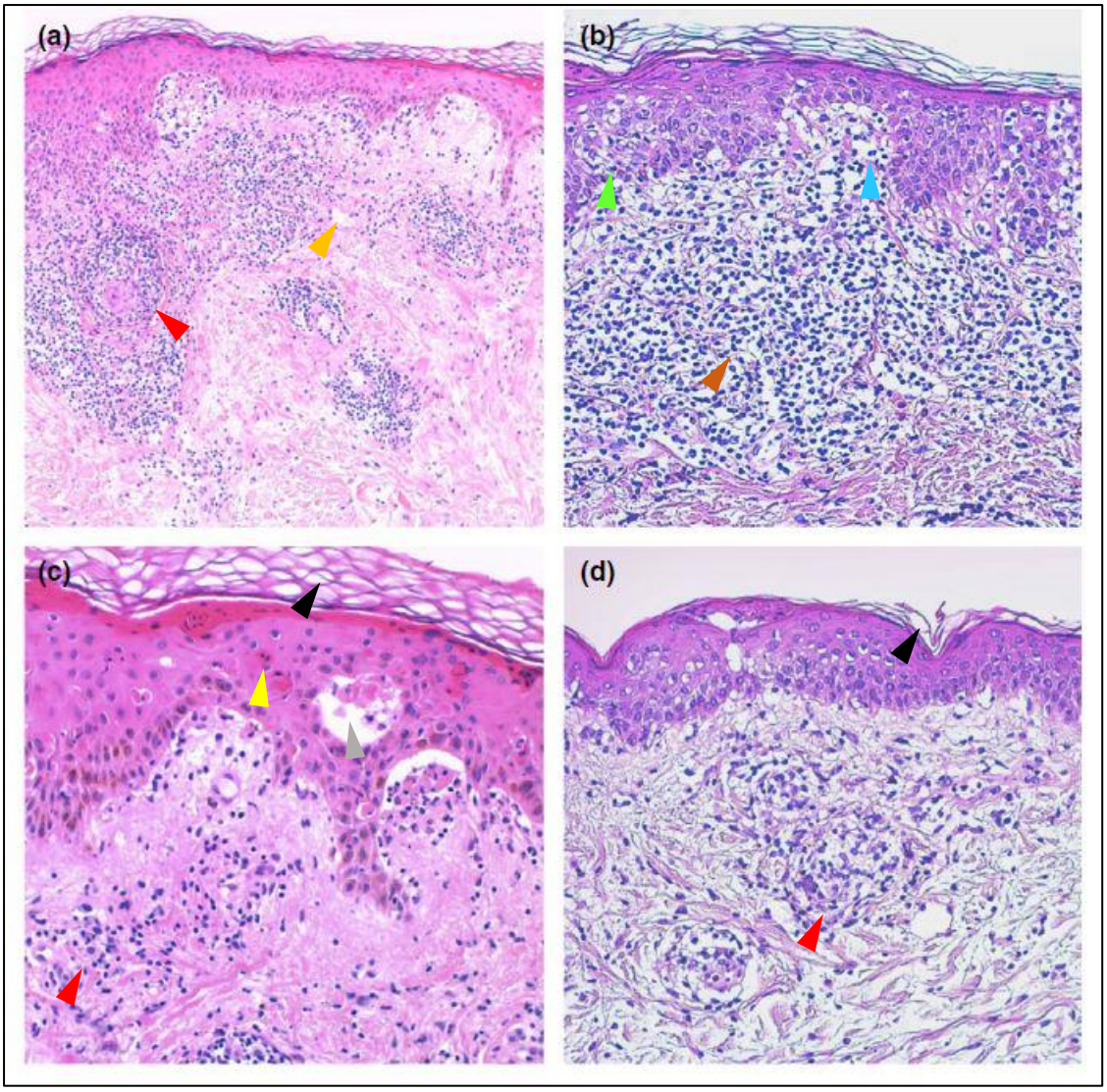

Figure 1-9: Histopathological patterns in skin lesions of DRESS syndrome. (**a**) Perivascular infiltrate (red arrowhead), dermal oedema (orange); (**b**) exocytosis (blue), spongiosis (green), lichenoid infiltrate (brown); (**c**) parakeratosis (black), perivascular infiltrate (red), necrotic keratinocytes (yellow), vacuolization of the basal layer (gray); (**d**) parakeratosis (black), perivascular infiltrate (red). Histological patterns are denoted by arrowheads. H&E stain, magnification 100x - (a); 200x - (b), (c), (d). Adapted from: (Weinborn et al., 2016)

Immunohistochemical (IHC) data in DRESS has revealed a dense dermal infiltration of activated lymphocytes and eosinophils. A case report by (Hansel et al., 2017) of a DRESS case secondary to ceftriaxone also revealed the presence of IL-5, granzyme B, perforin, fatty acid synthase ligand (FasL), tumour necrosis factor (TNF)-α and interferon (IFN)-γ, supporting the consideration of DRESS as a mixed immunological response (Chen et al., 2013). Additionally, in lesional skin of patients with severe DRESS, an increased proportion of CD8+ T cells expressing granzyme B has been observed (Kerl and Kerl, 2021, Ortonne et al., 2015).

1.7.2. SJS/TEN

SJS/TEN generally display subepidermal blisters with overlying necrosis of the epidermis. Early stages of SJS/TEN often display scattered apoptotic keratinocytes in the lower epidermis. Fully developed lesions feature a vacuolar interface dermatitis, with basal cell vacuolar degeneration, often leading to subepidermal blisters. Complete necrosis is characteristic. The accompanying perivascular lymphocytic infiltrate and exocytosis in the upper dermis are usually sparse, although increased concentrations of lymphocytes and monocytes have been observed in blister fluid at later stages of disease. (Bellon, 2019, Phillips, 2018). Eosinophils are usually rare (Kerl and Kerl, 2021).

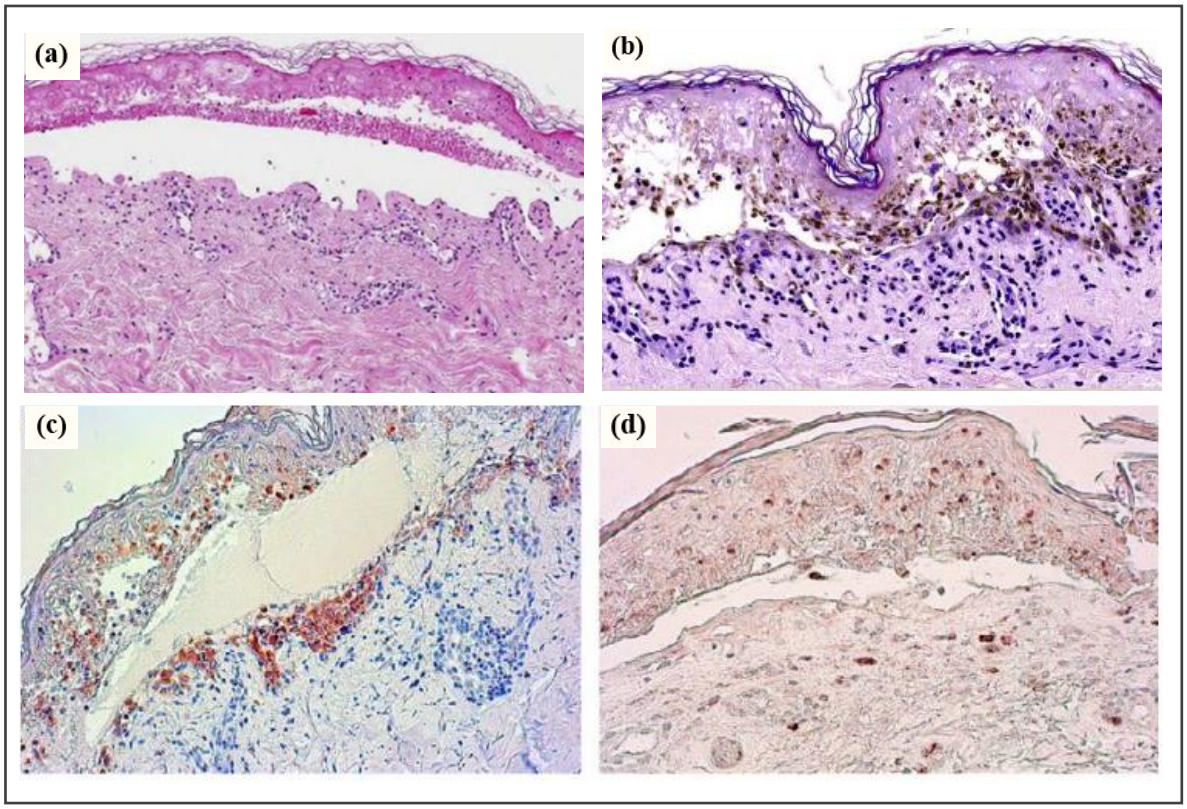

Figure 1-10: Histopathology patterns in skin lesion of Stevens-Johnson syndrome/toxic epidermal necrosis (SJS/TEN). (a) TEN. Subepidermal bulla and full thickness necrosis in the blister roof, sparse superficial lymphocytic infiltrate. (b) Splitting at the subepidermal level; a necrotic but otherwise complete epidermis forms the blister roof. Granulysin expression in TEN (c) and SJS (d). Images (a) and (b) were adapted from (Kerl and Kerl, 2021), images (c) and (d) were adapted from (Weinborn et al., 2016)

1.8. Special populations of T-cells in the skin and HIV

1.8.1. Effector memory cells in the skin – focus on tissue resident cells

Immunological memory is an essential feature of adaptive immune responses. Upon activation of naïve T cells into effector T cells by APCs, a percentage of these cells differentiate into memory T cell subsets which include effector memory T cells (TEM), central memory T cells (TCM) and TRM. Skin TRM cells are a memory T cell subset that provide immune surveillance to secondary antigen exposure. A key feature of these cells is their long term survival which can persist for months or years, and their ability to stay localized in the skin and not egress to blood as TEM do (Chen and Shen, 2020). Both CD4+ and CD8+ TRM cells have been shown to exist in the skin, although protective properties are best defined for CD8+ T cells. CD8+ TRM cells mediate immunity through immediate effector function and rapid recruitment of circulating immune cells (Steinbach et al., 2018). TRM, similar to TEM, differ from TCM cells as they have low expression of CD62L (L-selectin) or the chemokine receptor-7 (CCR7), while expression of markers of tissue residency including CD69 is increased (CD103 may also be increased), as well as the skin-homing marker cutaneous lymphocyte antigen (CLA) and chemokine receptors (CCR4/-6/-8/-10 and CXCR6) (Topham and Reilly, 2018, Chen and Shen, 2020, Schunkert et al., 2021). CD69 retains TRM cells in skin by inhibiting expression and function of the receptor sphingosine 1-phosphate receptor type 1 (S1PR1) which is vital for T cell egress from the skin. CD103 mediates TRM retention by interacting with E-Cadherin, a cell adhesion molecule. CD49a is also reported to be expressed on TRM cells, depending on the subset of TRM and peripheral tissue (Topham and Reilly, 2018). CD49a mediates retention by binding to collagen and attachment to the extracellular matrix (Chen and Shen, 2020, Steinbach et al., 2018). In human healthy skin, TRM cells are best phenotypically identified as CD3+, CD4+/ CD8+, CD45RO+CD69+CLA+CCR7-CD62^{low} and CD103+/- (Schunkert et al., 2021). Due to their long-term survival and low migratory properties, TRM cells have been implicated in several chronic inflammatory skin disease pathologies including psoriasis, vitiligo and allergic contact dermatitis (Chen and Shen, 2020). Studies of CADR such as FDE that recur in the same location after re-exposure to the offending drug, have indicated that localised skin TRM cells may be driving inflammatory responses (Trubiano et al., 2020, Shiohara and Mizukawa, 2012).

Due to availability of a wide variety of structurally unrelated drugs used to treat conditions, the need to rechallenge patients with causative drugs in the context of SCAR has reduced. However, there are cases where there may be no viable treatment options or alternative treatments are associated with higher risk. This is often seen in the case of comorbid HIV/TB-associated SCAR, whereby patients react to first-line drugs and the alternative treatment of second-line drug is less

effective and associated with poor outcomes (Peter et al., 2017, Lehloenya and Dheda, 2012). With SDC being the gold standard in identifying the offending drug, a positive reaction on rechallenge suggests the presence of drug-specific memory T cells in the skin or in circulation. Interestingly, a case report by Iriki et. al described an SJS/TEN patient with severe lymphopenia, and demonstrated the presence of CD45RO+CD69+CD4+ and CD8+ T cells in the absence of circulating leukocytes, raising the possibility that TRM cells are key mediators of these reactions (Iriki et al., 2014). Furthermore, Trubiano et al examined the role of TRM cells in the recovery phase of patients with a history DRESS or maculopapular exanthema (MPE) (Trubiano et al., 2020). They found an increased number of CD45RO+CD69+CD4+CD8+ T-cell in the skin after resolution of DRESS. Furthermore, they rechallenged the patients by applying the drug intradermally at a site of initial drug reaction. Skin biopsies sampled acutely after rechallenging and 8 weeks after resolution showed accumulation of this resident phenotype. These findings showed that T cells infiltrate and convert to the TRM phenotype following drug rechallenge, supporting the idea that skin TRM cells may contribute to drug hypersensitivity. Recent immunofluorescence work by Romar G. investigated the role of TRM cells in mediating DRESS, SJS/TEN or morbilliform drug eruption (MDE) by staining lesional skin for CD3+, CD103+, CD45RO+ and CD45RA+ T cells (Romar, 2020). They demonstrated that T-cells were more commonly CD45RO+ than CD45RA+, although a few CD103+ cells were observed. Despite these recent advances in characterising TRM, the predominant T-cell type (TCM or TRM) mediating these drug reactions remains unknown.

1.8.2. Effector memory cells in HIV

The concept of heterologous immunity, whereby a single TCR might recognize pathogens derived from more than one pathogen, is thought to contribute to the pathogenesis of T-cell mediated hypersensitivity reactions (White et al., 2015). Viral infection or reactivation, particularly herpes family viruses (HHV6, HHV7, EBV, CMV), is thought to contribute to development of drug hypersensitivity through heterologous immunity, and the proposed models are highlighted in Figure 1-11 (Pavlos et al., 2017, Picard et al., 2010, Ushigome et al., 2013). Infection with HHV (or other pathogen) results in generation of virus-specific CD4+ and CD8+ T-cell responses and development of a TRM population which persists at the site of antigen encounter in the skin. These TRM cells can cross react with drug-induced peptides presented by HLA risk allele, resulting in drug hypersensitivity. (White et al., 2015, Schunkert et al., 2021). The role HIV-specific T-cells, particularly TRM, play in mediating SCAR is unknown, although HIV-specific T-cell clones have been demonstrated to react *in vitro* against abacavir-altered peptide repertoire (Almeida et al., 2019), suggesting that HIV-specific memory T-cells may contribute to hypersensitivity reactions through heterologous immunity.

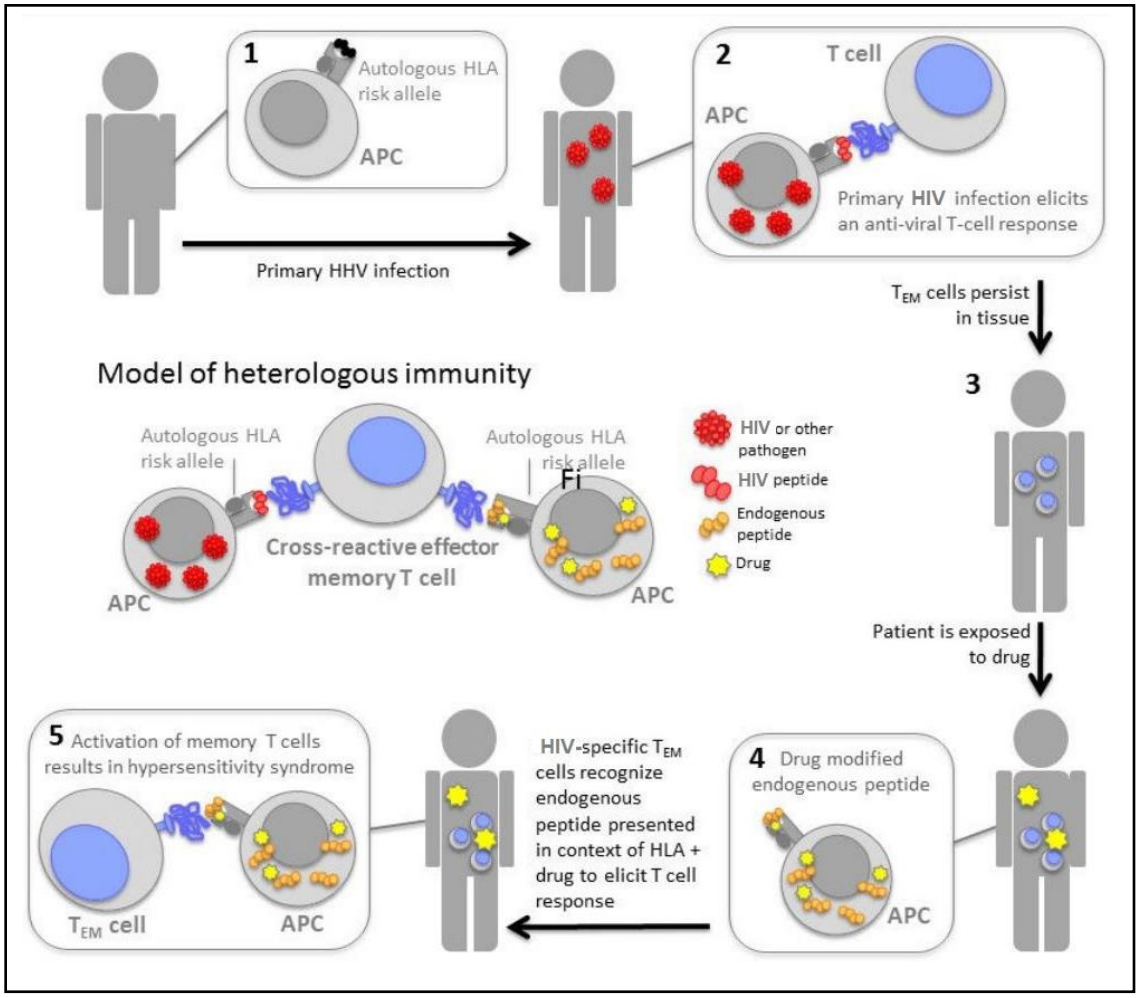

Figure 1-11: Generation of heterologous immune responses that may contribute to the pathogenesis of SCAR. The pathogenesis of SCAR can be summarized as follows: 1) HLA risk allele is a prerequisite for SCAR; however, it is not sufficient for development disease. 2) Infection with HIV (or other pathogen i.e., HHV) induces a polyclonal T cell response. 3) HIV-specific effector memory T cells are generated and persist in host. 4) Exposure to offending drug and drug-endogenous peptide-HLA epitopes are generated. 5) HIV-specific effector memory T cells cross react with drug-endogenous peptide-HLA epitopes, are activated and result in clinical symptoms of SCAR. Modified and adapted from (Pavlos et al., 2017).

1.9. Regulatory T-cells

1.9.1. Regulatory T-cells in the skin

Regulatory T cells are a subset of CD4+ T cells that play a crucial role in inducing and maintaining tissue immune homeostasis and in the termination of immune responses (de Boer et al., 2007). Two subsets of Treg cells exist, differing in terms of development, specificity, and effector mechanisms. These include naturally occurring Treg cells, which are induced in the thymus; and adaptive Treg

cells which develop from mature T cells in peripheral tissues under certain conditions of antigen-specific stimulation (de Boer et al., 2007). Tregs display a low expression of CD127 (IL-7 receptor) and a high cell surface expression CD25 (alpha chain of the IL-2 receptor), and their differentiation is regulated by the transcription factor forkhead box protein 3 (FOXP3) (Okoye and Picker, 2013). Although Tregs express CD25, the simultaneous expression of this marker on recently activated CD4 T cells has made it difficult to accurately identify these cells during immune activation (Ali and Rosenblum, 2017). There have been several reported mechanisms by which Tregs regulate the immune system. These include production of suppressor cytokines such as IL-10 and TGFβ, granzyme and perforin mediated cytolysis of effector cells, modulation of DC maturation and/or function required for effector T cell activation, and metabolic interruption through inhibition of proliferative response via IL-2 receptor (Vignali et al., 2009). Tregs in peripheral circulation have been shown to express the skin homing receptors CCR6 and CLA, enabling them to infiltrate into the skin (Ali and Rosenblum, 2017). A balance between effector cells and Tregs must always be established to maintain immune homeostasis. A dysfunction in Treg cells or abnormalities in their numbers is thought to disturb the control mechanism of immune regulation potentially leading to autoimmunity or aggravated pathogen induced inflammation.

Tregs have been shown to comprise up to ~10% of all T cells in normal human skin; and ~20% of the CD4+ T cell compartment (Rodriguez et al., 2014). Majority of these cells are localized in the epidermis and dermis near hair follicles. This brings them in close proximity to localized APCs and effector T cells. Majority of skin Tregs have also shown to exhibit an activated effector memory phenotype (CD45RO+) suggestive of previous antigen exposure (Rodriguez et al., 2014, Boothby et al., 2020). Inflammation or tissue damage in the skin allows more Treg cells to home from circulation into the skin to suppress effector cells following antigen presentation in primary lymphoid organs.

It has been reported that Tregs play a protective role against the development of SCAR. Using a transgenic mouse model that mimicked TEN, Azukizawa et al. demonstrated that transfer of CD4+CD25+ cells prevented epidermal damage; more efficiently when co-transferred with DCs (Azukizawa et al., 2005). This demonstrated that Tregs likely play a key role in the pathogenesis of TEN. Furthermore, a study by Takahashi et al. compared the number and function of peripheral blood Tregs in patients with DRESS and SJS/TEN at different time points after disease onset (Takahashi et al., 2009). They demonstrated that both peripheral blood and skin Tregs were expanded in the acute phase of DRESS, and that expansion of Treg cells occurred as the disease resolved. In TEN patients however, although Tregs were present in peripheral blood, their function and migratory capacity to skin was impaired and was later gained upon clinical improvement.

These findings may explain the delayed onset of DRESS in relation to introduction of causative drug, as well as why severe epidermal damage cannot be seen in DRESS as it is in SJS/TEN, besides activation of effector T cells (Shiohara et al., 2012, Takahashi et al., 2009). Additionally, it has been noted that Tregs eventually exhaust following resolution of DRESS, suggesting this could contribute to ongoing HHV viral replication as well as recurrence of clinical symptoms, the presence of autoantibodies and the onset of autoimmune diseases (Peter et al., 2017, Shiohara et al., 2015, Takahashi et al., 2009).

1.9.2. Regulatory T-cells in HIV

In persons living with HIV, the role of Tregs may be both beneficial and detrimental. Tregs express receptors CXCR4 and CCR5, and are therefore targets for HIV infection; human Tregs have been shown to be susceptible to HIV infection (Moreno-Fernandez et al., 2009). A number of factors have been shown to influence the frequency of Tregs detected in samples from HIV-infected patients including viral load, disease progression and antiretroviral therapy (de St Groth and Alan, 2008). Interestingly, several studies have reported that Tregs in HIV infection are partially spared, based on the observation that despite the decrease in their absolute counts in circulation, their frequency increases in acute HIV infection (Kleinman et al., 2018, de St Groth and Alan, 2008). In addition, other studies have shown that effector cells are more preferentially infected with HIV compared to Tregs in vivo (Moreno-Fernandez et al., 2009, Simonetta and Bourgeois, 2013). This sparing mechanism has not yet been fully elucidated.

Tregs have been shown to play a role in preventing the pathogenic consequences of chronic immune activation associated with ongoing HIV viral replication, by controlling the immune activation of virus producing cells, shifting them into the resting state and limiting the number of susceptible cells (Kleinman et al., 2018). However, this immunosuppression by Tregs may contribute to inefficient cell-mediated immunity in HIV infection and promote more viral replication (Moreno-Fernandez et al., 2009). Conflicting data has been published regarding the effect of HIV infection on Treg suppressive function. In vitro studies have reported HIV infection to either have no effect on Treg function (Moreno-Fernandez et al., 2009) or result in a loss of functionality (Angin et al., 2014). The different findings observed have been largely due to the different identification markers for Tregs used. The immunophenotype of Tregs in the context of HIV induced DRESS or SJS/TEN is poorly defined. There is little to no data on whether Tregs are spared in peripheral tissue such as skin in a similar manner as they are in circulation. Furthermore, it remains unclear whether Treg cell deficiency or dysfunction is causative in the induction of SCAR. Yang et al demonstrated a paucity of skin-directed CD4+ T-cells in HIV-infected TEN patients but found no difference between peripheral blood T-reg numbers amongst HIV-infected

and uninfected TEN patients (Yang et al., 2014). It must be noted that this study utilized CD25 as a marker for Treg cells, which is also upregulated in all activated T-cells abundant in TEN and thus this data may be skewed by CD25+ activated T-cells which are not Tregs.

HIV-specific effector CD8+ T cells are known to expand through disease progression (Peter et al., 2019, Jones and Walker, 2016). The loss of CD4+ T cells result in an increase in the ratio of CD8/CD4 T-cells in circulation, as well as skin (Yang et al., 2014). Furthermore, the possible depletion or dysfunction of Tregs as a result of CD4+ depletion could also drive this marked increase of effector CD8+ T-cells. In the context of SCAR, ongoing HIV viremia, as well as HIV-specific memory T-cells can result in this increased pool of virus-specific effector CD8+ T cells (White et al., 2015). This expansion of CD8+ T-cells in an aid to fight viral infection, together with the possible depletion of immunoregulatory mechanisms, further drives the pathogenesis of inflammatory and hypersensitivity skin disorders and is associated with a higher degree of cytotoxicity and increased levels of tissue damage. This project aimed to expand on the findings from Yang et al. in our cohort of FLTD-induced SCAR, using improved site-of-disease techniques, better target immune cell markers and an increased sample size, with a hypothesis that the depletion of CD4+ T cells in HIV infection may cause a possible depletion of protective Tregs in the skin and an expansion of CD8+ effector cells, contributing to SCAR in context of HIV.

1.10. Aims and objectives

Hypothesis:

Basic and advanced immune profiling of the skin in SCAR, the site of disease, is non-existent for drug-SCAR combinations in African HIV TB endemic settings. Site-of-disease study has proved to be preferable in several immune-mediated pathologies and SCAR is likely to be similar, especially in the context of HIV immune dysregulation and the known importance of skin resident innate and adaptive immune cells. **We hypothesize a role of HIV-related immune dysregulation in the skin to be important in the development of SCAR in HIV-infected populations. Immune dysregulation may cause depletion of protective T regulatory cells in the skin and increased infiltration of CD8+ or tissue resident effector cells, which will be addressed with immunohistochemistry approaches in the skin of patients.**

Overall aim:

To characterize the immune phenotype of skin from SJS/TEN and DRESS to first-line anti-tuberculosis drugs and cotrimoxazole comparing HIV-infected and uninfected patients.

Objectives:

Immunohistochemistry and immunofluorescence to enumerate differences in T-cell subsets (effector memory and regulatory T-cells) in lesional skin of SJS/TEN and DRESS:

1. comparing HIV-infected and uninfected cases
2. comparing different offending drugs, and patients reacting to single or multiple different drugs on rechallenge
3. comparing to non-lesional skin of HIV-infected and uninfected controls

2. MATERIALS AND METHODS

2.1. Ethical considerations

Ethics approval for this laboratory study was obtained from the University of Cape Town (UCT), Faculty of Health Sciences Human Research Ethics Committee (HREC), Reference number 377/2019. All participants (cases and controls) considered for this study were registered with the parent Immune-mediated Adverse Drug Reactions in African TB/HIV Endemic Settings (IMARI Africa) registry and biorepository (HREC Reference number R031/2018).

2.2. Study design and selection of participants

2.2.1. Inclusion criteria

This was a sub-study of the IMARI-Africa registry and biorepository. This registry approaches patients ages 12 and older, diagnosed with a treatment-limiting immune-mediated adverse drug reaction. The focus of this study was a subset of the parent study that met the following additional requirements:

i) Informed consent for examination of either stored or prospectively collected specimens (HREC R01/2018)
ii) Age ≥ 18 years
iii) Validated RegiSCAR phenotype of DRESS or SJS/TEN
iv) Highest drug causality score for one of the four first-line anti-tuberculosis drugs (rifampicin, isoniazid, pyrazinamide, or ethambutol) and cotrimoxazole.
v) Availability of formalin fixed paraffin embedded (FFPE) skin biopsy specimens from the National Health Laboratory Service (NHLS) collected for routine diagnostic histopathology.
vi) Skin biopsies were to have been take during the acute phase of drug reaction (1 to 20 days from the onset of clinical symptoms).
vii) Patient not on oral/intravenous corticosteroids or other immunosuppressive treatments at the time of skin biopsy.
viii) Availability of Registry or folder data for clinical records and laboratory reports.

2.2.2. Clinical and laboratory data

The following clinical and laboratory data were collected in all SCAR cases and normal skin controls in relation to the time the skin biopsy was taken including age, gender, HIV status, most recent CD4 cell count, HIV viral loads, chronological drug exposure history prior to onset of clinical symptoms, dates of start of symptoms onset of SCAR, routine histopathologic skin biopsy

report and laboratory parameters. Laboratory findings extracted included liver function tests (LFTs); alanine aminotransferase (ALT), aspartate transaminase (AST), alkaline phosphatase (ALP) and gamma-glutamyl transferase (GGT), as well as eosinophil blood counts.

2.2.3. Drug causality assessment

Drug causality assessment reports were carried out for all possible offending drugs. These included Naranjo (DRESS) or Alden (SJS/TEN) probability scores suggesting a "possible", "probable" or "definite" reaction for all possible offending drugs. For patients with a positive reaction upon SDC to a specific drug, a detail of the type of rechallenge reaction was recorded.

Adjunctive data including Enzyme-linked Immunospot assay (ELISpot), and HLA data were extracted, where possible to aid confirmation of most likely causative drug and phenotype. The ELISpot assay has been used as an *in vitro* diagnosis of offending drugs (Lehloenya et al., 2020). This assay involves stimulation of T-cells with varying suspected offending drugs or metabolites, allowing for quantification of the number of spot-forming cells that release cytokine markers (i.e., IFN-γ or IL-5) or cytolytic molecules (i.e., granzyme B or granulysin) (Lehloenya et al., 2020). Other in-vitro and ex vivo diagnostic tests used include lymphocyte transformation testing (LTT) and flow cytometry. In this study, an IFN-γ ELISpot assay was run on patient peripheral blood mononuclear cells (PBMCs) using optimized stimulating drug concentrations for rifampicin (RIF) (25µg/ml), isoniazid (INH) (50µg/ml), pyrazinamide (PZA) (50µg/ml), and ethambutol (EMB) (50µg/ml) and Cotrimoxazole (TMP/SMX = 50/250µg/ml or 500/2500µg/ml; and the cotrimoxazole metabolite 4-Nitro-Sulfamethoxazole (4-NIT-10µg/ml or 4-NIT-100µg/ml). A positive Elispot result was considered to be greater than or equal to 50 spot forming units (SFU)/million cells (Copaescu et al., 2021, Porter et al., 2021, Porter et al., 2022).

2.2.4. Sampling of skin biopsies

We compared the biopsies from FLTD-induced HIV-infected DRESS or SJS/TEN cases to two control groups:

i) HIV-uninfected DRESS or SJS/TEN cases
ii) HIV-infected and uninfected normal skin

DRESS cases were sampled from areas of maximal redness and infiltration, and SJS/TEN cases were sampled from active inflammatory areas adjacent to areas of epidermal necrosis. Where known, the site where the skin biopsy was taken is highlighted in the patient timelines. Discarded healthy skin collected from surgical procedures served as control normal skin, and a 4 mm biopsy punch was obtained at a morphologically normal site. For patients with non-invasive cancers

undergoing breast mastectomies, normal non-cancerous skin was obtained at a site away from the tumour in the case of unilateral mastectomies, or from the non-cancerous breast in the case of bilateral mastectomies.

2.2.5. Histopathological characterization

To characterize the histopathological features of DRESS and SJS/TEN, the skin biopsy pathology diagnosis was retrieved and parameters were assessed as per (Ortonne et al., 2015). These included (i) changes of the stratum corneum including hyperkeratosis, orthokeratosis or parakeratosis; (ii) changes of the spinous layers including acanthosis, spongiosis, apoptotic keratinocytes, necrotic keratinocytes, epidermal blisters or detachment; (iii) changes of the dermoepidermal junction including focal/widespread interface dermatitis with or without basal vacuolar degeneration and exocytosis; (iv) characterization of inflammatory infiltrates (lymphocytes, eosinophils, neutrophils, plasma cells); (v) dermal infiltrate including architecture (i.e., lichenoid, perivascular); (vi) dermal changes: oedema and pigmentary incontinence. The degree or extent of morphological changes or inflammatory patterns (e.g., mild/severe lymphocytic infiltrate) observed was not recorded.

2.3. Antibodies

Primary antibodies to the following cell surface and intracellular markers were used (Table 2-1). Detection was performed as per assay description (Section 2.43.) using secondary antibodies detailed in Table A-1. Where possible, monoclonal primary antibodies were used in order to prevent cross-reactivity and limit background staining associated with polyclonal antibodies (Magaki et al., 2019). With triple staining of antibodies as in the regulatory T cell assay, a combination of primary antibodies generated from different host species was used to prevent cross reactivity (i.e., rabbit anti-CD4, mouse anti-FOXP3 or rat anti-CD3).

Anti-CD3 antibody was used as the pan T cell marker which enables identification of all mature T-lymphocytes. Helper T cells and cytotoxic T cells form the two major T cell subtypes that fall under CD3+ lymphocytes (Tripodo and Pileri, 2021, Vallejo et al., 2004). To identify the helper T lymphocyte subset, anti-CD4 antibody was used as a marker. Naïve CD4+ helper T cells recognize antigens presented by MHC-II molecule on APCs and differentiate into various helper T subtypes. Regulatory T cells form a subset of CD4+ T cells, and were identified using the antibodies anti-CD3, -CD4+ and -FOXP3. To identify effector T cells, anti-CD8 antibody was used as a marker. CD8+ T-cells recognize antigens presented by MHC-I molecule and upon stimulation, mediate direct killing of antigen-presenting target cells (Tripodo and Pileri, 2021, Vallejo et al., 2004). CD4+ and CD8+ T cells can differentiate into effector memory T cells upon antigen exposure. Memory T cells were identified using the antibody anti-CD45RO.

Table 2-1: Primary antibodies

Panel	Primary antibody (clone) [a]	Supplier	Antigen Retrieval	Dilution in PBS	Incubation time	Positive control tissue
STANDARD IHC	Rabbit anti-CD3 (SP7)	Abcam	Citrate	1:150	1 hour	Tonsil
	Rabbit anti-CD4 (EPR6855)	Abcam	Tris-EDTA	1:400	1 hour	
	Rabbit anti-CD8 (Ab4055)	Abcam	Tris-EDTA	1:250	1 hour	
	Mouse anti-CD45RO (UCHL1)	Biolegend	Tris-EDTA	1:200	1 hour	
TREG ASSAY	Rat anti-CD3 (CD3-12)	Abcam	Tris-EDTA	1:250	Overnight	Appendix
	Rabbit CD4 (EPR6855)	Abcam	Tris-EDTA	1:50	Overnight	
	Mouse anti-FOXP3 (236A/E7)	Abcam	Tris-EDTA	1:50	Overnight	
CD4+/CD8+ & CD45RO+ co-expression	Rabbit anti-CD4 (EPR6855)	Abcam	Tris-EDTA	1:400	1 hour	Tonsil
	Rabbit anti-CD8 (Ab4055)	Abcam	Tris-EDTA	1:250	1 hour	
	Mouse anti-CD45RO (UCHL1)	Biolegend	Tris-EDTA	1:200	1 hour	

[a] Reactivity species human. **Abbreviations**: CD3 – cluster of differentiation 3, EDTA - ethylenediaminetetraacetic acid, FOXP3 - forkhead box P3, IHC - immunohistochemistry, Treg - regulatory T cell.

Table 2-2: Cell markers and justification for use

Cell Name	Markers	Justification
T-lymphocytes	CD3+	(Clevers et al., 1988, Vallejo et al., 2004, Mousset et al., 2019)
Helper T-cells	CD4+	(Vallejo et al., 2004, Mousset et al., 2019)
Cytotoxic T-cells	CD8+	(Vallejo et al., 2004, Mousset et al., 2019)
Memory T-cells	CD45RO+	(Mousset et al., 2019, Farber et al., 2014)
Regulatory T-cells	CD3+CD4+CD25+ FoxP3+	(Atif et al., 2020, Miyara et al., 2009, Nishimura et al., 2004)

*Make reference to antibody specification sheets.

2.4. Immunohistochemistry of FFPE skin biopsies

Immunohistochemistry (IHC) utilizes basic antibody-antigen interactions to confirm the presence and distribution of various peptides or proteins within a tissue of interest. A primary or suitable secondary antibody is labelled with a fluorescent, chromogenic, radioactive, or colloidal gold marker and binds to the antigen or primary antibody bound to the antigen in a thin tissue slice. Binding is visualized by light or fluorescence microscopy, enabling qualitative and quantitative analysis. IHC has become a routine tool in both diagnostic and research laboratories and was used in this study to determine the phenotype of T cell infiltrates.

2.4.1. Slide preparation

Freshly collected skin from surgical procedures was processed by a qualified histology technician using the Leica TP1020 Automatic Benchtop Tissue Processor. Briefly, the skin tissue was placed in suitably labelled cassettes (small, perforated baskets) and then fixed with 10% formalin for 24 hours at room temperature. The tissue was then dehydrated in graded ethanol (70% (15min), 2x 90% (15min each) and 3x 100% (15min, 30min and 45min each, respectively) ethanol) to remove most of the water. The tissue was then cleared through 3 changes of xylene for 20 minutes each. Thereafter, the tissue was immersed in 3 changes of paraffin wax for 30 minutes, at 60°C. The tissue cassettes were then transferred to a tissue embedding station, placed on top of a mold. Molten wax was then added, completely covering the tissue cassette in the mold, and the mold was placed on a cold plate to solidify, forming a tissue wax block. Thereafter, the cassette was removed from the mold, and the wax block was ready for microtomy. For SCAR cases, an already processed FFPE tissue block for each case was retrieved from the National Health Laboratory Service (NHLS) archives. Sections of 10µm thickness were cut from the wax embedded blocks using a microtome, floated on a warm water bath (42°C), and picked up onto an aminopropyltriethoxysilane (APES) coated slide. The slides were incubated at 56 degrees Celsius overnight and dewaxed by three changes in 100% xylene for 1 minutes with 10 seconds of agitation. The slides were rehydrated in graded ethanol (3x 100%, 2x 90% and 1x 70%) for 1 min each and were washed in water. For standard histology (H&E), slides were stained with haematoxylin solution for 8 mins, rinsed in running tap water for 5 mins and then stained with eosin solution for 3 minutes. To stain specifically for eosinophils, slides were stained in Sirius red stain for 2 hrs instead of eosin stain (*cells were not quantified). Thereafter, the slides were then dehydrated in graded ethanol and xylene and mounted with Entellan mounting media.

2.4.2. Antigen retrieval for immunohistochemistry

For immunohistochemistry, after rehydration, the slides were treated with 1% hydrogen peroxide (H_2O_2) in water solution for 15mins to block endogenous peroxidase activity. After, slides were washed well in water. Due to fixation of tissue blocks with formalin and substitution of water with paraffin, this results in formation of cross-linking of proteins that mask epitopes of interest (Bogen et al., 2009, Scalia et al., 2017). Antigen retrieval was performed prior to performing immunohistochemistry staining with antibodies of interest. Heat-induced antigen (HIER) and proteolytic-induced antigen retrieval (PIER) are the most popular antigen retrieval methods for FFPE tissue. However, HIER has become the most common antigen retrieval method, often recommended by most antibody manufacturing companies (Kim et al., 2016). Furthermore, HIER using a pressure cooker has been reported to give optimal staining results compared to other retrieval methods (i.e., microwave-HIER or PIER) (Pileri et al., 1997). As per antibody manufacturer recommendations for all antibodies used, HIER retrieval was applied on these FFPE slides. After rehydrating and blocking endogenous peroxidase, slides were pressure cooked in either citrate buffer (1.92g Citric acid (anhydrous), 1L d.H_2O, pH 6) or Tris-EDTA buffer (1.21g Tris, 0.37g EDTA, 1L dH2O, pH 9) as per antibody specification, for 2 minutes at full pressure. Slides were then immediately placed in water.

2.4.3. Immunostaining

i) Basic Immunohistochemistry

After antigen retrieval, slides were rinsed with phosphate buffer saline (PBS) 1X (8g NaCL, 0.2g KCl, 1.44g $Na_2HPO_42H_2O$, 0.24g KH_2PO_4, 1L d.H_2O pH 7.4) to prevent them from drying. Non-specific binding was blocked by treating slides with 1% Bovine Serum Albumin (BSA) in PBS for 1 hour. The excess serum was drained off the slide and sections were incubated with 200 µL of the primary antibodies at room temperature at optimized dilutions and times as specified in Table 2-1 above. The slides were washed well with PBS-tween (PBST) 1X (8g NaCL, 0.2g KCl, 1.44g $Na_2HPO_42H_2O$, 0.24g KH_2PO_4, 500µl Tween-20 1L d.H_2O pH 7.4) and the sections were incubated with 100ul DAKO envision labelled Polymer, HRP Rabbit (DAKO #K4003) or Mouse (DAKO #K4001) for 30 minutes at room temperature. Sections were then washed well with PBS. Positive staining of sections was obtained by applying 100ul chromogenic substrate 3.3. diaminobenzidine (DAB) (DAKO K3468) or Vector VIP substrate HRP (SK-4600) for 5-10 minutes and slides were washed with running tap water. To enhance the positive staining, slides were immersed in a 1% copper sulphate (CuSO4) solution in d.H_2O for 5 minutes and slides were washed in running tap water. Slides were counterstained in haematoxylin for 8 minutes, washed in running tap water for

5 minutes and blued in Scott's tap water for 3 minutes. Slides were then washed in water, dehydrated in graded ethanol, cleared with xylene, and mounted with Entellan mounting medium. For every case stained, positive control tissue was also stained (tonsil or appendix), as well as a negative control for each antibody (primary antibody replaced by PBS buffer).

ii) TREG assay

Slides were incubated overnight at 4 ̊C with 200 µL of a primary antibody cocktail of CD3, CD4 and FOXP3 at an optimized concentration as shown in Table 2-1. The slides were washed well with PBST, and the sections were incubated with 200ul of a cocktail of secondary antibodies (Donkey anti-rat A488, donkey anti-mouse A647 and Donkey anti-rabbit Cy3) for 1 hour at room temperature in the dark. Slides were washed well with PBST. To acquire a total cell count, the slides were stained for 10 minutes with 4′,6-diamidino-2-phenylindole (DAPI) (2µl DAPI stock in 10 mL 1X PBS for working solution), a fluorescent stain which binds strongly to adenine-thymine regions of deoxyribonucleic acid (DNA) allowing visualization of cell nuclei (Tarnowski et al., 1991). Slides were washed well with PBST and were incubated with 0.1% Sudan Black B in 70% ethanol for 10 minutes to reduce autofluorescence background. Slides were washed well with PBST and immediately immersed in d.H_2O. Slides were then air dried, mounted with fluorescent aqueous mounting medium, and left overnight at room temperature to allow medium to set.

iii) CD4+/CD8+ and CD45RO+ co-expression

As described above, slides were incubated overnight at 4 ̊C with 200 µL of a primary antibody cocktail of CD4/CD8, and CD45RO at their optimized concentration. The slides were washed well with PBST and were incubated with 200ul of a cocktail of secondary antibodies (Donkey anti-rabbit Cy3 and donkey anti-mouse A647) for 1 hour at room temperature in the dark. Slides were washed well with PBST. Slides were then stained with DAPI for 10 minutes. Thereafter, slides were washed with PBST and were incubated with 0.1% Sudan Black B in 70% ethanol for 10 minutes, washed well with PBST and immediately immersed in d.H_2O. Slides were then air dried, mounted with fluorescent aqueous mounting medium, and left overnight at room temperature to allow medium to set.

Confocal microscopy

Visualization of stained slides was done at the Confocal & Light Microscope Imaging Facility at the Institute of Infectious Disease & Molecular Medicine at UCT. Stained sections were visualized with a Zeiss LSM880 confocal scanning microscope using a 488nm (Green Emission), 561nm (Red Emission) and 633nm (Far Red Emission) laser as well as a DAPI laser (405nm). Training and

oversight on the confocal microscope was assisted by A/Prof Dirk Lang, an internationally recognized expert in advanced light microscopy imaging.

2.5. Quantification methods

Table 2-2 shows the different methods that have been used in the published literature to quantify lymphocytes in immunohistochemistry and immunofluorescence antibody staining skin tissue. The two most common methods for standard immunohistochemistry include visual semi-quantitative analysis scoring systems or a quantitative analysis counting positive cells per high powered field.

Table 2-3: Quantification methods of lymphocytes in IHC and confocal microscopy

Assay	Quantification		Target cell markers [a] (Tissue)	Reference
	Number of fields counted/magnification	Expression of cells		
Basic IHC	Whole section/x20	% CD3+ cells.	**CD3+**, **CD4+**, **FOXP3**+, GITR+, CD25+ (Skin)	(de Boer et al., 2007)
	3 fields/ x40	Positive cells normalized to CD3+ cells present.	**CD3+, CD8+, CD4+**, CD25+ (Skin)	(Yang et al., 2014)
	5 fields/ x40	Positive cells per high power field.	**CD3+, CD4+, CD8+, CD45RO+, FOXP3+** (Skin)	(Galhardo et al., 2004) (Morito et al., 2014)
	Whole sections/ x40	Semi-quantitative (scoring system).	**CD3+, CD8+, CD4+, FOXP3+** (Skin, tonsil)	(Ortonne et al., 2015, Galhardo et al., 2004, Signh et al., 2018)
Confocal microscopy	≥4 fields/ x60 (Oil objective)	Positive cells/mm^2	**CD3+CD4+**CCR5+, **CD8+α**CD8+βPerforin+ (Skin)	(Gray et al., 2020a, Zhu et al., 2013)

[a] Cell surface markers that have been stained for and quantified using the stipulated method. Antibody markers used in this study are in **bold**.

2.6. Quantification

i) Basic IHC

Imaging was performed using the ZEISS Primo Star Light Microscope (Zeiss, Germany). Standard immunohistochemistry staining was quantified using the approach as described by (Yang et al., 2014). This group are the only ones reported in literature to have immunophenotyped the skin in SCAR, and thus we chose this method of quantification in order to have a refence point to compare our results. Briefly, for each antibody staining, a centre section of biopsy specimen was stained for

CD3 as a marker for lymphocytes. Adjacent sections were stained for CD4, CD8 or CD45RO antibodies. An area of high density CD3+ staining was identified at low-power magnification (10X) on the section for both epidermal and dermal compartments and captured. The selected area of high-density staining was retraced at high-power magnification (40X) in the corresponding set of adjacent CD4+, CD8+ or CD45RO+ staining, and images were captured. The total number of positive cells in interrelated images, normalized to CD3+ cells present were manually counted and averaged over 3 high-powered successive fields. Epidermal and dermal compartments were considered as two separate events, and cells appearing at the dermoepidermal junction were considered to be in the epidermis (Yang et al., 2014).

Confocal imaging

ii) Treg Assay

Visualization of positive cells was performed using the Zeiss LSM880 Confocal Scanning Microscope (Zeiss, Germany) and imaging and analysis using the Carl Zeiss ZEN 2.3 SP1 imaging software. There is no study in literature that has quantified Tregs in the skin using fluorescence microscopy. Due to the relatively low numbers of Tregs in the skin, and lack of any published data on quantifying skin Tregs, a quantification approach used by Gray et al was used (Gray et al., 2020a). Briefly, for each section, tilescan images (stitched panels) spanning the tissue to include the epidermis and dermis were captured at 60X magnification (Figure 2-1B). As the majority of Tregs infiltrated the superficial to mid dermis, we set our tilescans to include at least three X60 images spanning the dermis, and *n* X60 images depending on the thickness of the epidermis. A minimum of 4 tilescans spanning along the skin were captured for each section, depending on size of the specimen. Using the Carl Zeiss ZEN 3.1 (ZEN lite) software, CD3+CD4+FOXP3+ positive cells in both compartments were identified and manually marked using the "points" option. Positive cells were further analysed to truly confirm colocalization. Finally, the number of dermal or epidermal CD3+CD4+FOXP3+ cells in each capture tilescan image was divided by the area of each respective compartment to calculate density (cells/mm^2). This density of positive cells was averaged over the total number of images quantified for each section.

iii) CD4+/CD8+ and CD45RO co-expression

Images of positive cells were captured at 60X magnification spanning the epidermis and dermis of the skin. Cells counts were quantified over 4 successive 60X high power fields as shown in Figure 2-1A for both dermal and epidermal compartments. CD4+ or CD8+ cells co-expressing the memory marker CD45RO+ were expressed as a percentage of CD4+ or CD8+ cells present.

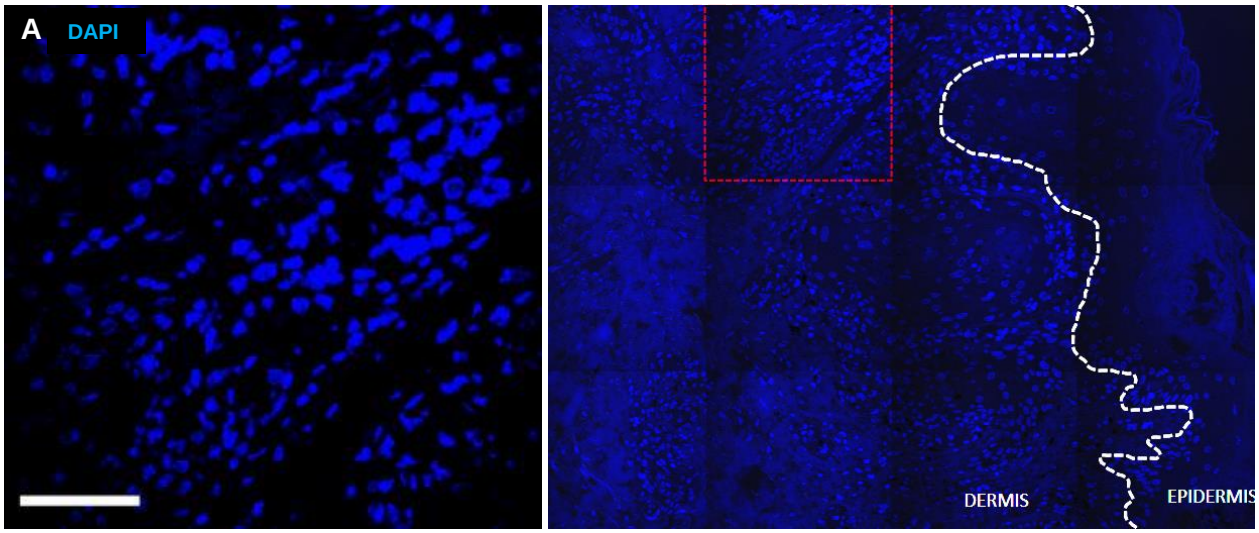

Figure 2-1: Confocal microscopy image of the skin. **(A)** An image captured using the 60x oil objective lens. (B) A tilescan image consisting of panels stitched together to form a single image (B). At least four tilescan images spanning the length of section were captured. Positive cells in each compartment were divided by the total area to obtain the density of cells/mm^2. Mean density was obtained over the total number of tilescan images captured. Blue staining denotes cell nuclear staining. Dashed white line denotes the dermoepidermal junction. Scale bar = 50μm.

2.7. Statistical analysis

Statistical analysis was performed using R Studio version 4.0.5 and SPPS Statistics 27. A comparison between the common pathological diagnoses of HIV-infected versus uninfected DRESS or SJS/TEN was performed using the Freeman-Halton extension of the Fisher's exact probability test; P-values < 0.05 was considered statistically significant. The Wilcoxon rank sum test was used to assess for significant differences in cell counts and ratios between case and control groups. Results were described as median (interquartile range) and were considered significant if P-values < 0.05. Linear regression analysis was used to assess any correlation between the density of dermal CD4+ or Treg cells and clinical or demographic characteristics. Standardized coefficients were used to signify relationships between variables and P-values < 0.005 were considered statistically significant, using a Bonferroni correction. Multivariate linear regression was used to assess any correlation between the density of Tregs and clinical characteristics; P-values < 0.05 were considered statistically significant.

3. RESULTS

3.1. Clinical description of included cases and controls.

A patient disease progression timeline was generated for all SCAR cases (e.g., Figure 3-2), to better understand the types of reactions observed, all the drugs the patients were exposed to during the course of sickness, as well as a full detailed summary of all the necessary laboratory data before and after onset of symptoms. SCAR phenotypes were validated by two expert dermatologists as DRESS (possible, probable, definite) using the RegiSCAR scoring system for DRESS (Table 3-5) (Kardaun et al., 2007, Kardaun et al., 2014), or SJS/TEN (possible, probable, definite) based on the international SCAR-group consensus (Table 3-6) (Bastuji-Garin et al., 1993, Rzany et al., 1999).

3.1.1. HIV-infected SCAR cases

HIV-infected SCAR cases consisted of 15 DRESS and 6 SJS/TEN patients. A summary of their clinical and laboratory data is provided in Table 3-1. DRESS cases consisted of 8 definite, 4 probable cases and 3 possible cases, with 10 of the cases having pulmonary TB, 4 disseminated TB and 1 with no active TB. SJS/TEN cases on the other hand consisted of 3 definite, 2 probable and 1 possible case, with 2 cases having pulmonary TB, 1 disseminated TB, and 3 with no active TB. The median age (IQR) for DRESS and SJS/TEN cases was 39 (30-45); and 40 (33-47) years, respectively. DRESS cases consisted of a median CD4 count of 137 (66-246) cells/mm^3 with 53% of the cases on ART, and SJS/TEN cases had a median CD4 count of 86 (55-116) cells/mm^3 with 67% of the cases on ART.

The median number of days between the onset of skin symptoms to sampling was 9 (5-18) days for DRESS cases and 6 (4-10) days for SJS/TEN. Most DRESS cases revealed a diffuse erythematous (12/15) as well as exanthematous eruption (6/15). Other common clinical features in DRESS cases included peeling (desquamation) and facial oedema. Six out of 15 cases were reported to have lesions in at least 1 mucosal area, predominantly oral mucosa (Table 3-3). The liver was the main extracutaneous organ involved. Nine out of 15 DRESS cases presented with liver involvement, manifesting as elevated liver enzymes**.** The median eosinophil count for DRESS cases was 0.57 (0.2-1.35) $x10^9$/L, with 60% of the cases presenting with elevated eosinophilia (>0.40 x 10^9/L). Five out of 6 SJS/TEN cases presented with epidermal necrosis and some degree of stripping (skin detachment). Other common clinical features in SJS/TEN cases included erythema, macules, and mucosal involvement. Two out of 6 cases presented with liver involvement.

Table 3-1: Summary of clinical and laboratory data for HIV-infected and uninfected SCAR

VARIABLES	DRESS (N=20)			SJS/TEN (N=7)	
	HIV-infected (n=15)	HIV-uninfected (n=5)	p-value	HIV-infected (n=6)	HIV-uninfected (n=1)
AGE IN YEARS, MEDIAN (IQR†)	39 (30-45)	46 (15-52)	0.72	40 (33-47)	33
FEMALE, N (%)	11/15 (73)	3/5 (60)	-	4/6 (67)	1/1 (100)
MALE, N (%)	4/15 (27)	2/5 (40)	-	2/6 (33)	0
CD4 CELL COUNT, MEDIAN (IQR†)	137 (66-246)	-	-	86 (55-115.5)	-
ON ANTIRETROVIRAL THERAPY AT TIME OF SCAR, N (%)	8/15 (53)	-	-	4/6 (67)	-
VALIDATED PHENOTYPE: DEFINITE, N (%)	8/15 (53)	3/5 (60)	-	3/6 (50)	0
PROBABLE, N (%)	4/15 (33)	2/5 (40)	-	2/6 (33)	1/1 (100)
POSSIBLE, N (%)	3/15	0	-	1/6 (17)	0
TYPE OF TUBERCULOSIS: PULMONARY, N (%)	10/15 (67)	1/5 (17)	-	2/6 (33)	1 (100)
DISSEMINATED, N (%)	4/15 (27)	0	-	1/6 (17)	0
NO ACTIVE TB, N (%)	1/15 (7)	4/5 (83)	-	3/6 (50)	0
DAYS FROM SYMPTOMS ONSET TO BIOPSY, MEDIAN (IQR†)	9 (5-18)	6 (3 - 8)	0.20	6 (4.3-10)	4
PERCENTAGE BODY SURFACE AREA (BSA) SKIN RASH	65 (57.5 – 77.5)	40 (40 – 40)	0.28	55 (35 - 75)	18
LIVER FUNCTION TESTS: (REFERENCE VALUES)					
AST (15-40 U/L)	63 (56-127.5)	197 (83-239)	0.19	69.5 (42.75-92.5)	234
ALP (10-40 U/L)	110 (81.5-220.5)	281 (105-430)	0.16	147.5 (88.5-208)	59
ALT (53-128 U/L)	56 (35-137.5)	159 (94-220)	0.09	52 (32-188.2)	661
GGT (<68 U/L)	134 (84.5-171.5)	139 (131-602)	0.39	137.5 (46.25-340.50)	50
EOSINOPHIL COUNT (0.0-0.4 X10^9/L)	0.57 (0.2-1.35)	1.36 (1.36-2.55)	0.09	0.42 (0.203-0.53)	0.04

Abbreviations: AST – Aspartate transaminase, ALT – Alanine transaminase, ALP – Alkaline phosphatase, GGT - Gamma-glutamyl transferase. † Interquartile range.

3.1.2. HIV-uninfected SCAR cases

The HIV-uninfected SCAR cases consisted of 5 DRESS and 1 SJS patient. A summary of their clinical and laboratory data is summarized in Table 3-1. DRESS cases consisted of 3 definite and 2 probable cases, with 1 case with pulmonary TB and 4 cases with no active TB. There was only 1 SJS/TEN case (probable), and the only one with active pulmonary TB. The median age for DRESS cases was 46 (15-52) years. The median number of days between the onset of skin symptoms to and when the biopsies were taken was 6 (3-8) days. Four out of 6 DRESS cases presented with at least one or more elevated liver enzymes, similarly with the one SJS/TEN case. The median eosinophil count for DRESS cases was 1.36 (1.36 - 2.55) $x10^9$/L, with all cases presenting with elevated eosinophilia (> 0.40 x 10^9/L).

3.1.2.1. HIV-infected versus uninfected DRESS cases

There were no statistically significant differences observed in the laboratory and clinical data between HIV-infected and uninfected DRESS cases. This includes the body surface area rash, number of days from symptoms onset to sampling, and the LFTs and eosinophils counts. There was no comparison done between HIV-infected and uninfected SJS/TEN cases due to the small sample size.

3.1.3. HIV-infected and uninfected normal skin

Table 3-2 shows a summary of the HIV-infected and uninfected participants with normal skin. Majority of breast cancer patients had a bilateral breast mastectomy procedure done, and normal skin was obtained from the non-cancerous breast. Where a unilateral breast mastectomy/reduction was done, normal tissue was obtained at a site away from the cancer tissue. The HIV-infected controls consisted of 3 females with a median age of 39 (37-41). The median CD4 count was 511 (509-512) and all participants had no active TB. The median (IQR) eosinophil count was 0.075 (0.057-0.09) $x10^9$/L cells. The HIV-uninfected controls consisted of 3 females with a median age of 52 (44-68) years. All participants had no active TB, and their median (IQR) eosinophil count was 0.03 (0.025-0.095) $x10^9$/L cells.

Table 3-2: Summary of clinical and laboratory data for HIV-infected and uninfected normal skin controls

Control	Age/Sex	HIV status	CD4 count (cells/ µl)/	Eosinophil count ($x10^9$/L cells)	Reason and type of surgical procedure
1	43/Female	Positive	508	0.11	Breast carcinoma, bilateral mastectomy
2	35/Female	Positive	513	0.04	Breast reduction
3[a]	39/Female	Positive	Unknown	Unknown	Fibroadenoma, unilateral breast reduction
4	83/Female	Negative	-	0.16	Breast carcinoma, bilateral mastectomy
5	36/Female	Negative	-	0.03	Breast carcinoma, bilateral mastectomy
6	52/Female	Negative	-	0.02	Excess stomach skin used for breast reconstruction

[a]CD4 and eosinophil counts data could not be retrieved for this patient.

3.2. Drug causality assessment: Naranjo or Alden scoring and adjunctive HLA & ELISpot data.

For all HIV-infected and uninfected SCAR cases, Naranjo or Alden drug causality assessment scores were calculated as applicable, and drugs were assessed as 'definite' or 'probable' offending drugs. The highest Naranjo or Alden scored offending drugs for HIV-infected cases are summarized in Table 3-3. Rifampicin, pyrazinamide and cotrimoxazole were the most frequently Naranjo or Alden defined definite or probable offending drugs. Upon SDC of all HIV-infected DRESS cases, 10 cases were clinically reacting to a single drug, 3 cases had a true positive reaction to two or more drugs and were classified as multiple reactors, and 2 cases were neither rechallenged nor did they have a positive ELISpot result and were classified as undetermined. Similarly, in HIV-infected SJS/TEN cases, 2 were clinically reacting to a single drug,1 case reacting to multiple drugs, and 3 cases were undetermined. Three HIV-infected cases, 2 DRESS and 1 SJS/TEN, that were on rifafour FDC and cotrimoxazole on baseline, tolerated and were discharged rifafour but were not rechallenged to cotrimoxazole were classified as single reactors on the basis of having a positive ELISpot result to cotrimoxazole. Table 3-4 also summarizes the drug causality assessment for HIV-uninfected SCAR cases. 3 DRESS cases were clinically reacting to a single drug, while 2 cases had a true positive reaction to two or more drugs. The only SJS/TEN case had a true positive reaction to two or more drugs. Out of all HIV-infected and uninfected DRESS and SJS/TEN patients in the

study, only two cases (patients 45 and 103) were on immunosuppressant treatment (both on prednisone) at the time of skin biopsy. Majority of patients were put on immunosuppressant treatment after withdrawal of offending drug.

In addition to Naranjo or Alden scoring the suspected offending drug, IFN-γ ELISpot assay results on peripheral blood mononuclear cells (PBMCS) of reactive patients sampled at baseline, pre- or post-oral drug rechallenge were used to further identify the culprit drug (Figure 3-1). This data proved to be very useful more especially in patients that could not be rechallenged for different reasons i.e., in the event of death, therefore making identification of culprit drugs even more difficult. Seven out of 21 HIV-infected SCAR cases had at least one matched positive ELISpot and positive drug rechallenge, confirming the suspected drug. In majority of the cases where there was a positive drug rechallenge reaction and a drug was Naranjo/Alden scored as the most probable culprit; a positive ELISpot result was recorded although not reaching the 50 SFU/million cells threshold.

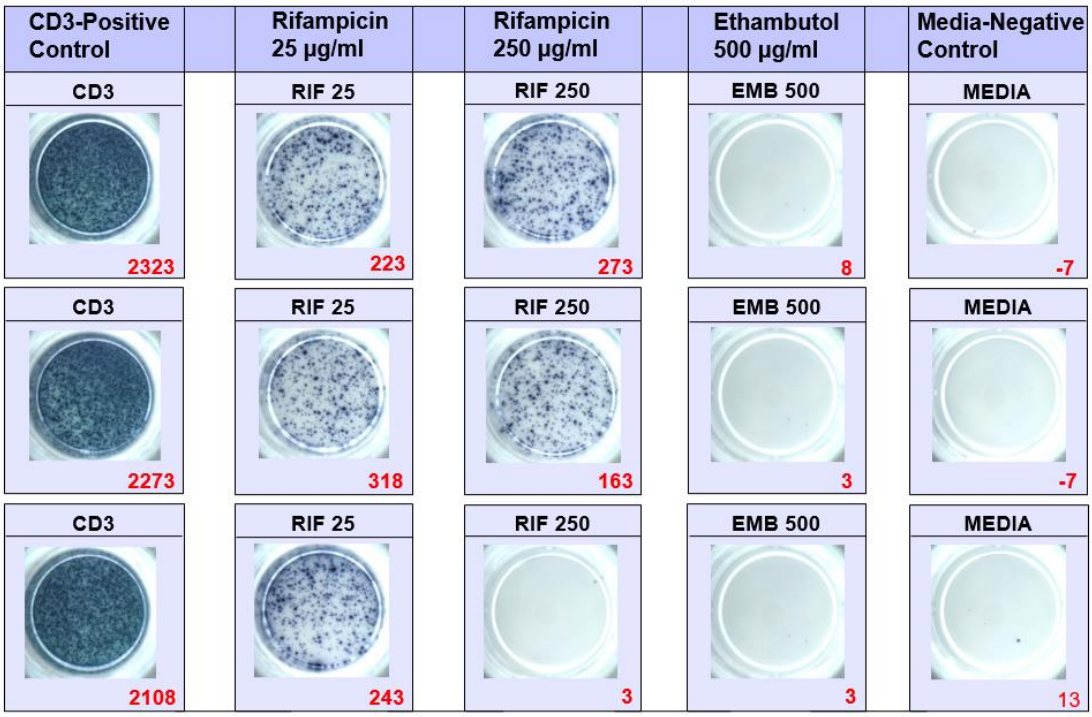

Figure 3-1: Interferon-gamma ELISpot assay result on patient 24 peripheral blood mononuclear cells. Patient 24 had a positive reaction to rifampicin on SDC and an ELISpot assay was run on 6-month follow-up PBMCs. IFN-γ responses were averaged over triplicates and positive results were given as ≥50SFU/million cells after subtracting of non-specific background staining (media-negative control) (Porter et al., 2022). Results were positive for rifampicin at concentrations 25µg/ml (261 SFU/million cells) and 250µg/ml (146 SFU/million cells). See patient timeline in Figure A-2.

Table 3-3: Description of type of reactions, laboratory findings and adjunct ELISpot and HLA data for HIV-infected SCAR patients

Patient	Age/ Sex	CD4 count/ ART (Y/N) [a]	Viral load copies/mL	Validated phenotype (RegiSCAR score)	Biopsy day [b]	Reaction characteristics at baseline and after drug rechallenge (timing) [c]	Highest Drug Causality Score [d]	Discharge regimen	Single or Multiple	Liver function tests and eosinophils	Elispot SFU [e]	HLA genotype
15	26/F	66/Y	59148	Probable DRESS (**5**)	8	**Baseline: RHZE –** 30% BSA skin rash, exanthema, pain over affected area, with liver involvement. **Rechallenge: INH (2 days) –** headache, abdominal pain, vomiting blood, elevated AST & ALT, hypotenuse, temperature 38°C. NOT STOPPED †**MXF & ETA reaction**: abdominal pain, temperature spike, tender palms	PZA (4), EMB (4), Cotrimoxazole (4), INH (3)	RIF, INH, TRD	Multiple¶	ALT (238), AST (304), ALP (173), GGT (156), Eosinophils (0.5)	INH: 130 EMB: 62 TMP/SMX§: 0	A 68:27:01G + 74:01:01G B 07:05:01G + 35:01:01G C 04:01:01G + 07:02:01G
31	22/F	384/Y	LDL	Definite DRESS (**6**)	5	**Baseline: Tribuss, Trivuda, INH –** 60% BSA skin rash involving the eyes, lip, and oral mucosa, exanthema, erythema, burning, nausea, muscle pain, sore throat, facial oedema (*Not rechallenged*)	INH (4), NVP (4) ‡	TDF, FTC, EFV (ART FDC)	Undetermined	ALT (227), AST (84), ALP (268), GGT (708), Eosinophils (0.57)	INH: 0	A 26:01:01G + 33:03:07G B 44:03:01G + 44:03:02G 02:10:01G + 07:01:01G
38	30/F	48/Y	17778	Definite DRESS (**7**)	5	**Baseline: RHZE, Cotrimoxazole –** 80% BSA skin rash, exanthema, peeling (desquamation), and erythema, with liver involvement, facial oedema	Cotrimoxazole (4) ‡	RIF, INH, EMB, PZA	Single¶	ALT (237), AST (136), ALP (81), GGT (78), Eosinophils (1.52)	TMP/SMX§: 5	A 23:01:01G + 68:02:01G B 15:03:01G + 53:01:01G C 0:10:01G + 04:01:01G
41	45/M	39/Y	93907	Definite DRESS (**6**)	11	**Baseline: RHZE –** 80% BSA skin rash, erythema, itching, facial oedema, liver involvement **Rechallenge: PZA (within 24hrs) –** itching, visible rash, fever, exanthema, erythema	PZA (6)	RIF, INH, EMB	Single¶	ALT (75), AST (137), ALP (120), GGT (140), Eosinophils (7.44)	PZA: 13 INH: 40	A 24:02:01G + 34:02:01G B 07:02:01G + 08:01:01G C 07:01:01G + 07:02:01G
46	38/F	87/N	LDL	Possible DRESS (**2**)	23	**Baseline: RHZE –** 75% BSA skin rash involving oral and genital mucosa, exanthema, itching, burning	RIF (4) ‡	INH, PZA, EMB, Rfb	Single¶	ALT (92), AST (58), ALP (110), GGT (91), Eosinophils (0.14)	RIF: 13 Rifabutin: 6	A 30:01:01G + 30:02:01G B 14:02:01G + 42:01:01G C 08:02:01G + 17:01:01G

71	26/F	330/N	262654	Definite DRESS (**7**)	4	**Baseline: RHZE –** 65% BSA skin rash, exanthema, and erythema, itching, burning, pain over affected area, facial oedema **Rechallenge: PZA (48hrs) –** itching, visible rash, exanthema, erythema	PZA (6)	RIF, INH, EMB	Single¶	ALT (49), AST (54), ALP (88), GGT (36), Eosinophils (2.91)	PZA: 0	A 32:01:01G + 68:01:01G B 58:01:01G + 58:02:01G C 06:02:01G + 06:02:01G
85	41/F	39/N	3475	Definite DRESS (**6**)	7	**Baseline: RHZE –** 55% BSA skin rash, exanthema, and erythema, itching and burning **Rechallenge: RIF (5 days) –** itching, burning, visible rash, exanthema, erythema. **Rechallenge: Rifabutin (5 days) –** eosinophilia, visible rash, erythema	RIF (6), Rifabutin (6)	INH, EMB, PZA	Single¶	ALT (68), AST (119), ALP (111), GGT (187), Eosinophils (1.49)	RIF: 60	A 02:01:01G + 68:02:01G B 15:10:01G + 44:03:02G C 03:04:02G + 07:01:01G
100	30/F	137/N	115989	Possible DRESS (3)	5	**Baseline: RHZE, Cotrimoxazole –** 65% BSA skin rash involving the lip and oral mucosa, peeling (desquamation), erosions, erythema itching, burning, cough **Rechallenge: INH (72hrs) –** visible rash, erythema, fever, nausea	INH (6)	PZA, EMB, MXF, Rfb	Single¶	ALT (13), AST (22), ALP (83), GGT (22), Eosinophils (1.04)	INH: 3	A 01:01:01G + 68:02:01G B 57:02:01G + 58:01:01G C 07:01:01G + 07:01:01G
103	45/F	66/N	-	Probable DRESS (**5**)	5	**Baseline: RHZE, Cotrimoxazole, Prednisone‡ -** 40% BSA skin rash involving the scalp, erythema, itching, peeling (desquamation), facial oedema, vomiting, anorexia, abdominal pain	RHZE (3), Cotrimoxazole (4) ‡	Deceased	Single¶ (Positive cotrimoxazole ELISpot)	ALT (35), AST (60), ALP (61), GGT (138), Eosinophils (0.68)	RIF, PZA, INH: 0 EMB: 25 4-NIT-10: 45 4-NIT-100: 5	A 02:01:01G + 34:02:01G B 15:03:01G + 45:01:01G C 02:10:01G + 16:01:01G
104	47/F	578/N	3862114	Definite DRESS (**7**)	9	**Baseline: RHZE –** 70% BSA skin rash involving the scalp, lips, oral and nasal mucosa, erythema, burning, fatigue, anorexia, sore throat, kidney, and liver involvement **Rechallenge: PZA (24hrs) –** abdominal pain, elevated AST and ALT, erythema	PZA (6)	RIF, INH, EMB, MXF	Single¶	ALT (183), AST (90), ALP (82), GGT (134), Eosinophils (0.19)	PZA: 0	A: *alleles not typed* B 15:03:01G + 15:03:01G C 02:10:01G + 04:01:01G

105	35/M	142/Y	LDL	Definite DRESS (**7**)	73	**Baseline: RHZE –** 80% BSA skin rash involving the eye, lip, oral and nasal mucosa, itching, burning, peeling (desquamation), facial oedema, liver involvement **†Rifinah reaction (unclear timing):** deranged liver functions **†RIF, INH reaction (non-FDC) (unclear timing):** deranged liver functions	RIF (6), INH (6)	RIF, INH (later reacted to individual RIF & INH and pushed through)	Multiple¶	ALT (35), AST (48), ALP (456), GGT (307), Eosinophils (0.37)	RIF; INH: 0	A 30:02:01G + 36:01:01G B 53:01:01G + 53:01:01G C 04:01:01G + 04:01:01G
111	39/F	360/Y	-	Possible DRESS (3)	22	**Baseline: RHZE –** 80% BSA skin rash involving oral mucosa, erythema, itching peeling (desquamation), nausea, joint and abdominal pain, cough, liver involvement **Rechallenge: RIF (3 days)** – worsening rash	RIF (6)	Deceased	Single¶	ALT (56), AST (190), ALP (790), GGT (749), Eosinophils (0.21)	PZA: 0 RIF:0 INH: 0 TMP/SMX§/#: 0 4-NIT10/100: 0	Not done
137	45/M	141/Y	-	Definite DRESS/EN overlap (6)	9	**Baseline: RHZE, Cotrimoxazole –** 65% BSA skin rash involving the nails, lips, oral and nasal mucosa, erythema, peeling (desquamation), erosions, liver, and lung involvement **Rechallenge: INH with EMB and Rifabutin (10 days) –** erythema, blisters, fever, peeling, epidermal necrosis (Possible TEN)**.**	INH (6), EMB (6), Rfb (6)	BDQ/LZD/ LVX/CFZ	Multiple¶	ALT (37), AST (63), ALP (70), GGT (102), Eosinophils (0.13)	EMB, PZA: 0 INH: 7 4-NIT-10: 52 TMP/SMX§: 2	A 29:02:01G + 68:02:01G B 44:03:02G + 53:01:01G C 04:01:01G + 07:01:01G
139	54/F	86/N	-	Probable DRESS (5)	23	**Baseline: RHZE, Cotrimoxazole –** 60% BSA skin rash involving the scalp, erythema, itching, burning, fatigue, headache, fever, enlarged lymph nodes.	Cotrimoxazole (4)	RIF, INH, PZA, EMB	Single¶ (Some cotrimoxazole ELISpot signal)	ALT (23), AST (27), ALP (71), GGT (46), Eosinophils (0.04)	TMP/SMX§ = 10	A 02:02:01G + 29:02:01G B 42:01:01G + 58:02:01G C 06:02:01G + 17:01:01G
167	41/M	162/Y	-	Probable DRESS (4)	14	**Baseline: RHZE –** 20% BSA skin rash, erythema, itching, infiltration, liver involvement	RIF (6), EMB (6)	BDQ, LZD, CFZ, TZD, LVX	Undetermined	ALT (31), AST (63), ALP (392), GGT (122), Eosinophils (1.21)	RIF, INH, PZA, EMB: 0 TMP/SMX§: 0	A 03:01:01G + 29:02:01G B 08:01:01G + 15:03:01G C 02:10:01G + 07:02:01G

						Rechallenge: RIF & EMB together – pruritis, induration, liver derangement						
24	40/F	117/N	LDL	Probable SJS/TEN (**2**)	19	**Baseline: RHZE –** 30% BSA skin rash, epidermal necrosis, liver involvement **Rechallenge: RIF (2-3hrs) –** vomiting, fever	RIF (6)	INH, PZA, EMB, MXF	Single¶	ALT (50), AST (96), ALP (225), GGT (690), Eosinophils (0.16)	RIF: 146	A 23:01:01G + 34:02:01G B 44:03:01G + 58:02:01G C 04:01:01G + 06:02:01G
39	68/M	53/Y	233	Probable SJS/TEN (**2**)	7	**Baseline: RHZE –** 10-15% BSA skin rash, epidermal necrosis, stripping (skin detachment), pain over affected area, liver, and kidney involvement	RHZE (4), Cotrimoxazole (4) ‡	Not done (TB diagnosis refuted)	Undetermined	ALT (769), AST (945), ALP (138), GGT (379), Eosinophils (0.54)	RIF: 3 INH, PZA, EMB: 0 TMP/SMX§: 40 TMP/SMX #: 10 4NIT-10;100: 43,33	A 30:01:01G + 30:01:01G B 42:01:01G + 42:02:01G C 17:01:01G + 17:01:01G
45	40/F	111/N	1719	Definite TEN (**3**)	11	**Baseline: Cotrimoxazole, Prednisone‡ -** 80% BSA skin rash, epidermal necrosis, stripping (skin detachment), erythema, macules, burning, sore throat, pain over affected area (*Not rechallenged*)	Cotrimoxazole (7)	Unknown	Undetermined	ALT (54), AST (38), ALP (72), GGT (50), Eosinophils (0.5)	Not done	A 29:02:01G + 30:01:01G B 42:01:01G + 81:01:01G C 04:01:01G + 17:01:01G
52	30/M	147/Y	732	Definite TEN (**3**)	4	**Baseline: Cotrimoxazole –** 60% BSA skin rash with eye, lip, oral, nasal, and genital mucosa involvement, epidermal necrosis, Nikolsky sign, stripping (skin detachment), itching, burning, sore throat †**Vancomycin reaction**: 36% BSA, fever, visible rash, exanthema, macules.	Cotrimoxazole (7), Vancomycin (7)	Dapsone	Multiple¶	ALT (26), AST (82), ALP (55), GGT (29), Eosinophils (0.64)	TMP/SMX§: 0 Vancomycin:2232	A 02:01:01G + 30:09 B 45:01:01G + 81:01:01G C 04:01:01G + 16:01:01G
83	49/F	24/Y	145579	Possible TEN **(1)**	4	**Baseline: Cotrimoxazole –** 80% BSA skin rash involving oral and nasal mucosa, Nikolsky sign, stripping (skin detachment) (*Not rechallenged*)	Cotrimoxazole (8)	Deceased	Undetermined	ALT (16), AST (31), ALP (157), GGT (45), Eosinophils (0)	Not done	Not done

99	27/F	61/Y	LDL	Definite TEN **(3)**	5	**Baseline: RHZE, Cotrimoxazole –** 50% BSA, skin rash involving the scalp, lip, nasal, oral and genital mucosa, facial oedema, stripping (skin detachment), epidermal necrosis, itching, night sweats, oedema, cough, facial oedema	Cotrimoxazole (6)	RHZE	Single¶ (Positive cotrimoxazole ELISpot)	ALT (233), AST (57), ALP (237), GGT (225), Eosinophils (0.33)	TMP/SMX§: 22	A 30:04:01G + 68:01:01G B 44:03:01G + 58:02:01G C 02:10:01G + 06:02:01G

[a] CD4 count (cells/µl)/On ART at time of sampling. [b] Days between onset of symptoms to biopsy. [c] Drug rechallenged (time from drug rechallenge to positive reaction). [d] Naranjo scoring applied in DRESS cases and Alden in SJS/TEN (Scores: ≥9 (Definite), 5 to 8 (Probable), 1 to 4 (Possible)). [e] Positive ELISpot ≥50 spot forming units (SFU) per million cells**.** † Not rechallenged to drug but had a separate CADR. ‡Patient not rechallenged to drug(s) – highest Naranjo/Alden scored most likely offending drug(s). ⁑ Patient on immunosuppressive treatment at the time of skin biopsy. ¶ Patient included in the analysis of HIV-infected single vs multiple drug reactors in Figures 3-24 and 3-27.

ELISpot drug concentrations: RIF (25µg/ml), INH (50µg/ml), PZA (50µg/ml), EMB (50µg/ml), Rifabutin (25µg/ml), TMP/SMX (50/250µg/ml§ or 500/2500µg/ml#), 4-NIT-10 (10µg/ml) 4-NIT-100 (100µg/ml), Vancomycin (250 µg/ml).

Abbreviations: ART – antiretroviral therapy, EFV – efavirenz, ETA – ethionamide, FDC – fixed-dose combination, FTC – emtricitabine, LDL – lower than detectable limit, LVX – levofloxacin, MXF – moxifloxacin, NVP – nevirapine, Rifabutin – Rfb, RHZE – rifampicin, isoniazid, pyrazinamide, ethambutol FDC, TMP/SMX – Trimethoprim/Sulfamethoxazole, TDF – tenofovir, TRD – terizidone, 4-NIT-10 – 4-Nitro Sulfamethoxazole-10.

Table 3-4: Description of type of reactions, laboratory findings and adjunct ELISpot and HLA data for HIV-uninfected SCAR patients

Patient	Age/Sex	Validated phenotype (RegiSCAR score)	Biopsy day [a]	Reaction characteristics at baseline, and after drug rechallenge (timing) [b]	Highest Drug Causality Score	Discharge regimen	Single or Multiple	Liver function tests and eosinophils	Elispot SFU [c]	HLA genotype
97	15/M	Definite DRESS (**6**)	3	**Baseline: Phenytoin –** 40% BSA, pustules and erythema, fatigue, headache, anorexia, nausea, liver involvement. (*Not rechallenged*)	Phenytoin (7)	Deceased	Single	ALT (94), AST (239), ALP (281), GGT (139), Eosinophils (0.62)	Not done	A: *alleles not typed* B 27:09 + 39:10:01G C 01:02:01G + 12:03:01G
102	57/F	Definite DRESS (**6**)	17	**Baseline: Phenytoin –** 90% BSA skin rash involving the scalp, lips, liver, and oral, nasal, and genital mucosa, peeling (desquamation), erythema, facial oedema (*Not rechallenged*)	Phenytoin (7)	Nil	Single	ALT (220), AST (327), ALP (95), GGT (602), Eosinophils (6.09)	Not done	A 30:01:01G + 66:01:01G B 42:02:01G + 58:02:01G C 06:02:01G + 17:01:01G
136	52/F	Probable DRESS (**5**)	3	**Baseline: Carbamazepine –** 40% BSA skin rash involving the eyes, erythema, itching, fever, liver, and lung involvement. (*Not rechallenged*)	Carbamazepine (7)	LEV	Single	ALT (564), AST (83), ALP (798), GGT (655), Eosinophils (1.36)	Not done	Not done
145	15/F	Probable DRESS (**5**)	6	**Baseline: RHZE –** 40% BSA skin rash involving the oral mucosa, erythema, facial oedema, itching, fatigue, nausea, abdominal pain, fever, cough, liver involvement. **Rechallenge**: **INH (14hrs)** – visible rash, itching, purpura, erythema, fever. **Rechallenge: RIF (8.5hrs)** – fever, burning eyes, morbilliform rash, palmar erythema, elevated AST & ALT	RIF (6), INH (6), EMB (6)	CFZ, BDQ, LZD, LVX	Multiple	ALT (159), AST (197), ALP (430), GGT (106), Eosinophils (1.36)	RIF: 520 EMB: 17 PZA: 0 INH: 33	A 25:01:01G + 32:01:01G B 07:02:01G + 15:01:01G C 02:10:01G + 03:03:01G
147	46/M	Definite DRESS (**7**)	8	**Baseline: Allopurinol –** 40% BSA skin rash, erythema, facial oedema, purpura, itching, burning, fever. †**Vancomycin rection** – visible rash, abnormal pain, jaundice, weakness of limbs	Allopurinol (7)	Nil	Multiple	ALT (67), AST (38), ALP (105), GGT (131), Eosinophils (2.55)	Not done	A 34:02:01G + 66:01:01G B 44:03:01G + 57:03:01G C 04:02:01G + 18:01:01G

28	33/F	Probable SJS/TEN (**2**)	4	**Baseline: RHZE-** 18% BSA skin rash, epidermal necrosis, erythema, itching, vomiting, diarrhoea, abdominal pain, liver involvement **Rechallenge: RIF (10-15mins)** – itching, burning, oedema, erythema **Rechallenge: INH (24hrs) –** itching, oedema **Rechallenge: EMB (10 days) –** burning, oedema, jaundice **Rechallenge: PZA (13 days) –** burning, oedema, jaundice, later tolerated **Rechallenge: Rifabutin (19 days) –** burning, oedema, jaundice	RIF/Rfb (6), INH (6), PZA (3), EMB (6)	BDQ, LVX, MXF, CFZ	Multiple	ALT (661), AST (234), ALP (59), GGT (50), Eosinophils (0.04)	RIF: 33 INH: 47 PZA: 45 EMB: 28	A 30:02:01G + 74:01:01G B 42:02:01G + 45:01:01G C 16:01:01G + 17:01:01G

[a] Days between onset of symptoms to biopsy. [b] Drug rechallenged (time from drug rechallenge to positive reaction). [c] Positive ELISpot ≥50 spot forming units (SFU) per million cells.

ELISpot drug concentrations: RIF (25µg/ml); INH (50µg/ml), PZA (50µg/ml), EMB (50µg/ml).

Abbreviations: BDQ – bedaquiline, CFZ – clofazimine, EMB – ethambutol, INH – isoniazid, LEV – levetiracetam, LVX – levofloxacin, LZD – linezolid, PZA – pyrazinamide, RHZE – rifampicin, isoniazid, pyrazinamide, ethambutol, RIF – rifampicin.

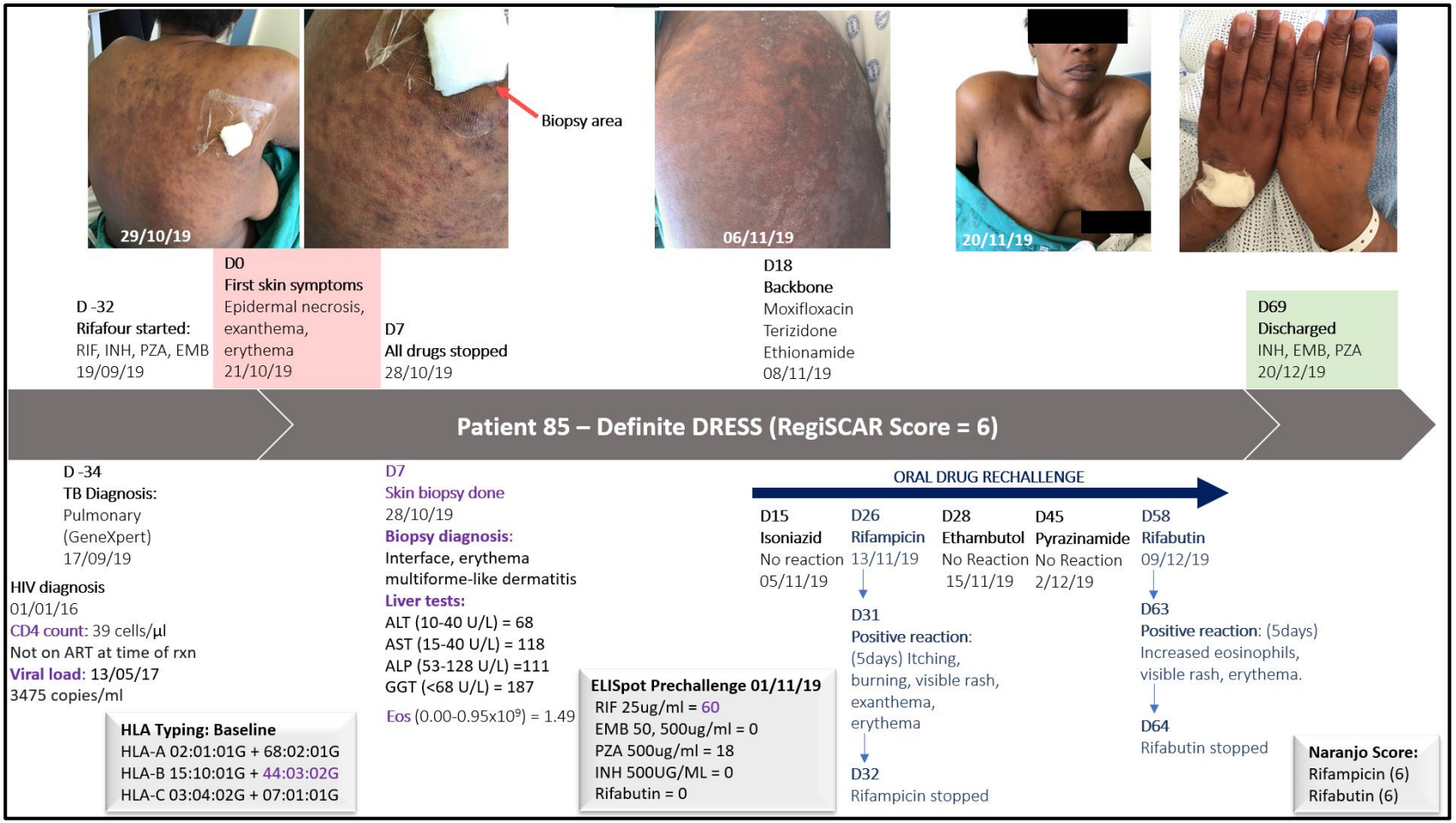

Figure 3-2: Disease progression timeline for a DRESS case. (**Patient 85**) A 41-year-old HIV positive female with active TB and on FLTD therapy. She developed first skin symptoms 32 days after initiation of rifafour FDC. She also presented with deranged LFTs, eosinophilia, and an interface dermatitis biopsy diagnosis. On day 15, she started her oral drug rechallenge to RHZE, and was put on a backbone regimen on day 18. She had a positive reaction to rifampicin and rifabutin on day 31 and 63 respectively. IFN-γ ELISpot assay on pre-challenge PBMCs showed positivity to rifampicin (60 SFU/million cells). The patient was discharged on day 69 on INH, EMB and PZA.

Table 3-5: RegiSCAR validation for DRESS cases

Patient 85, Definite DRESS

SCORE	-1	0	1	2	min	max
Fever ≥ 38.5 ^{0}C (No fever during stay in hospital)	N/U	Y	-	-	-1	0
Lymphadenopathy	-	N/U	Y	-	0	1
Eosinophilia (Eos 1.57 on 23 Oct 2019)	-	N/U	-	-	0	2
Eosinophils	-	-	700-1499/µl	≥1500/µl	-	-
Eosinophils, if leukocytes <4000	-	-	10-19.9%	≥20%	-	-
Atypical lymphocytes	-	N/U	Y		0	1
Skin involvement	-	-	-	-	-2	2
Skin rash extent (% BSA) (50-60%)	-	N/U	>50%	-	-	-
Skin rash suggests DRESS	N	U	Y	-	-	-
Biopsy suggests DRESS	N	Y/U	-	-	-	-
Organ involvement *	-	-	-	-	0	2
Liver: AST = 118 (28 Oct 2019)	-	N/U	Y	-	-	-
ALT = 69 (01 Nov 2019)	-	N/U	Y	-	-	-
Kidney	-	N/U	Y	-	-	-
Lung	-	N/U	Y	-	-	-
Muscle/heart	-	N/U	Y	-	-	-
Pancreas	-	N/U	Y	-	-	-
Other organ(s)						
Resolution ≥ 15 days (Y)	N/U	Y	-	-	-1	0
Evaluation other potential causes:	-	-	-	-	0	1
ANA: Neg (01 Nov 19)	-	-	-	-	-	-
Blood culture	-	-	-	-	-	-
Serology: HBV = Pos (30 Oct 2019)	-	N/U -	-	-	-	-
HAV, HCV = Neg (30 Oct 19)	-	-	-	-	-	-
Chlamydia-/ Mycoplasma pneumoniae	-	-	-	-	-	-
Other serology/PCR: RPR = Neg (30 Oct 19)	-		-	-	-	-
If no positive and ≥ 3 of above negative	-	-	-	-	-	-
TOTAL SCORE					-4	9

Abbreviations: U = unknown/unclassifiable; N = No; Y = Yes; ULN = upper limit of normal
* After exclusion of other explanations: 1 = 1 organ, 2 = ≥ 2 organs

Case Validation Score: 6

<2: No case
2-3: Possible case
4-5: Probable case
>5: Definite case

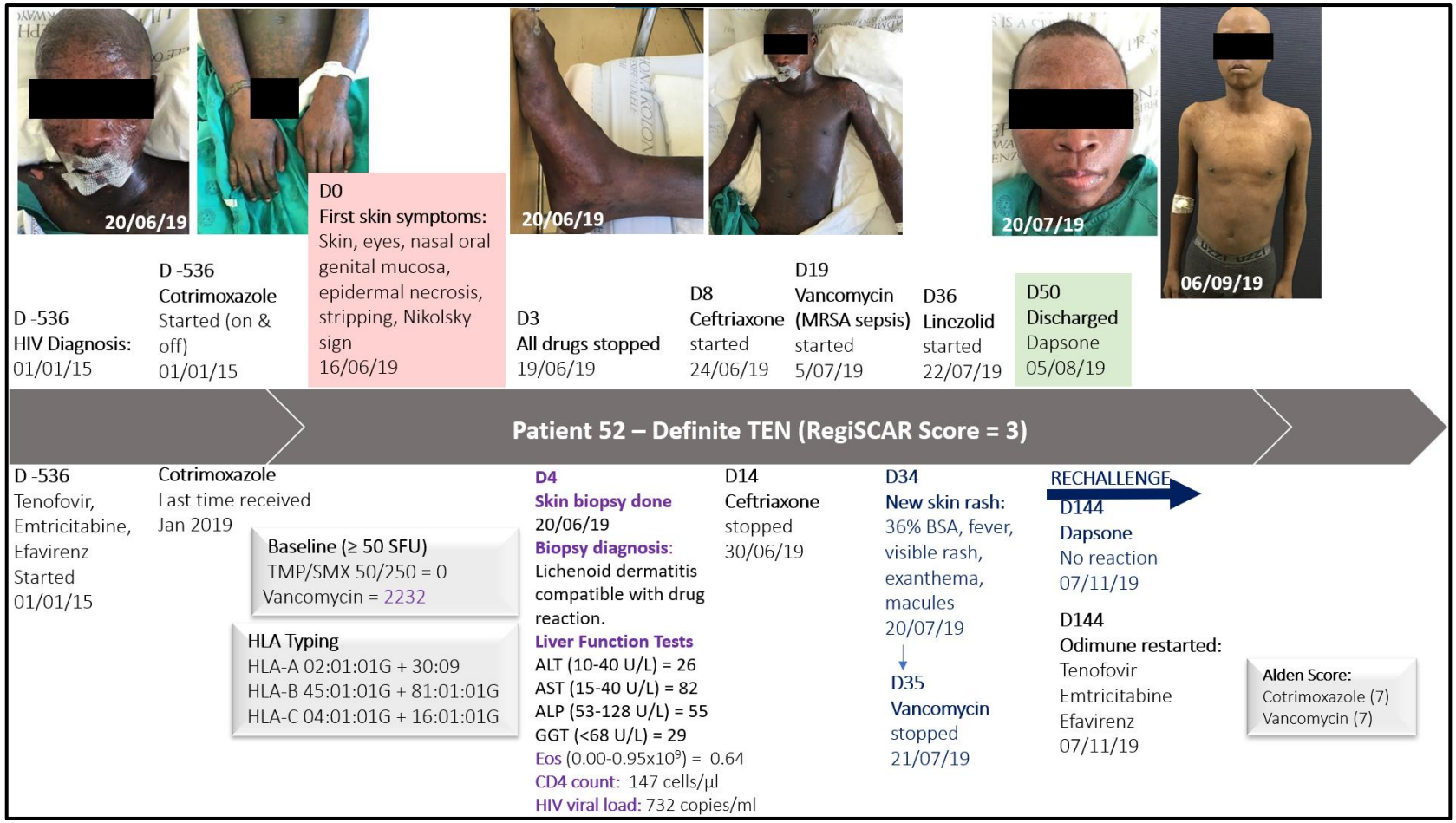

Figure 3-3: Disease progression timeline for a TEN case. (**Patient 52**) A 30-year-old HIV positive male on antiretroviral therapy and Cotrimoxazole, and with no active TB. The patient had a history of on and off Cotrimoxazole intake 4 years prior and presented with first skin symptoms ~6 months after last receiving Cotrimoxazole. He also presented with eosinophilia and a lichenoid dermatitis skin diagnosis compatible with a drug reaction. He developed methicillin-resistant *Staphylococcus aureus* (MRSA) sepsis on day 19 and was put on vancomycin. He developed a new skin rash on day 34 and vancomycin was stopped. The patient was discharged on day 50 (discharge medication not clear) and was further rechallenged to Dapsone on day 144 and tolerated the drug. Antiretroviral therapy was also restarted and was tolerated. ELISpot assay on acute PBMCs showed positivity to Vancomycin.

Table 3-6: International SCAR-group consensus validation for SJS/TEN cases

Patient 52, Definite TEN

Date of first symptoms: 14 June 2019 Date of admission: 20 June 2019

Photos: Yes Skin Biopsy: Yes; 20 June 2019

PARAMETER	FEATURES	STATUS (Y/N) OR VALUE	DATE
1. Max. involvement	Erythema	95%	
	Blisters and erosions	70%	
2. Blisters and erosions of the skin		Y	20/06/19
3. Epidermal detachment > 5 cm		Y	20/06/19
4. Mucous membranes	Red or stinging eyes	Y	
	Conjunctivitis or blepharitis	Y	12/06/19
	Severe conjunctivitis or blepharitis diagnosed by an ophthalmologist	Y	
	Erosions of lips	Y	20/06/19
	Oral erosions	Y	20/0619
	Genital erosions	Y	26/06/19
	Erosions of other mucosa	Y	
5a. Skin burning before		Y	16/06/19
5b. Skin pain before		Y	16/06/19
6. Nikolski's sign		Y	20/06/19
7. Erythema / large plaques without single spots		Y	
8. Targets or spots		Y	
9. Diagnosed by a dermatologist	Diagnosis if Yes:	TEN	
10. Photographs		Y	
11. Biopsy		Y	20/06/19
	Date of first blister / erosion of the skin or mucosa		16/06/19
	ad 8. targets - spots, type:		
	1. spots	Y	
	2. typical targets	N	
	3. atypical targets raised	Y	
	4. atypical targets flat	N	
	5. type of targets unknown	N	

Case Validation Score: 3

No Case = 0
Possible SJS/TEN = 1
Probable SJS/TEN = 2
Definite TEN = 3

3.3. Antibody optimization

Human tonsil tissue was used as a positive control for immunohistochemistry staining. The staining protocol was performed as previously described, and antibody concentrations and incubation times were optimized on the positive control tissue prior to skin tissue staining. Figure 3-4 shows CD3 staining of tonsil tissue displaying different staining intensities. A negative control slide in which the primary antibody was excluded was done for all staining (Figure 3-4A). The secondary antibody and DAB detection chromogen were used at 'neat' (undiluted) concentration. The primary antibody concentration was adjusted by a titration series until optimal staining was achieved, similarly with antibody incubation times. The same optimization procedure was repeated for CD8, CD4 and CD45RO antibodies.

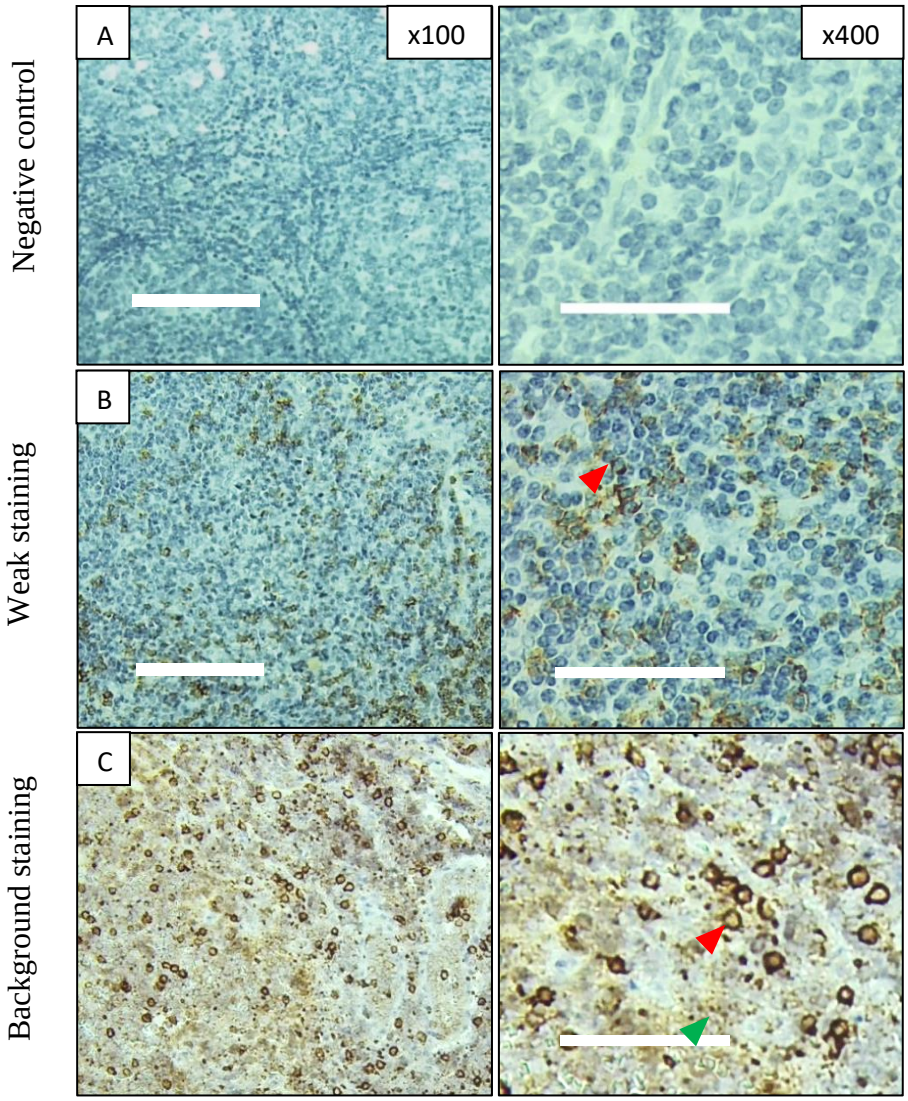

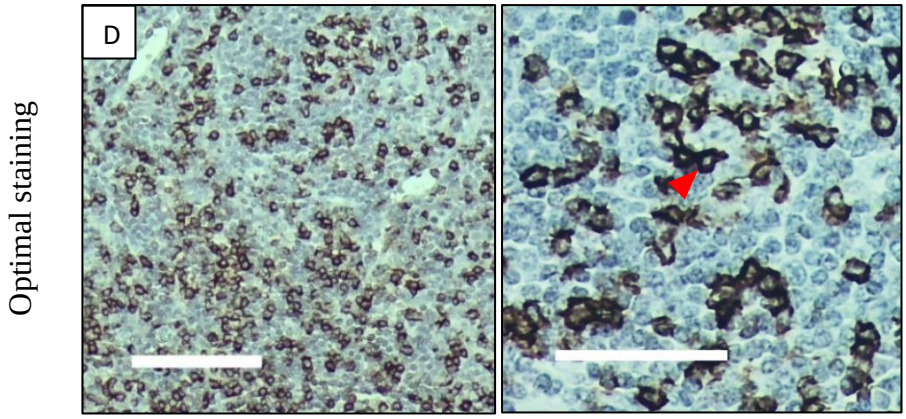

Figure 3-4: CD3 antibody optimization staining in positive control tonsil tissue. Positive CD3 cells (red arrowhead) can be seen marked by the brown cell surface staining. The primary antibody was titrated until optimal concentration was achieved (**D**) and non-specific background staining was eliminated (green arrowhead). Images are at x100 magnification (left), scale bar = 100µm; and x400 (right), **s**cale bar = 50µm.

The optimized antibody concentrations and incubation times were applied for skin tissue staining as shown in Figure 3-5. In cases where certain skin samples exhibited excessive background and non-specific staining, the samples were blocked in H_2O_2 for longer (at least ≥ 20mins), depending on the extent of background staining. Stronger positive staining was enhanced by increasing the antigen retrieval treatment time.

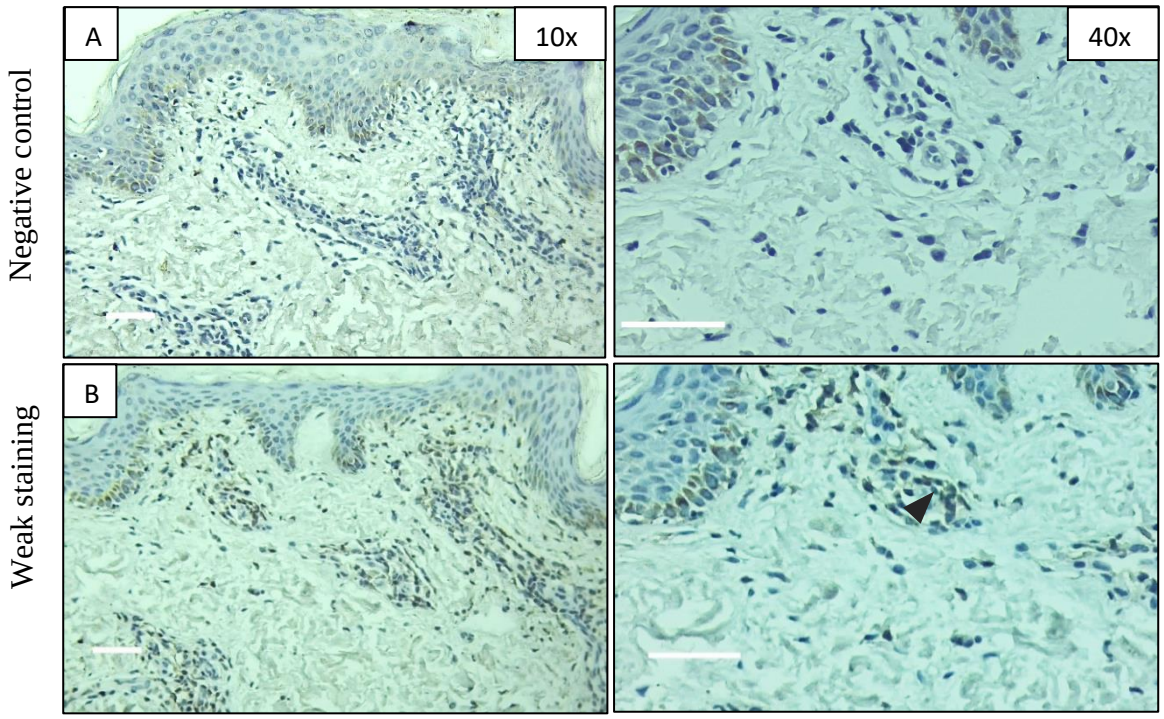

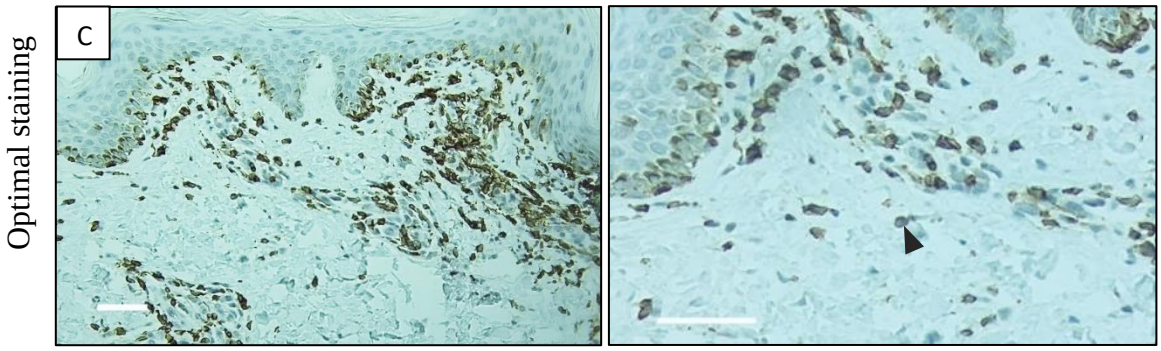

Figure 3-5: CD3 antibody staining optimization in the skin of a DRESS case. Black arrowhead denotes positive CD3 lymphocyte. Images are at x200 magnification (left), scale bar = 50µm; and x400 (right), **s**cale bar = 50µm

Human appendix tissue was used as the positive control for immunofluorescence staining of Tregs. Both primary and secondary antibody concentrations were titrated until optimal staining was achieved (Figure 3-6). A similar approach was used for optimizing CD45RO+CD4+/CD8+ co-expression staining using tonsil tissue (Figure 3-7).

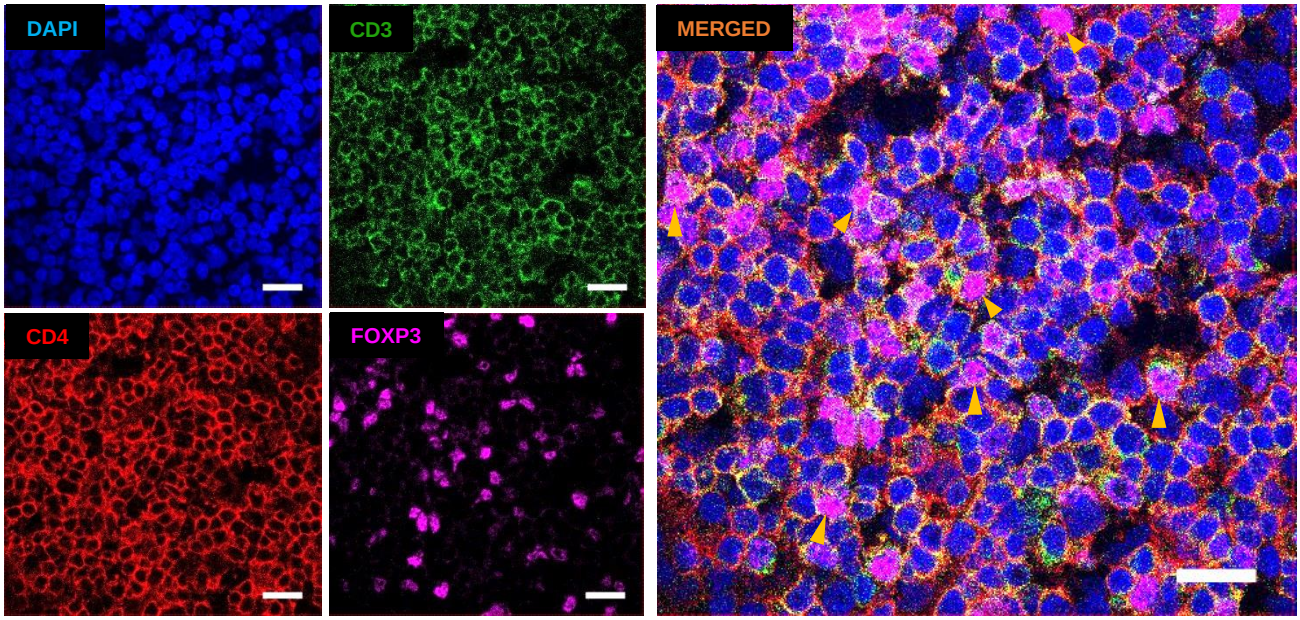

Figure 3-6: Confocal microscopy Treg cell staining optimization in positive control appendix tissue. Sections were stained with anti-CD3 (green), anti-CD4 (red), anti-FOXP3 (purple), and nuclear staining with DAPI (blue). The orange arrowheads denote Treg cells (CD3+CD4+FOXP3+). Images at 60x (oil objective), scale bar = 50µm.

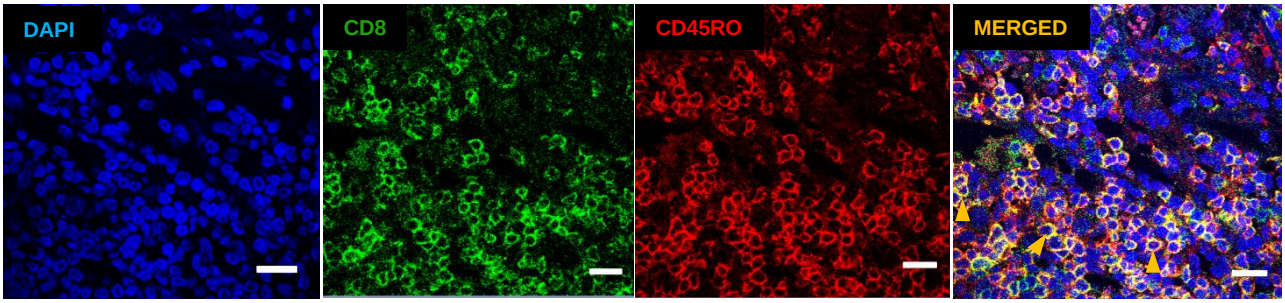

Figure 3-7: Confocal microscopy of CD8+CD45RO+ co-expression optimization staining in positive control tonsil tissue. CD8+CD45RO+ co-expressed cells appear orange and are denoted by the yellow arrowheads. Scale bar = 50µm

3.4. Histological features in DRESS & SJS/TEN cases

Several histopathology patterns were displayed in the SCAR cases. Figures 3-8 and 3-9 highlight the major patterns observed in DRESS and SJS/TEN cases, respectively.

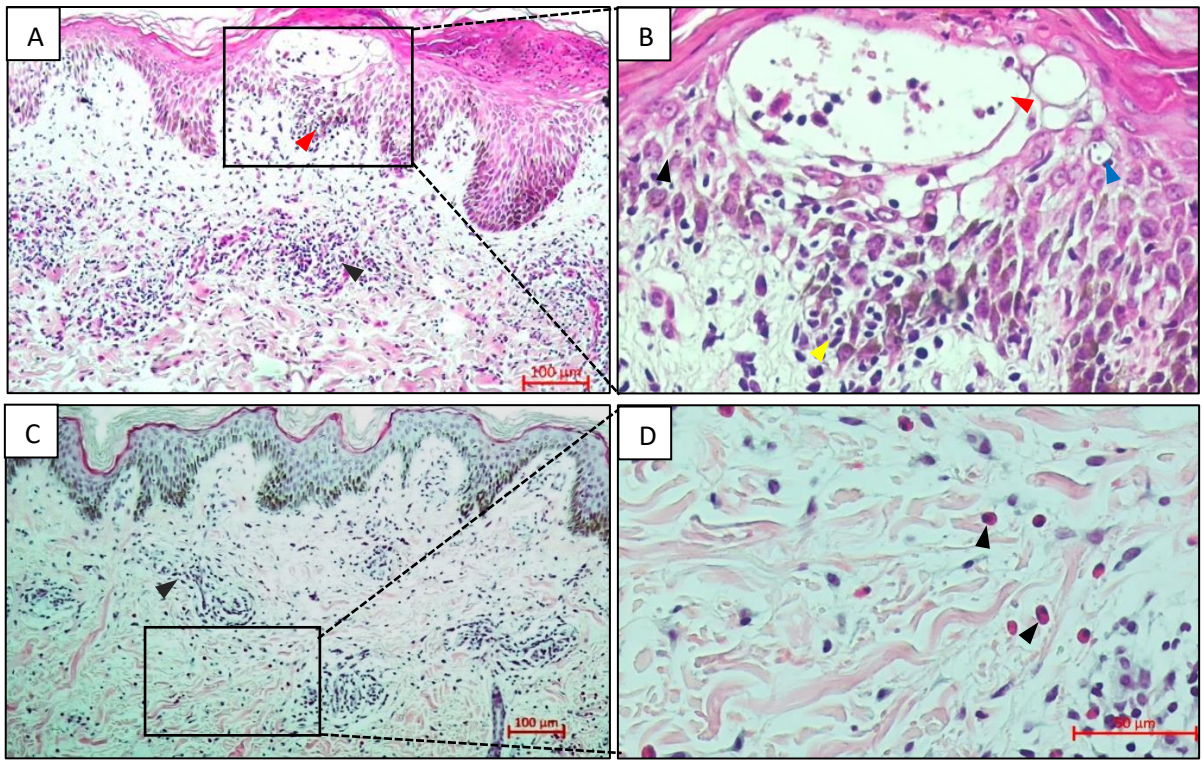

Figure 3-8: Major histopathological patterns revealed in DRESS cases. **A.** Skin biopsy from a case of DRESS showing interface dermatitis (red arrowhead) at the dermoepidermal junction and a band like lichenoid dermatitis in the dermis (black arrowhead) (x100). Apoptotic keratinocytes (**B**. blue arrowhead), and basal vacuolar degeneration (yellow arrowhead) resulting from interface dermatitis leading to epidermal spongiosis (black arrowhead) and intra epidermal vesicle formation (red arrowhead). **C**. Another case of DRESS displaying mild superficial perivascular lymphocytic dermatitis

(black arrowhead) with scattered dermal eosinophils (**D.** black arrowheads). Scale bars: A and C: 100µm, B and D: 50µm.

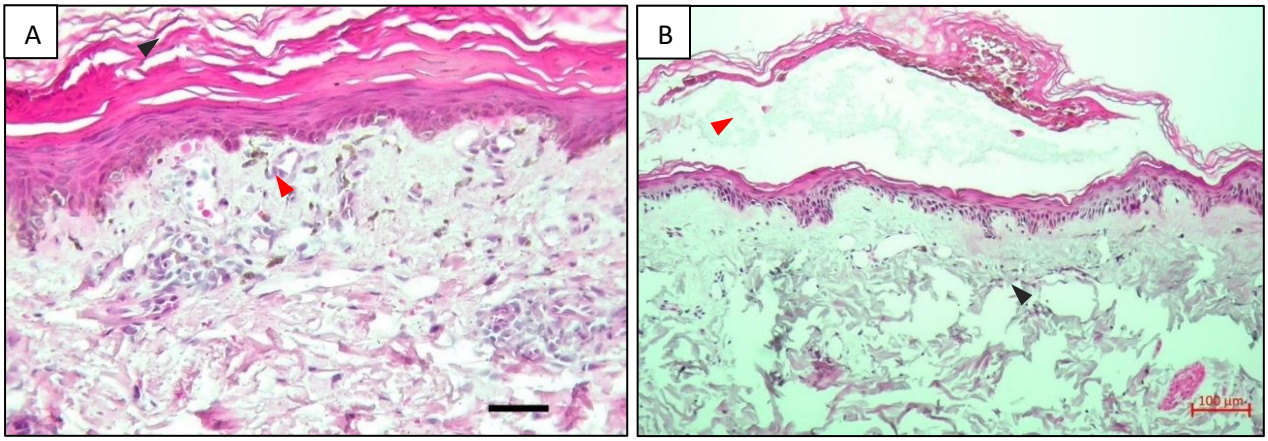

Figure 3-9: Major histopathological patterns revealed in SJS/TEN cases. **A**. Skin biopsy from a case of SJS/TEN (patient 24) showing hyperkeratosis (black arrowhead) and pigmentary incontinence (red arrowhead) **B.** Another case of SJS/TEN (patient 28) displaying a subcorneal blister (red arrowhead) in the epidermis, and a sparse dermal lymphocytic infiltrate (black arrowhead) with no eosinophils. Scale bars: A, C, E, and F: 100µm, B and D: 50µm.

Histopathological features of diagnostic or prognostic importance were identified and the histopathologic diagnosis was confirmed by a Consultant Anatomical Pathologist. Changes in the epidermis, at the dermoepidermal junction and in dermis for both HIV-infected, and uninfected DRESS and SJS/TEN cases were revealed upon histological analysis. Various degrees of morphological changes and inflammatory patterns were observed in these cases. The main epidermal changes and patterns observed in both DRESS and SJS/TEN cases included hyperkeratosis, spongiosis and basal vacuolar degeneration, and apoptotic keratinocytes with interface dermatitis. In the dermis a perivascular infiltration of inflammatory cells was commonly noted, as well as pigmentary incontinence and dermal oedema. A detailed description of the patients' skin biopsy histopathological changes is shown in Tables A-2 and A-3.

Table 3-7 shows a summary of these histopathologic findings for both HIV-infected and uninfected SCAR patients. Hyperkeratosis was observed in 9/15 HIV-infected DRESS cases and in 4/6 HIV-infected SJS/TEN cases. Epidermal spongiosis was also commonly observed, occurring in 13/15 of HIV-infected DRESS cases, 3/4 HIV-uninfected DRESS cases and 3/6 HIV-uninfected SJS/TEN cases. Apoptotic keratinocytes were observed in 12/15 HIV-infected DRESS cases, and in only 1/4 HIV-uninfected DRESS. A focal interface dermatitis at the dermoepidermal junction was observed in 7/15 HIV-infected DRESS cases and 4/4 HIV-uninfected DRESS cases. A widespread interface dermatitis was only observed in 4/15 HIV-infected DRESS cases. Eight out

of 15 HIV-infected DRESS cases revealed basal vacuolar degeneration at the dermoepidermal junction, with only 1/15 cases exhibiting lymphocytic exocytosis. All 2/4 HIV-uninfected DRESS cases with basal vacuolar degeneration were accompanied with lymphocytic exocytosis. Pigmentary incontinence was observed in 9/19 DRESS cases and in all SJS/TEN cases. Superficial perivascular dermatitis was the most commonly observed dermal inflammatory pattern in both DRESS (12/19) and SJS/TEN (5/7) cases. Lichenoid dermatitis was only observed in 3/19 of DRESS cases and only 1/7 SJS/TEN cases. A predominant infiltration of lymphocytes and eosinophils was observed in 10/19 HIV-infected and uninfected DRESS cases.

Table 3-7: Summary of histopathologic findings in HIV-infected and uninfected SCAR cases

LOCATION/PARAMETER	HISTOLOGICAL FEATURE	DRESS (N=19)				SJS/TEN (N=7)		
		HIV-infected (n=15)	HIV-uninfected (n=4) [a]	Total (n=19)	p-value	HIV-infected (n=6)	HIV-uninfected (n=1)	Total (n=7)
EPIDERMAL STRATUM CORNEUM	Parakeratosis	5/15 (33%)	1/4 (25%)	6/19 (32%)	1.00	2/6 (33%)	1/1 (100%)	2/7 (29%)
	Hyperkeratosis	9/15 (60%)	1/4 (25%)	10/19 (52%)	0.30	3/6 (50%)	1/1 (100%)	5/7 (71%)
	Orthokeratosis	0	0	1/19 (5%)	1.00	2/6 (33%)	0	1/7 (14%)
EPIDERMAL SPINOUS LAYER	Acanthosis	3/15 (20%)	0	3/19 (16%)	1.00	1/6 (17%)	0	1/7 (14%)
	Spongiosis	13/15 (87%)	3/4 (75%)	16/19 (84%)	0.53	3/6 (50%)	0	3/7 (43%)
	Necrotic keratinocytes	0	0	0	1.00	2/6 (33%)	1/1 (100%)	3/7 (43%)
	Apoptotic keratinocytes	12/15 (80%)	1/4 (25%)	13/19 (68%)	0.07	1/6 (17%)	1/1 (100%)	2/7 (29%)
	Epidermal oedema	1/15 (7%)	0	1/19 (5%)	1.00	0	0	0
	Epidermal blister	0	0	0	1.0	1/6 (17%)	1/1 (100%)	2/7 (29%)
	Epidermal detachment	0	0	0	1.00	1/6 (17%)	0	1/7 (14%)
	Intraepidermal vesicle	1/15 (7%)	0	0	1.00	0	0	0
DERMOEPIDERMAL JUNCTION	Focal interface dermatitis	7/15 (47%)	4/4 (100%)	11/19 (58%)	0.10	1/6 (17%)	0	1/7 (14%)
	Widespread interface dermatitis	4/15 (27%)	0	4/19 (21%)	0.53	0	0	0
	Basal vacuolar degeneration	8/15 (53%)	2/4 (50%)	10/19 (52%)	1.00	2/6 (33%)	0	2/7 (29%)
	Exocytosis	1/15 (6%)	2/4 (50%)	3/19 (16%)	0.09	1/6 (17%)	0	1/7 (14%)
DERMIS	Pigmentary incontinence	7/15 (47%)	2/4 (50%)	9/19 (47%)	1.00	6/6 (100%)	1/1 (100%)	7/7 (100%)
	Dermal oedema	1/15 (7%)	0	1/19 (5%)	1.00	1/6 (17%)	0	1/7 (14%)
DERMAL INFLAMMATION	Lichenoid	2/15 (13%)	1/4 (25%)	3/19 (16%)	0.53	1/6 (17%)	0	1/7 (14%)
	Perivascular	8/15 (53%)	4/4 (100%)	12/19 (63%)	0.25	4/6 (67%)	1/1 (100%)	5/7 (71%)
PREDOMINANT DERMAL INFLAMMATORY INFILTRATES	Lymphocytes only	1/15 (7%)	0	1/19 (5%)	1.00	1/6 (17%)	1/1 (100%)	3/7 (43%)
	Lymphocytes and eosinophils	9/15 (60%)	2/4 (50%)	10/19 (53%)	1.00	2/6 (33%)	0	4/7 (57%)
	Mixed: lymphocytes and/or eosinophils, neutrophils, plasma cells	5/15 (33%)	2/4 (50%)	7/19 (37%)	0.60	3/6 (50%)	0	0

Values are given as n (%). Freeman-Halton extension of the Fisher's exact probability test was used for statistical analysis. P-values ≤ 0.05 were considered significant.
[a] 1 out of the 5 HIV-uninfected DRESS cases was not histopathologically evaluated, therefore analysis was done on 4 HIV-uninfected DRESS cases only.

3.5. Standard IHC by marker

Distribution of cell infiltrates in normal and SCAR tissue

Figure 3-10 is an H&E staining showing overall distribution of inflammatory infiltrates in the skin of HIV-infected and uninfected DRESS compared to normal skin. As expected, a higher infiltration of cells can be noted in the skin undergoing a SCAR reaction, whereas very little activity is noted in normal skin. The absence of any epidermal or dermal histopathological or morphological changes characteristic of a drug reaction can also be noted in normal skin (Figure 3-10C-D).

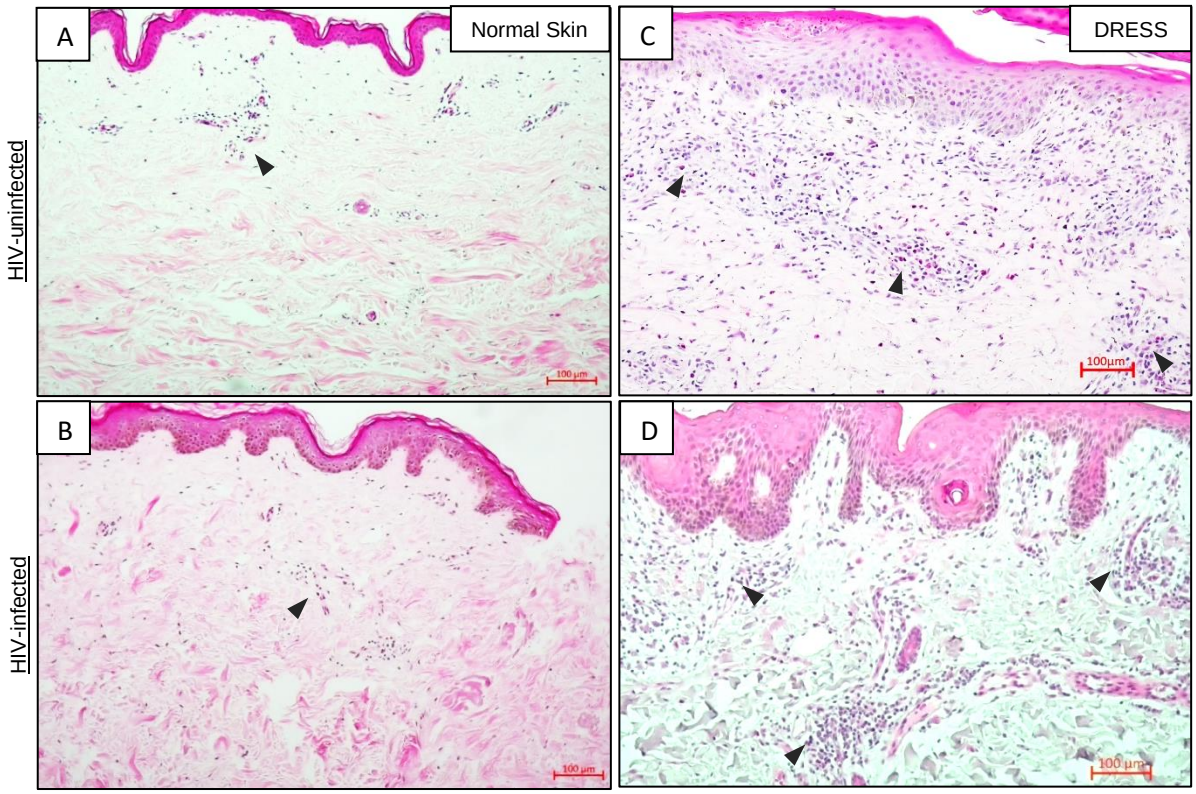

Figure 3-10: Distribution of inflammatory infiltrates (denoted by black arrowheads) in the skin of HIV-uninfected (A) and infected normal skin (B) compared to HIV-uninfected (C) and infected (D) DRESS lesional skin. All images at 100x magnification, scale bar = 100µm

Infiltration of lymphocytes confirmed by CD3+ cells

The presence of lymphocytes in the skin was confirmed using anti-CD3, a pan T-cell marker. Figure 3-11 shows an example case, patient 38 (See patient timeline Figure A-4), an HIV-infected DRESS patient, showing immunohistochemistry of CD3, CD4, CD8 and CD45RO T-cells. Predominant infiltration of CD8+ and CD45RO+ T-cells can be noted, and CD4+ T-cells to a lesser extent.

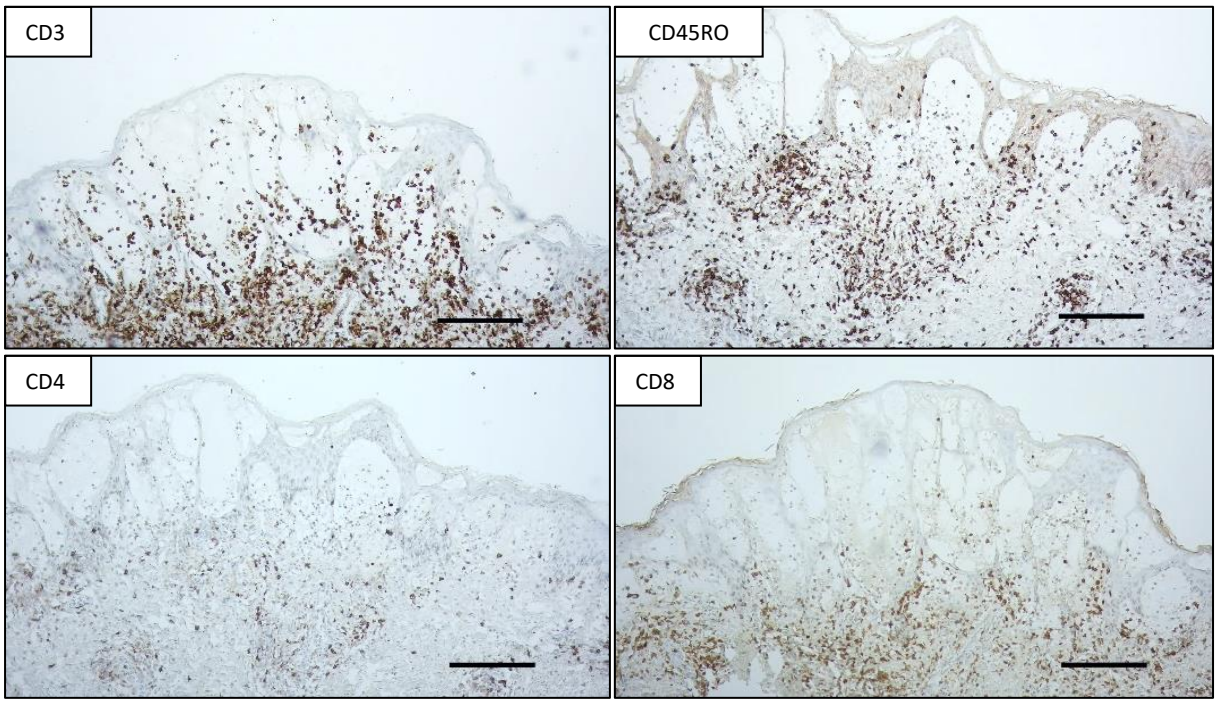

Figure 3-11: Distribution of T cells in skin biopsy of acute HIV-infected DRESS**.** Immunohistochemistry of CD3+, CD4+, CD8+ and CD45RO+, confirming a T cell infiltrate of predominantly CD45RO+ and CD8+ T-cells, and to a lesser extent CD4+ T-cells. Scale bars = 200µm.

CD3 T cells

Upon revealing histopathological patterns and distribution of inflammatory patterns in SCAR cases on H&E staining, the immunophenotypes of these infiltrates between HIV-infected and uninfected cases and normal skin was studied. No comparison between HIV-infected and uninfected SJS/TEN cases was done due to the small sample size. DRESS cases were quantified separately, and an overall combined count of DRESS and SJS/TEN (SCAR) was done for both HIV-infected and uninfected cases. Patient disease progression timelines for example cases used are shown in the appendix section.

As revealed on histological evaluation, there was an increased infiltration of lymphocytes in the dermis compared to the epidermis of this skin in both HIV-infected and uninfected SCAR, Figure 12A-B. HIV-uninfected DRESS patients (n=5) were associated with significant increased infiltration of dermal CD3+ T-cells when compared to HIV-infected DRESS (n=15); median (IQR) CD3+ T-cell count (81 (63 - 106) versus 53 (45-62) cells/high-powered field, p = 0.0326), (Figure 3-13A). A similar pattern was observed in the counts of DRESS and SJS/TEN combined, although not statistically significant, p = 0.0915 (Figure 3-13B).

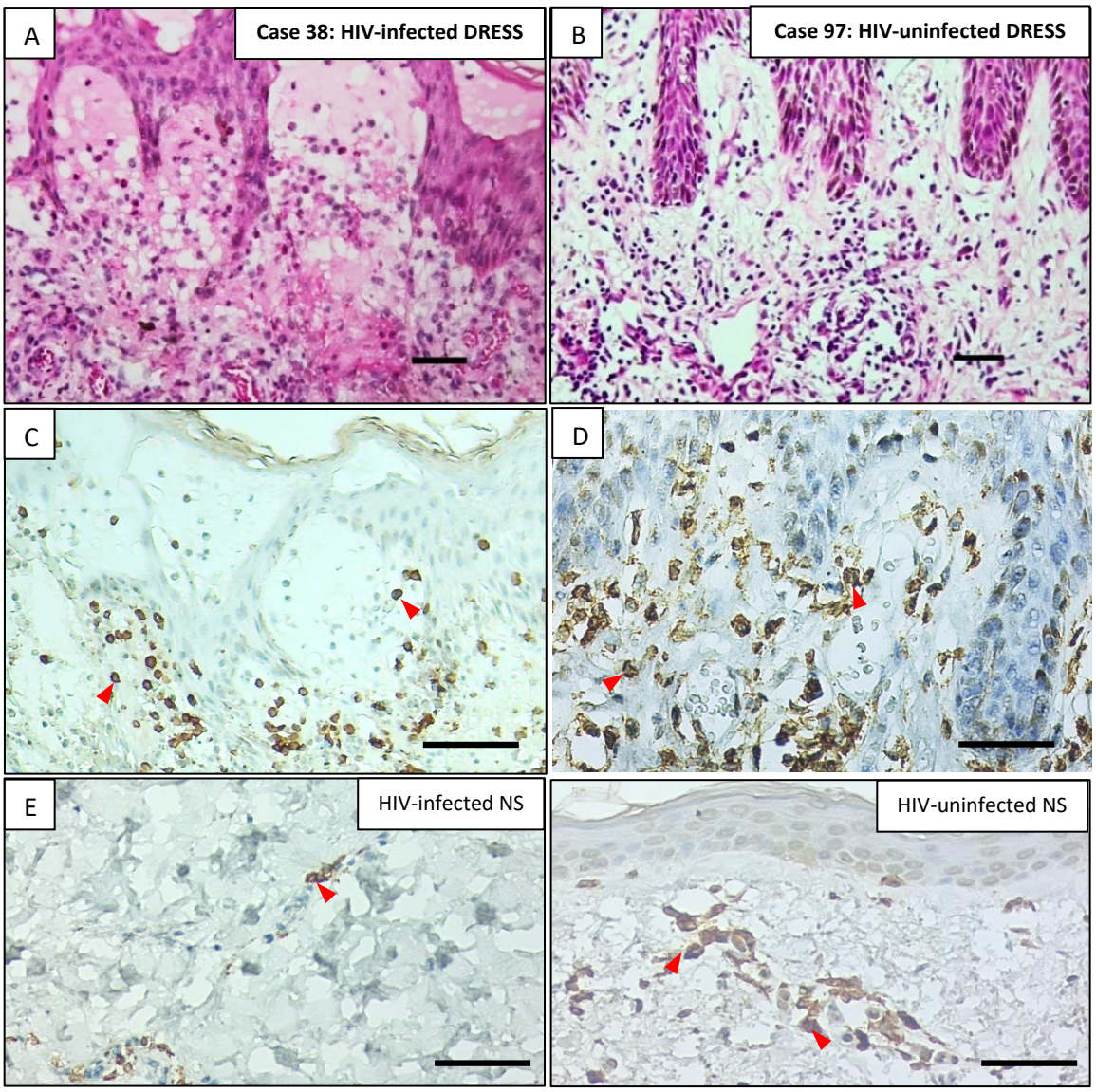

Figure 3-12: Immunohistochemistry staining of CD3+ T-cells in HIV-infected and HIV-uninfected DRESS. (**A**) Histopathological examination for case 38 on H&E staining revealed spongiotic dermatitis with intraepidermal vesicle formation and eosinophils (See patient timeline in Figure A-4). (**B**) Case 97 displayed a focal interface change with spongiosis, and superficial perivascular dermatitis composed of

lymphocytes and eosinophils (See patient timeline in Figure A-5). H&E images are at 200x, scale bar = 50µm; IHC images are at 400x, scale bar = 50µm.

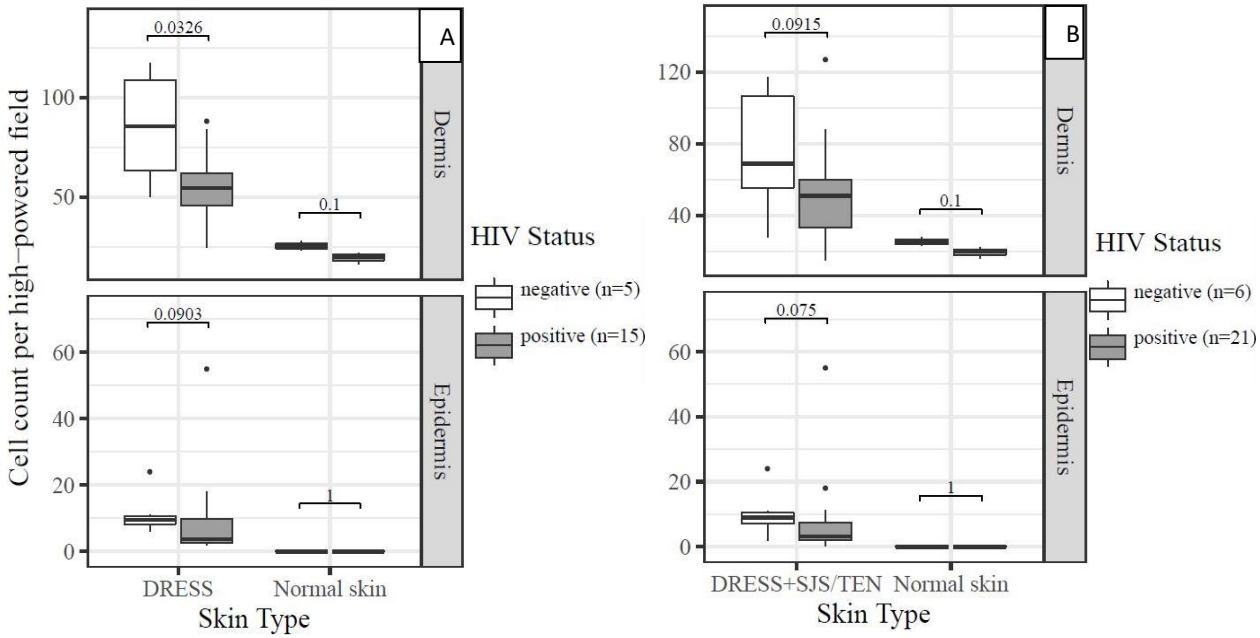

Figure 3-13: Comparison of CD3 T-cell staining in dermal and epidermal compartments of HIV-infected and uninfected DRESS only and DRESS + SJS/TEN combined (SCAR). (**A**) A significant increase in dermal CD8+ T-cell counts is noted in HIV-infected compared to HIV-uninfected DRESS. A significant increase in dermal and epidermal CD3+ T-cell counts is noted in HIV-infected and uninfected DRESS (and SCAR) compared to HIV-infected and uninfected normal skin, respectively.

CD8 cytotoxic T cells

Immunohistochemistry revealed a significantly increased dermal and epidermal infiltration of CD8+ T-cells in both HIV-infected and uninfected DRESS and SJS/TEN cases compared to normal skin (HIV-infected and uninfected) (Figure 3-14). In DRESS cases, there was a predominant dense dermal infiltrate of CD8+ T-cells, observed in both HIV-infected and uninfected cases (Figure 3-14 C&D). Surprisingly, there was only a sparse to mild infiltrate of effector CD8+ T-cells in both HIV-infected and uninfected SJS/TEN cases (Figure 3-15A-D). One TEN case had a high distribution of effector CD8+ T-cells, that presented with a lymphocytic lichenoid dermatitis histopathological pattern on H&E (Figure 3-15 E-F). Overall, there were no significant differences observed in the epidermal and dermal CD8+ T-cell counts between HIV-infected and uninfected DRESS cases, although in the dermis of HIV-uninfected versus HIV-infected DRESS cases there was a higher CD8+ T-cell count; (56 (27 - 87) versus 37 (30-51) cells/high-powered field, p =

0.601) (Figure 3-16A); and a similar trend observed in the counts of DRESS and SJS/TEN combined (Figure 3-16B).

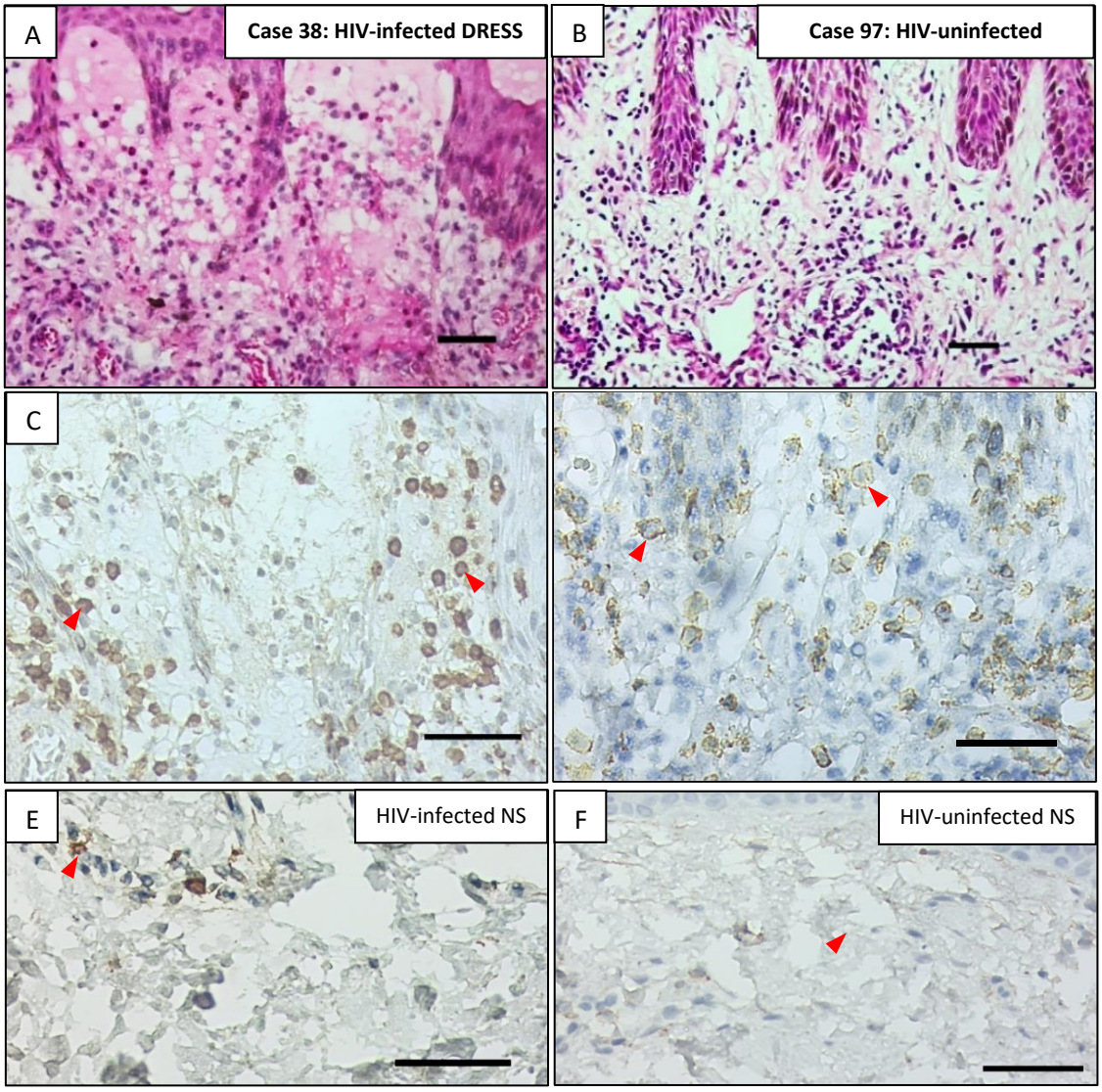

Figure 3-14: A. Immunohistochemistry staining of CD8+ cells in HIV-infected and uninfected DRESS. Dense infiltration of CD8 T-cells can be observed in HIV-infected (**C**) and uninfected (**D**) DRESS, compared to HIV-infected (**E**) and uninfected (**F**) normal skin. H&E images are at 200x, scale bar = 50μm; IHC images are at 400x, scale bar = 50μm. Abbreviations: NS – normal skin.

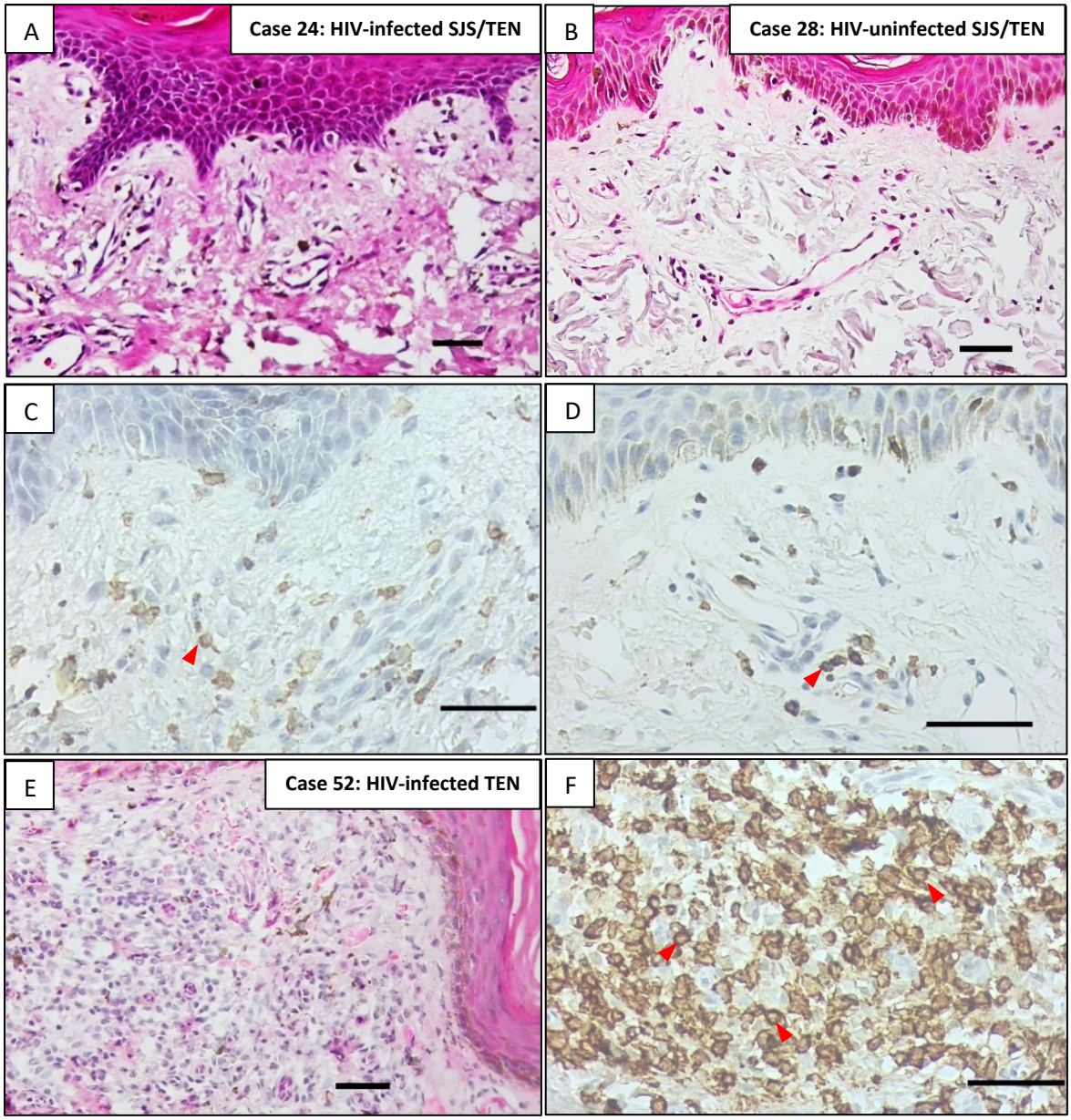

Figure 3-15: **A**. Immunohistochemistry staining of CD8+ T-cells in HIV-infected and HIV-uninfected SJS/TEN; and HIV-infected TEN. (**A**) Histopathologic examination for the HIV-infected SJS/TEN case 24 on H&E staining revealed spongiosis in the epidermis and mild perivascular lymphocytic dermatitis with no eosinophils in the dermis (See patient timeline in Figure A-2). (**B**) HIV-uninfected SJS/TEN case 28 displayed epidermal hyperkeratosis and parakeratosis with a perivascular lymphocytic dermal infiltrate (See patient timeline in Figure A-3). (**E**) The HIV-infected TEN case 52 displayed a lymphocytic lichenoid dermatitis, compatible with a drug reaction (See patient timeline in Figure 3-3). A sparse distribution of CD8+ cells can be noted in both HIV-infected (**C**) and uninfected (**D**) SJS/TEN cases, whereas the HIV-infected TEN case (**F**), displayed a dense infiltration of cells. H&E images are at 200x, scale bar = 50µm; IHC images are at 400x, scale bar = 50µm.

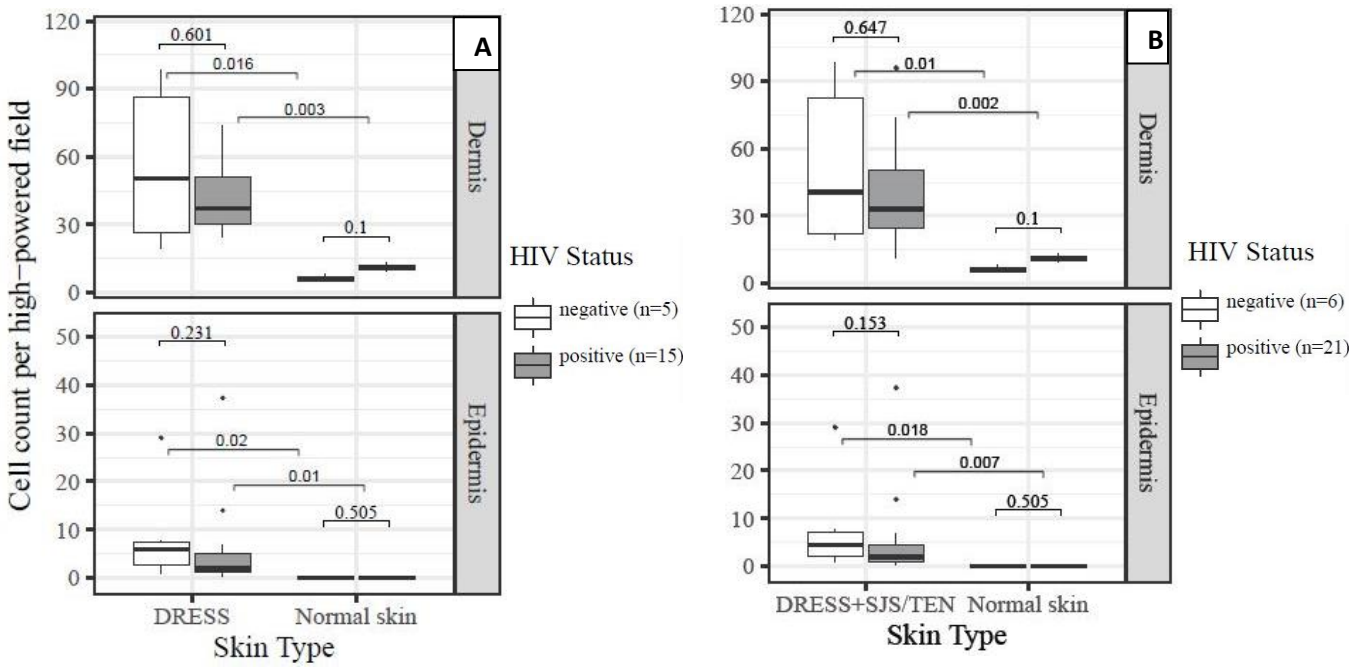

Figure 3-16: Comparison of CD8 T-cell staining as a percentage of all CD3+ cells in dermal and epidermal compartments of HIV-infected and uninfected DRESS only and DRESS + SJS/TEN combined (SCAR). (**A**) A significant increase in dermal (P = 0.003; 0.016) and epidermal (P = 0.01; 0.02) CD8+ T-cell counts is noted in HIV-infected and uninfected DRESS compared to HIV-infected and uninfected normal skin, respectively. (**B**) A similar pattern is observed in the counts of DRESS and SJS/TEN combined.

CD4 helper T cells

HIV-uninfected DRESS showed an increased infiltration of dermal and epidermal CD4+ T-cells when compared to normal skin. There was, however, a significant decrease in the dermal and epidermal infiltration of CD4+ T-cells in HIV-infected DRESS cases, compared to HIV-uninfected cases, p = 0.0007 and p = 0.004) respectively (Figures 3-17A-D and 3-18A). A similar trend was observed in the overall combined counts of DRESS and SJS/TEN (Figure 3-18B). This decrease in CD4+ T-cells was associated with up to a 3-fold increase in the ratio of dermal and epidermal CD8+/CD4+ T-cells in HIV-infected DRESS cases, p = 0.009 and p = 0.032 respectively, compared to HIV-uninfected cases (Table A-3) and similarly in the counts of DRESS and SJS/TEN combined.

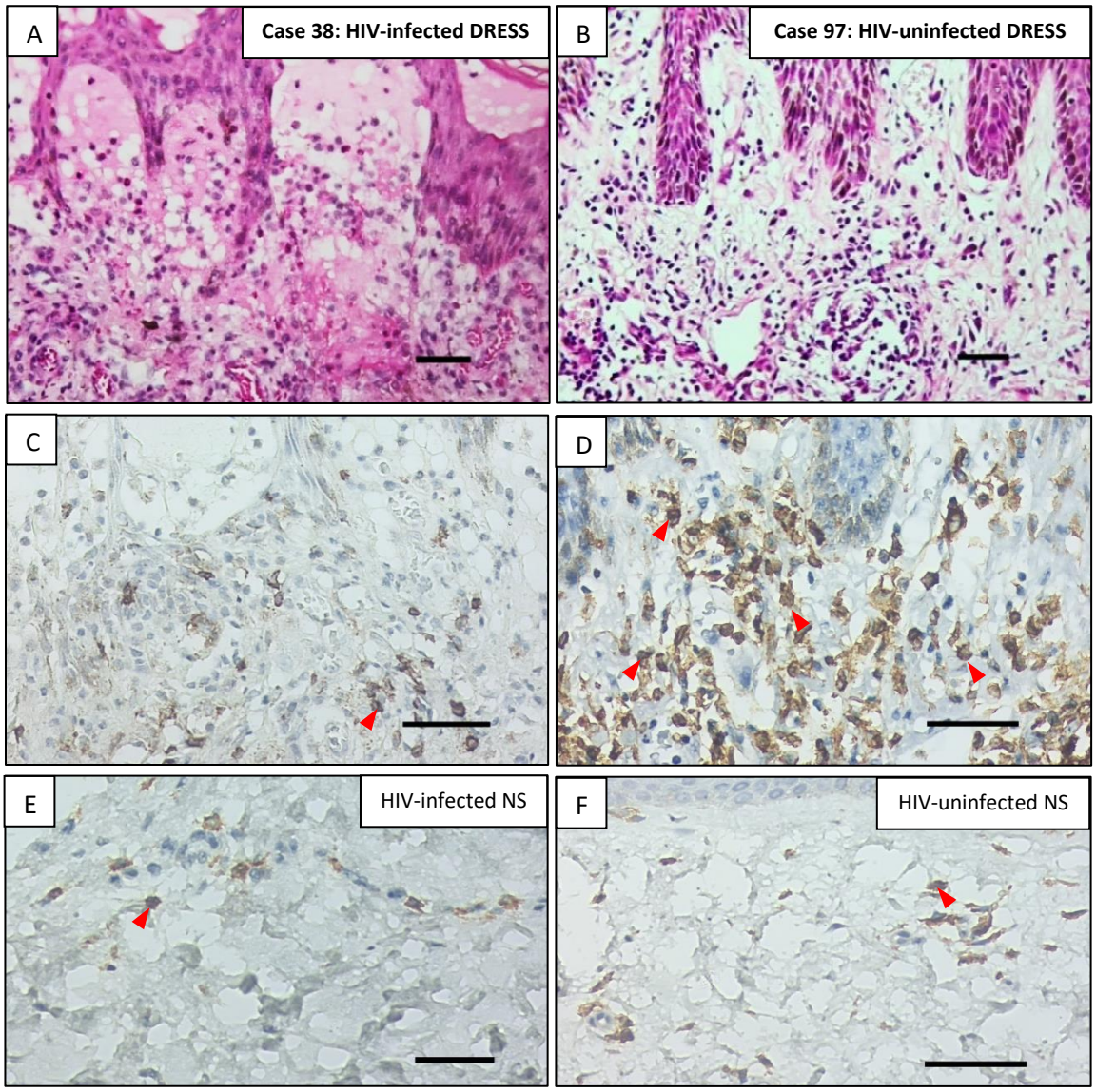

Figure 3-17: A. Immunohistochemistry staining of CD4+ cells in HIV-infected and HIV-uninfected DRESS. A significant decrease in CD4 T-cells can be noted in HIV-infected DRESS (**C**) compared to HIV-uninfected DRESS (**D**). Similarly, a very low distribution of CD4 T-cells can be observed in both HIV-infected (**E**) and HIV-uninfected (**F**) normal skin. H&E images are at 200x, scale bar = 50µm; IHC images are at 400x, scale bar = 50µm. Abbreviations: NS – normal skin.

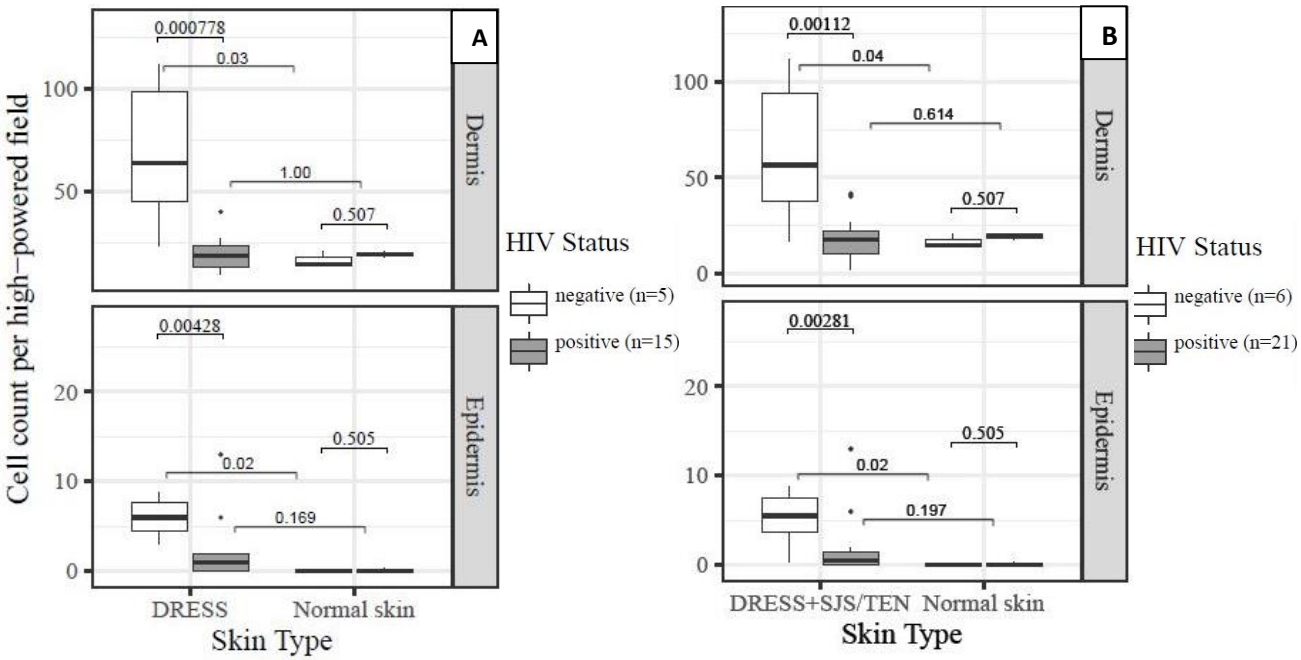

Figure 3-18: Comparison of CD4 T-cell staining as a percentage of all CD3+ cells in dermal and epidermal compartments of HIV-infected and uninfected DRESS only and DRESS + SJS/TEN combined (SCAR). (**A**) A significant decrease in CD4+ T-cells can be noted in both dermal (P = 0.000778) and epidermal (P = 0.00428) compartments of HIV-infected DRESS compared to HIV-uninfected DRESS. (**B**) A significant increase in dermal (P = 0.03) and epidermal (P = 0.02) CD4+ T-cells can be noted in HIV-uninfected DRESS compared to HIV-uninfected normal skin. Similar trends can be observed in the counts of DRESS and SJS/TEN combined.

CD45RO+ memory T cells

Expression of effector memory cells was assessed using the CD45RO marker. This single marker method is not able to distinguish T-cell (CD4 versus CD8) or T-cell memory subsets (effector central or tissue resident memory). Both HIV-infected and uninfected SCAR cases showed a dense expression CD45RO memory T-cells in the skin (Figure 3-19A-D), and significantly higher when compared to normal skin (Figure 3-19E-F, Figure 3-20). This suggested that most of the inflammatory infiltrates had previously encountered antigen/drug interaction. Overall, there were no significant differences in the dermal and epidermal CD45RO+ expression observed between HIV-infected and uninfected SCAR cases, although a trend toward an increase was observed in the dermis of HIV-uninfected DRESS patients, (55 (37 - 81) versus 42 (33 - 50) cells/high-powered

field; p = 0.224) (Figure 3-20A-B). A similar trend was observed in the counts of DRESS and SJS/TEN combined.

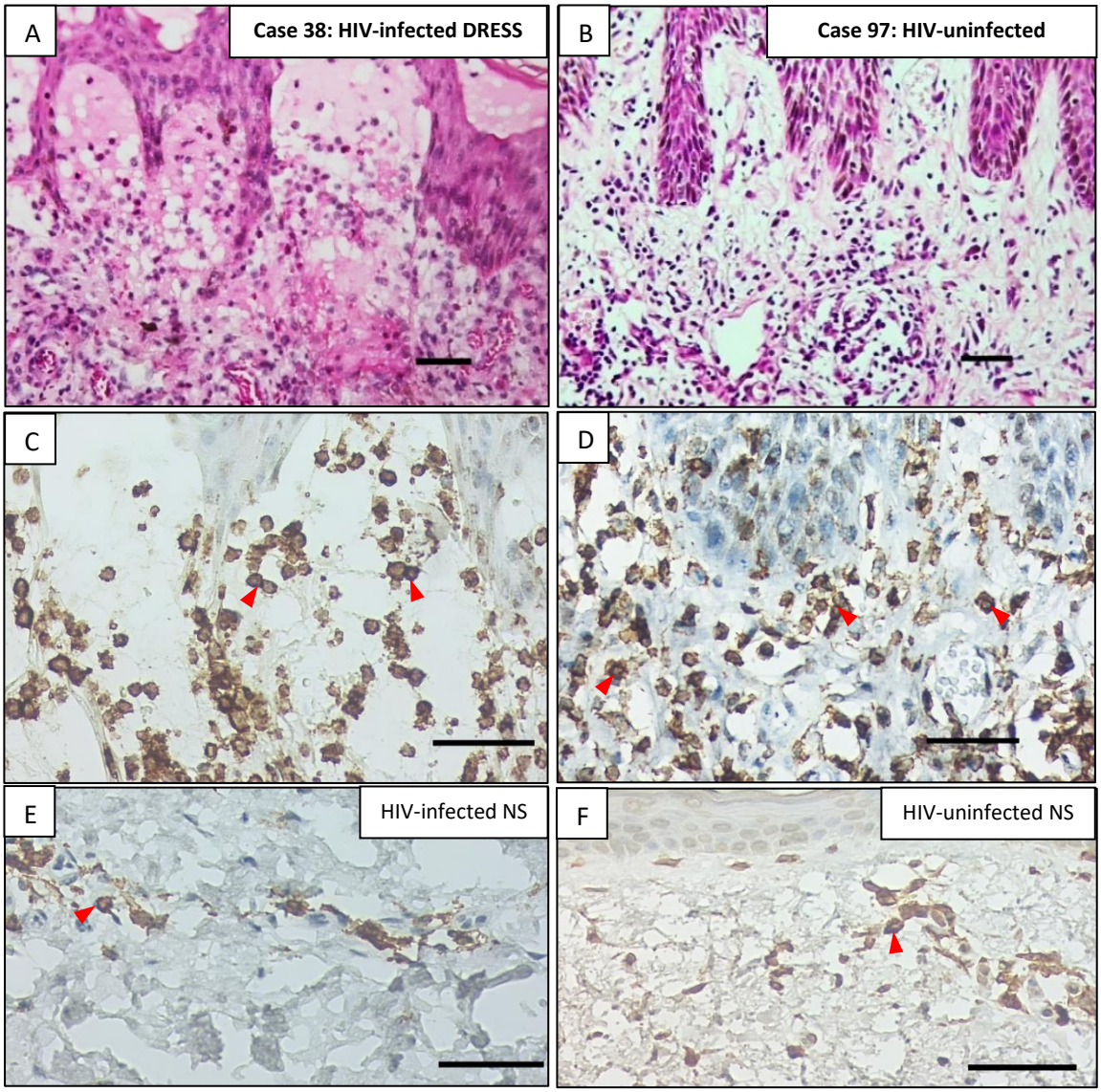

Figure 3-19: Immunohistochemistry staining of CD45RO+ T-cells in HIV-infected and HIV-uninfected DRESS. Dense infiltration of CD45RO+ T-cells can be observed in both HIV-infected (**C**) and uninfected DRESS (D**)** compared to HIV-infected (**E**) and uninfected normal skin (**F**). H&E images are at 200x, scale bar = 50µm; IHC images are at 400x, scale bar = 50µm.

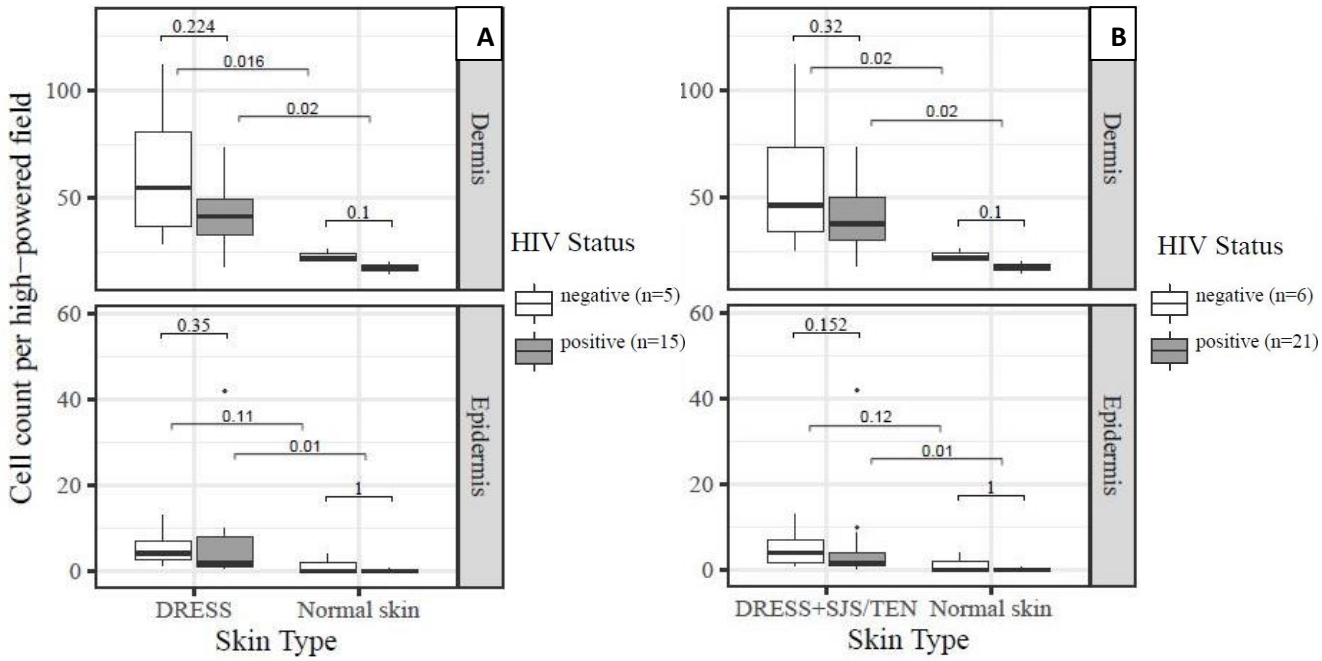

Figure 3-20: Comparison of CD45RO+ T-cell staining as a percentage of all CD3+ cells in dermal and epidermal compartments of HIV-infected and uninfected DRESS only and DRESS + SJS/TEN combined (SCAR). (**A**) A significant increase in dermal (P = 0.02; 0.016) and epidermal (P = 0.01; 0.11) CD45RO+ T-cell staining is noted in HIV-infected and uninfected DRESS compared to HIV-infected and uninfected normal skin, respectively. (**B**) A similar trend can be noted in the counts of DRESS and SJS/TEN combined.

To determine which T-cell sub-population displayed a higher effector memory phenotype, a CD4+/CD8+ and CD45RO+ cells double fluorescent staining was performed (Figure 3-21). On gross appearance, both CD4+ and CD8+ cells displayed CD45RO+ co-expression amongst HIV-infected DRESS and SJS/TEN. However, due to CD4+ T-cell depletion observed in HIV-infected cases, co-expression of CD4+ with CD45RO+ (Figure 3-21C) was observed to a lesser extent when compared to CD8+CD45RO+ co-expression (Figure 3-21B). Both CD4+ and CD8+ cells displayed a high CD45RO+ co-expression amongst HIV-uninfected SCAR. These cells were quantified amongst 4 HIV-infected and 3 HIV-uninfected DRESS cases only. Overall, no significant differences were observed in the number of dermal CD8+ cells co-expressing CD45RO+ as a percentage of CD8+ cells present amongst HIV-infected (n=4) versus HIV-uninfected DRESS patients (n=3); [median IQR %CD8+ co-expressing CD45RO+, 80 (78 - 83) versus 78 (74 - 82); p =0.47]. Similarly, no significant differences were observed in the number of dermal CD4+ cells co-expressing CD45RO+ as a percentage of CD4+ cells present amongst HIV-infected versus uninfected DRESS; [77 (76 - 78) versus 76 (76 - 78); p = 1.00] (Figure 3-22).

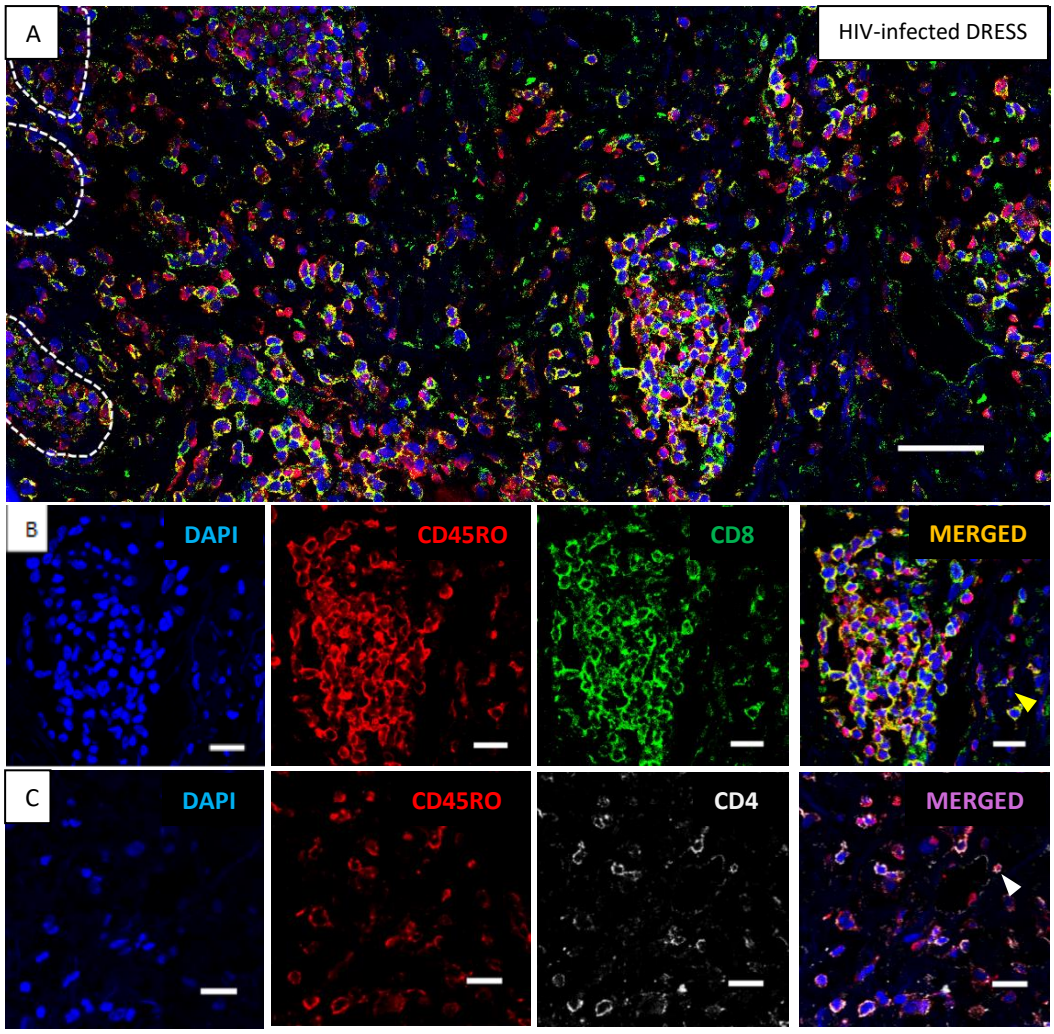

Figure 3-21: Co-expression of CD45RO+ with CD8+ and CD4+ cells in HIV-infected DRESS (**A**). CD8+CD45RO+ (**B**, white arrowhead) and CD4+CD45RO+ double staining (**C**, yellow arrowhead). Scale bars: A = 20µm; B&C = 50µm.

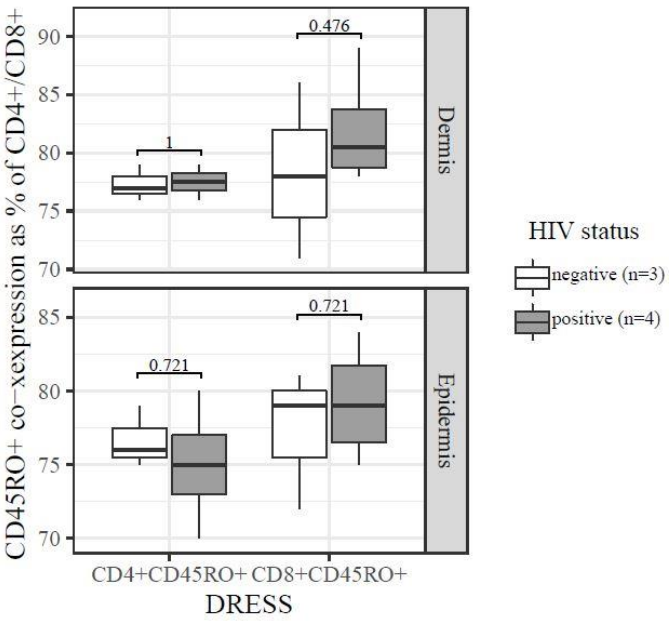

Figure 3-22: Comparison of dermal and epidermal infiltration of CD4+/CD8+ cells co-expressing CD45RO amongst HIV-infected and uninfected DRESS patients. No Significant differences can be observed although a trend towards an increase in dermal and epidermal CD8+CD45RO+ co-expression is seen amongst HIV-infected DRESS patients.

Basic IHC differences between HIV single and multiple drug reactors

The immunohistological phenotypes between HIV-infected SCAR patients clinically reacting to a single drug were compared to those reacting to multiple unrelated medications. HIV-infected DRESS and SCAR patients reacting to multiple unrelated medications were associated with a non-significant increase in the infiltration of dermal and epidermal CD3+ lymphocytes compared to single drug reactors. This was associated with a significant increase in dermal CD4+ T-cells in multiple drug reactors (n=4) compared to single drug reactors (n=12) amongst HIV-infected SCAR patients; (32 (23 - 41) versus 15 (11 - 20) cells/high-powered field, p = 0.0336). A similar trend was observed amongst HIV-infected DRESS patients, although not statistically significant; (24 (22 - 32) versus 18 (12 - 21) cells/high-powered field, p = 0.15). No difference in the peripheral blood CD4 cell counts were noted between DRESS single versus multiple drug reactors, mean CD4 count (IQR) 86.5 (52.5 – 281.8) cells/µl and 141 (103.5 – 141.5) cells/µl respectively, p = 0.73; similarly in the counts of DRESS and SJS/TEN cases combined (p = 0.39).

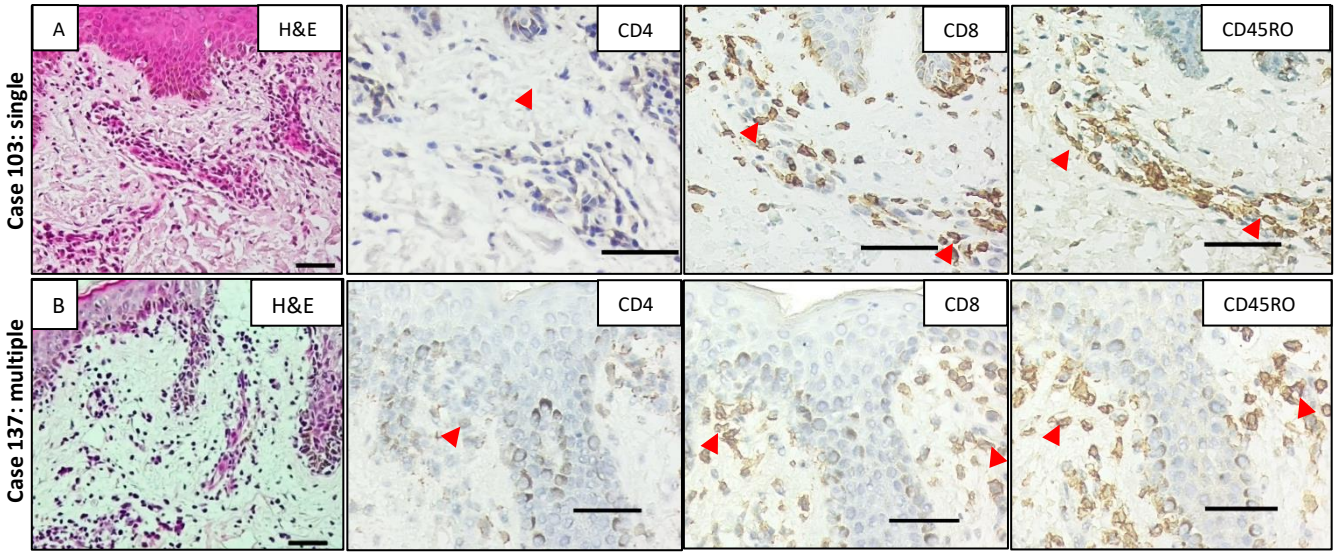

Figure 3-23: Immunohistochemistry staining of CD4+, CD8+ and CD45RO+ cells in HIV-infected DRESS single and multiple drug reactors. (**A**) Histopathologic examination for case 103 revealed a perivascular dermatitis with focal interface inflammations and isolated eosinophils. (**B**) Case 137 on H&E staining revealed interface dermatitis with mild eosinophilia compatible with a drug

reaction; and CD8+ and CD45RO+ cells display a similar distribution of cells for both cases, with an expected decrease in CD4+ cells. H&E images are at 200x, scale bar = 50µm; IHC images are at 400x, scale bar = 50µm.

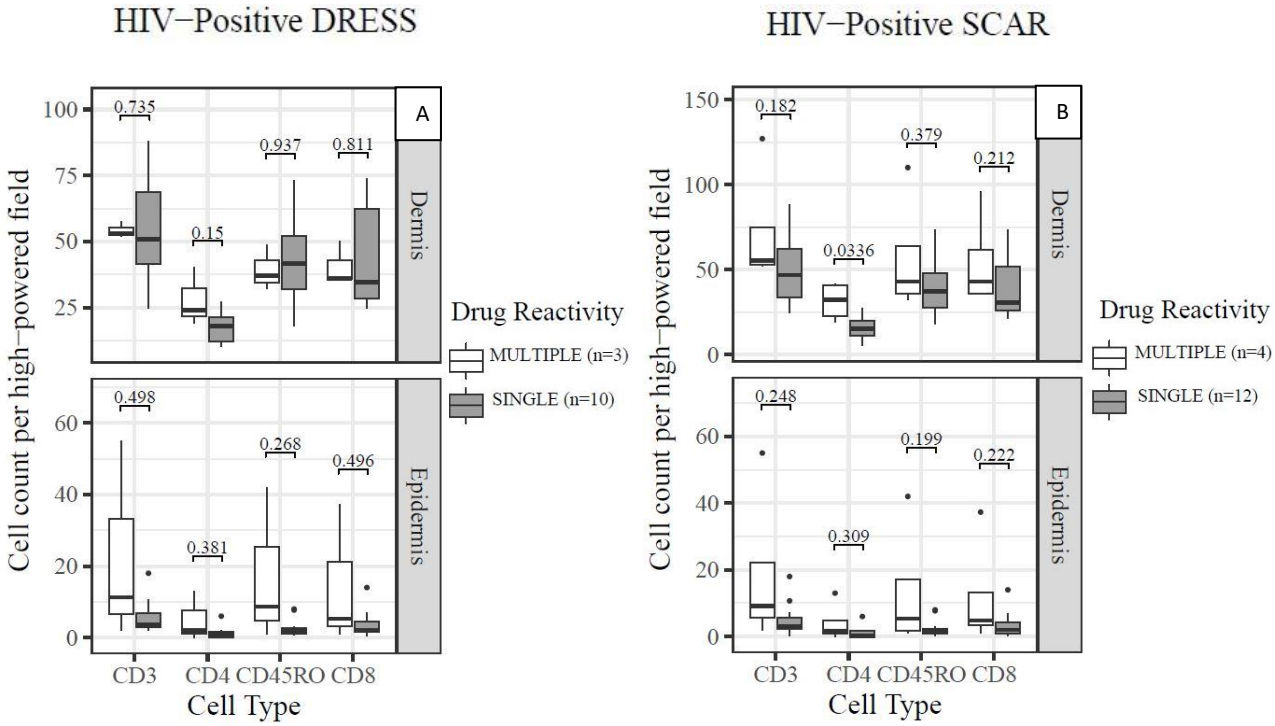

Figure 3-24: Comparison of dermal and epidermal infiltrates of the different T cell types amongst single and multiple drug reactors in HIV-infected DRESS only and DRESS + SJS/TEN combined (SCAR). A significant increase in the dermal infiltration of CD4+ T-cells in multiple drug reactors can be seen amongst HIV-infected SCAR cases (**B**). A similar trend is observed in HIV-infected DRESS cases (**A**), although not significant.

3.6. Regulatory T-cell assay

Treg-specific confocal microscopy was performed on skin sections, staining for CD3+, CD4+, and FOXP3+ colocalization. Due to the relatively low numbers of Tregs observed, a larger area of the section was analysed. Treg counts were reported as density of cells/mm^2, as well as frequency as a percentage of CD4+ T cells. Overall, very few cells were observed in the epidermis or at dermoepidermal junction, while majority were detected in the superficial to mid dermis, appearing in areas of clustered CD4+ cells.

HIV-infected cases

There were no significant differences observed in the epidermal distribution of Tregs amongst HIV-infected DRESS (Figure 3-25) versus HIV-infected SJS/TEN (Figure 3-26), although a non-significant increase in dermal Tregs was observed in DRESS cases (10 (0-26) versus 9 (3 - 19) cells/mm^2), p = 1.0). These low Treg numbers observed in SJS/TEN (n=2) corresponded to a sparse lymphocytic infiltration revealed by H&E staining, while a higher infiltration was observed in TEN cases (n=4); [2 (1-2) cell/mm^2 versus 17 (10 – 26) cells/ mm^2, p =0.133].

HIV-infected DRESS patients with true positive reactions to multiple drugs (n=2) showed a non-significant increase in the density of dermal Tregs compared to those reacting to a single drug (n=10); (42 (37 - 47) cells/mm^2 versus 10 (2-19) cells/mm^2, p = 0.064) (Figure 3-27). A significant increase in Treg infiltration was observed in the epidermis of multiple drug reactors, p = 0.0344. In the counts of DRESS and SJS/TEN combined (SCAR), there was a significant increase in the dermal Treg infiltration in multiple drug reactors (n=3) compared to single drug reactors (n=12); (39 (36-48) versus 10 (1-22), p-value = 0.0241, similarly in epidermal Treg counts, p = 0.007. We further categorized the Treg counts in HIV-infected SCAR patients by the number of days from symptoms onset to skin biopsy sampling; patients sampled ≤7 days versus >7 days from the onset of clinical symptoms (Figure 3-28). A trend towards an increase in the dermal infiltration of Tregs was observed in DRESS patients sampled ≤7 days from onset of symptoms.

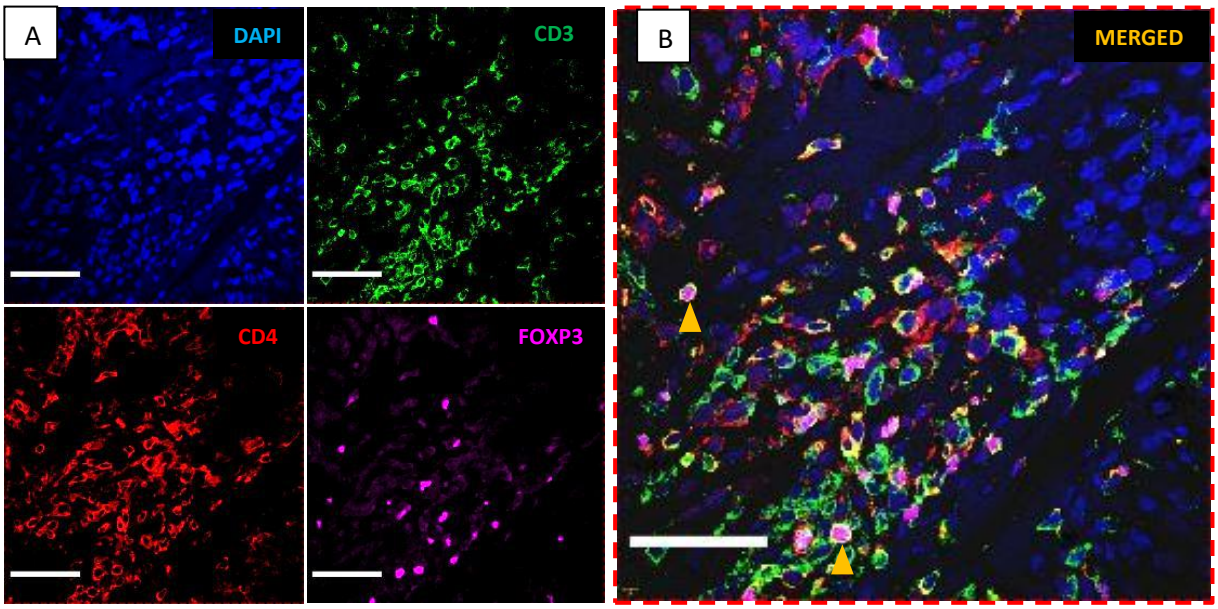

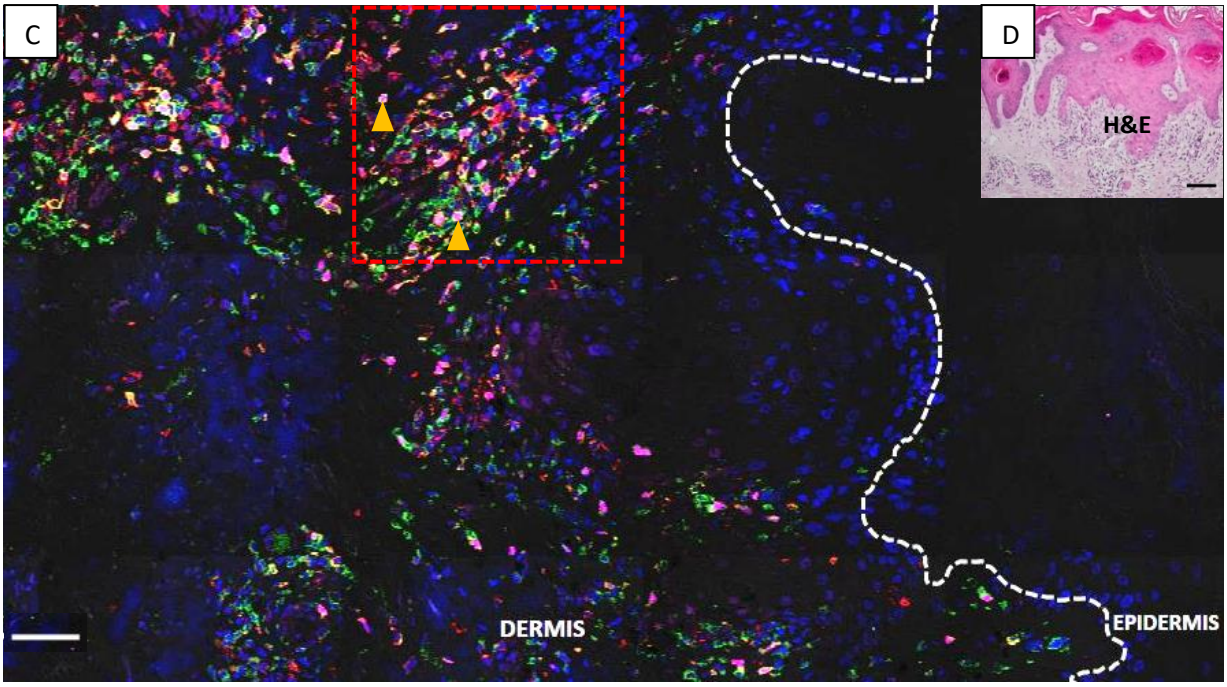

Figure 3-25: Confocal microscopy Treg staining in case 15, HIV-infected DRESS. (See patient timeline in Figure A-1) (**D**) Histopathologic examination on H&E staining revealed a basketweave hyperkeratosis with spongiosis in the epidermis and a dermal superficial perivascular interface dermatitis with eosinophils. The red arrowheads denote colocalization of CD3+CD4+FOXP3+ Treg cells (**B**). Most Treg cells can be observed in the superficial to mid dermis, and a few in the epidermis (**C**). Dotted white line denote the boundary between the epidermis and dermis (dermoepidermal junction). Scale bar = 100µm

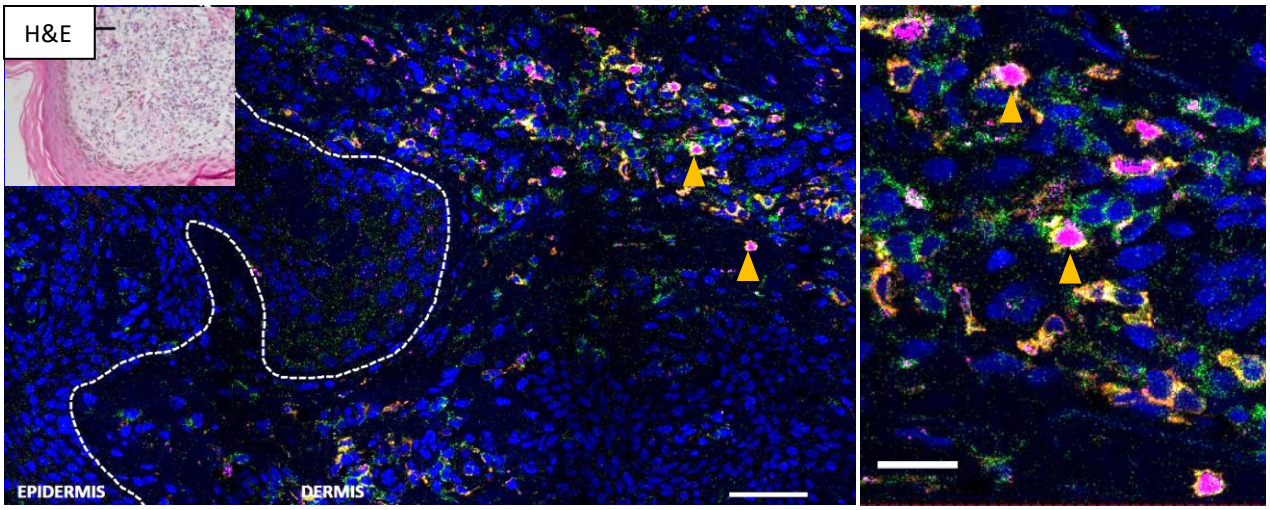

Figure 3-26: Confocal microscopy Treg staining in case 52, HIV-infected TEN. (See patient timeline in Figure 3-3). Histopathologic examination on H&E staining revealed a lichenoid dermatitis, compatible with a drug reaction. Similar to DRESS, Tregs were mostly distributed in the superficial dermis. Scale bar, 100µm.

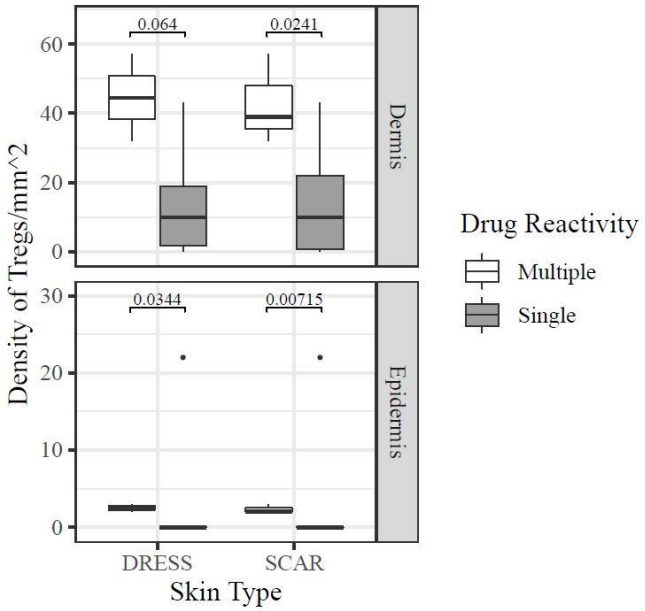

Figure 3-27: Density of Tregs/mm^2 between HIV-infected single and multiple drug reactors. DRESS single drug reactors (n=10) and multiple drug reactors (n=2). SCAR single drug reactors (n=12) and multiple drug reactors (n=3). A significant increase in Tregs is observed in both the dermis and epidermis of multiple drug reactors amongst HIV-infected SCAR cases. A similar trend is observed amongst HIV-infected DRESS cases.

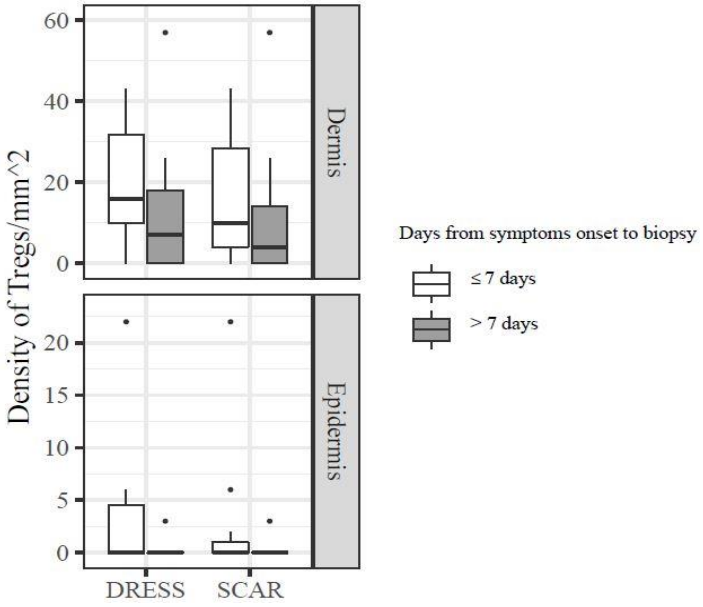

Figure 3-28: Density of Tregs in HIV-infected DRESS and SCAR (DRESS + SJS/TEN) cases sampled ≤7 days versus >7 days from onset of clinical symptoms.

HIV-uninfected cases

As demonstrated by immunohistochemistry staining, HIV-uninfected DRESS was associated with a high infiltrate of CD4+ T-cells in the dermis. In contrast, a low and very sparse distribution of Tregs was observed in the dermis, with little to none in the epidermis of HIV-uninfected cases (Figure 3-29 A&B). The frequency of Tregs in relation to the number CD3+CD4+ T-cells present was also decreased when compared to HIV-infected DRESS & SCAR (Figure 3-31 B&D.). Overall, the density of dermal Tregs was depleted in HIV-uninfected DRESS (n=5) compared to HIV-infected DRESS (n=14), although this was not statistically significant (4 (3 -8) cells/mm^2 versus 10 (0 - 30) cells/mm^2, p = 0.325). A similar observation was observed in the overall dermal counts of SCAR (DRESS and SJS/TEN combined), (4 (3 - 7) cells/mm^2 versus 10 (1 - 27) cells/mm^2, p = 0.28).

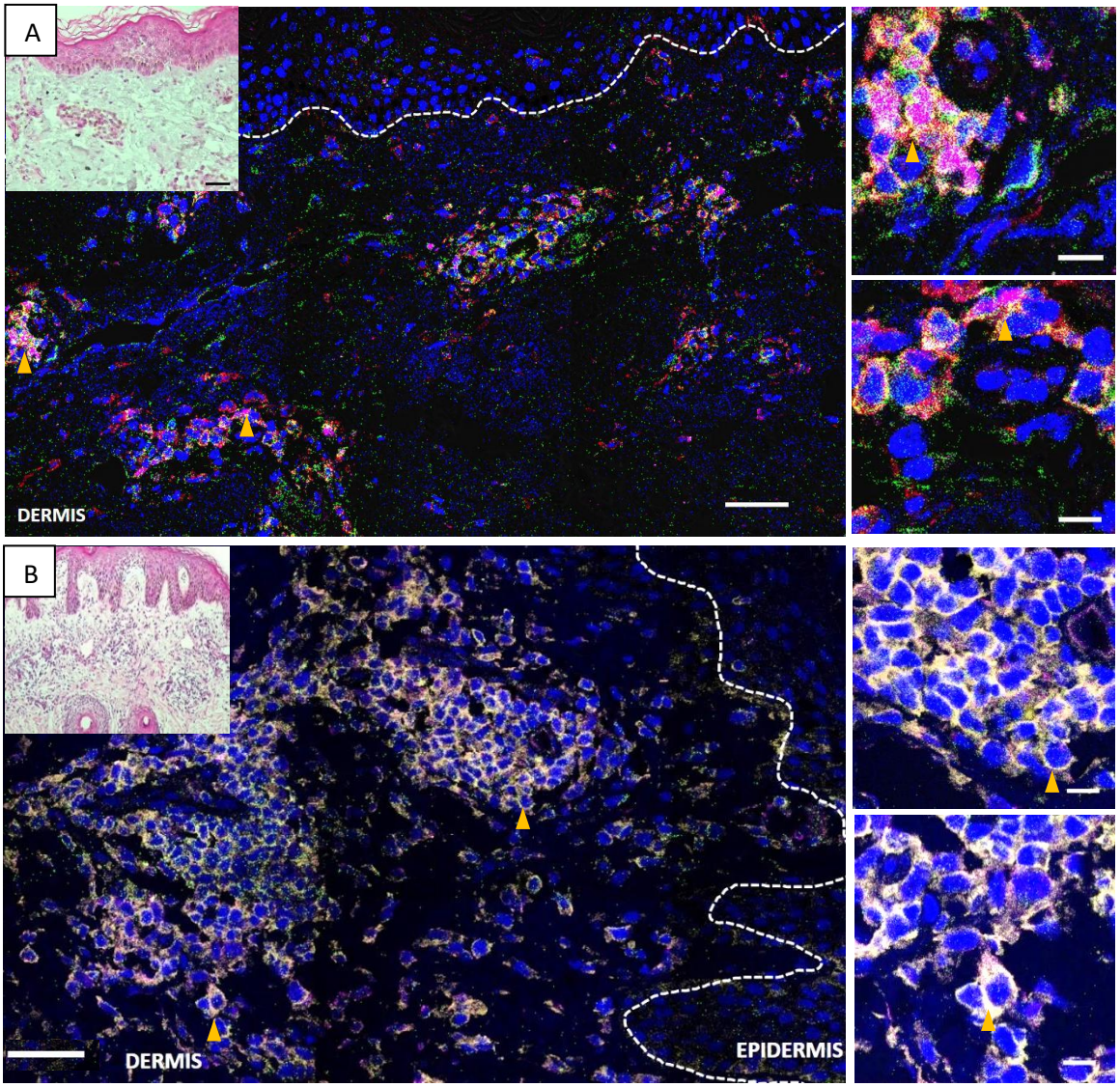

Figure 3-29: Confocal microscopy Treg staining in HIV-uninfected DRESS cases 102 (A) and case 97 (B). (A) See disease progression timeline for patient 102 in Figure A-6. (B) Histopathologic

examination on H&E for case 97 staining revealed a mild superficial dermal perivascular lymphocytic inflammation with low eosinophils on histopathological examination (See patient timeline in Figure A-5). A sparse dermal distribution of Tregs can be noted for case 102. Case 97 displayed a very high CD4+ skin count, although little to no active Tregs were present. Scale bar, 50µm (A) and 100µm (B).

HIV-infected and uninfected normal skin

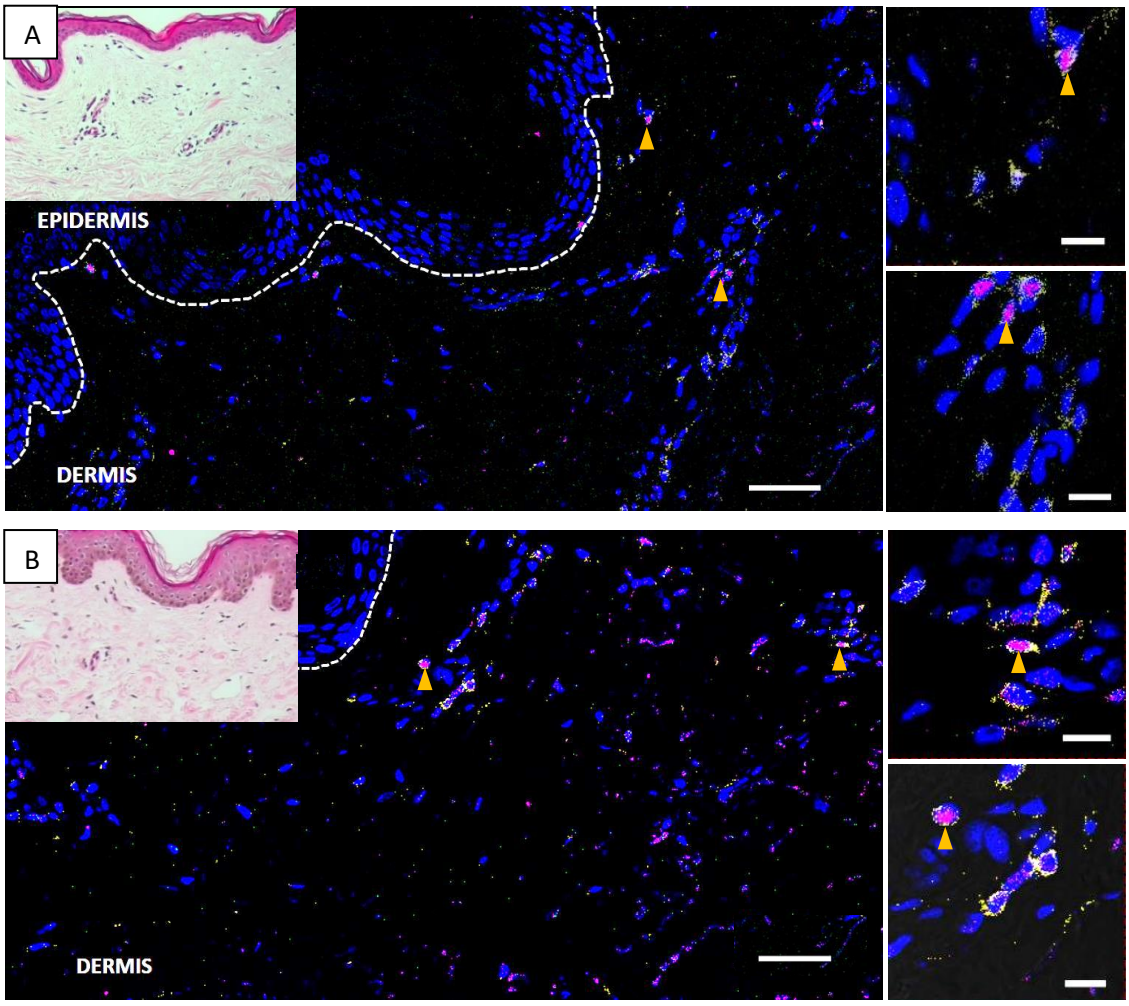

Figure 3-30: Distribution of Tregs in HIV-infected (A) and HIV-uninfected (B) normal skin. Low distribution of Tregs can be observed for both, however a high frequency in relation to the number of CD4+ cells present can be noted. Scale bars, 50µm.

Despite the dense infiltration of CD4+ T cells observed in HIV-uninfected DRESS cases, there was no significant differences in the density of dermal and epidermal Tregs observed when compared to HIV-uninfected normal skin, $p = 0.71$ and $p = 0.86$ respectively (Figure 3-31 A); similarly in the counts of DRESS and SJS/TEN combined (Figure 3-31 D). A similar trend was observed between HIV-infected DRESS and SCAR versus HIV-infected normal skin (Figure 3-31 A-D). Notably, there was a trend toward an increase in the frequency of Tregs as a percentage of CD4+ T-cells

observed in the dermis of HIV-infected normal skin compared to HIV-infected DRESS [13 (8 - 21) versus 7 (0 – 24), p = 0.73]; and similarly, between HIV-uninfected normal skin versus HIV-uninfected DRESS [12 (11 - 13) versus 3 (0 - 5), p = 0.25] (Figure 3-31B). A similar trend was observed in frequency of Tregs in the counts of DRESS and SJS/TEN combined (Figure 3-31D). However, no differences were observed in the frequency of Tregs between HIV-infected and uninfected normal skin.

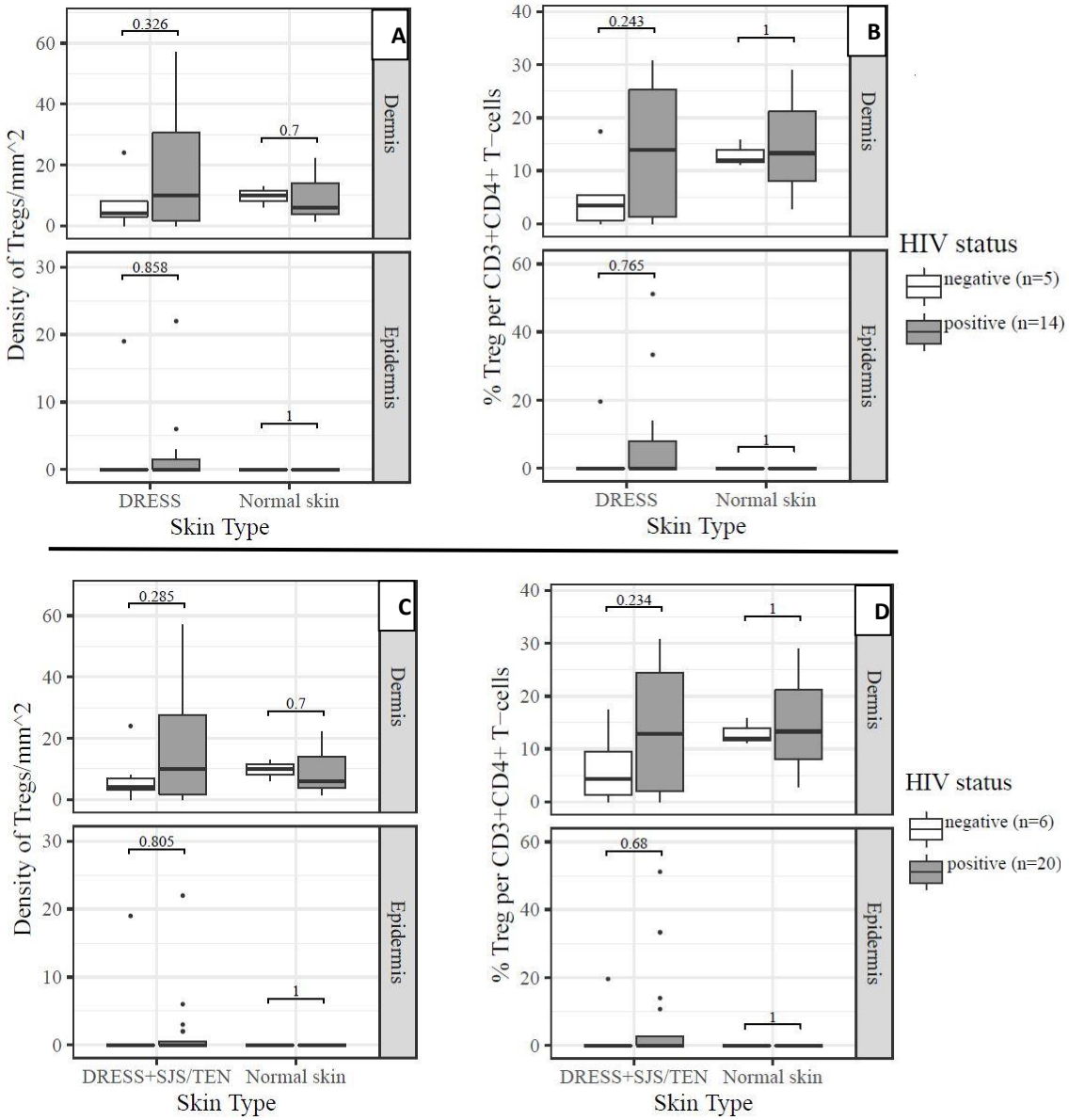

Figure 3-31: Quantification of Tregs amongst HIV-infected and uninfected DRESS only and DRESS + SJS/TEN combined (SCAR). Density of Tregs/mm^2 in HIV-infected and uninfected DRESS (**A**) and SCAR (DRESS+ SJS/TEN) (**C**). Frequency of Tregs expressed as a percentage of CD4+ T-cells present in DRESS (**B**) and SCAR (DRESS+ SJS/TEN) (**D**).

3.7. Increased skin infiltrating Tregs in an HIV-infected DRESS patient with a long delay between symptoms onset and skin biopsy.

A definite DRESS patient secondary to rifampicin and isoniazid, stood out amongst the HIV-infected SCAR cases. This patient was sampled 73 days after the onset of clinical symptoms, and not in the acute stage of reaction. The patient is HIV positive on ART and was diagnosed with extrapulmonary TB (urine LAM+). They were started on rifafour (FDC), which was later changed to rifinah, and they presented with first skin symptoms characterized by an 80% BSA skin rash, erythema, epidermal necrosis, and typical target lesions, and all drugs were stopped. Their most recent serum CD4 count at the time of reaction was 142 cells/mm^3 and the patient was on ART. They presented with deranged LFTs (AST (43), ALP (456) and GGT (307)), although eosinophils were normal (0.37 x 10^9/l). Histopathologic examination on H&E was consistent with a drug reaction, revealing hyperkeratosis, parakeratosis, and acanthosis in the epidermis, with an interface dermatitis resulting in epidermal spongiosis and basal vacuolar degeneration. Scattered dermal eosinophils were present. On day 71, the patient was restarted on rifinah and ART, and they developed a new rash. rifinah was changed to individual rifampicin and isoniazid and another rash developed, with deranged LFTs. However, skin symptoms were managed by applying topical dovate and the rash resolved and LFTs normalized, and the patient was discharged on rifampicin, isoniazid and dovate. They were readmitted again on day 92 after developing new skin symptoms secondary to the discharge regimen. The concentration for topical dovate was increased and temporarily managed the rash, but symptoms later worsened, and all treatment was stopped. On readmission, the patient had a positive polymerase chain reaction (PCR) to CMV accompanied by as positive IgG test for CMV and EBV. A timeline for the patients' disease progression is shown in Figure 3-32.

Immunohistochemistry staining revealed a very dense infiltration of CD8+ and CD45RO+ T-cells in both dermal and epidermal compartments, and CD4+ T-cells to a lesser extent (Figure 3-33). Despite the low infiltration of CD4+ T-cells compared to CD8+ and CD45RO+ cells, the CD4+ infiltration was higher for this patient when compared to that observed in all HIV-infected SCAR cases sampled in the acute phase of reaction. Of note though was the comparatively high infiltration of Tregs, with a density of 107 and 193 cells/mm^2 in both epidermal and dermal compartments, respectively.

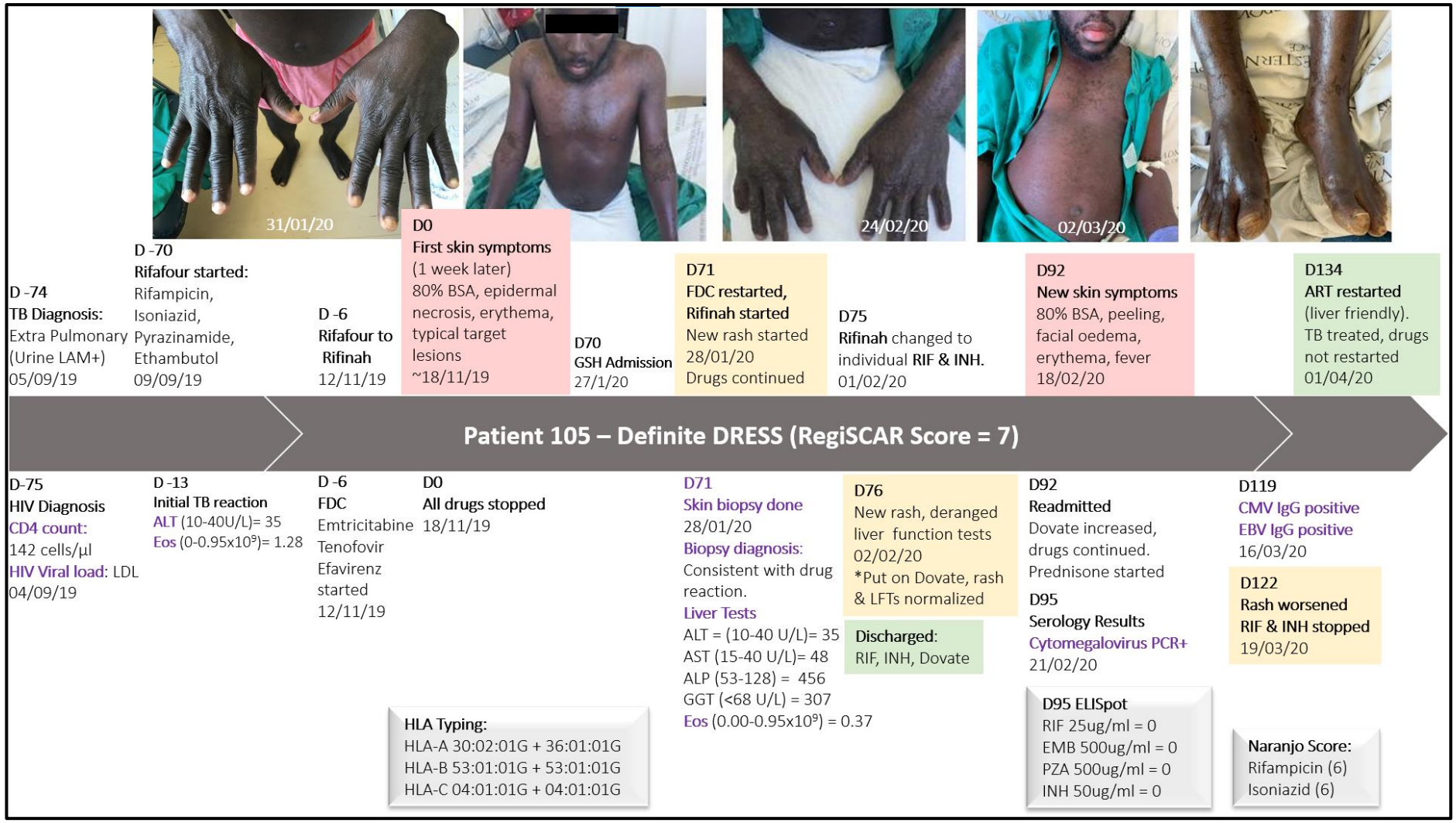

Figure 3-32: Disease progression timeline for patient 105. An HIV positive 35-year-old male definite DRESS patient with extrapulmonary TB. The patient was on ART and rifafour at the time of reaction.

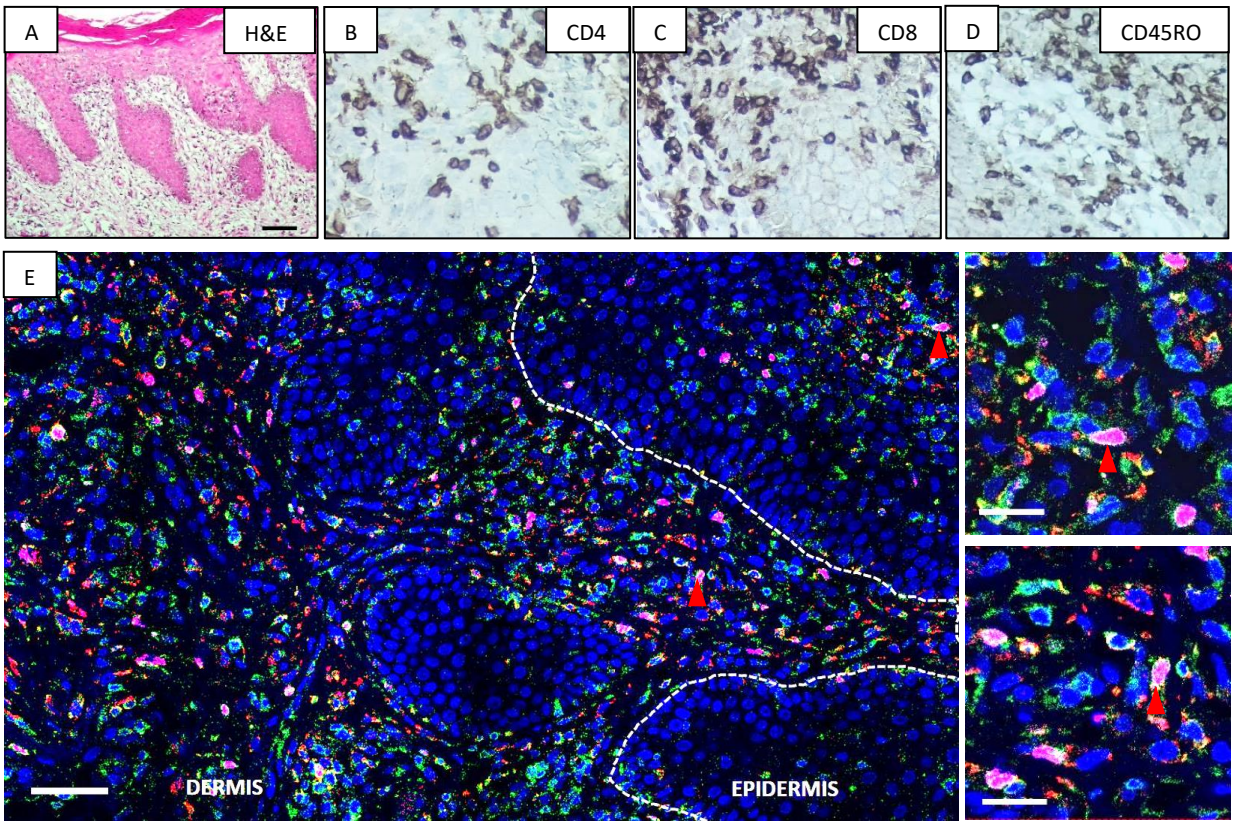

Figure 3-33: Increased infiltration of Tregs and effector T cells in case 105, HIV-infected DRESS patient. Histopathologic examination on H&E (**A**) staining showed hyperkeratosis, acanthosis, spongiosis and parakeratosis. The epidermis showed multiple apoptotic keratinocytes and an interface inflammation with basal vacuolar degeneration, all compatible with a drug. A dense infiltration of CD8+ (**C**) and CD45RO (**D**) T-cells can be noted, and to a lesser extent CD4+ T-cells (**B**). The skin was infiltrated with a high number of Tregs (**E**) in both dermal and epidermal compartments. Scale bar, 100µm.

3.8. Association between dermal CD4+ or Treg counts with demographic or clinical characteristics.

We examined for correlations between clinical or demographic characteristics with dermal numbers of CD4 T cells and Tregs. Figure 3-34, Figure 3-35, and Table A-6 summarize the correlation analysis in HIV-infected and uninfected DRESS patients; and Table A-7 shows association with SCAR patients (DRESS & SJS/TEN combined), respectively. We found a significant negative correlation between age and dermal Tregs counts in HIV-infected SCAR patients ($R^2 = 0.396$, $p = 0.003$). A similar trend was observed amongst HIV-infected DRESS ($R^2 = 0.402$, $p = 0.015$). We found a trend toward a positive correlation between dermal Tregs and days from onset of symptoms to sampling amongst HIV-uninfected SCAR ($R^2 = 0.869$, $p = 0.007$); and similarly, amongst HIV-uninfected DRESS ($R^2 = 0.869$, $p = 0.021$). There was a positive correlation between dermal Tregs and eosinophil counts amongst HIV-uninfected DRESS ($R^2 = 0.945$, $p = 0.006$); and similarly, amongst HIV-uninfected SCAR ($R^2 = 0.878$, $p = 0.006$). Amongst HIV-uninfected DRESS, there was an association between dermal Tregs and BSA skin rash ($R^2 = 0.909$, $p = 0.012$); and similarly, amongst HIV-uninfected SCAR ($R^2 = 0.781$, $p = 0.02$). Dermal Tregs and CD4 counts were positively associated with the enzyme ALT amongst HIV-infected DRESS ($R^2 = 0.441$, $p = 0.01$ and $R^2 = 0.289$, $p = 0.047$ respectively. However, using Bonferroni correction for multiple comparisons, p values ≥ 0.005 were considered not statistically significant. No significant correlations were observed between serum CD4 counts or log viral loads with dermal CD4+ and Tregs counts amongst HIV-infected DRESS and SCAR patients. It must be noted that majority of the viral loads and CD4 counts recorded were not within the same time frame as the biopsy sampling period, and thus may not give an accurate indication of HIV disease state. No significant correlation was observed between dermal CD4 or Treg counts with RegiSCAR severity scores amongst HIV-infected and uninfected patients.

An exploratory multivariate linear regression analysis was performed to determine predictors for dermal Tregs amongst HIV-infected and uninfected SCAR cases (n=26) and HIV-infected SCAR cases (n=20) (Table 3-8). Independent variables tested for included days from symptoms onset to biopsy, HIV status, SCAR phenotype, eosinophil count, ALT, serum CD4 count and the BSA skin rash. No significant association was observed between dermal Tregs, and all the independent variables tested.

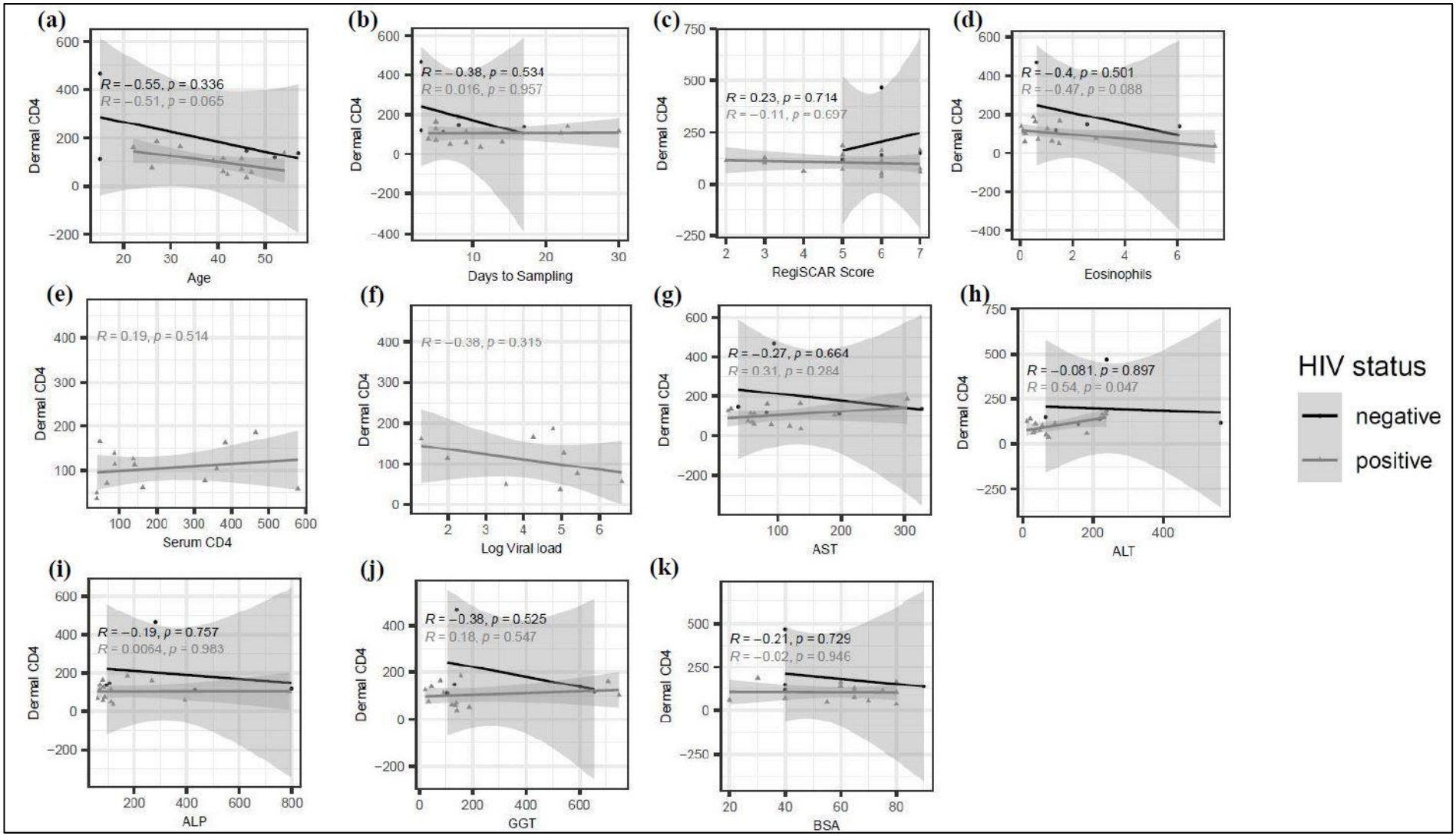

Figure 3-34: Association between dermal CD4 counts with demographic and clinical characteristics in HIV-infected & uninfected DRESS. Using Bonferroni correction, P-values ≤ 0.005 were considered significant. *HIV viral loads were log transformed to permit the use of a linear model.

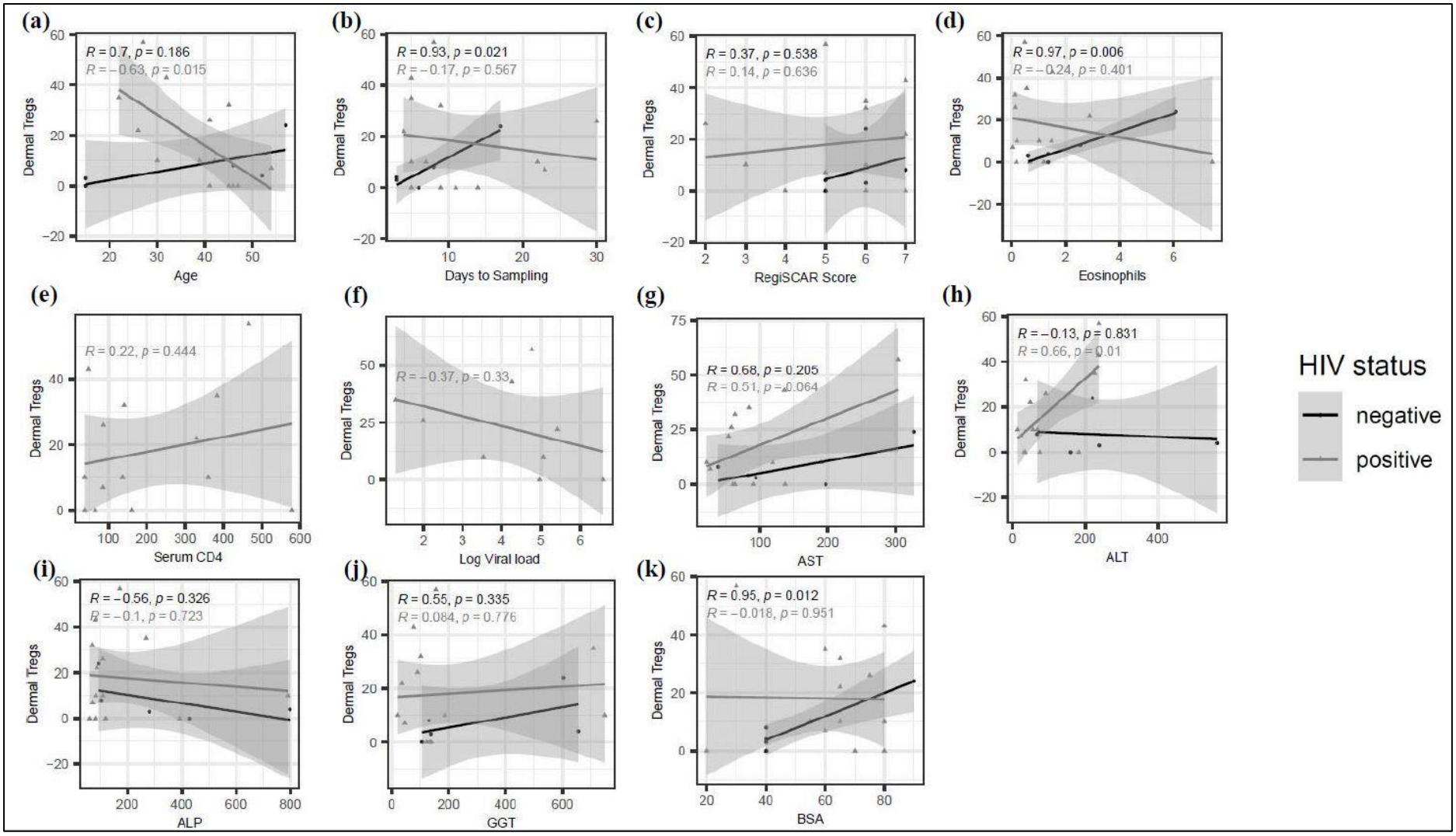

Figure 3-35: Association between dermal Treg counts with demographic and clinical characteristics in HIV-infected & uninfected DRESS. Using Bonferroni correction, P-values ≤ 0.005 were considered significant. *HIV viral loads were log transformed to permit the use of a linear model.

Table 3-8: Association between dermal Treg counts clinical characteristics in all DRESS and SJS/TEN patients.

INDEPENDENT VARIABLE	DEPENDENT VARIABLE = DERMAL TREG COUNTS (CELLS/MM^2)	
	Multivariate r^2 (coefficient, p value)	
	All patients (n=26) [a]	HIV-infected patients (n=20)
	r^2 = 0.168	r^2 = 0.187
Days from symptoms onset to sampling	(-0.161, 0.482)	(-0.266, 0.338)
HIV status	(-0.271, 0.294)	-
SCAR phenotype	(-0.177, 0.459)	(-0.191, 0.543)
Eosinophil count	(-0.140, 0.573)	(-0.259, 0.379)
Alanine aminotransferase (ALT)	(0.182, 0.506)	(0.142, 0.634)
Serum CD4 count	-	(0.137, 0.641)
Percentage BSA skin rash	(0.322, 0.236)	(0.206, 0.483)

[a] Serum CD4 count variable excluded from analysis due to missing data for HIV-uninfected patients.

*****Multivariate regression for HIV-uninfected patients not done due to small sample size.

4. DISCUSSION

Globally, DRESS and SJS/TEN are the two most frequent SCAR clinical manifestations, with an up to 100-fold increased risk amongst persons living with HIV (Peter et al., 2019). In South Africa, the high prevalence of TB coinfection amongst persons living with HIV generates a considerable prescribing pressure, and first-line anti-tuberculosis drugs (FLTD) and cotrimoxazole prophylaxis antibiotics are the most common offenders for SCAR. DRESS and SJS/TEN cause considerably high morbidity and mortality globally, and in the context of advanced HIV-related immunosuppression create massive treatment complexity and considerable healthcare costs (Knight et al., 2019). Research to better understand the immune mechanisms underlying these SCAR in the context of the vulnerable and immunologically distinct HIV population is urgently required to aid any prevention, diagnostic or treatment tools and strategies.

The hallmark feature of advancing HIV is CD4 T cell depletion, but several aspects of immune dysregulation such as expansion of effector memory cells and possible depletion of immunoregulatory mechanism have been proposed to be important drivers of SCAR (Peter et al., 2019). Detailed immunohistological study of site-of-disease samples is the starting point in understanding the key pathological immune cell subsets and getting early insights into immunopathogenesis. Surprisingly though, to date there is only one immunohistological study amongst persons with HIV and SCAR that have examined both effector and regulatory T-cells subsets. Thus, in the current study, we sought to characterize the immunophenotype of DRESS and SJS/TEN in our cohort of comorbid HIV-TB infection, with predominantly FLTD as offending agents. We outline histopathological and immunohistological differences of DRESS and SJS/TEN patients with and without HIV co-infection, and furthermore we examine for immunohistological features that may predict patients likely to have clinical reactivity to more than one drug during SDC.

Histological appearance of DRESS and SJS/TEN similar in HIV-infected and uninfected cases

The diagnosis of DRESS and SJS/TEN can be challenging due to heterogeneity in clinical presentations, as well as overlapping dermatological and other clinical features with non-drug driven skin diseases. Certain histopathologic features are associated with SCAR phenotypes, and histology is included in most published validation tools for DRESS and SJS/TEN (Kardaun et al., 2007, Kardaun et al., 2014, Bastuji-Garin et al., 1993, Sasidharanpillai et al., 2022). A female predominance of our study population, the clinical presentations of skin eruptions, haematological changes and histopathologic findings were consistent with existing DRESS (Ortonne et al., 2015,

Walsh et al., 2013, Chi et al., 2014, Borroni et al., 2014, Wongkitisophon et al., 2012, Maoz and Brenner, 2007, Weinborn et al., 2016) and SJS/TEN cohorts reported in literature (Orime, 2017, Wetter and Camilleri, 2010, Weinborn et al., 2016), thus the majority of HIV-infected SCAR cases were RegiSCAR validated as definite or probable DRESS or SJS/TEN cases. Consistent histopathological changes in DRESS have been reported in several studies in literature. Ortone et al. compared histopathological changes between DRESS and maculopapular rash (MPR) patients and revealed various inflammatory patterns frequently seen in DRESS including foci of interface dermatitis, apoptotic keratinocytes, lymphocytic exocytosis, and a dermal infiltration of predominantly neutrophils and eosinophils (Ortonne et al., 2015). A similar study by Chi et al. compared clinicohistopathological features of 32 patients with RegiSCAR defined probable/definite DRESS to 17 patients with MPE. They revealed that major pathological changes more frequent in DRESS than in MPE included dyskeratosis and spongiosis in the epidermis, interface vacuolization at the dermoepidermal junctional, and a perivascular lymphocytic infiltration with eosinophils (Chi et al., 2014). In some studies, these histopathologic findings in DRESS have been used as prognostic markers for disease outcome and severity. Walsh et al. reported the most frequent histopathological changes in a series of 27 DRESS to be spongiotic dermatitis and basal cell vacuolization with apoptotic keratinocytes. They reported that the presence of apoptotic keratinocytes was associated with a more severe phenotype, with liver injury and an erythema multiforme-like eruption of atypical targets (Walsh et al., 2013). Sasidharanpillai et al. in a study of 40 cases of DRESS showed a significant association between interface dermatitis with hepatic involvement (Sasidharanpillai et al., 2020). In the current study, similar histological patterns were observed in both HIV-infected and uninfected DRESS cases, with the most frequently reported findings including hyperkeratosis, spongiosis and apoptotic keratinocytes in the epidermis, focal interface dermatitis with basal vacuolar degeneration and exocytosis at the dermoepidermal junction, and a perivascular lymphocytic inflammatory pattern and pigmentary incontinence in the dermis. Of note amongst HIV-infected DRESS cases, apoptotic keratinocytes were observed in 80% of the cases (12 out of 15), compared to 25% (1 out 0f 4) in HIV-uninfected cases ($p = 0.07$). Seven out of the 12 HIV-infected DRESS cases with apoptotic keratinocytes presented with severe liver involvement, presenting as deranged LFTs. This finding supports reports in literature suggesting that apoptotic keratinocytes may be a prognostic marker in predicting severity of liver complications (Chi et al., 2014, Ortonne et al., 2015, Skowron et al., 2015, Walsh et al., 2013, Orime, 2017). Similar to DRESS, histopathologic changes observed in SJS/TEN cases were consistent with data reported in literature including formation of epidermal blisters, necrotic and apoptotic keratinocytes, and pigmentary incontinence (Wetter and Camilleri, 2010). These findings put together, reveal the diverse histopathologic presentations of these

reactions and further highlight that no finding is specific to confirm diagnosis, hence why a combination of these histopathological changes often serves as a diagnostic clue for clinical pathologists. The absence of any histopathological and morphological changes in both dermal and epidermal compartments of normal skin, and the low distribution of inflammatory infiltrates compared to those observed in SCAR further highlight the extent of cutaneous damage and severity of these reactions. Although this data suggest the overall histopathological picture of SCAR is similar in HIV-infected and uninfected patients, these numbers are small, particularly for SJS/TEN, and larger numbers for each phenotype are required to confirm these findings.

Effector T-cell infiltrates differ amongst HIV-infected and uninfected SCAR patients.

IHC staining of CD3, CD4 and CD8+ T-cells confirmed large numbers of these T-cells at the site of pathology in both HIV-infected and uninfected DRESS and SJS/TEN compared to normal skin. This support the primary role of drug-specific lymphocytes in the immune pathology of these reactions (Peter et al., 2017, White et al., 2015, Miyagawa and Asada, 2021). CD4+ T-cell infiltrates were reduced in the dermis of HIV-infected DRESS and SJS/TEN cases, with resultant increase in the ratio of CD8+/CD4+. These findings are consistent with the only other small previous study. Yang et at. characterized the composition of inflammatory infiltrates in 12 cases of TEN amongst HIV-infected and uninfected patients, reporting a decrease in CD4+ T-cell infiltrates and resultant significant increase in the ratio of CD8+/CD4+ cells in the dermis of HIV-infected patients (Yang et al., 2014). Notably, the changes in the CD8/CD4 ratio were mainly driven by the decrease in dermal CD4+ cells rather than an increase in CD8+ cells in HIV-infected SCAR cases when compared to HIV-uninfected SCAR cases. We did not find a correlation between serum and dermal CD4 T-cell counts in HIV-infected DRESS cases, indicating that although overall depletion of the circulating CD4+ T-cell pool is likely a major driver of this finding, several additional factors may impact individual CD4+ T-cell dermal infiltrates including CD4 cell activation and exhaustion status, migratory capacity/skin homing receptor expression and extent/duration of drug-induced antigenic stimulation.

The relationship between the peripheral CD4 T-cell counts and likelihood of developing drug reactions has produced conflicting data. Smith et al. observed an increased likelihood of developing drug reactions with decreasing serum CD4 counts and CD4/CD8 ratio in HIV-infected individuals, predominantly secondary to cotrimoxazole and other sulphonamide drugs. However, early studies have identified higher CD4 cell counts to be a predictor for SCAR. For instance, short-term nevirapine therapy in non-HIV-infected patients has been linked with serious hepatic and cutaneous reactions (Patel et al., 2004). In HIV-infected patients initiating nevirapine-containing cART, the risk for developing SJS and DILI was observed at CD4 cells counts

higher than 200 cells/mm^3 (Hasan et al., 2022, Tseng et al., 2014, Dube et al., 2013). There have also been studies where no association between CD4 counts and disease onset was found (Peters et al., 2010, Phanuphak et al., 2007). Mechanistically, a possible explanation to the increased risk for developing SCAR with decreasing CD4 cell counts is the direct effect of depleted CD4 T cells on professional APCs phenotype and expression of costimulatory markers essential for naïve and memory T cells activation. Cardone et al. developed a mechanism of tolerance or hypersensitivity to abacavir in an HLA-B*57:01-trangenic mouse model (Cardone et al., 2018, Phillips and Mallal, 2018). They reported that *in vivo* depletion of CD4+ T-cells in HLA-B57:01+ mice prior to abacavir administration enhanced the maturation of DCs to a $CD68^{hi}CD80^{hi}PD\text{-}L1^{hi}$ phenotype that is capable of co-stimulation and induction of ABC-reactive effector CD8+ T cells that can traffic to the skin and induce hypersensitivity. In immunocompetent transgenic mice and in the presence of CD4 T-cells, DCs remain in an immature state, and the mouse tolerates the altered peptide repertoire (Cardone et al., 2018, Phillips and Mallal, 2018).

CD45RO+ T-cells predominated across CD3+ T-cell infiltrates in the dermis of both DRESS and SJS/TEN patients, with no differences noted between HIV-infected and uninfected patients. There was, however, a trend toward increased dermal CD45RO+ T cell expression observed in HIV-uninfected DRESS and SJS/TEN cases compared to HIV-infected cases. The decrease in CD45RO+ expression in HIV-infected cases reflects depletion in CD4+ T cell counts observed when compared to HIV-uninfected cases, as further reflected by the decreased CD4+CD45RO+ co-expression as highlighted in Figure 3-19C. The presence of these memory cells in normal skin, particularly HIV-uninfected skin, shows that even in the resting unaffected/non-lesional skin, majority of resident skin T cells have previously encountered pathogen, and are antigen-primed to allow for a swift response on secondary antigen exposure (Bos et al., 1989). There is increasing evidence that effector memory T cells, particularly TRM cells, play a role in mediating skin disorders. Withing drug reactions, their role in FDE are the best described, where skin lesions reappear at the same skin site when patients are re-exposed to a causative drug (Schunkert et al., 2021, Mizukawa et al., 2002). In the context of SCAR, Iriki et al. reported a case of TEN that occurred in the absence of circulating drug-reactive T cells, but in the presence of skin resident CD69+CD45RO+CD4+ and CD8+ T cells, suggesting their role in disease pathogenesis (Iriki et al., 2014). Furthermore, Trubiano et al reported increased number of CD45RO+CD69+CD4+ and CD8+ TRM cells in DRESS patients after resolution of disease (Trubiano et al., 2020). These cells have also been described in other inflammatory skin disorders such as psoriasis and mycosis fungoides (Clark, 2015, Cheuk et al., 2014, Aladily et al., 2022). In psoriasis patients with

progressive psoriatic lesions and regressed plaques at remission, an excess of CD45RO+ T cells was observed when compared to the skin of healthy volunteers (Khairutdinov et al., 2017).

Activation of the TCR by the appropriate peptide-MHC ligand results in proliferation of peptide-specific lymphocytes into effector T cells which further generate effector memory T cells which are generally characterized by the cellular marker CD45RO, and lack of the naïve T cell marker CD45RA (White et al., 2015, Farber et al., 2014). The majority of CD45RO+ T-cells lack expression of the lymph node homing receptor CCR7, allowing them to maintain surveillance at peripheral tissues, including the skin (White et al., 2015). CD45RO+ memory T cells generally require fewer costimulatory signals/lower threshold for activation upon secondary antigen exposure (White et al., 2015). In the context of SCAR, these memory T cells likely migrate to the skin when exposed to antigens specific to drug, and may differentiate into skin TRM, residing indefinitely in the skin. Memory T cells against viral infections i.e., HHV or HIV constitute a significant proportion of the memory T cell pool, and have been proposed as contributory to SCAR in the heterologous immunity model (White et al., 2015). It has been proposed that these viral directed effector memory T-cells can cross-react with drug-specific epitopes resulting in SCAR (Almeida et al., 2019, Schunkert et al., 2021, White et al., 2015). The exploration of the viral-specificities of skin memory T-cells was beyond the scope of this project, but the specificities and role of HIV-specific tissue effector memory T-cells is a key future research focus. Although the percentage of CD4+ and CD8+ T cells expressing CD45RO+ amongst HIV-infected versus uninfected DRESS patients was similar, further phenotyping with additional cell surface markers of tissue residency including CLA+, CD69+ and CD103+ (effector central versus tissue resident memory) is required to better define tissue resident subsets where differences may be noted.

Inflammatory T-cell infiltrates differ between DRESS patients reacting to more than one versus a single anti-TB drug.

Sequential drug rechallenge remains the gold standard in establishing drug causality and is currently the preferred method to identifying offending drugs and rapidly allow the recommencement of tolerated anti-TB medications. The high mortality associated with TB in advanced HIV-infection means that patients frequently also need a bridging regimen of anti-TB drugs, that are not FLTDs, while the clinical and laboratory features of acute SCAR settle prior to SDC. Multiple drug hypersensitivities, neosensitisations and non-specific flare-up reactions are all described and debated in the DRESS literature (Pichler et al., 2017, Pichler et al., 2011, Jorg et al., 2020a, Jorg et al., 2020b, Jorg-Walther et al., 2015, Peter, 2016, Jin et al., 2021) Amongst patients having SCAR to FLTDs, reactions to multiple chemically distinct drugs is described amongst HIV-infected and uninfected cohorts (Jin et al., 2021, Lehloenya and Dheda, 2012, Lehloenya et al.,

2012). Patients reacting to multiple anti-TB drugs during bridging and SDC pose a particular challenge for both current and future treatment of TB, as this requires a minimum of four-drug therapy for six months. Thus, an improved understanding of the risk factors of reacting to multiple TB drugs, and the immunopathogenesis would be very useful to define which reactions can be treated through and which need to be permanently avoided. Current hypotheses included host and drug-related factors such as: i) true sensitization of T-cells to multiple, chemically distinct drugs, facilitated by the activated immune environment of acute DRESS, ii) lower thresholds for non-specific flare ups, and iii) viral reactivation of HHV (Pichler et al., 2017). The majority of these hypothesis have evidence for and against. For example, a study by Mardivirin et al. reported seven cases of amoxicillin-induced flare-ups in patients with DRESS induced by other drugs; demonstrating that amoxicillin increased the replication of HHV-6 *in vitro* (Mardivirin et al., 2010); the clinical implications of this are unclear. Similarly, *in vivo* (e.g., skin patch testing) or *in vitro* (lymphocyte transformation tests or ELISpot assay) has confirmed the presence of drug-specific T-cell reactivity to multiple drugs in the context of DRESS – whether this represents last sensitisation is unclear (Peter et al., 2017, Shiohara et al., 2012). Thus, there is a major unmet need to identify biomarkers and better define the different phenotypes of rechallenge reactions in the context of SCAR and in particular DRESS.

In this small cohort, there were three DRESS patients and one SJS/TEN patient that had positive drug challenge reactions to two or more structurally unrelated drugs, while 10 DRESS and two SJS/TEN patients only had a positive reaction to a single drug. Patient 15 is one HIV-infected SCAR case with multiple reactions and demonstrates the complexity of positive drug reactions in the acute DRESS period. Upon developing first skin symptoms and discontinuation of all treatment, the patient was put on a backbone regimen of MXF, ETA and TRZ prior to SDC. On SDC the patient had isoniazid positive rechallenge reaction with symptoms including headache, abdominal pain, vomiting blood, fever, deranged LFTs and temperature spike - clinically distinct from the admission reaction, but the drug was treated through successfully. Thereafter, MXF and ETA were erroneously omitted for 2 days, and when the patient was restarted on the drugs, they developed a transient reaction (abdominal pain, temperature spike and tender palms). Furthermore, *in vivo* ELISpot assay (done in the first six weeks post DRESS) showed a positive result for all four FLTDs, including rifampicin that was tolerated on drug rechallenge. Interestingly, our data suggests that HIV-infected patients reacting to multiple medications tended to have more dermal infiltration of CD4 T cells. This was noted in both DRESS and SJS/TEN phenotypes. Similarly, we noted a trend towards an increase in other inflammatory T cells (CD3, CD8 and CD45RO) as well as regulatory T-cell infiltrates amongst the multiple compared to single drug reactors. A larger sample size is required to validate these preliminary observations, but it interesting to consider

possible explanations. Could this imply a stochastic relationship whereby the magnitude of the initial T-cell response to an offending drug creates a larger pool from where even a small group of non-specifically activated T-cells may produce clinical reactivity to a different drug or create a greater opportunity for neosensitisations (Zgolli et al., 2021). In this context it is also worth noting that we saw a trend amongst HIV-uninfected patients between Treg dermal infiltrate and DRESS BSA, suggesting that Treg infiltrates may be linked to DRESS severity. Of course, there may be several other factors at play including the activation status of T-cells as well as alteration in the inflammatory milieu e.g., innate immune activation that may provide important second signals necessary to cross thresholds of T-cell activation. To our knowledge there is no other reported data in literature examining T cell infiltrates in the skin amongst single and multiple drug reactors, and more research is required to better detail their immunohistological phenotypes, as this may confirm these initial findings, and given the wide use of skin biopsy/histology could provide a relatively easily accessible risk stratification tool to guide drug introduction in the post DRESS period.

No difference in dermal Tregs between HIV-infected compared to uninfected DRESS

Tregs play a crucial role in regulating immune homeostasis and inflammation, through suppression of effector T-cells at sites of inflammation, and in a simplistic model are thereby thought to limit disease mediated by effector T-cells (Belkaid and Rouse, 2005). Skin infiltration of T-regs has been studied across several inflammatory skin diseases including atopic dermatitis, psoriasis, systemic lupus erythematous and cutaneous adverse drug reactions (Lin et al., 2011, Mehta et al., 2021, Keijsers et al., 2013, Fujimura et al., 2008, Biswas et al., 2021, Schmidt et al., 2017, Teraki and Shiohara, 2003, Morito et al., 2014). Surface staining markers to identify Treg cell infiltrates have included: CD4, CD25, FOXP3 and or other markers such as Helios (Matavele Chissumba et al., 2022, Biswas et al., 2021, Mehta et al., 2021, Mizutani et al., 2020, Snelgrove et al., 2019, Speiser et al., 2019, Rossi et al., 2018, Gorman et al., 2018, Schmidt et al., 2017, Keijsers et al., 2013, Fujimura et al., 2008); but it is worth noting that functionality of Treg populations with similar surface markers can be different, meaning caution is required in direct extrapolation from number to function (Lin et al., 2011).

Treg studies from SCAR are limited but increases in circulating and dermal skin infiltrating Tregs in the acute phase of DRESS has been reported, with a positive correlation between dermal Treg numbers with days from rash onset found in one study (Morito et al., 2014). Takahashi et al, in a study of 11 TEN patients noted depletion of circulating Tregs in the acute phase of TEN patients, hypothesising that the low frequency may relate to severe epidermal damage and Treg trafficking into skin in an attempt to control immune-mediated damage (Takahashi et al., 2009). The increase of skin infiltrating Tregs across inflammatory diseases, including with SCAR suggests most likely

that Treg infiltrations follow effector T cell responses in a homeostatic manner. This is supported by data from Mizukawa et al. that investigated epidermal damage in evolving FDE lesions, by analysing FDE skin lesions induced by causative drug rechallenge (Mizukawa et al., 2008). They reported that FOXP3+ Tregs were detected predominantly in the vicinity of CD8+ T cells after rechallenging with the causative drug, but not in resting lesions before drug rechallenge. This indicated that Treg infiltration, likely with a homeostatic suppressor function of activated effector CD8+ T cells, follows drug-induced T cell activation (Mizukawa et al., 2008). Mouse data has examined Treg migration into uninflamed and inflamed skin and demonstrated that molecular mechanisms controlling intraepidermal Treg migration, particularly integrin binding and intracellular signalling pathways, differ considerably depending on the phase of the inflammatory response (Norman et al., 2021). Additional mice data examining the behaviour of Tregs following their arrest on the endothelial surface demonstrated that adhesion and transmigration of Tregs in dermal microvasculature can be driven by different molecular mechanisms at different stages of an antigen driven inflammatory response (Snelgrove et al., 2019). Furthermore, Chow et al. characterized the actions of peripheral Tregs under resting conditions and during T cell-driven inflammatory response, and showed that tissue-resident Tregs are immotile in the resting state, whereas following innate or adaptive induced inflammation, an increased proportion of Tregs actively migrated throughout the dermis (Chow et al., 2013).

In persons living with HIV, the architecture of circulating immune cells is dysregulated (Van de Wijer et al., 2021). HIV-related immune dysregulation can impact the proportion and phenotype of Tregs, although the relationship is complex with several modulating factors; peripheral blood Treg numbers being shown to vary depending on the particular HIV population studies, as well as the way Tregs were characterized (Presicce et al., 2011). Treg frequencies in circulation vary according to the stage of HIV disease, antiretroviral therapy, and the direct effect from APCs activation/maturation states. A study by Chen et al. showed that the percentage of CD4+CD25+ Tregs amongst HIV-infected/AIDS patients was only increased in the late stage of disease (Chen et al., 2021). Similarly, Presicce et al. revealed increased proportions of circulating CD3+CD4+FOXP3+ Tregs but reduced absolute numbers in patients with chronic HIV infection (Presicce et al., 2011). Politou et al. also revealed that CD4+CD25+FOXP3+ Treg cell counts were shown to be significantly higher in HIV-infected patients with high viral load and patients with virological failure to ART (Politou et al., 2020). In patients with chronic or late-stage HIV disease, increased Treg frequencies have been associated with decreased proportions of CD8+ T cells (Matavele Chissumba et al., 2022, van Eekeren et al., 2022, Van de Wijer et al., 2021), while a negative correlation with CD4+ T cell counts has been observed (Politou et al., 2020, Liu et al., 2022) . Combination ART has been shown to contribute to changes in Treg frequencies in people

living with HIV. Hu et al. showed that in the short-term after ART initiation, CD4+CD25^{high}CD127^{low} Treg counts gradually increased, and further increased with long-term ART use (Hu et al., 2022). Nobrega et al. showed that Treg percentages were higher at ART onset in patients with CD4 cell counts <200µl at baseline (Nobrega et al., 2016). However, the frequency of Tregs is reported to eventually decrease with continued and successful cART use, reaching normal levels similar to that of healthy controls (Nobrega et al., 2016, Presicce et al., 2011, Yero et al., 2021). In addition, DCs also contribute to alterations in Treg frequencies, with studies showing that DCs derived from monocytes of HIV-infected patients, and lymph node DCs from untreated HIV-infected patients induced proliferation of T cells and conversion of Tregs (Krathwohl et al., 2006, Carbonneil et al., 2004). Furthermore, Stiksrud et al. showed that immunological non-responders displayed higher activation of both myeloid and plasmacytoid DCs, and this was associated with increased T-cell activation and activated Tregs (Stiksrud et al., 2019). In our small cohort, the majority of patients had advanced immune suppression (CD4 < 200 cells/µl) but over half were established on ART, therefore making it hard to predict Treg proportions, numbers, or functional state in the context of a new SCAR.

This study is the first study to use robust surface markers for Treg cells (CD3, CD4+ and FOXP3) to examine skin infiltration of Treg cells in the context of DRESS and SJS/TEN patients with HIV infection. Contrary to our initial hypothesis that Tregs could be depleted in the context of advanced HIV infection and poorly migrate into skin, we did not note a difference between Tregs density amongst HIV-infected or uninfected DRESS or SJS/TEN patients. In fact, there was a trend to an increased number of Treg cells in HIV-infected DRESS patients, which may reach statistical significance with an increased sample size. We explored and did not find any obvious impact of confounders such as demographic and clinical characteristics to account for differences in dermal Tregs between HIV-infected and uninfected cases; we particularly examined any impact on the number of days between the onset of clinical symptoms to skin biopsy, the BSA of skin rash, and eosinophils counts or LFTs. To our knowledge, there is no reported data in literature on Tregs in circulation or at the site of disease (skin) in the context of HIV-infected DRESS or SJS/TEN, with the majority of Treg data limited to peripheral blood and not in the context of SCAR. However, it may be that the continued immune activation in both HIV, TB, and DRESS drive expansion of Treg populations, and that this may be occurring in both peripheral blood and the site of disease. Mouse data suggest that exposure of hapten to naïve mice can induce an increase in the proportion of migratory Tregs demonstrating that innate signals can induce Treg migration (Chow et al., 2013). Thus, it could be that in HIV-infected patients under skin inflammatory conditions, with innate and antigen-specific adaptive stimuli drive an increase of Tregs in the context of HIV-infected SCAR. Further work on a larger sample size is now required to confirm these findings.

Increased dermal and epidermal Treg infiltration in a case of DRESS with a longer delay between symptoms onset to biopsy.

The above suggested factors driving an increased Treg infiltration into skin in the context of HIV and ongoing antigenic stimulation is supported by patient 105, a definite DRESS case sampled 71 days after the onset of clinical symptoms. This patient presented with a profound increased dermal infiltration of CD4+ and Treg T cells when compared to all of the other SCAR patients in the cohort sampled in the acute phase of disease (1 to 20 days from the onset of clinical symptoms). There was also an increased infiltration of effector CD8+ and memory CD45RO+ T cells in both dermal and epidermal compartments. The patient's disease progression timeline in Figure 3-32 reveals that despite the patient presenting with ongoing clinical symptoms suggestive of a drug reaction, there was continued attempts by the treating clinicians to treat through the grumbling reaction, and thus the patient had prolonged drug exposure prior to biopsy and after the development of the initial symptoms/DRESS. Thus, it is reasonable to propose that this ongoing drug exposure continued to drive infiltration of effector and memory T cells in the skin, and simultaneously Tregs infiltration. Although simplistic, the relative dominant Treg infiltration, extreme in comparison to the other DRESS cases, may have led to a somewhat abrogated clinical phenotype in this patient and meant that the clinicians felt it reasonable to try and treat through the reaction. A differential impact of topical steroid therapy may also have played a factor in explaining this picture.

5. LIMITATIONS OF STUDY

The major limitation of this study was the small sample size, particularly for HIV-infected and uninfected SJS/TEN cases, as well as matching HIV-uninfected FLTD SCAR. In many cases this meant the inability to draw substantiative conclusions or compare groups e.g., SJS/TEN. Case accumulation is ongoing beyond this thesis where we hope to be able to confirm many of these preliminary findings with larger study numbers. The inability to rechallenge some patients (i.e., in the event of death) limited our ability for complete validation of some cases as single or multiple drug reactors. Therefore, in the analysis for single versus multiple reactors, some cases were classified as 'undetermined' and were not able to be included in the comparative analysis. All of these findings warrant further investigation with a larger sample size in order to deduce robust conclusions, however case accumulation across the span of this thesis was negatively impacted by the COVID19 pandemic.

The study design did not allow possible follow-up biopsy sampling on patients to be able to compare the immunohistological profiles at different stages of disease progression (i.e., acute versus recovery phase). This longitudinal repeat biopsy data would be useful to strengthen some of

the observations, particular around T-regulatory cell changes across the post DRESS period. Sampling timeframes were based on clinical time-points and not strictly specified; therefore, some laboratory results i.e., HIV viral loads or CD4 counts were unavailable to match with the timing of skin biopsy sampling. Thus, the lack of correlation between some of these values and skin biopsy findings may have been impacted.

Experimental variables such as tissue fixation, concentration of fixatives or duration of tissue fixation could not be directly controlled in this study, as this was done within the context of routine pathological services. It has been reported that under/over fixation of specimens and use of tissue preservatives other than formalin may impact antigen retrieval (Yaziji and Barry, 2006). We feel that the technical aspects of this study were well performed, and that these factors, although noted as possible limitations, were unlikely to have significantly contributed to failure or false negative results of immunohistochemical staining.

6. FUTURE WORK

The accumulation of additional cases is the first and ongoing work to be completed. Thereafter, we plan to broaden the immune cell focus to investigate the role of skin TRM cells, as well as tissue macrophages and DCs. There still remains several research gaps around the role of specific subsets of T-cells mediating disease e.g., central TCM or TRM effector memory or both. Further analysis would be valuable, more especially to understand the role and function of TRM cells in the context of HIV-infection and disease progression itself, and then in HIV-infected patients who develop SCAR.

Single-cell RNA sequencing (scRNA-seq) and spatial transcriptomic techniques have been successfully applied to characterize immune and non-immune cell populations in inflammatory and hypersensitivity skin disorders including SCAR, helping identify transcriptomic changes at the site-of-disease which include identifying key pathogenic T-cell populations, overexpressed genes and altered cellular pathways; all of which can provide increased resolution to understanding complex immunopathology. At present, there is neither a transcriptomic atlas of normal skin in persons living with HIV in sub-Saharan Africa, nor in HIV-infected patient who develop SCAR making the ability to interpret scRNA-seq data in these populations a major challenge. Mapping the spatial or single cell transcriptomic atlas of HIV-infected and uninfected normal skin in FLTD drug tolerant patients will give more insight on the immune cell and gene expression profiles of normal skin in the context of HIV infection at different levels of advancing immunosuppression and during the immune reconstitution associated with ART. Comparing this normal skin transcriptomic atlas with that of HIV-infected and uninfected patients with FLTD-induced SCAR will help characterize

disease causing cell populations and further supplement the nature and local distribution of transcriptomic changes observed in diseased skin.

7. CONCLUSION

Although uncommon, SCARs remain a major clinical challenge for TB HIV co-infected patients. HIV infection is associated with increased risk of skin disorders including SCARs, and HIV-induced immune dysregulation is consistently thought to play a role in triggering onset of these conditions, yet this remains poorly understood. This novel study uncovered some excellent preliminary findings to guide further study. HIV-infected and uninfected SCAR was associated with an increased infiltration of cytotoxic CD8+ T-cells compared to normal skin, displaying their role as key mediators of tissue damage. CD4+ T-cells were decreased in HIV-infected SCAR patients, in line with the known HIV-related peripheral circulation decline in CD4 cell counts. Interestingly, this data suggests that higher dermal infiltrates of CD4 T-cells were associated with an increased risk for reactivity to multiple unrelated medications within the post drug rechallenge period. Lastly, the finding of higher dermal Tregs in HIV-infected DRESS was unexpected and the functional significance of this requires further research to understand the role, if any, that these cells play in the observed lower-than expected mortality in HIV-infected SCAR patients.

8. APPENDIX

Table A-1: Secondary antibodies

Panel	Secondary Antibody	Supplier	Dilution in PBS	Incubation time (mins)	Emission wavelength	Excitation wavelength
STANDARD IHC	EnVision+ HRP Anti-rabbit (K4003)	DAKO	Neat	30 mins	-	-
	EnVision+ HRP Anti-mouse (K4001)	DAKO	Neat	30 mins	-	-
TREG ASSAY	Anti-rat Alexa 488	UCT Imaging Facility	1:250	1 hour	494nm	517nm
	Anti-mouse Cy3	UCT Imaging Facility	1:1000	1 hour	555nm	569nm
	Anti-rabbit Alexa 674	UCT Imaging Facility	1:500	1 hour	594nm	633nm
	DAPI	UCT Imaging Facility	1:5000	10 mins	345nm	475nm

Table A-2: Histopathology of skin lesions of HIV-infected DRESS and SJS/TEN cases

Case	Age/Sex	Validated phenotype (RegiSCAR Score)	Clinical description of skin rash at baseline	Biopsy [a]	Histology
15	26/F	Probable DRESS (**5**)	30% BSA skin rash, exanthema	8	Basketweave hyperkeratosis, spongiosis, focal lichenoid dermatitis with basal vacuolar degeneration, pigmentary incontinence in the dermis and an inflammatory infiltrate of lymphocytes and eosinophils
31	22/F	Definite DRESS (**6**)	60% BSA skin rash involving the eyes, lip, and oral mucosa, exanthema, erythema,	5	Hyperkeratosis, mild spongiosis, apoptotic keratinocytes, focal interface dermatitis with lymphocytic exocytosis and associated pigmentary incontinence, dermal perivascular infiltration of lymphocytes, eosinophils, and plasma cells.
38	30/F	Definite DRESS (**7**)	80% BSA skin rash, exanthema, peeling (desquamation), and erythema,	5	Moderate spongiosis and intraepidermal oedema, intraepidermal vesicle formation, dermal perivascular infiltrate of lymphocytes and eosinophils
41	45/M	Definite DRESS (**6**)	80% BSA skin rash, erythema, itching, facial oedema, liver involvement	11	Mild spongiosis and apoptotic keratinocytes, widespread interface dermatitis with basal vacuolization, perivascular infiltrate of lymphocytes and eosinophils
46	38/F	Possible DRESS (**2**)	75% BSA skin rash involving oral and genital mucosa, exanthema	23	Hyperkeratosis, irregular acanthosis, mild spongiosis, and apoptotic keratinocytes, widespread interface dermatitis with lymphocytic and eosinophilic dermal infiltrate, pigmentary incontinence
71	26/F	Definite DRESS (**7**)	65% BSA skin rash, exanthema, and erythema	4	Epidermal spongiosis and apoptotic keratinocytes, focal interface dermatitis with basal vacuolar degeneration, dermal perivascular infiltrate of lymphocytes and eosinophils
85	41/F	Definite DRESS (**6**)	55% BSA skin rash, exanthema, and erythema	7	Basketweave hyperkeratosis, spongiosis, widespread interface dermatitis with basal vacuolar degeneration, perivascular lymphocytic infiltrate with no eosinophils, dermal oedema, and pigmentary incontinence

100	30/F	Possible DRESS (3)	65% BSA skin rash involving the lip and oral mucosa, peeling (desquamation), erosions, erythema	5	Hyperkeratosis, epidermal spongiosis and apoptotic keratinocytes, basal vacuolar degeneration, perivascular lymphocytic infiltrate with plasma cells and scattered eosinophils, neutrophil margination
103	45/F	Probable DRESS (**5**)	40% BSA skin rash involving the scalp, erythema, itching, peeling (desquamation)	5	Parakeratosis and hyperkeratosis, epidermal irregular acanthosis and apoptotic keratinocytes, focal interface dermatitis, perivascular lymphocytic infiltrate with plasma cells and scattered eosinophils
104	47/F	Definite DRESS (**7**)	70% BSA skin rash involving the scalp, lips, oral and nasal mucosa, erythema	9	Basketweave hyperkeratosis, spongiosis and apoptotic keratinocytes, lichenoid dermatitis comprising of lymphocytes and eosinophils and plasma cells, pigmentary incontinence
105	35/M	Definite DRESS (**7**)	80% BSA skin rash involving the eye, lip, oral and nasal mucosa, itching, burning, peeling (desquamation)	73	Parakeratosis and hyperkeratosis, irregular acanthosis, spongiosis, apoptotic keratinocytes, widespread interface dermatitis with basal vacuolization, lymphocyte and eosinophil infiltration, pigmentary incontinence
111	39/F	Possible DRESS (3)	80% BSA skin rash involving oral mucosa, erythema, itching peeling (desquamation)	22	Parakeratosis, spongiosis, apoptotic keratinocytes, focal interface dermatitis with basal vacuolization, perivascular infiltration of lymphocytes and eosinophils
137	45/M	Definite DRESS (6)	65% BSA skin rash involving the nails, lips, oral and nasal mucosa, erythema, peeling (desquamation), erosions	9	Parakeratosis, spongiosis, apoptotic keratinocytes, focal interface dermatitis with basal vacuolization, lymphocyte, and eosinophil infiltration
139	54/F	Probable DRESS (5)	60% BSA skin rash involving the scalp, erythema	23	Hyperkeratosis, apoptotic keratinocytes, focal interface dermatitis, lymphocyte and eosinophil infiltration, pigmentary incontinence
167	41/M	Probable DRESS (4)	20% BSA skin rash, erythema, infiltration,	14	Parakeratosis, spongiosis, apoptotic keratinocytes, focal interface dermatitis, lymphocytic inflammation with plasma cells and eosinophil infiltration
24	40/F	Probable SJS/TEN (**2**)	30% BSA skin rash, epidermal necrosis	19	Basketweave orthokeratosis and hyperkeratosis, irregular acanthosis, necrotic keratinocytes, perivascular lymphocytic infiltration with plasma cells and a few eosinophils, pigmentary incontinence

39	68/M	Probable SJS/TEN (**2**)	10-15% BSA skin rash, epidermal necrosis, stripping (skin detachment)	7	Spongiosis, mild perivascular lymphocytic infiltration with plasma cells and no eosinophils, pigmentary incontinence
45	40/F	Definite TEN (**3**)	80% BSA skin rash, epidermal necrosis, stripping (skin detachment), erythema, macules	11	Basketweave hyperkeratosis and orthokeratosis, spongiosis, interstitial oedema, perivascular lymphocytic infiltration, pigmentary incontinence
52	30/M	Definite TEN (**3**)	60% BSA skin rash with eye, lip, oral, nasal and genital mucosa involvement, epidermal necrosis, Nikolsky sign, stripping (skin detachment)	4	Hyperkeratosis and parakeratosis, apoptotic keratinocytes, focal interface dermatitis with basal vacuolar degeneration, lichenoid dermatitis with lymphocytes, plasma cells and some eosinophils, dermal oedema, and pigmentary incontinence
83	49/F	Possible TEN **(1)**	80% BSA skin rash involving oral and nasal mucosa, Nikolsky sign, stripping (skin detachment)	4	Full thickness epidermal necrosis, Lymphocytic exocytosis, perivascular infiltration of lymphocytes and some eosinophils, pigmentary incontinence
99	27/F	Definite TEN **(3)**	50% BSA, skin rash involving the scalp, lip, nasal, oral, and genital mucosa, facial oedema, stripping (skin detachment), epidermal necrosis.	5	Parakeratosis, spongiosis, epidermal blister, necrotic keratinocytes, basal vacuolization, lymphocyte infiltration with some eosinophils, pigmentary incontinence

a Days from onset of symptoms to biopsy

Table A-3: Histopathology of skin lesions of HIV-uninfected DRESS and SJS/TEN cases

Patient	Age/Sex	Validated Phenotype (RegiSCAR Score)	Clinical description of skin rash at baseline	Biopsy [a]	Histology
97	15/M	Definite DRESS (**6**)	40% BSA, pustules and erythema	3	Spongiosis, focal interface dermatitis, perivascular infiltration of mixed inflammatory components: lymphocytes, eosinophils, plasma cells and neutrophils, pigmentary incontinence
102*	57/F	Definite DRESS (**6**)	90% BSA skin rash involving the scalp, lips, oral, nasal, and genital mucosa, peeling (desquamation), erythema	17	-
136	52/F	Probable DRESS (**5**)	40% BSA skin rash involving the eyes, erythema	3	Hyperkeratosis, spongiosis, focal interface dermatitis with basal vacuolar degeneration and lymphocytic exocytosis, perivascular lymphocytic infiltration with eosinophils, pigmentary incontinence
145	15/F	Probable DRESS (**5**)	40% BSA skin rash involving the oral mucosa, erythema	6	Apoptotic keratinocytes, focal interface dermatitis with basal vacuolization, focal lichenoid dermatitis and perivascular infiltrate of lymphocytes and eosinophils
147	46/M	Definite DRESS (**7**)	40% BSA skin rash, erythema, facial oedema, purpura	8	Parakeratosis, spongiosis, focal interface dermatitis with lymphocytic exocytosis, perivascular infiltration of mixed inflammatory components: lymphocytes, eosinophils, plasma cells, pigmentary incontinence
28	33/F	Probable SJS/TEN (**2**)	18% BSA skin rash, epidermal necrosis, erythema	4	Parakeratosis and hyperkeratosis, subcorneal blister containing necrotic keratinocytes, apoptotic keratinocytes, perivascular lymphocytic infiltration, pigmentary incontinence

*No histological analysis done

[a] Days from onset of symptoms to biopsy

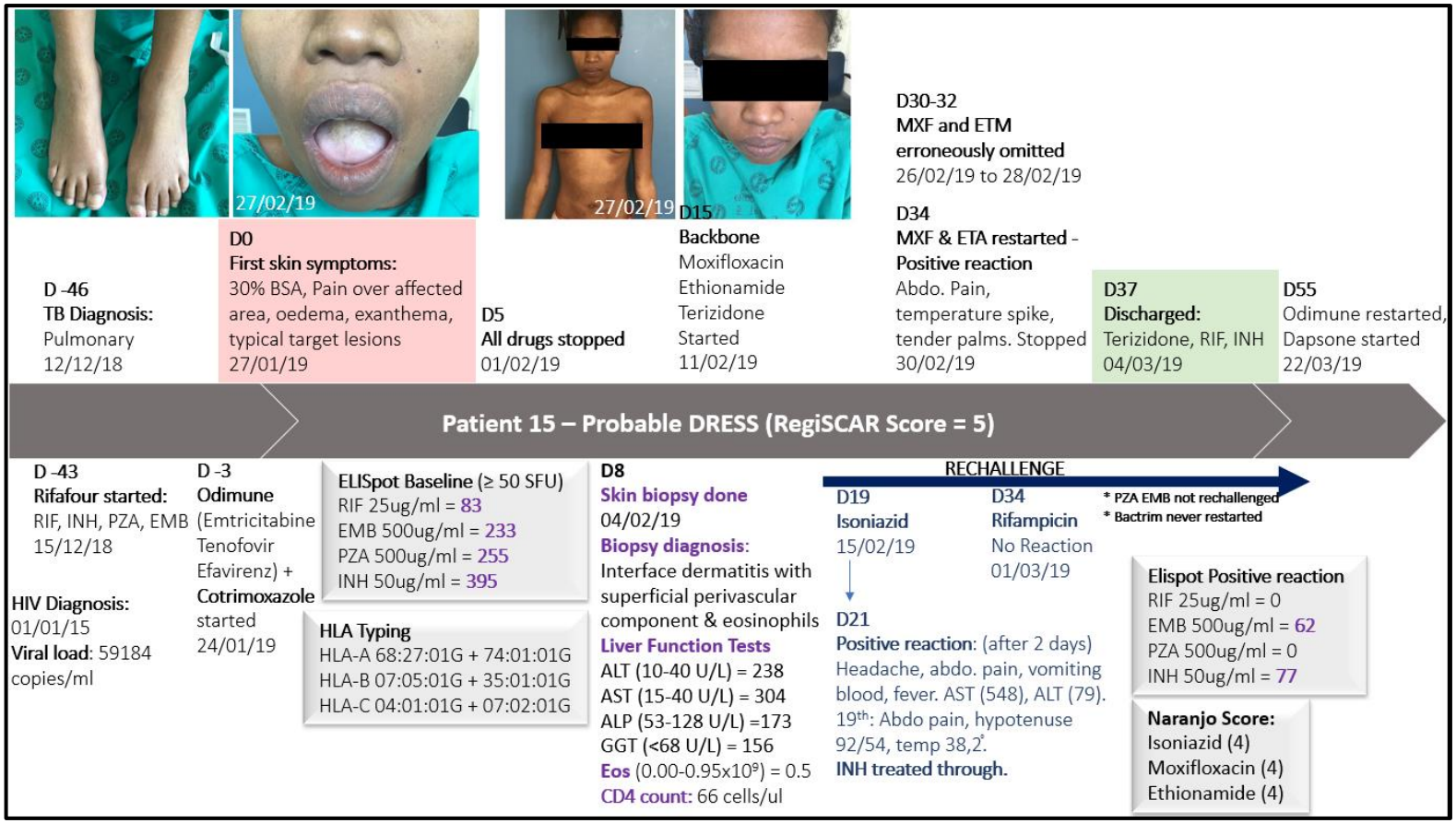

Figure A-1: Disease progression timeline of patient 15. A 27-year-old HIV-positive female with pulmonary TB. The patient was started on rifafour and Odimune prior to developing first skin symptoms. They also presented with deranged LFTs, and skin biopsy diagnosis revealed an interface dermatitis with eosinophils. They were put on backboned treatment and were rechallenged to INH ad RIF. They had a positive reaction to INH but was treated through. Moxifloxacin and ethionamide were erroneously omitted for two days, and when the patient was restarted on treatment, they developed symptoms. The patient was later discharged on RIF, INH and Terizidone. Odimune was restarted and tolerated, and dapsone was started.

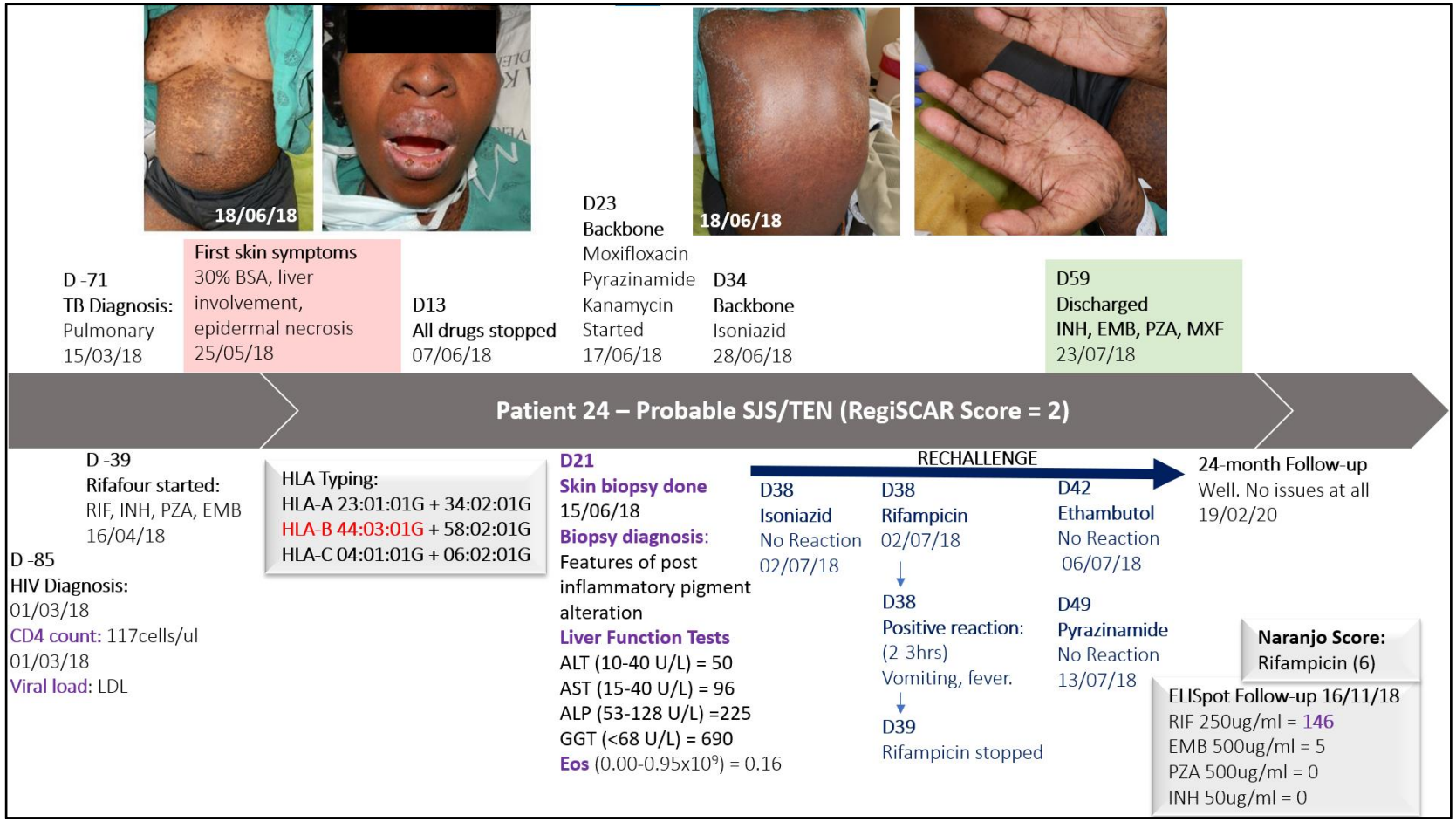

Figure A-2: Disease progression timeline of patient 24. A 41-year-old HIV positive female with pulmonary TB. They were started on rifafour and developed new skin symptoms 39 days later. They presented with deranged LFTs, and skin biopsy diagnosis showed features of post inflammatory pigment alteration. They were put on a backbone and rechallenged to all four drugs. The patient had a positive reaction to rifampicin and treatment was stopped. IFN-γ ELISpot assay also showed positivity to rifampicin.

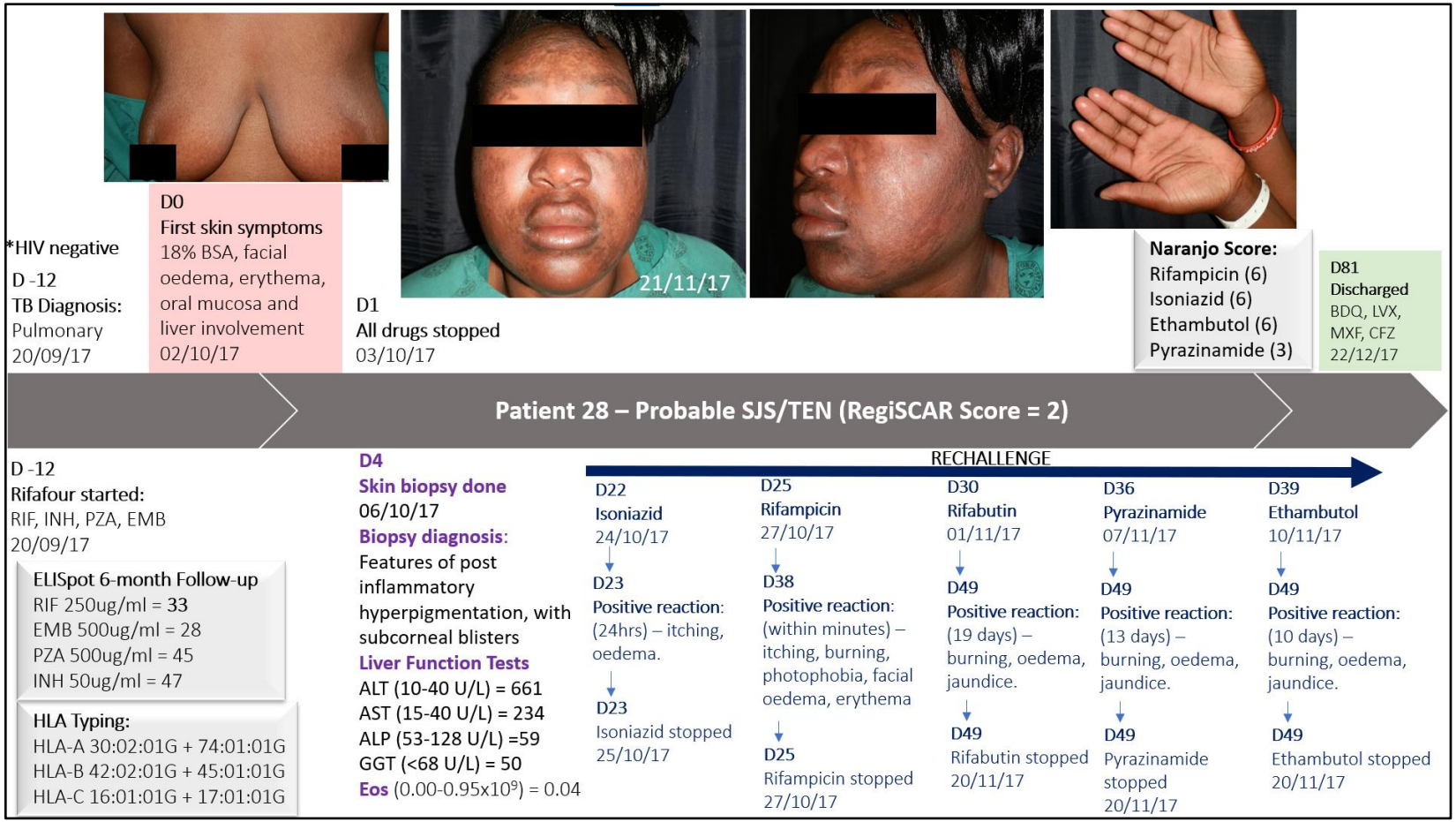

Figure A-3: Disease progression timeline of patient 28. A 33-year-old HIV negative female with pulmonary TB. She was started on rifafour 12 days before developing first skin symptoms. She presented with deranged LFTs, and skin biopsy diagnosis revealed featured of post inflammatory hyperpigmentation with subcorneal blisters. She was put on a backbone regimen and was rechallenged to all four drugs. She had a positive reaction to all drugs and treatment was stopped. IFN-γ ELISpot assay showed positivity to all four drugs.

Figure A-4: Disease progression timeline of patient 38. A 32-year-old HIV positive female on ART and with pulmonary TB. She was started on rifafour 24 days before developing first skin symptoms. She presented with deranged LFTs and eosinophilia, and skin biopsy diagnosis revealed a spongiotic dermatitis with eosinophils. She was put on a backbone regimen and rechallenged to all four drugs. She tolerated all drugs and was later discharged.

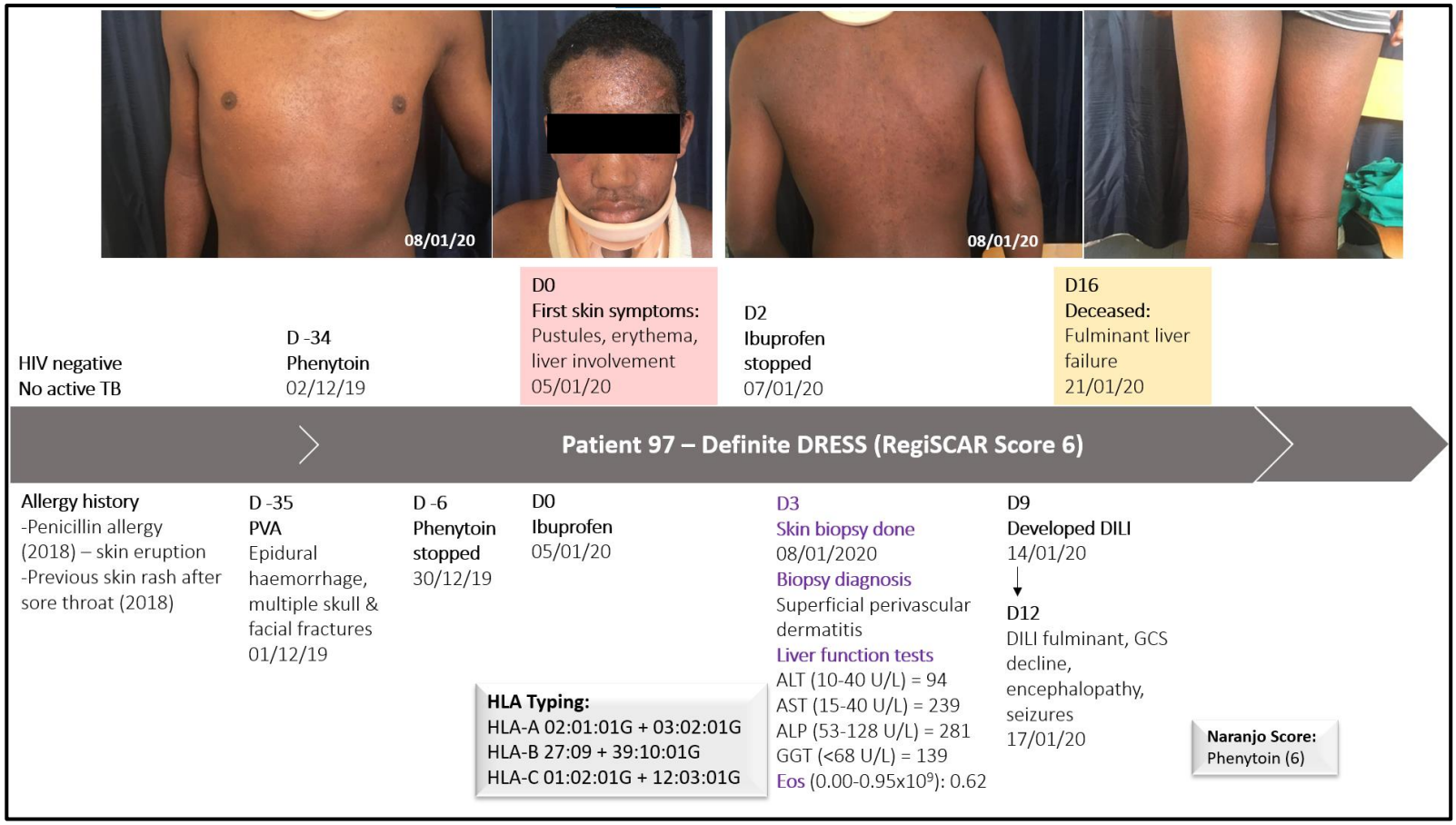

Figure A-5: Disease progression timeline of patient 97. An 18-year-old male with a history of penicillin allergy. He was phenytoin following PVA and developed first skin symptoms 6 days later. He presented with deranged LFTs and eosinophilia, and skin biopsy diagnosis revealed a superficial perivascular dermatitis. Patient later developed fulminant liver failure.

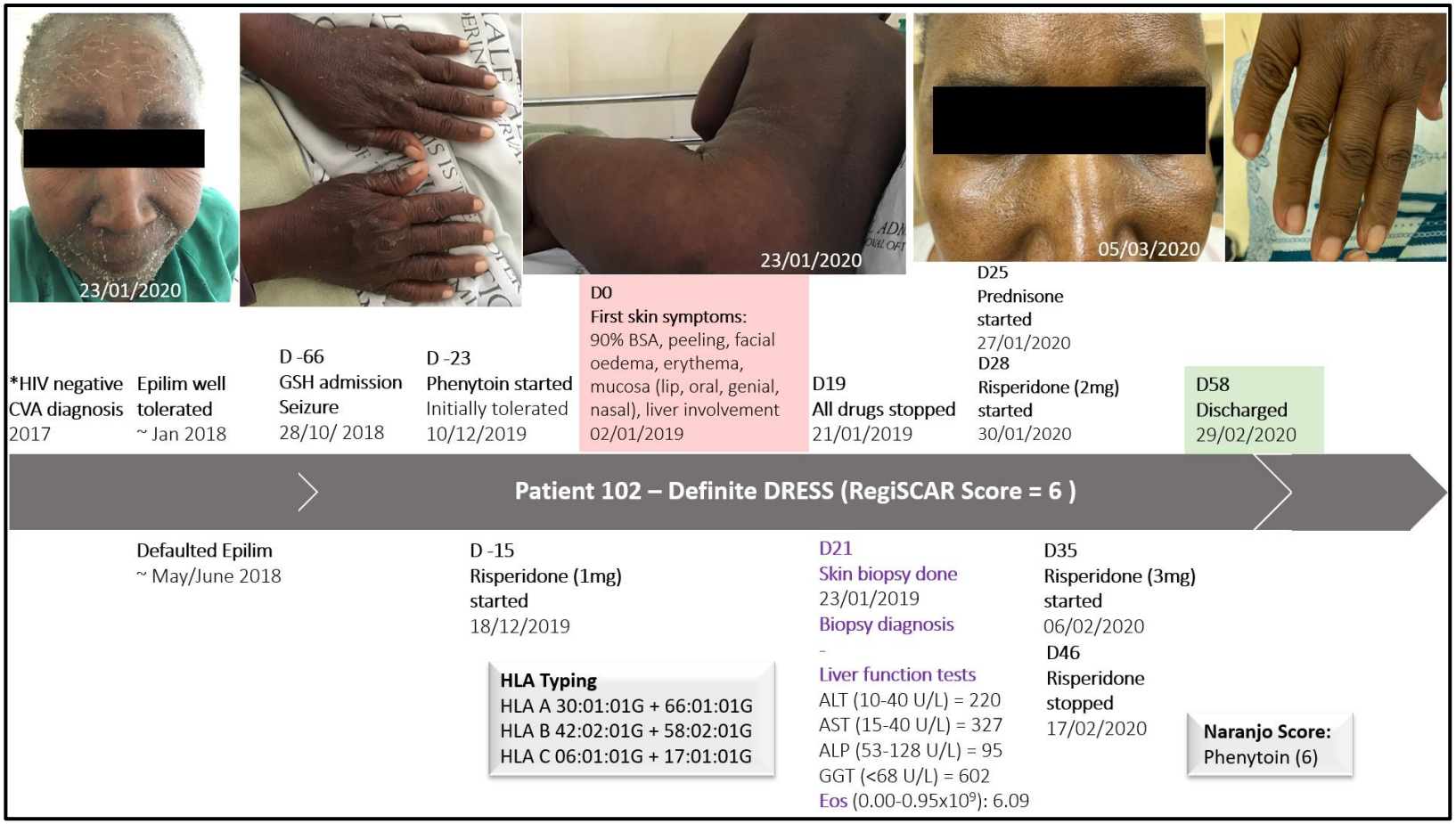

Figure A-6: Disease progression timeline of patient 102. A 58-year-old psychiatric patient with a history of seizures. She was put on phenytoin 23 days before developing first skin symptoms. She presented with deranged LFTs and eosinophilia. She was put on an increased dosage of risperidone and was later discharged.

Table A-4: Association between dermal CD4+ and Treg densities and clinical/demographic characteristics in HIV-infected and uninfected DRESS patients.

Independent variable	Dependent variable R^2 (coefficient, p value)			
	HIV-infected DRESS (n=14)		HIV-uninfected DRESS (n=5)	
	Dermal CD4	Dermal Tregs	Dermal CD4	Dermal Tregs
Age	0.256 (-0.506, 0.065)	0.402 (-0.634, 0.015)	0.304 (-0.551, 0.336)	0.494 (0.703, 0.189)
Days (symptoms to onset)	0.00 (-0.016, 0.957)	0.028 (-0.168, 0.567)	0.141 (-0.375, 0.534)	0.869, (0.932, 0.021)
Serum CD4 count	0.039 (0.191, 0.514)	0.05 (0.223, 0.444)	-	-
Log Viral load [a]	0.143 (-0.379, 0.315)	0.136 (-0.368, 0.33)	-	-
Eosinophils	0.223 (-0.472, 0.089)	0.06 (-0.244, 0.401)	0.163 (-0.403, 0.501)	0.945 (0.972, 0.006)
Liver enzymes: AST	0.095 (0.308, 0.284)	0.258 (0.508, 0.064)	0.071 (-0.267, 0.664)	0.465 (0.682, 0.205)
ALP	0.00 (0.006, 0.983)	0.011 (-0.104, 0.723)	0.037 (-0.192, 0.757)	0.314 (-0.560, 0.326)
ALT	0.289 (0.538, 0.047)	0.441 (0.664, 0.01)	0.006 (-0.081, 0.897)	0.018 (-0.133, 0.831)
GGT	0.031 (0.176, 0.547)	0.013 (0.112, 0.715)	0.146 (-0.382, 0.525)	0.304 (0.552, 0.335)
Body surface area of rash	0.00 (-0.02, 0.946)	0.00 (-0.018, 0.951)	0.046 (-0.215, 0.729)	0.909, (0.954, 0.012)
RegiSCAR Severity Score	0.013 (-0.114, 0.697)	0.019 (0.139, 0.636)	0.051 (0.227, 0.714)	0.138 (-0.371, 0.538)

[a] HIV viral loads were log transformed to permit the use of a linear model. Using Bonferroni correction, P-values ≤ 0.005 were considered significant.

Table A-5: Association between dermal CD4+ and Treg densities and clinical/demographic characteristics in HIV-infected and uninfected SCAR (DRESS + SJS/TEN) patients.

Independent variable	Dependent variable R^2 (coefficient, p value)			
	HIV-infected SCAR (n=20)		HIV-uninfected SCAR (n=6)	
	Dermal CD4	Dermal Tregs	Dermal CD4	Dermal Tregs
Age	0.180 (-0.424, 0.062)	**0.396 (-0.629, 0.003)**	0.163 (-0.404, 0.427)	0.513 (0.716, 0.109)
Days (symptoms to onset)	0.001 (-0.027, 0.910)	0.042 (-0.206, 0.385)	0.046 (-0.215, 0.683)	0.869 (0.932, 0.007)
Serum CD4 count	0.065 (0.255, 0.278)	0.068 (0.261, 0.267)	-	-
Log Viral load	0.043 (-0.207, 0.460)	0.026 (-0.162, 0.564)	-	-
Eosinophils	0.114 (-0.338, 0.145)	0.025 (-0.158, 0.507)	0.018 (-0.135, 0.799)	0.878 (0.937, 0.006)
Liver enzymes: AST	0.010 (0.102, 0.667)	0.002 (-0.044, 0.855)	0.135 (-0.367, 0.474)	0.334 (0.578, 0.230)
ALP	0.00 (-0.018, 0.939)	0.015 (0.122, 0.609)	0.00 (0.017, 0.974)	0.185 (-0.431, 0.394)
ALT	0.044 (0.209, 0.375)	0.007 (0.081, 0.735)	0.127 (-0.296, 0.488)	0.048 (-0.220, 0.676)
GGT	0.001 (0.037, 0.877)	0.009 (-0.093, 0.698)	0.018 (-0.134, 0.800)	0.323 (0.568, 0.239)
Body surface area of rash	0.00 (-0.009, 0.969)	0.01 (0.10, 0.674)	0.005 (0.074, 0.889)	0.781 (0.884, 0.02)
RegiSCAR Severity Score	0.012 (0.110, 0.645)	0.055 (0.234, 0.321)	0.228 (0.478, 0.338)	0.103 (0.320, 0.536)

Using Bonferroni correction, P-values ≤ 0.005 were considered significant, recorded in **bold.**

9. REFERENCES

ALADILY, T. N., ABUSHUNAR, T., ALHESA, A., ALRAWI, R., ALMAANI, N. & ABDALJALEEL, M. 2022. Immunohistochemical Expression Patterns of CD45RO, p105/p50, JAK3, TOX, and IL-17 in Early-Stage Mycosis Fungoides. *Diagnostics (Basel),* 12.

ALI, N. & ROSENBLUM, M. D. 2017. Regulatory T cells in skin. *Immunology,* 152**,** 372-381.

ALMEIDA, C. A., VAN MIERT, P., O'DRISCOLL, K., ZOET, Y. M., CHOPRA, A., WITT, C., JOHN, M., CLAAS, F. H. J. & D'ORSOGNA, L. J. 2019. Virus-specific T-cell clonotypes might contribute to drug hypersensitivity reactions through heterologous immunity. *J Allergy Clin Immunol,* 144**,** 608-611 e4.

ANGIN, M., SHARMA, S., KING, M., MUROOKA, T., GHEBREMICHAEL, M., MEMPEL, T., WALKER, B., BHASIN, M. & ADDO, M. 2014. HIV-1 infection impairs regulatory T-cell suppressive capacity on a per-cell basis. *The Journal of Infectiouos Diseases,* 210**,** 899-903.

ATIF, M., CONTI, F., GOROCHOV, G., OO, Y. H. & MIYARA, M. 2020. Regulatory T cells in solid organ transplantation. *Clin Transl Immunology,* 9**,** e01099.

AZUKIZAWA, H., SANO, S., KOSAKA, H., SUMIKAWA, Y. & ITAMI, S. 2005. Prevention of toxic epidermal necrolysis by regulatory T cells. *European Journal of Immunology,* 35**,** 1722-1730.

BAKKUM, R. S., WAARD-VAN DER SPEK, F. B. & THIO, H. B. 2002. Delayed-type hypersensitivity reaction to ethambutol and isoniazid. *Contact Dermatitis,* 46**,** 359.

BASTUJI-GARIN, S., RZANY, B., STERN, R. S., SHEAR, N. H., NALDI, L. & ROUJEAU, J. C. 1993. Clinical classification of cases of toxic epidermal necrolysis, Stevens-Johnson syndrome, and erythema multiforme. *Arch Dermatol,* 129**,** 92-6.

BELKAID, Y. & ROUSE, B. T. 2005. Natural regulatory T cells in infectious disease. *Nat Immunol,* 6**,** 353-60.

BELLON, T. 2019. Mechanisms of Severe Cutaneous Adverse Reactions: Recent Advances. *Drug Safety* 42**,** 973-992.

BISWAS, D., SETHY, M., BEHERA, B., PALIT, A. & MITRA, S. 2021. T-Regulatory Cells in Erythema Nodosum Leprosum: An Immunohistochemical and Image Morphometric Study. *Am J Dermatopathol,* 43**,** e149-e157.

BLAUVELT, A. & KATZ, S. I. 1995. The skin as target, vector, and effector organ in human immunodeficiency virus disease. *J Invest Dermatol,* 105**,** 122S-126S.

BLUMENTHAL, K. G., PETER, J. G., TRUBIANO, J. A. & PHILLIPS, E. J. 2019. Antibiotic allergy. *Lancet,* 393**,** 183-198.

BOGEN, S. A., VANI, K. & SOMPURAM, S. R. 2009. Molecular mechanisms of antigen retrieval: antigen retrieval reverses steric interference caused by formalin-induced cross-links. *Biotech Histochem,* 84**,** 207-15.

BOOTHBY, I. C., COHEN, J. N. & ROSENBLUM, M. D. 2020. Regulatory T cells in skin injury: At the crossroads of tolerance and tissue repair. *Science Immunology,* 5**,** eaaz9631.

BORRAS-BLASCO, J., NAVARRO-RUIZ, A., BORRAS, C. & CASTERA, E. 2008. Adverse cutaneous reactions associated with the newest antiretroviral drugs in patients with human immunodeficiency virus infection. *J Antimicrob Chemother,* 62**,** 879-88.

BORRONI, G., TORTI, S., PEZZINI, C., VASSALLO, C., ROSSO, R., D'OSPINA, R. M., TOMASINI, C. & BRAZZELLI, V. 2014. Histopathologic spectrum of Drug Reaction with Eosinophilia and Systemic Symptoms (DRESS): a diagnosis that needs clinico-pathological correlation. *G Ital Dermatol Venereol,* 149**,** 291-300.

BOS, J. D., HAGENAARS, C., DAS, P. K., KRIEG, S. R., VOORN, W. J. & KAPSENBERG, M. L. 1989. Predominance of "memory" T cells (CD4+, CDw29+) over "naive" T cells (CD4+, CD45R+) in both normal and diseased human skin. *Arch Dermatol Res,* 281**,** 24-30.

BRENCHLEY, J. M., PAIARDINI, M., KNOX, K. S., ASHER, A. I., CERVASI, B., ASHER, T. E., SCHEINBERG, P., PRICE, D. A., HAGE, C. A., KHOLI, L. M., KHORUTS, A., FRANK, I., ELSE, J., SCHACKER, T., SILVESTRI, G. & DOUEK, D. C. 2008. Differential Th17 CD4 T-cell depletion in pathogenic and nonpathogenic lentiviral infections. *Blood,* 112**,** 2826-35.

CAMPBELL, G. R., TO, R. K. & SPECTOR, S. A. 2019. TREM-1 Protects HIV-1-Infected Macrophages from Apoptosis through Maintenance of Mitochondrial Function. *mBio,* 10**,** e02638-19.

CARBONNEIL, C., DONKOVA-PETRINI, V., AOUBA, A. & WEISS, L. 2004. Defective dendritic cell function in HIV-infected patients receiving effective highly active antiretroviral therapy: neutralization of IL-10 production and depletion of CD4+CD25+ T cells restore high levels of HIV-specific CD4+ T cell responses induced by dendritic cells generated in the presence of IFN-alpha. *J Immunol,* 172**,** 7832-40.

CARDONE, M., GARCIA, K., TILAHUN, M. E., BOYD, L. F., GEBREYOHANNES, S., YANO, M., RODERIQUEZ, G., AKUE, A. D., JUENGST, L., MATTSON, E., ANANTHULA, S., NATARAJAN, K., PUIG, M., MARGULIES, D. H. & NORCROSS, M. A. 2018. A transgenic mouse model for HLA-B*57:01-linked abacavir drug tolerance and reactivity. *J Clin Invest,* 128**,** 2819-2832.

CHANTARANGSU, S., MUSHIRODA, T., MAHASIRIMONGKOL, S., KIERTIBURANAKUL, S., SUNGKANUPARPH, S., MANOSUTHI, W., TANTISIRIWAT, W., CHAROENYINGWATTANA, A., SURA, T., CHANTRATITA, W. & NAKAMURA, Y. 2009. HLA-B*3505 allele is a strong predictor for nevirapine-induced skin adverse drug reactions in HIV-infected Thai patients. *Pharmacogenetics and genomics,* 19**,** 139-146.

CHEN, H., REN, C., SONG, H., MA, L. L., CHEN, S. F., WU, M. J., ZHANG, H., XU, J. C. & XU, P. 2021. Temporal and spatial characterization of negative regulatory T cells in HIV-infected/AIDS patients raises new diagnostic markers and therapeutic strategies. *J Clin Lab Anal,* 35**,** e23831.

CHEN, L. & SHEN, Z. 2020. Tissue-resident memory T cells and their biological characteristics in the recurrence of inflammatory skin disorders. *Cell and Molecular Immunology,* 17**,** 64-75.

CHEN, Y.-C., CHO, Y.-T., CHANG, C.-Y. & CHU, C.-Y. 2013. Drug reaction with eosinophilia and systemic symptoms: A drug-induced hypersensitivity syndrome with variable clinical features. *Dermatologica Sinica,* 31.

CHEUK, S., WIKEN, M., BLOMQVIST, L., NYLEN, S., TALME, T., STAHLE, M. & EIDSMO, L. 2014. Epidermal Th22 and Tc17 cells form a localized disease memory in clinically healed psoriasis. *J Immunol,* 192**,** 3111-20.

CHI, M. H., HUI, R. C., YANG, C. H., LIN, J. Y., LIN, Y. T., HO, H. C., CHUNG, W. H. & KUO, T. T. 2014. Histopathological analysis and clinical correlation of drug reaction with eosinophilia and systemic symptoms (DRESS). *Br J Dermatol,* 170**,** 866-73.

CHO, Y.-T., YANG, C.-W. & CHU, C.-Y. 2017. Drug reaction with eosinophilia and systemic symptoms (DRESS): an interplay among drugs, viruses, and immune system. *International journal of molecular sciences,* 18**,** 1243.

CHOMPUNUD NA AYUDHYA, C., ROY, S., THAPALIYA, M. & ALI, H. 2020. Roles of a Mast Cell-Specific Receptor MRGPRX2 in Host Defense and Inflammation. *J Dent Res,* 99**,** 882-890.

CHOW, Z., MUELLER, S. N., DEANE, J. A. & HICKEY, M. J. 2013. Dermal regulatory T cells display distinct migratory behavior that is modulated during adaptive and innate inflammation. *J Immunol,* 191**,** 3049-56.

CHUNG, W.-H., HUNG, S.-L., HONG, H.-S., HSIH, M.-S., YANG, L.-C., HO, H.-C., WU, J.-Y. & CHEN, Y.-T. 2004. Medical genetics: a marker for Stevens-Johnson syndrome. *Nature* 428**,** 486.

CLARK, R. A. 2015. Resident memory T cells in human health and disease. *Sci Transl Med,* 7**,** 269rv1.

CLEVERS, H., ALARCON, B., WILEMAN, T. & TERHORST, C. 1988. The T cell receptor/CD3 complex: a dynamic protein ensemble. *Annu Rev Immunol,* 6**,** 629-62.

COATES, M., LEE, M. J., NORTON, D. & MACLEOD, A. 2019. The Skin and Intestinal Microbiota and Their Specific Innate Immune Systems. *Frontiers in Immunology***,** 1-11.

COLDIRON, B. M. & BERGSTRESSER, P. R. 1989. Prevalence and clinical spectrum of skin disease in patients infected with human immunodeficiency virus. *Arch Dermatol,* 125**,** 357-61.

COLEBUNDERS, R., VANWOLLEGHEM, T., MEURRENS, P. & MOERMAN, F. 2004. Efavirenz-associated Stevens-Johnson syndrome. *Infection,* 32**,** 306-7.

COPAESCU, A., CHOSHI, P., PEDRETTI, S., MOUHTOURIS, E., PETER, J. & TRUBIANO, J. A. 2021. Dose Dependent Antimicrobial Cellular Cytotoxicity-Implications for ex vivo Diagnostics. *Front Pharmacol,* 12**,** 640012.

DE BOER, O. J., VAN DER LOOS, C. M., TEELING, P., VAN DER WAL, A. C. & TEUNISSEN, M. B. M. 2007. Immunohistochemical Analysis of Regulatory T Cell Markers in FOXP3 and GITR on CD4+CD25+ T cells in Normal Skin and Inflammatory Dermatoses. *Journal of Histochemistry & Cytochemistry,* 55**,** 891-898.

DE ST GROTH, B. & ALAN, L. 2008. Regulatory T cells in HIV infection: pathogenic or protective participants in immune response? *AIDS,* 22**,** 671-683.

DHEDA, K., BARRY, C. & MAARTENS, G. 2016. Tuberculosis. *Lancet,* 387**,** 1211-1226.

DUBE, N., ADEWUSI, E. & SUMMERS, R. 2013. Risk of nevirapine-associated Stevens-Johnson syndrome among HIV-infected pregnant women: the Medunsa National Pharmacovigilance Centre, 2007 - 2012. *S Afr Med J,* 103**,** 322-5.

FARBER, D. L., YUDANIN, N. A. & RESTIFO, N. P. 2014. Human memory T cells: generation, compartmentalization and homeostasis. *Nat Rev Immunol,* 14**,** 24-35.

FOUCHARD, N., BERTOCCHI, M., ROUJEAU, J.-C., REVUZ, J. & WOLKENSTEIN, P. 2000. SCORTEN: A severity-of-illness score for Toxic Epidermal Necrolysis. *Journal of Investigative Dermatology,* 115**,** 149-153.

FUJIMURA, T., OKUYAMA, R., ITO, Y. & AIBA, S. 2008. Profiles of Foxp3+ regulatory T cells in eczematous dermatitis, psoriasis vulgaris and mycosis fungoides. *Br J Dermatol,* 158**,** 1256-63.

GAIDE, O., EMERSON, R. O., JIANG, X., GULATI, N., NIZZA, S., DESMARAIS, C., ROBINS, H., KRUEGER, J. G., CLARK, R. A. & KUPPER, T. S. 2015. Common clonal origin of central and resident memory T cells following skin immunization. *Nat Med,* 21**,** 647-53.

GALHARDO, M. C., ALVARENGA, F. F., SCHUELER, G., PEREZ, M., MORGADO, M. G., FERREIRA, H., AZEVEDO, L. M., SAMPAIO, E. P. & SARNO, E. N. 2004. Normal skin of HIV-infected individuals contains increased numbers of dermal CD8 T cells and normal numbers of Langerhans cells. *Braz J Med Biol Res,* 37**,** 745-53.

GIRLING, D. 1997. Adverse reactions to rifampicin in antituberculosis regimens. *The journal of antimicrobial chemotherapy,* 3**,** 115-132.

GONCALO, M., CARDOSO, J., GOUVEIA, M., COUTINHO, I., GAMEIRO, A., BRITES, M. & TELLECHEA, O. 2016. Histopathology of the Exanthema in DRESS Is Not Specific but May Indicate Severity of Systemic Involvement. *The American Journal of Dermatology,* 38.

GORMAN, S., GELDENHUYS, S., WEEDEN, C. E., GRIMBALDESTON, M. A. & HART, P. H. 2018. Investigating the roles of regulatory T cells, mast cells and interleukin-9 in the control of skin inflammation by vitamin D. *Arch Dermatol Res,* 310**,** 221-230.

GRAY, C., O'HAGAN, K., LORENZO-REDONDO, R., OLIVIER, A., AMU, S., CHIGORIMBO-MUREFU, N., HARRTPARSAD, R., SEBAA, S., MAZIYA, L., DIETRICH, J., OTWOMBE, K., MARTINSON, N., FERRIAN, S., MKHIZE, N., LEWIS, D., LANG, D., CARIAS, A., JASPAN, H., WILSON, D., MCGILVRAY, M., CIANCI, G., ANDERSON, M., DINH, M., WILLIAMSON, A.-L., PASSMORE, J.-A., CHIODI, F. & HOPE, T. 2020a. Impact of chemokine C-C ligand 27, foreskin anatomy and sexually transmitted infections on HIV-1 target cell availability in adolescent South African males. *Mucosal Immunology,* 13**,** 118-127.

GRAY, C. M., O'HAGAN, K. L., LORENZO-REDONDO, R., OLIVIER, A. J., AMU, S., CHIGORIMBO-MUREFU, N., HARRYPARSAD, R., SEBAA, S., MAZIYA, L., DIETRICH, J., OTWOMBE, K., MARTINSON, N., FERRIAN, S., MKHIZE, N. N., LEWIS, D. A., LANG, D., CARIAS, A. M., JASPAN, H. B., WILSON, D. P. K., MCGILVRAY, M., CIANCI, G. C., ANDERSON, M. R., DINH, M. H., WILLIAMSON, A. L., PASSMORE, J. S., CHIODI, F. & HOPE, T. J. 2020b. Impact of chemokine C-C ligand 27, foreskin anatomy and sexually transmitted infections on HIV-1 target cell availability in adolescent South African males. *Mucosal Immunol,* 13**,** 118-127.

HANIFFA, M., GUNAWAN, M. & JARDINE, L. 2015. Human skin dendritic cells in health and disease. *J Dermatol Sci,* 77**,** 85-92.

HANSEL, K., BELLINI, V., BIANCHI, L., BROZZI, J. & STINGENI, L. 2017. Drug reaction with eosinophilia and systemic symptoms from ceftriaxone confirmed by positive patch test: An immunohistochemical study. *The journal of allergy and clinical immunology. In practice,* 5**,** 808-810.

HASAN, M., YUNIHASTUTI, E., TEGUH, H. K. & ABDULLAH, M. 2022. Incidence and predictors of nevirapine and efavirenz-associated rash among Indonesian HIV patients. *Asian Pac J Allergy Immunol,* 40**,** 141-146.

HIRANSUTHIKUL, A., RATTANANUPONG, T., KLAEWSONGKRAM, J., RERKNIMITR, P., PONGPRUTTHIPAN, M. & RUXRUNGTHAM, K. 2016. Drug-induced hypersensitivity syndrome/drug reaction with eosinophilia and systemic symptoms (DIHS/DRESS): 11 years retrospective study in Thailand. *Allergol Int,* 65**,** 432-438.

HU, R., CHEN, T., YAN, Y., ZHOU, Y., YANG, R. & XIONG, Y. 2022. Short- and long-term effects of antiretroviral therapy on peripheral regulatory CD4+/CD25hi/CD127low T lymphocytes in people living with HIV/AIDS. *Rev Inst Med Trop Sao Paulo,* 64**,** e11.

ILLING, P. T., VIVIAN, J. P., DUDEK, N. L., KOSTENKO, L., CHEN, Z., BHARADWAJ, M., MILES, J. J., KJER-NIELSEN, L., GRAS, S., WILLIAMSON, N. A., BURROWS, S. R., PURCELL, A. W., ROSSJOHN, J. & MCCLUSKEY, J. 2012. Immune self-reactivity triggered by drug-modified HLA-peptide repertoire. *Nature,* 486**,** 554-8.

IRIKI, H., ADACHI, T., MORI, M., TANESE, K., FUNAKOSHI, T., KARIGANE, D., SHIMIZU, T., OKAMOTO, S. & NAGAO, K. 2014. Toxic epidermal necrolysis in the absence of circulating T cells: a possible role for resident memory T cells. *Journal of the American Academy of Dermatology,* 71**,** e214-216.

JIN, H. J., KANG, D. Y., NAM, Y. H., YE, Y. M., KOH, Y. I., HUR, G. Y., KIM, S. H., YANG, M. S., KIM, S., JEONG, Y. Y., KIM, M. H., CHOI, J. H., KANG, H. R., JO, E. J., PARK, H. K. & KOREAN SEVERE CUTANEOUS ADVERSE REACTIONS, C. 2021. Severe Cutaneous Adverse Reactions to Anti-tuberculosis Drugs in Korean Patients. *Allergy Asthma Immunol Res,* 13**,** 245-255.

JONES, R. B. & WALKER, B. D. 2016. HIV-specific CD8(+) T cells and HIV eradication. *J Clin Invest,* 126**,** 455-63.

JORG-WALTHER, L., SCHNYDER, B., HELBLING, A., HELSING, K., SCHULLER, A., WOCHNER, A. & PICHLER, W. 2015. Flare-up reactions in severe drug hypersensitivity: infection or ongoing T-cell hyperresponsiveness. *Clin Case Rep,* 3**,** 798-801.

JORG, L., HELBLING, A., YERLY, D. & PICHLER, W. J. 2020a. Drug-related relapses in drug reaction with eosinophilia and systemic symptoms (DRESS). *Clin Transl Allergy,* 10**,** 52.

JORG, L., YERLY, D., HELBLING, A. & PICHLER, W. 2020b. The role of drug, dose, and the tolerance/intolerance of new drugs in multiple drug hypersensitivity syndrome. *Allergy,* 75**,** 1178-1187.

KABASHIMA, K., HONDA, T., GINHOUX, F. & EGAWA, G. 2019. The immunological anatomy of the skin. *Nat Rev Immunol,* 19**,** 19-30.

KARDAUN, S., SIDOROFF, A., VALEYRIE-ALLANORE, L., HALEVY, S., DAVIDOVICI, B., MOCKENHAUPT, M. & ROUJEAU, J.-C. 2007. Variability of clinical pattern of cutaneous side-effects of drugs with systemic symptoms : does a DRESS syndrome really exist? *The British Journal of Dermatology,* 156**,** 609-611.

KARDAUN, S. H., MOCKENHAUPT, M. & ROUJEAU, J. C. 2014. Comments on: DRESS syndrome. *J Am Acad Dermatol,* 71**,** 1000-1000 e2.

KARNES, J., MILLER, M., WHITE, K., KONVINSE, K., PAVLOS, R., REDWOOD, A., PETER, J., LEHLOENYA, R., MALLAL, S. & PHILLIPS, E. 2019. Applications of immunopharmacogenomics: predicting, preventing, and understanding immune-mediated adverse drug reactions. *Annual review of pharmacology and toxicology,* 59**,** 463-486.

KEIJSERS, R. R., VAN DER VELDEN, H. M., VAN ERP, P. E., DE BOER-VAN HUIZEN, R. T., JOOSTEN, I., KOENEN, H. J. & VAN DE KERKHOF, P. C. 2013. Balance of Treg vs. T-helper cells in the transition from symptomless to lesional psoriatic skin. *Br J Dermatol,* 168**,** 1294-302.

KERL, K. & KERL, H. 2021. Severe cutaneous adverse drug reactions. *Diagnostic Histopathology,* 27**,** 1-5.

KHAIRUTDINOV, V. R., MIKHAILICHENKO, A. F., BELOUSOVA, I. E., KULIGINA, E. S., SAMTSOV, A. V. & IMYANITOV, E. N. 2017. The role of intradermal proliferation of T-cells in the pathogenesis of psoriasis. *An Bras Dermatol,* 92**,** 41-44.

KIM, S. W., ROH, J. & PARK, C. S. 2016. Immunohistochemistry for Pathologists: Protocols, Pitfalls, and Tips. *J Pathol Transl Med,* 50**,** 411-418.

KLEINMAN, A., SIVANANDHAM, R., PANDREA, I., CHOUGNET, C. & APETREI, C. 2018. Regulatory T cells as potential targets for HIV cure research. *Frontiers in Immunology,* 9.

KNIGHT, L. K., LEHLOENYA, R. J., SINANOVIC, E. & POORAN, A. 2019. Cost of managing severe cutaneous adverse drug reactions to first-line tuberculosis therapy in South Africa. *Trop Med Int Health,* 24**,** 994-1002.

KO, T.-M., CHUNG, W.-H., WEI, C.-Y., SHIH, H.-Y., CHEN, J.-K., LIN, C.-H., CHEN, Y.-T. & HUNG, S.-L. 2011. Shared and restricted T-cell receptor use is crucial for carbamazepine-induced Stevens-Johnson syndrome. *The journal of allergy and clinical immunology,* 128**,** 1266-1276.

KRATHWOHL, M. D., SCHACKER, T. W. & ANDERSON, J. L. 2006. Abnormal presence of semimature dendritic cells that induce regulatory T cells in HIV-infected subjects. *J Infect Dis,* 193**,** 494-504.

KUPPER, T. S. & FUHLBRIGGE, R. C. 2004. Immune surveillance in the skin: mechanisms and clinical consequences. *Nat Rev Immunol,* 4**,** 211-22.

LEHLOENYA, R. & DHEDA, K. 2012. Cutaneous adverse drug reactions to anti-tuberculosis drugs: state of the art and into the future. *Expert review of anti-infective therapy,* 10**,** 475-486.

LEHLOENYA, R., WALLACE, J., TODD, G. & DHEDA, K. 2012. Multiple drug hypersensitivity reactions to anti-tuberculosis drugs: five cases in HIV-infected patients. . *The international journal of tuberculosis and lung disease : the official journal of the International Union against Tuberculosis and Lung Disease,* 16**,** 1260-1264.

LEHLOENYA, R. J., DLAMINI, S., MULOIWA, R., KAKANDE, B., NGWANYA, M. R., TODD, G. & DHEDA, K. 2016. Therapeutic Trial of Rifabutin After Rifampicin-Associated DRESS Syndrome in Tuberculosis-Human Immunodeficiency Virus Coinfected Patients. *Open Forum Infect Dis,* 3**,** ofw130.

LEHLOENYA, R. J. & KGOKOLO, M. 2014. Clinical presentations of severe cutaneous drug reactions in HIV-infected Africans. *Dermatol Clin,* 32**,** 227-35.

LEHLOENYA, R. J., PETER, J. G., COPASCU, A., TRUBIANO, J. A. & PHILLIPS, E. J. 2020. Delabeling Delayed Drug Hypersensitivity: How Far Can You Safely Go? *J Allergy Clin Immunol Pract,* 8**,** 2878-2895 e6.

LIN, C. C., CHEN, C. B., WANG, C. W., HUNG, S. I. & CHUNG, W. H. 2020. Stevens-Johnson syndrome and toxic epidermal necrolysis: risk factors, causality assessment and potential prevention strategies. *Expert Rev Clin Immunol,* 16**,** 373-387.

LIN, Y. T., WANG, C. T., CHAO, P. S., LEE, J. H., WANG, L. C., YU, H. H., YANG, Y. H. & CHIANG, B. L. 2011. Skin-homing CD4+ Foxp3+ T cells exert Th2-like function after staphylococcal superantigen stimulation in atopic dermatitis patients. *Clin Exp Allergy,* 41**,** 516-25.

LIU, L., YUAN, G., SUN, F., SHI, J., CHEN, H. & HU, Y. 2022. Treg Cell Evaluation in Patients with Acquired Immune Deficiency Syndrome with Poor Immune Reconstitution and Human Immunodeficiency Virus-Infected Treg Cell Prevention by Polymeric Nanoparticle Drug Delivery System. *J Biomed Nanotechnol,* 18**,** 818-827.

MA, J. D., LEE, K. C. & KUO, G. M. 2010. HLA-B*5701 testing to predict abacavir hypersensitivity. *PLoS Curr,* 2**,** RRN1203.

MAGAKI, S., HOJAT, S. A., WEI, B., SO, A. & YONG, W. H. 2019. An Introduction to the Performance of Immunohistochemistry. *Methods Mol Biol,* 1897**,** 289-298.

MALLAL, S., PHILLIPS, E. J., CAROSI, G., MOLINA, J.-M., WORKMAN, C. J., TOMAZIC, J., JAGEL-GUEDES, E., RUGINA, S., KOZYREV, O., CID, F., HAY, P., NOLAN, D., HUGHES, S., HUGHES, A., RYAN, S.,

FITCH, N., THORBORN, D. & BENBOW, A. 2008. HLA-B*5701 screening for hypersensitivity to abacavir. *The New England Journal of Medicine,* 358 568-579.

MANCHES, O., FRLETA, D. & BHARDWAJ, N. 2014. Dendritic cells in progression and pathology of HIV infection. *Trends in immunology,* 35**,** 114-122.

MAOZ, K. B. & BRENNER, S. 2007. Drug rash with eosinophilia and systemic symptoms syndrome: sex and the causative agent. *Skinmed,* 6**,** 271-3.

MARDIVIRIN, L., VALEYRIE-ALLANORE, L., BRANLANT-REDON, E., BENETON, N., JIDAR, K., BARBAUD, A., CRICKX, B., RANGER-ROGEZ, S. & DESCAMPS, V. 2010. Amoxicillin-induced flare in patients with DRESS (Drug Reaction with Eosinophilia and Systemic Symptoms): report of seven cases and demonstration of a direct effect of amoxicillin on Human Herpesvirus 6 replication in vitro. *Eur J Dermatol,* 20**,** 68-73.

MATAVELE CHISSUMBA, R., MAGUL, C., MACAMO, R., MONTEIRO, V., ENOSSE, M., MACICAME, I., CUMBANE, V., BHATT, N., VIEGAS, E., IMBACH, M., ELLER, L. A., POLYAK, C. S., KESTENS, L. & GROUP, R. V. S. 2022. Helios expressing regulatory T cells are correlated with decreased IL-2 producing CD8 T cells and antibody diversity in Mozambican individuals living chronically with HIV-1. *BMC Immunol,* 23**,** 12.

MCCORMACK, M., ALFIREVIC, A., BOURGEOIS, S., FARRELL, J., KASPERAVICIUTE, D., CARRINGTON, M., SILLS, G., MARSON, T., JIA, X., DE BAKKER, P., CHINTHAPALLI, K., MOLOKHIA, M., JOHNSON, M., O'CONNOR, G., CHAILA, E., ALHUSAINI, S., SHIANNA, K., RADTKE, R., HEINZEN, E., WALLEY, N., PANDOLFO, M., PICHLER, W., PARK, K., DEPONDT, C., SISODIYA, S., GOLDSTEIN, D., DELOUKAS, P., DELANTY, N., CAVALLERI, G. & PIRMOHAMED, M. 2011. HLA-A*3101 and carbamazepine-induced hypersensitivity reactions in Europeans. *New England Journal of Medicine,* 364**,** 1134-1143.

MEHTA, H., MASHIKO, S., ANGSANA, J., RUBIO, M., HSIEH, Y. M., MAARI, C., REICH, K., BLAUVELT, A., BISSONNETTE, R., MUNOZ-ELIAS, E. J. & SARFATI, M. 2021. Differential Changes in Inflammatory Mononuclear Phagocyte and T-Cell Profiles within Psoriatic Skin during Treatment with Guselkumab vs. Secukinumab. *J Invest Dermatol,* 141**,** 1707-1718 e9.

MILLER, E. & BHARDWAJ, N. 2013. Dendritic cell dysregulation during HIV-1 infection. *Immunol Rev,* 254**,** 170-89.

MIYAGAWA, F. & ASADA, H. 2021. Current Perspective Regarding the Immunopathogenesis of Drug-Induced Hypersensitivity Syndrome/Drug Reaction with Eosinophilia and Systemic Symptoms (DIHS/DRESS). *International Journal of Molecular Sciences,* 22**,** 2147.

MIYARA, M., YOSHIOKA, Y., KITOH, A., SHIMA, T., WING, K., NIWA, A., PARIZOT, C., TAFLIN, C., HEIKE, T., VALEYRE, D., MATHIAN, A., NAKAHATA, T., YAMAGUCHI, T., NOMURA, T., ONO, M., AMOURA, Z., GOROCHOV, G. & SAKAGUCHI, S. 2009. Functional delineation and differentiation dynamics of human CD4+ T cells expressing the FoxP3 transcription factor. *Immunity,* 30**,** 899-911.

MIZUKAWA, Y., YAMAZAKI, Y. & SHIOHARA, T. 2008. In vivo dynamics of intraepidermal CD8+ T cells and CD4+ T cells during the evolution of fixed drug eruption. *Br J Dermatol,* 158**,** 1230-8.

MIZUKAWA, Y., YAMAZAKI, Y., TERAKI, Y., HAYAKAWA, J., HAYAKAWA, K., NURIYA, H., KOHARA, M. & SHIOHARA, T. 2002. Direct evidence for interferon-gamma production by effector-memory-type intraepidermal T cells residing at an effector site of immunopathology in fixed drug eruption. *Am J Pathol,* 161**,** 1337-47.

MIZUTANI, N., KANGSANANT, S., SAGARA, A., MIYAZAKI, M. & NABE, T. 2020. CD8(+) T cells regulated by CD4(+)CD25(+) regulatory T cells in the early stage exacerbate the development of Dermatophagoides farinae-induced skin lesions via increasing mast cell infiltration in mice. *Eur J Pharmacol,* 868**,** 172843.

MOCKENHAUPT, M., VIBOUD, C., DUNANT, A., NALDI, L., HALEVY, S., BOUWES BAVINCK, J. N., SIDOROFF, A., SCHNECK, J., ROUJEAU, J. C. & FLAHAULT, A. 2008. Stevens-Johnson syndrome and toxic epidermal necrolysis: assessment of medication risks with emphasis on recently marketed drugs. The EuroSCAR-study. *J Invest Dermatol,* 128**,** 35-44.

MORENO-FERNANDEZ, M., ZAPATA, W., BLACKARD, J., FRANCHINI, G. & CLAIRE, C. 2009. Human regulatory T cells are targets for Human Immunodeficiency Virus (HIV) infection, and their susceptivility differes depending on the HIV Type 1 strain. *Journal of Virology,* 83**,** 12925-12933.

MORITO, H., OGAWA, K., FUKUMOTO, T., KOBAYASHI, N., MORII, T., KASAI, T., NONOMURA, A., KISHIMOTO, T. & ASADA, H. 2014. Increased ratio of FoxP3+ regulatory T cells/CD3+ T cells in skin lesions in drug-induced hypersensitivity syndrome/drug rash with eosinophilia and systemic symptoms. *Clin Exp Dermatol,* 39**,** 284-91.

MOUNTON, J., NJUGUNA, C., KRAMER, N., STEWART, A., MEHTA, U., BLOCKMAN, M., FORTUIN-DE SMIDT, M., DE WAAL, R., PARRISH, A., WILSON, D., ILGUMBOR, E., AYNALEM, G., DHEDA, M., MAARTENS, G. & COHEN, K. 2016. Adverse Drug Reactions Causing Admission to Medical Wards: A Cross-Sectional Survey at 4 Hospitals in South Africa. *Medicine,* 95**,** e3437.

MOUSSET, C. M., HOBO, W., WOESTENENK, R., PREIJERS, F., DOLSTRA, H. & VAN DER WAART, A. B. 2019. Comprehensive Phenotyping of T Cells Using Flow Cytometry. *Cytometry A,* 95**,** 647-654.

MOUTON, J., MEHTA, U., PARRISH, A., WILSON, D., STEWART, A., NJUGUNA, C., KRAMER, N., MAARTENS, G., BLOCKMAN, M. & COHEN, K. 2015. Mortality from adverse drug reactions in adult medical inpatients at four hospitals in South Africa: a cross-sectional survey. *British journal of clinical pharmacology,* 80**,** 818-826.

NAGARAJAN, S. & WHITAKER, P. 2018. Management of adverse reactions to first-line tuberculosis antibiotics. *Curr Opin Allergy Clin Immunol,* 18**,** 333-341.

NALITYE HAITEMBU, B. N., PORTER, M. N., BASERA, W., HICKMANN, R., DLAMINI, S. K., SPEARMAN, C. W., PETER, J. G. & LEHLOENYA, R. J. 2021. Pattern and impact of drug-induced liver injury in South African patients with Stevens-Johnson syndrome/toxic epidermal necrolysis and a high burden of HIV. *J Allergy Clin Immunol Pract*.

NARANJO, C., BUSTO, U., SELLERS, E., SANDOR, P., RUIZ, I., ROBERTS, E., JANECEK, E., DOMECQ, C. & GREENBLATT, D. 1981. A method for estimating the probability of adverse drug reactions. *Clinical Pharmacology and Therapeutics,* 30**,** 239-245.

NASSIF, A., BENSUSSAN, A., BOUMSELL, L., DENIAUD, A., MOSLEHI, H., WOLKENSTEIN, P., BAGOT, M. & ROUJEAU, J.-C. 2004. Toxic epidermal necrolysis: effector cells are drug-specific cytotoxic T cells. *The journal of allergy and clinical immunology,* 114**,** 1209-1215.

NESTLE, F. O., DI MEGLIO, P., QIN, J. Z. & NICKOLOFF, B. J. 2009. Skin immune sentinels in health and disease. *Nat Rev Immunol,* 9**,** 679-91.

NGUYEN, A. V. & SOULIKA, A. M. 2019. The Dynamics of the Skin's Immune System. *Int J Mol Sci,* 20.

NISHIMURA, E., SAKIHAMA, T., SETOGUCHI, R., TANAKA, K. & SAKAGUCHI, S. 2004. Induction of antigen-specific immunologic tolerance by in vivo and in vitro antigen-specific expansion of naturally arising Foxp3+CD25+CD4+ regulatory T cells. *Int Immunol,* 16**,** 1189-201.

NOBREGA, C., HORTA, A., COUTINHO-TEIXEIRA, V., MARTINS-RIBEIRO, A., BALDAIA, A., RB-SILVA, R., SANTOS, C. L., SARMENTO-CASTRO, R. & CORREIA-NEVES, M. 2016. Longitudinal evaluation of regulatory T-cell dynamics on HIV-infected individuals during the first 2 years of therapy. *AIDS,* 30**,** 1175-86.

NORMAN, M. U., CHOW, Z., SNELGROVE, S. L., PRAKONGTHAM, P. & HICKEY, M. J. 2021. Dynamic Regulation of the Molecular Mechanisms of Regulatory T Cell Migration in Inflamed Skin. *Front Immunol,* 12**,** 655499.

OKOYE, A. A. & PICKER, L. J. 2013. CD4+ T cell depletion in HIV infection: mechanisms of immunological failure. *Immunological Reviews,* 254**,** 54-64.

OLADOKUN, R. E., LEHLOENYA, R. J., HLELA, C., UBESIE, A. C., KATIBI, S. O., MALANDE, O. O. & ELEY, B. 2018. *Atlas of Paediatric HIV Infection*, University of Cape Town Libraries.

ORIME, M. 2017. Immunohistopathological Findings of Severe Cutaneous Adverse Drug Reactions. *Journal of Immunology Research,* 2017**,** 6928363.

ORTONNE, N., VALEYRIE-ALLANORE, L., BASTUJI-GARIN, S., WECHSLER, J., DE FERAUDY, S., DUONG, T.-A., DELFAU-LARUE, M.-H., CHOSIDOW, O., WOLKENSTEIN, P. & ROUJEAU, J.-C. 2015.

Histopathology of drug rash with eosinophilia and systemic symptoms syndrome: a morphological and phenotypical study. *The British Journal of Dermatology,* 173**,** 50-58.

OSTROV, D. A., GRANT, B. J., POMPEU, Y. A., SIDNEY, J., HARNDAHL, M., SOUTHWOOD, S., OSEROFF, C., LU, S., JAKONCIC, J., DE OLIVEIRA, C. A., YANG, L., MEI, H., SHI, L., SHABANOWITZ, J., ENGLISH, A. M., WRISTON, A., LUCAS, A., PHILLIPS, E., MALLAL, S., GREY, H. M., SETTE, A., HUNT, D. F., BUUS, S. & PETERS, B. 2012. Drug hypersensitivity caused by alteration of the MHC-presented self-peptide repertoire. *Proc Natl Acad Sci U S A,* 109**,** 9959-64.

OZEKI, T., MUSHIRODA, T., YOWANG, A., TAKAHASHI, A., KUBO, M., SHIRAKATA, Y., IKEZAWA, Z., IIJIMA, M., SHIOHARA, T., HASHIMOTO, K., KAMATANI, N. & NAKAMURA, Y. 2010. Genome-wide association study identifies HLA-A*3101 allele as a genetic risk factor for carbamazepine-induced cutaneous adverse drug reactions in Japanese population. *Human molecular genetics,* 20**,** 1034-1041.

PANDA, S. & COLONNA, M. 2019. Innate Lympid Cells in Mucosal Immunity. *Frontiers in Immunology,* 10**,** 1-13.

PASPARAKIS, M., HAASE, I. & NESTLE, F. O. 2014. Mechanisms regulating skin immunity and inflammation. *Nat Rev Immunol,* 14**,** 289-301.

PATEL, S. M., JOHNSON, S., BELKNAP, S. M., CHAN, J., SHA, B. E. & BENNETT, C. 2004. Serious adverse cutaneous and hepatic toxicities associated with nevirapine use by non-HIV-infected individuals. *J Acquir Immune Defic Syndr,* 35**,** 120-5.

PAVLOS, R., WHITE, K. D., WANJALLA, C., MALLAL, S. A. & PHILLIPS, E. J. 2017. Severe Delayed Drug Reactions: Role of Genetics and Viral Infections. *Immunol Allergy Clin North Am,* 37**,** 785-815.

PEGRAM, P. S., JR., MOUNTZ, J. D. & O'BAR, P. R. 1981. Ethambutol-induced toxic epidermal necrolysis. *Arch Intern Med,* 141**,** 1677-8.

PETER, J., CHOSHI, P. & LEHLOENYA, R. 2019. Drug hypersensitivity in HIV infection. *Current opinion in allergy and clinical immunology,* 19**,** 272-282.

PETER, J. G. 2016. Multiple-drug intolerance syndrome Case records from the multi-disciplinary drug hypersensitivity clinic : guest review. *Current Allergy & Clinical Immunology,* 29**,** 152-156.

PETER, J. G., LEHLOENYA, R., DLAMINI, S., RISMA, K., WHITE, K., KONVINSE, K. & PHILLIPS, E. 2017. Severe delayed cutaneous and systemic reactions to drugs: a global perspective on the science and art of current practice. *The journal of allergy and clinical immunology. In practice,* 5**,** 547-563.

PETERS, P. J., STRINGER, J., MCCONNELL, M. S., KIARIE, J., RATANASUWAN, W., INTALAPAPORN, P., POTTER, D., MUTSOTSO, W., ZULU, I., BORKOWF, C. B., BOLU, O., BROOKS, J. T. & WEIDLE, P. J. 2010. Nevirapine-associated hepatotoxicity was not predicted by CD4 count >/=250 cells/muL among women in Zambia, Thailand and Kenya. *HIV Med,* 11**,** 650-60.

PHANUPHAK, N., APORNPONG, T., TEERATAKULPISARN, S., CHAITHONGWONGWATTHANA, S., TAWEEPOLCHAROEN, C., MANGCLAVIRAJ, S., LIMPONGSANURAK, S., JADWATTANAKUL, T., EIAMAPICHART, P., LUESOMBOON, W., APISARNTHANARAK, A., KAMUDHAMAS, A., TANGSATHAPORNPONG, A., VITAVASIRI, C., SINGHAKOWINTA, N., ATTAKORNWATTANA, V., KRIENGSINYOT, R., METHAJITTIPHUN, P., CHUNLOY, K., PREETIYATHORN, W., AUMCHANTR, T., TORO, P., ABRAMS, E. J., EL-SADR, W. & PHANUPHAK, P. 2007. Nevirapine-associated toxicity in HIV-infected Thai men and women, including pregnant women. *HIV Med,* 8**,** 357-66.

PHILLIPS, E. 2018. New strategies to predict and prevent serious immunologically mediated adverse drug reactions. *Transactions of the American Clinical and Climatological Association* 129**,** 74-78.

PHILLIPS, E. & MALLAL, S. 2009. Successful translation of pharmacogenetics into the clinic: the abacavir example. *Mol Diagn Ther,* 13**,** 1-9.

PHILLIPS, E. & MALLAL, S. 2018. Active suppression rather than ignorance: tolerance to abacavir-induced HLA-B*57:01 peptide repertoire alteration. *The Journal of Clinical Investigation,* 128**,** 2746-2749.

PICARD, D., JANELA, B., DESCAMPS, V., D'INCAN, M., COURVILLE, P., JACQUOT, S., ROGEZ, S., MARDIVIRIN, L., MOINS-TEISSERENC, H., TOUBERT, A., BENICHOU, J., JOLY, P. & MUSETTE, P. 2010. Drug reaction with eosinophilia and systemic symptoms (DRESS): a multiorgan antiviral T cell response. *Sci Transl Med,* 2**,** 46ra62.

PICHLER, W. J., DAUBNER, B. & KAWABATA, T. 2011. Drug hypersensitivity: flare-up reactions, cross-reactivity and multiple drug hypersensitivity. *J Dermatol,* 38**,** 216-21.

PICHLER, W. J., SRINOULPRASERT, Y., YUN, J. & HAUSMANN, O. 2017. Multiple Drug Hypersensitivity. *Int Arch Allergy Immunol,* 172**,** 129-138.

PILERI, S. A., RONCADOR, G., CECCARELLI, C., PICCIOLI, M., BRISKOMATIS, A., SABATTINI, E., ASCANI, S., SANTINI, D., PICCALUGA, P. P., LEONE, O., DAMIANI, S., ERCOLESSI, C., SANDRI, F., PIERI, F., LEONCINI, L. & FALINI, B. 1997. Antigen retrieval techniques in immunohistochemistry: comparison of different methods. *J Pathol,* 183**,** 116-23.

PIVARCSI, A., KEMENY, L. & DOBOZY, A. 2004. Innate Immune Functions of the Keratinocytes. *Acta Microbiologica et Immunologica Hungarica,* 51**,** 303-310.

POLESE, B., ZHANG, H., THURAIRAJAH, B. & KING, I. 2020. Innate Lymphocytes in Psoriasis. *Fronitiers in Immunology,* 11**,** 1-13.

POLITOU, M., BOTI, S., ANDROUTSAKOS, T., KONTOS, A., POULIAKIS, A., KAPSIMALI, V., PANAYIOTAKOPOULOS, G., KORDOSSIS, T., KARAKITSOS, P. & SIPSAS, N. V. 2020. Regulatory T Cell Counts and Development of Malignancy in Patients with HIV Infection. *Curr HIV Res,* 18**,** 201-209.

PORTER, M., CHOSHI, P., PEDRETTI, S., CHIMBETETE, T., SMITH, R., MEINTJES, G., PHILLIPS, E., LEHLOENYA, R. & PETER, J. 2022. IFN-gamma ELISpot in Severe Cutaneous Adverse Reactions to First-line Anti-tuberculosis Drugs in an HIV Endemic Setting. *J Invest Dermatol*.

PORTER, M. N., CHOSHI, P., PEDRETTI, S., BUCK, C., CHIMBETETE, T., LEHLOENYA, R. & PETER, J. Limited Adjunctive Diagnostic Utility of IFN-Gamma Elispot to Identify Offending Drug(s) in Severe Cutaneous Adverse Reactions to First-Line AntiTuberculous Drugs in HIV Endemic Setting. SJS/TEN 2021: Collaboration, Innovavtion and Commnity, 28-29 August 2021 2021.

PRESICCE, P., ORSBORN, K., KING, E., PRATT, J., FICHTENBAUM, C. J. & CHOUGNET, C. A. 2011. Frequency of circulating regulatory T cells increases during chronic HIV infection and is largely controlled by highly active antiretroviral therapy. *PLoS One,* 6**,** e28118.

RODRIGUEZ, R. S., MARIELA, P. L., NEUHAUS, I. M., YU, S. S., ARRON, S. T., HARRIS, H. W., YANG, S. H., ANTHONY, B. A., SVERDRUP, F. M., KROW-LUCAL, E., MACKENZIE, T. C., JOHNSON, D. S., MEYER, E. H., LOHR, A., HSU, S., KOO, J., LIAO, W., GUPTA, R., DEBBANEH, M. G., BUTLER, D., HUYNH, M., LEVIN, E. C., LEON, A., HOFFMAN, W. Y., MCGRATH, M. H., ALVARADO, M. D., LUDWIG, C. H., TRUONG, H.-A., MAURANO, M. M., GRATZ, I. K., ABBAS, A. K. & ROSENBLUM, M. D. 2014. Memory regulatory cells reside in human skin *The Jounal of Clinical Investigation,* 124**,** 1027-1036.

ROMAR, G. A. 2020. *Investigating the Role of Skin-Resident Memory T Cells in Cutaneous Delayed-Type Drug Hypersensitivity Reactions.* PhD Thesis, Havard Medical School.

ROSSI, M. T., ARISI, M., LONARDI, S., LORENZI, L., UNGARI, M., SERANA, F., FUSANO, M., MOGGIO, E., CALZAVARA-PINTON, P. G. & VENTURINI, M. 2018. Cutaneous infiltration of plasmacytoid dendritic cells and T regulatory cells in skin lesions of polymorphic light eruption. *J Eur Acad Dermatol Venereol,* 32**,** 985-991.

RZANY, B., CORREIA, O., KELLY, J. P., NALDI, L., AUQUIER, A. & STERN, R. 1999. Risk of Stevens-Johnson syndrome and toxic epidermal necrolysis during first weeks of antiepileptic therapy: a case-control study. Study Group of the International Case Control Study on Severe Cutaneous Adverse Reactions. *Lancet,* 353**,** 2190-4.

SALLUSTO, F., LENIG, D., FORSTER, R., LIPP, M. & LANZAVECCHIA, A. 1999. Two subsets of memory T lymphocytes with distinct homing potentials and effector fucntions. *Nature,* 401**,** 708-712.

SANCHEZ-BORGES, M., THONG, B., BLANCA, M., ENSINA, L. F., GONZALEZ-DIAZ, S., GREENBERGER, P. A., JARES, E., JEE, Y. K., KASE-TANNO, L., KHAN, D., PARK, J. W., PICHLER, W., ROMANO, A. &

JAEN, M. J. 2013. Hypersensitivity reactions to non beta-lactam antimicrobial agents, a statement of the WAO special committee on drug allergy. *World Allergy Organ J,* 6**,** 18.

SARFO, F., SARFO, M., NORMAN, B., PHILLIPS, R. & CHADWICK, D. 2014. Incidence and determinants of nevirapine and efavirenz-related skin rashes in West Africans: nevirapine's epitaph? *PloS One,* 9**,** e94854.

SASIDHARANPILLAI, S., AJITHKUMAR, K., JISHNA, P., KHADER, A., ANAGHA, K. V., BINITHA, M. P. & CHATHOTH, A. T. 2022. RegiSCAR DRESS (Drug Reaction with Eosinophilia and Systemic Symptoms) Validation Scoring System and Japanese Consensus Group Criteria for Atypical Drug-Induced Hypersensitivity Syndrome (DiHS): A Comparative Analysis. *Indian Dermatol Online J,* 13**,** 40-45.

SASIDHARANPILLAI, S., GOVINDAN, A., AJITHKUMAR, K., CHATHOTH, A. T., KHADER, A., REENA MARIYATH, O. K., FARSHA, R., SHERIN, N. & DAVID, E. M. 2020. Interface dermatitis as an indicator of hepatic involvement in drug reaction with eosinophilia and systemic symptoms (DRESS). *J Cutan Pathol,* 47**,** 800-808.

SASSOLA, B., HADDAD, C., MOCKENHAUPT, M., DUNANT, A., LISS, Y., BORK, K., HAUSTEIN, U., VIELUF, D., ROUJEAU, J.-C. & LE LOUET, H. 2010. ALDEN, an algorithm for assessmentof drug causality in Stevens-Johnson Syndrom and toxic epidermal necrolysis: comparison with case-control analysis. *Clinical Pharmacology and Therapeutics,* 88**,** 60-68.

SCALIA, C. R., BOI, G., BOLOGNESI, M. M., RIVA, L., MANZONI, M., DESMEDT, L., BOSISIO, F. M., RONCHI, S., LEONE, B. E. & CATTORETTI, G. 2017. Antigen Masking During Fixation and Embedding, Dissected. *J Histochem Cytochem,* 65**,** 5-20.

SCHMIDT, A., RIEGER, C. C., VENIGALLA, R. K., ELIAS, S., MAX, R., LORENZ, H. M., GRONE, H. J., KRAMMER, P. H. & KUHN, A. 2017. Analysis of FOXP3(+) regulatory T cell subpopulations in peripheral blood and tissue of patients with systemic lupus erythematosus. *Immunol Res,* 65**,** 551-563.

SCHUNKERT, E. M., SHAH, P. N. & DIVITO, S. J. 2021. Skin Resident Memory T Cells May Play Critical Role in Delayed-Type Drug Hypersensitivity Reactions. *Front Immunol,* 12**,** 654190.

SHIOHARA, T., KANO, Y., TAKAHASHI, R., ISHIDA, T. & MIZUKAWA, Y. 2012. Drug-Induced Hypersensitivity Syndrome: Recent Advances in the Diagnosis, Pathogenesis and Management. *Chemical Immunology and Allergy,* 97**,** 122-138.

SHIOHARA, T. & MIZUKAWA, Y. 2012. Fixed drug eruption: the dark side of activation of intraepidermal CD8+ T cells uniquely specialized to mediate protective immunity. *Chemical Immunology and Allergy,* 97**,** 106-121.

SHIOHARA, T., USHIGOME, Y., KANO, Y. & TAKAHASHI, R. 2015. Crucial Role of Viral Reactivation in the Development of Severe Drug Eruptions: a Comprehensive Review. *Clin Rev Allergy Immunol,* 49**,** 192-202.

SIGNH, U., CUI, Y., DIMAANO, N., MEHTA, S., PRUITT, S., YEARLEY, J., LATERZA, O., JUCO, J. & DOGDAS, B. 2018. Analytical validation of quantitative immunohistochemical assays of tumor infiltrating lymphocyte biomarkers. *Biotechnic & histochemistry,* 93**,** 411-423.

SIMONETTA, F. & BOURGEOIS, C. 2013. CD4+FOXP3+ regulatory T-cell subsets in human immunodeficiency virus infection. *Frontiers in Immunology,* 30**,** 215.

SISAY, M., BUTE, D., EDESSA, D., MENGISTU, G., AMARE, F., GASHAW, T. & BIHONEGN, T. 2018. Appropriateness of Cotrimoxazole Prophylactic Therapy Among HIV/AIDS Patients in Public Hospitals in Eastern Ethiopia: A Retrospective Evaluation of Clinical Practice. *Front Pharmacol,* 9**,** 727.

SKOWRON, F., BENSAID, B., BALME, B., DEPAEPE, L., KANITAKIS, J., NOSBAUM, A., MAUCORT-BOULCH, D., BERARD, F., D'INCAN, M., KARDAUN, S. & NICOLAS, J. 2015. Drug reaction with eosinophilia and systemic symptoms (DRESS): clinicopathological study of 45 cases,. *Journal of the European Academy of Dermatology and Venereology,* 29**,** 2199-2205.

SNELGROVE, S. L., ABEYNAIKE, L. D., THEVALINGAM, S., DEANE, J. A. & HICKEY, M. J. 2019. Regulatory T Cell Transmigration and Intravascular Migration Undergo Mechanistically Distinct Regulation at Different Phases of the Inflammatory Response. *J Immunol,* 203**,** 2850-2861.

SPEISER, J. J., MONDO, D., MEHTA, V., MARCIAL, S. A., KINI, A. & HUTCHENS, K. A. 2019. Regulatory T-cells in alopecia areata. *J Cutan Pathol,* 46**,** 653-658.

STAINSBY, C., PERGER, T., VANNAPPAGARI, V., MOUNZER, K., HSU, R., HENEGAR, C., OYEE, J., URBAITYTE, R., LANE, C., CARTER, L., PAKES, G. & SHAEFER, M. 2019. Abacavir Hypersensitivity Reaction Reporting Rates During a Decade of HLA-B*5701 Screening as a Risk-Mitigation Measure. *Pharmacotherapy,* 39**,** 40-54.

STEINBACH, K., VINCENTI, I. & MERKLER, D. 2018. Resident-Memory T Cells in Tissue-Restricted Immune Responses: For Better or Worse? *Frontiers in Immunology,* 30**,** 2827.

STEWART, A., LEHLOENYA, R., BOULLE, A., DE WAAL, R., MAARTENS, G. & COHEN, K. 2016. Severe antiretroviral-associated skin reactions in South African patients: a case series and case-control analysis. *Pharmacoepidemiology and drug safety,* 25**,** 1313-1319.

STIKSRUD, B., AASS, H. C. D., LORVIK, K. B., UELAND, T., TROSEID, M. & DYRHOL-RIISE, A. M. 2019. Activated dendritic cells and monocytes in HIV immunological nonresponders: HIV-induced interferon-inducible protein-10 correlates with low future CD4+ recovery. *AIDS,* 33**,** 1117-1129.

SUAREZ-FARINAS, M., FUENTES-DUCULAN, J., LOWES, M. A. & KRUEGER, J. G. 2011. Resolved psoriasis lesions retain expression of a subset of disease-related genes. *J Invest Dermatol,* 131**,** 391-400.

SUNDSTROM, J. B., ELLIS, J. E., HAIR, G. A., KIRSHENBAUM, A. S., METCALFE, D. D., YI, H., CARDONA, A. C., LINDSAY, M. K. & ANSARI, A. A. 2007. Human tissue mast cells are an inducible reservoir of persistent HIV infection. *Blood,* 109**,** 5293-300.

SURJAPRANATA, F. J. & RAHAJU, N. N. 1979. A case of Stevens-Johnson's syndrome caused by ethambutol. *Paediatr Indones,* 19**,** 195-201.

TAKAHASHI, R., KANO, Y., YAMAKAZI, Y., KIMISHIMA, M., MIZUKAWA, Y. & SHIOHARA, T. 2009. Defective Regulatory T Cells In Patients with Severe Drug Eruptions: Timing of the Dysfunction Is Associated with the Pathological Phenotype and Outcome. *Journal of Immunology* 182**,** 8071-8079.

TAN, W. C., ONG, C. K., KANG, S. C. & RAZAK, M. A. 2007. Two years review of cutaneous adverse drug reaction from first line anti-tuberculous drugs. *Med J Malaysia,* 62**,** 143-6.

TARNOWSKI, B. I., SPINALE, F. G. & NICHOLSON, J. H. 1991. DAPI as a useful stain for nuclear quantitation. *Biotech Histochem,* 66**,** 297-302.

TERAKI, Y. & SHIOHARA, T. 2003. IFN-gamma-producing effector CD8+ T cells and IL-10-producing regulatory CD4+ T cells in fixed drug eruption. *J Allergy Clin Immunol,* 112**,** 609-15.

THOMAS, M., HOPKINS, C., DUFFY, E., LEE, D., LOULERGUE, P., RIPAMONTI, D., OSTROV, D. & PHILLIPS, E. J. 2017. Association of the HLA-B*53:01 Allele With Drug Reaction With Eosinophilia and Systemic Symptoms (DRESS) Syndrome During Treatment of HIV Infection With Raltegravir. *Clinical infectious diseases: an official publication of the Infectious Disease Society of America,* 64**,** 1198-1203.

TOPHAM, D. J. & REILLY, E. C. 2018. Tissue-Resident Memory CD8(+) T Cells: From Phenotype to Function. *Front Immunol,* 9**,** 515.

TRIPODO, C. & PILERI, S. A. 2021. The Fundamentals of T-cell Lymphocyte Biology. *The Peripheral T-Cell Lymphomas.*

TRUBIANO, J. A., GORDON, C. L., CASTELLUCCI, C., CHRISTO, S. N., PARK, S. L., MOUHTOURIS, E., KONVINSE, K., ROSE, M., GOH, M., BOYD, A. S., PHILLIPS, E. J. & MACKAY, L. K. 2020. Analysis of skin-resident memory T cells following drug hypersensitivity reactions. *Journal of Investigative Dermatology,* 140**,** 1442-1445.

TSENG, Y. T., YANG, C. J., CHANG, S. Y., LIN, S. W., TSAI, M. S., LIU, W. C., WU, P. Y., SU, Y. C., LUO, Y. Z., YANG, S. P., HUNG, C. C. & CHANG, S. C. 2014. Incidence and risk factors of skin rashes and

hepatotoxicity in HIV-infected patients receiving nevirapine-containing combination antiretroviral therapy in Taiwan. *Int J Infect Dis,* 29**,** 12-7.

USHIGOME, Y., KANO, Y., ISHIDA, T., HIRAHARA, K. & SHIOHARA, T. 2013. Short- and long-term outcomes of 34 patients with drug-induced hypersensitivity syndrome in a single institution. *J Am Acad Dermatol,* 68**,** 721-8.

UTHAYAKUMAR, S., NANDWANI, R., DRINKWATER, T., NAYAGAM, A. T. & DARLEY, C. R. 1997. The prevalence of skin disease in HIV infection and its relationship to the degree of immunosuppression. *Br J Dermatol,* 137**,** 595-8.

VALLEJO, A. N., DAVILA, E., WEYAND, C. M. & GORONZY, J. J. 2004. Biology of T lymphocytes. *Rheum Dis Clin North Am,* 30**,** 135-57.

VAN DE WIJER, L., VAN DER HEIJDEN, W. A., TER HORST, R., JAEGER, M., TRYPSTEEN, W., RUTSAERT, S., VAN CRANENBROEK, B., VAN RIJSSEN, E., JOOSTEN, I., JOOSTEN, L., VANDEKERCKHOVE, L., SCHOOFS, T., VAN LUNZEN, J., NETEA, M. G., KOENEN, H., VAN DER VEN, A. & DE MAST, Q. 2021. The Architecture of Circulating Immune Cells Is Dysregulated in People Living With HIV on Long Term Antiretroviral Treatment and Relates With Markers of the HIV-1 Reservoir, Cytomegalovirus, and Microbial Translocation. *Front Immunol,* 12**,** 661990.

VAN EEKEREN, L. E., MATZARAKI, V., ZHANG, Z., VAN DE WIJER, L., BLAAUW, M. J. T., DE JONGE, M. I., VANDEKERCKHOVE, L., TRYPSTEEN, W., JOOSTEN, L. A. B., NETEA, M. G., DE MAST, Q., KOENEN, H., LI, Y. & VAN DER VEN, A. 2022. People with HIV have higher percentages of circulating CCR5+ CD8+ T cells and lower percentages of CCR5+ regulatory T cells. *Sci Rep,* 12**,** 11425.

VIGNALI, D. A. A., COLLISON, L. W. & WORKMAN, C. J. 2009. How regulatory T cells work. *Nature Reviews Immunology,* 8**,** 523-532.

VISWANATH, B. K., RANKA, P. & RAMANJANAYALU, M. 2012. Severe cutaneous adverse reactions due to isoniazid in a HIV positive patient. *Indian J Lepr,* 84**,** 227-32.

WALMSLEY, S. L., ANTELA, A., CLUMECK, N., DUICULESCU, D., EBERHARD, A., GUTIERREZ, F., HOCQUELOUX, L., MAGGIOLO, F., SANDKOVSKY, U., GRANIER, C., PAPPA, K., WYNNE, B., MIN, S., NICHOLS, G. & INVESTIGATORS, S. 2013. Dolutegravir plus abacavir-lamivudine for the treatment of HIV-1 infection. *N Engl J Med,* 369**,** 1807-18.

WALSH, S., DIAZ-CANO, S., HIGGINS, E., MORRIS-JONES, R., BASHIR, S., BERNAL, W. & CREAMER, D. 2013. Drug reaction with eosinophilia and systemic symptoms: Is cutaneous phenotype a prognostic marker for outcome? A review of clinicopathological features of 27 cases. *The British Journal of Dermatology,* 168**,** 391-401.

WANG, B., ABBOTT, L., CHILDS, K., TAYLOR, C., AGARWAL, K., CORMACK, I., MIQUEL, R. & SUDDLE, A. 2018. Dolutegravir-induced liver injury leading to sub-acute liver failure requiring transplantation: a case report and review of literature. *Internation journal of STD and AIDS,* 29**,** 414-417.

WEINBORN, M., BARBAUD, A., TRUCHETET, F., BEUREY, P., GERMAIN, L. & CRIBIER, B. 2016. Histopathological study of six types of adverse cutaneous drug reactions using granulysin expression. *Int J Dermatol,* 55**,** 1225-1233.

WETTER, D. A. & CAMILLERI, M. J. 2010. Clinical, etiologic, and histopathologic features of Stevens-Johnson syndrome during an 8-year period at Mayo Clinic. *Mayo Clin Proc,* 85**,** 131-8.

WHITE, K., CHUNG, W.-H., HUNG, S.-L., MALLAL, S. & PHILLIPS, E. 2015. Evolving models of the immunopathogenesis of T cell-mediated drug allergy: The role of host, pathogens, and drug response. *The journal of allergy and clinical immunology,* 136**,** 219-234.

WONGKITISOPHON, P., CHANPRAPAPH, K., RATTANAKAEMAKORN, P. & VACHIRAMON, V. 2012. Six-year retrospective review of drug reaction with eosinophilia and systemic symptoms. *Acta Derm Venereol,* 92**,** 200-5.

WU, P.-Y., CHENG, C.-Y., LIU, C.-E., LEE, Y.-C., YANG, C.-J., TSAI, M.-S., CHENG, S.-H., LIN, S.-P., LIN, D.-Y., WANG, N.-C., LEE, Y.-C., SUN, H.-Y., TANG, H.-J. & HUNG, C.-C. 2017. Multicenter study of skin rashes and hepatotoxicity in antiretroviral-naïve HIV-positive patients receiving non-

nucleoside reverse-transcriptase inhibitor plus nucleoside reverse-transcriptase inhibitors in Taiwan. *PloS One,* 12**,** e0171596.

YANG, C., MOSAM, A., MANKAHLA, A., DLOVA, N. & SAAVEDRA, A. 2014. HIV infection predisposes skin to toxic epidermal necrolysis via depletion of skin-directed CD4+ T cells. *Journal of the American Academy of Dermatology,* 70**,** 1096-1102.

YAZIJI, H. & BARRY, T. 2006. Diagnostic Immunohistochemistry: what can go wrong? *Adv Anat Pathol,* 13**,** 238-46.

YERO, A., SHI, T., FARNOS, O., ROUTY, J. P., TREMBLAY, C., DURAND, M., TSOUKAS, C., COSTINIUK, C. T. & JENABIAN, M. A. 2021. Dynamics and epigenetic signature of regulatory T-cells following antiretroviral therapy initiation in acute HIV infection. *EBioMedicine,* 71**,** 103570.

YUNIHASTUTI, E., WIDHANI, A. & KARJADI, T. H. 2014. Drug hypersensitivity in human immunodeficiency virus-infected patient: challenging diagnosis and management. *Asia Pac Allergy,* 4**,** 54-67.

ZGOLLI, F., CHARFI, O., AOUINTI, I., CHARFI, O., LAKHOUA, G., EL AIDLI, S., DAGHFOUS, R. & ZAIEM, A. 2021. Neosensitization to Multiple Drugs Following Trimethoprim/Sulfamethoxazole-induced Drug Reaction with Eosinophilia and Systemic Symptoms syndrome. *Acta Scientific Medical Sciences,* 5**,** 24-25.

ZHU, J., PENG, T., JOHNSTON, C., PHASOUK, K., KASK, A. S., KLOCK, A., JIN, L., DIEM, K., KOELLE, D. M., WALD, A., ROBINS, H. & COREY, L. 2013. Immune surveillance by CD8alphaalpha+ skin-resident T cells in human herpes virus infection. *Nature,* 497**,** 494-7.

chmtaf003:Thesis.pdf

ORIGINALITY REPORT

18%	14%	10%	3%
SIMILARITY INDEX	INTERNET SOURCES	PUBLICATIONS	STUDENT PAPERS

PRIMARY SOURCES

1	hdl.handle.net Internet Source	1%
2	livrepository.liverpool.ac.uk Internet Source	1%
3	Submitted to University of Cape Town Student Paper	1%
4	researchrepository.murdoch.edu.au Internet Source	1%
5	open.uct.ac.za Internet Source	1%
6	www.ncbi.nlm.nih.gov Internet Source	<1%
7	"Advances in Diagnosis and Management of Cutaneous Adverse Drug Reactions", Springer Science and Business Media LLC, 2019 Publication	<1%
8	Mireille Porter, Phuti Choshi, Sarah Pedretti, Tafadzwa Chimbetete et al. "IFN-γ ELISpot in Severe Cutaneous Adverse Reactions to First-	<1%